

Creating Tertiary and Quaternary Carbon Centers by Nickel and Copper-Catalyzed Cross-Coupling Reactions of Alkyl Electrophiles

THÈSE N° 5567 (2012)

PRÉSENTÉE LE 16 NOVEMBRE 2012

À LA FACULTÉ DES SCIENCES DE BASE

LABORATOIRE DE SYNTHÈSE ET DE CATALYSE INORGANIQUE

PROGRAMME DOCTORAL EN CHIMIE ET GÉNIE CHIMIQUE

ÉCOLE POLYTECHNIQUE FÉDÉRALE DE LAUSANNE

POUR L'OBTENTION DU GRADE DE DOCTEUR ÈS SCIENCES

PAR

Peng REN

acceptée sur proposition du jury:

Prof. J. Zhu, président du jury

Prof. X. Hu, directeur de thèse

Dr R. Martin, rapporteur

Prof. Ph. Renaud, rapporteur

Prof. J. Waser, rapporteur



ÉCOLE POLYTECHNIQUE
FÉDÉRALE DE LAUSANNE

Suisse
2012

ACKNOWLEDGEMENTS

First, I would like to thank my advisor, Prof. Xile Hu, for his trust and support, and for giving me the chance to do my PhD work in such an exciting research environment. Thanks to his constant guidance and encouragement. I have been able to develop my abilities as a chemist in a promising and important research field.

I would like to thank my thesis jury for agreeing to examine this thesis: Prof. Jieping Zhu, Prof. Jérôme Waser, Prof. Philippe Renaud, Dr. Ruben Martin.

I would like to thank my past and present group members. They made EPFL a wonderful working atmosphere, not only giving me valuable advice in academics, but also helping me to enjoy the multicultural lab atmosphere. I would especially like to thank Dafa for mentoring me in my research. Thanks to Heron for teaching me lots of experimental techniques and for helping me to solve many difficulties over the years. Thanks to Kate for the corrections and proof of SNSF documents and my thesis. Thanks to Gerald who introduced me to HPLC. Thanks to Thomas for translating the French abstract of my thesis. Many thanks to all of the master students who worked with me. Big thanks to our group apprentice Isuf who synthesized ligands and substrates for me and made my research more efficient.

I am thankful to all of my teachers during my Ph.D. study. Also, I would like to thank the Waser group for the use of the GC-MS instrument. Thanks to Dr. Rosario Scopelliti and Dr. Euro Solari for the X-ray and elemental analyses which contributed a lot to my thesis; Gladys Pache, Annelise Carrupt, Giovanni Petrucci and Benjamin Kronenberg from chemical stores for ordering plenty of chemicals for me. Francisco Sepulveda, Daniel Baumann and Dr. Laure Menin for the mass-spectro analysis. Dr Martial Rey for help with the NMR spectrometers. Patrick Favre and Donald Zbinden for the IT support. Anne-Lene Odegaard and Christina Zamanos-Epremian for the always kind help and administrative work. I thank Dr. Ning Yan, Dr. Bo Yao, Dr. Zhengren Xu for insightful discussion about my research.

Foremost, I would like to express my gratitude to my parents, family and girlfriend Xin for their support and encouragement during my study. Your love brightened my life.

ABSTRACT

Transition-metal-catalyzed C-C coupling reactions have been extensively studied in the past three decades. These reactions have become invaluable to fundamental research and industrial applications, because they can be used to construct complicated molecules from simple precursors. Among them, the coupling systems of aryl, alkenyl, and alkynyl halides have been well-optimized, while the coupling of non-activated alkyl halides, especially secondary alkyl halides, is still difficult. In the first chapter, the development of the transition-metal-catalyzed alkyl-alkyl cross-coupling reactions is introduced and summarized, and the difficulties and potential improvements are discussed.

In chapter 2, a structure-activity study is described for Ni-catalyzed alkyl-alkyl Kumada-type cross coupling reactions. A series of new nickel(II) complexes bearing bidentate and tridentate amino-amide ligands were synthesized and structurally characterized. The coordination geometries of these complexes include square planar, tetrahedral, and square pyramidal. The complexes had been examined as pre-catalysts for the cross coupling of non-activated alkyl halides, particularly secondary alkyl iodides, with alkyl Grignard reagents. Comparison was made to the results obtained with the previously reported Ni pincer complex $[(^{\text{Me}}\text{N}_2\text{N})\text{NiCl}]$ (**1**). A transmetalation site in the pre-catalysts is necessary for the catalysis. The coordination geometries and spin-states of the pre-catalysts have little or no influence. The work led to the discovery of several well-defined Ni catalysts that are significantly more active and efficient than the pincer complex (**1**) for the coupling of secondary alkyl halides. The best catalysts are $[(^{\text{H}}\text{NN})\text{Ni}(\text{PPh}_3)\text{Cl}]$ (**24**) and $[(^{\text{H}}\text{NN})\text{Ni}(2,4\text{-lutidine})\text{Cl}]$ (**27**). The improved activity and efficiency were attributed to the fact that the phosphine and lutidine ligands in these complexes could dissociate from the Ni center during catalysis. The activation of alkyl halides was shown to proceed via a radical mechanism.

After investigating how secondary alkyl halides could couple with primary Grignard reagents in high yields using nickel catalysts, the complementary methodology, the coupling of non-activated alkyl electrophiles with secondary and tertiary alkyl nucleophiles, is described in chapter 3. It was found that simple copper(I) chloride could catalyze the cross-coupling of non-activated primary alkyl halides and tosylates with secondary and tertiary alkyl Grignard reagents. The method is highly efficient, practical, and general. A wide range of functional groups can be tolerated, such as ester, ketone, amide, nitrile, and heterocyclic groups.

In chapter 4, a series of new copper complexes bearing hemilabile ligands were synthesized and structurally characterized. Among them, the copper complex $[(^{\text{Me}}\text{N}_2\text{N})\text{Cu}(\text{PPh}_3)]$ (**36**) was shown to have the highest catalytic activity towards alkylation of benzoxazoles with secondary alkyl halides. The higher efficiency of **36** relative to other copper catalysts might result from a hemilabile property of the pincer ligand. An important additive, bis[2-(N,N-dimethylamino)ethyl] ether (BDMAEE) is also identified. This is the first time that non-activated secondary alkyl halides have been used as electrophiles in the alkylation of benzoxazoles.

Keywords: cross coupling, C-H functionalization, alkyl electrophiles, coordination chemistry, alkylation, mechanism, nickel, copper, Kumada coupling, Grignard reagents, secondary alkyl halides.

RESUME

Les réactions de couplage C-C catalysées par des métaux de transition ont été beaucoup étudiées durant les trois dernières décennies. Ces réactions sont devenues incontournables dans la recherche fondamentale et dans les applications industrielles, puisqu'elles peuvent être utilisées dans la synthèse de molécules complexes à partir de précurseurs simples. Parmi celles-ci, les systèmes de couplage d'halogénures d'aryle, d'alcène et d'alcyne ont été très bien optimisés, tandis que le couplage d'halogénures d'alkyle non-activés, et notamment les halogénures d'alkyle secondaires, est encore difficile. Dans le premier chapitre, le développement de réactions de couplage croisé alkyle-alkyle catalysées par des métaux de transition est introduit et résumé, puis les difficultés et les améliorations potentielles sont examinées.

Dans le chapitre 2, une étude activité-structure est décrite pour les réactions de couplage croisé alkyle-alkyle de type Kumada et catalysées par le nickel. Une série de nouveaux complexes à base de nickel(II) portant des ligands amino-amide bidenté et tridenté ont été synthétisés et caractérisés structurellement. Ces complexes possèdent des géométries de coordination plan-carré, tétraèdre ou pyramide à base carrée. Les complexes ont été étudiés comme pré-catalyseurs pour le couplage croisé d'halogénures d'alkyle, et en particulier d'iodures d'alkyle secondaires, avec des organomagnésiens de type alkyle. Les résultats ont été comparés avec ceux obtenus avec le complexe de nickel pincer [$^{\text{Me}}\text{N}_2\text{N}$] NiCl (**1**) déjà étudié par le *Laboratory of Inorganic Synthesis and Catalysis*. Un site de transmétallation sur les pré-catalyseurs est nécessaire pour la catalyse. Les géométries de coordination et les états de spin des pré-catalyseurs n'ont que peu d'influence voire aucune. Les travaux ont mené à la découverte de différents catalyseurs de nickel bien définis qui sont sensiblement plus actifs et efficaces que le complexe pincer (**1**) pour le couplage des halogénures d'alkyle secondaires. Les meilleurs catalyseurs sont les complexes [$^{\text{H}}\text{NN}$] $\text{Ni}(\text{PPh}_3)\text{Cl}$ (**24**) et [$^{\text{H}}\text{NN}$] $\text{Ni}(2,4\text{-lutidine})\text{Cl}$ (**27**). L'activité améliorée et l'efficacité ont été attribuées au fait que les ligands phosphine et lutidine de ces complexes pourraient se dissocier du centre métallique de Ni pendant la catalyse. Il a été montré que l'activation d'halogénures d'alkyle procède via un mécanisme radicalaire.

Après avoir étudié comment les halogénures d'alkyle secondaires pouvaient se coupler avec des organomagnésiens primaires avec des rendements élevés en utilisant des catalyseurs de nickel, la méthodologie complémentaire, à savoir le couplage d'électrophiles alkyles non-

activés avec des nucléophiles alkyles secondaires et tertiaires, est décrite dans le chapitre 3. Il a été trouvé que le chlorure de cuivre(I) pouvait catalyser le couplage croisé d'halogénures et de tosylates d'alkyle primaires non activés avec des organomagnésiens de type alkyle secondaire et tertiaire. La méthode est hautement efficace, facilement réalisable et générale. Une grande variété de groupes fonctionnels peut être tolérée, comme les esters, les cétones, les amides, les nitriles et les groupes hétérocycliques.

Dans le chapitre 4, une série de nouveaux complexes à base de cuivre possédant des ligands hémilabiles ont été synthétisés et caractérisés structurellement. Parmi eux, le complexe de cuivre $[(^{\text{Me}}\text{N}_2\text{N})\text{Cu}(\text{PPh}_3)]$ (**36**) a montré la plus haute activité à travers l'activation de benzoxazoles avec des halogénures d'alkyle secondaires. L'efficacité du complexe **36**, plus élevée que celle des autres catalyseurs de cuivre, pourrait résulter de la propriété hémilabile du ligand pincer. Un additif important, le bis[2-(N,N-diméthylamino)éthyl] éther (BDMAEE) est également identifié. Des halogénures d'alkyle secondaires non-activés ont été employés comme électrophiles dans l'alkylation de benzoxazoles pour la première fois.

Mots-clés: couplage croisé, fonctionnalisation de la liaison C–H, électrophiles alkyles, chimie de coordination, alkylation, mécanisme, nickel, cuivre, couplage de Kumada, organomagnésiens, halogénures d'alkyle secondaires.

LIST OF SYMBOLS AND ABBREVIATIONS

Å	angstrom
δ	chemical shift
°	degree
λ	wavelength
acac	acetylacetonate
APPI	atmospheric pressure photoionization
aq.	aqueous
atm	atmosphere
BBN	9-borobicyclo[3.3.1]-nonane
BDMAEE	bis[(2-(<i>N,N</i> -dimethylaminoethyl)]ether
B. E.	β-H elimination
Bn	Benzyl
Boc	tert-butyloxycarbonyl
br	broad
Bu	butyl
Bz	benzyl
calcd	calculated
cat	catalyst
cod	1,5-cyclooctadiene
Cy	cyclohexyl
Cyp	cyclopentyl
d	doublet
dba	dibenzylideneacetone
DBU	1,8-diazabicycloundec-7-ene
dd	doublet of doublets
DFT	density functional theory
DIBAL	diisobutylaluminum hydride
DMA	<i>N,N</i> -dimethylacetamide
dme	1,2-dimethoxyethane
dmeda	<i>N,N'</i> -dimethylethane-1,2-diamine
DMI	1,3-dimethyl-2-imidazolidinone

dmiy	1,3-dimethylimidazolin-2-ylidene
DMF	<i>N,N</i> -dimethylformamide
DMSO	dimethyl sulfoxide
dppf	1,1'-bis(diphenylphosphino)ferrocene
dq	doublet of quartets
dt	doublet of triplets
e.e.	enantiomeric excess
eq.	equation
equiv.	equivalent
ESI	electrospray ionization
Et	ethyl
Et ₃ N	triethylamine
FID	flame ionization detector
g	gram
GC	gas chromatography
^{HiPr} N ₂ NH	(2-isopropylaminophenyl)amine
^{HMe} N ₂ ^{Me} N	<i>N,N</i> -bis(2-methylaminophenyl)methylamine
^{HMe} N ₂ NH	bis(2-methylaminophenyl)amine
^H NNH	<i>N</i> ¹ , <i>N</i> ¹ -dimethyl- <i>N</i> ² -phenylbenzene-1,2-diamine
hr	hour
HR	high resolution
HPLC	high-performance liquid chromatography
ⁱ Bu	iso-butyl
ⁱ Pr	iso-propyl
K	Kelvin
Lut	2,4-lutidine
Me	methyl
Me ₂ NH	dimethylamine
^{Me} N ^{Me} N ^{Me} NH	2-(2-(dimethylamino)ethyl)- <i>N,N</i> -dimethylaniline
Me ₂ SO ₄	dimethyl sulfate
^{Me} N ₂ ^{Me} N	<i>N,N</i> -bis(2-dimethylaminophenyl)methylamine
^{Me} NNH	<i>N</i> ¹ , <i>N</i> ¹ -dimethyl- <i>N</i> ² -(<i>o</i> -tolyl)benzene-1,2-diamine
^{Me} N ₂ NH	bis[(2-dimethylamino)phenyl]amine

mer	meridional
mg	mili-gram
MHZ	mega-hertz
mL	mili-liter
mmol	mili-mole
mol	mole
MS	mass spectrometry
NaOMe	sodium methoxide
ⁿ Bu	normal-butyl
NMI	<i>N</i> -methylimidazole
NMP	<i>N</i> -Methylpyrrolidone
NMR	nuclear magnetic resonance
NNOH	<i>N</i> ¹ -(2-methoxyphenyl)- <i>N</i> ² , <i>N</i> ² -dimethylbenzene-1,2-diamine
ⁿ Non	normal-nonyl
NPH	2-(diphenylphosphino)- <i>N</i> -phenylaniline
O. A.	oxidative addition
OAc	acetate
Oct.	octyl
OTf	triflate
Pd ₂ (dba) ₃	tris(dibenzylideneacetone)dipalladium(0)
Ph	phenyl
^{Ph} NNH	<i>N</i> ¹ -([1,1'-biphenyl]-2-yl)- <i>N</i> ² , <i>N</i> ² -dimethylbenzene-1,2-diamine
ppm	part per million
Pybox	2,6-bis[(4 <i>R</i>)-4-phenyl-2-oxazolinyl]pyridine
R. E.	reductive elimination
r.t.	room temperature
rxn	reaction
s	second
s	singlet
^s Bu	sec-butyl
t	triplet
T	temperature
^t Bu	tert-butyl

terpy	terpyridine
td	triplet of doublets
THF	tetrahydrofuran
T. M.	transmetalation
TMEDA	tetramethylethylenediamine
TMS	trimethylsilyl
TOF-MS	time-of-flight mass spectrometry
TON	turnover number
Xantphos	9,9-dimethyl-4,5-bis(diphenylphosphino)xanthene

Table of Contents

Acknowledgements.....	I
Abstract.....	II
Résumé.....	IV
List of Symbols and Abbreviations.....	VI
Table of Contents.....	X
Chapter 1. Introduction.....	1
1.1 Transition-metal-catalyzed C-C cross-coupling reactions.....	2
1.2 Alkyl-alkyl Kumada-Corriu-Tamao coupling reactions.....	4
1.3 Alkyl-alkyl Negishi coupling reactions.....	9
1.4 Alkyl-alkyl Suzuki-Miyaura coupling reactions.....	13
1.5 Reductive alkyl-alkyl coupling reactions.....	17
1.6 Summary and outlook.....	18
1.7 References.....	19
Chapter 2. A Structure-Activity Study of Nickel-Catalyzed Alkyl-Alkyl Kumada Coupling. Improved Catalysts for Coupling of Secondary Alkyl Halides.....	23
2.1 Introduction.....	24
2.2 Synthesis and structure of nickel catalysts.....	25
2.2.1 Ligand synthesis.....	25
2.2.2 Metallation using organo lithium and magnesium reagents.....	27
2.2.3 Synthesis of nickel complexes of ligands 3-9	31
2.2.4 Structures of Ni complexes.....	34
2.3 Kumada coupling of secondary alkyl halides using Nickel complexes as catalysts.....	42
2.3.1 Test reactions.....	42
2.3.2 Ranking of catalysts.....	48
2.3.3 Probing the origin of the activity and efficiency for catalysts 1 , 24 , and 27	54
2.4 Radical clock.....	58
2.5 Substitution reactions for complexes 24 , 25 , and 27	60
2.6 Inhibition study for pre-catalysts 24 and 27	61
2.7 Discussion.....	62
2.7.1 Synthesis of Ni complexes.....	62
2.7.2 Alkyl-alkyl Kumada coupling using preformed Ni complexes.....	62
2.8 Conclusions.....	66

2.9 Experimental section	66
2.9.1 Chemicals and Reagents	66
2.9.2 Physical methods	67
2.9.3 Synthetic methods	67
2.9.4 Crystallographic Details	79
2.9.5 Typical Procedure for the Alkyl-Alkyl Kumada Coupling	85
2.9.6 Coupling of radical clocks	86
2.9 References and Notes	86
2.9 GC-MS Spectra of Products	89
Chapter 3. Copper-Catalyzed Cross-Coupling of Functional Alkyl Halides and Tosylates	
with Secondary and Tertiary Alkyl Grignard Reagents	103
3.1 Introduction	104
3.2 Optimization of the reaction conditions for coupling of 5-bromopentyl acetate with ^t BuMgCl	104
3.3 Scope of Kumada-Corriu-Tamao coupling of functionalized alkyl halides with alkyl Grignard reagents	106
3.4 Attempts at asymmetric catalysis of alkyl-alkyl Kumada-Corriu-Tamao coupling	112
3.5 Mechanistic investigations	113
3.6 Conclusions	114
3.7 Experimental section	114
3.7.1 Chemicals and Reagents	114
3.7.2 Physical methods	115
3.7.3 General procedures for the entries reported in Tables 1, 3, 4	115
3.7.4 General procedures for the entries reported in Table 2	116
3.7.5 General procedures for Cross coupling reactions employing chiral ligands in scheme 1	116
3.7.6 Hg-test experiment	116
3.7.7 Radical probe experiments	116
3.7.8 Detailed descriptions for products	117
3.8 References and Notes	123
Chapter 4. Synthesis of Copper Complexes with Hemilabile Ligands; Copper-Catalyzed	
Direct Alkylation of Benzoxazoles Using Secondary Alkyl Halides	127
4.1 Introduction	128
4.2 Copper complexes	128

4.2.1 Ligand synthesis	128
4.2.2 Synthesis and structures of copper complexes	130
4.3 Optimization of the coupling reaction conditions between benzoxazole and cyclopentyl iodide	139
4.4 Scope of the copper-catalyzed alkylation of benzoxazoles	144
4.5 Mechanistic investigations	148
4.6 Conclusions	149
4.7 Experimental section	149
4.7.1 Chemicals and Reagents	149
4.7.2 Physical methods	150
4.7.3 Synthetic methods for ligands and copper complexes	150
4.7.4 Crystallographic details	156
4.7.5 General procedures for Table 3, 5, 6 and Scheme 6	160
4.7.6 General procedures for Table 4	160
4.7.7 Stereochemical assignment of ring-closed product (Scheme 6, eq. 2)	160
4.7.8 Detailed descriptions for products in Table 4	161
4.8 References and Notes	167
Concluding Remarks and Outlook	171
Curriculum Vitae	175

Chapter 1

Introduction

1.1 Transition metal-catalyzed C-C cross-coupling reactions

Transition metal-catalyzed cross-coupling reactions, such as C-C and C-heteroatom bond formation reactions, are extremely powerful in organic synthesis.¹⁻³ Since the first Ni-catalyzed Kumada coupling reaction was discovered in 1972,⁴ the development of coupling reactions has reached a level of sophistication that allows for a wide range of coupling partners to be combined efficiently. A variety of reactions have been used in the synthesis of natural products, pharmaceuticals, and materials.⁵⁻⁹ In 2010, the importance of this chemistry was recognized by the award of the Nobel prize to Heck, Negishi, and Suzuki “for palladium-catalyzed cross-couplings in organic synthesis”.

A C-C coupling reaction is the connection of two hydrocarbon fragments. Generally, one of the substrates is an organometallic reagent and the other is an electrophile. Because of the diversity of these two coupling partners, numerous new molecules can be formed. This is why the C-C coupling chemistry has been popular for more than three decades. Some of the most important “name reactions” are presented in Table 1.

Table 1. Important metal-catalyzed C-C cross-coupling reactions.

$RX + R'-[M] \xrightarrow{\text{cat.}} R-R' + [M]-X$		
Reaction	[M]	Year
Kumada-Corriu-Tamao	$R'MgY$	1972
Negishi	$R'ZnY$ or R'_2Zn	1977
Suzuki-Miyaura	$R'B(OY)_2$	1979
Heck	$R''-\text{CH=CH}_2$, no $R'-[M]$ is formed, the mechanism is different, alkene insert into the palladium-carbon bond intermediate	1972
Sonogashira	$R''-\text{C}\equiv\text{C}-\text{Cu}$ <i>In situ</i> form from terminal alkyne with base and CuI	1975
Stille	$RSnR''_3$	1979

Table 1. (continued)

Reaction	[M]	Found Year
Hiyama	RSiR'' ₃	1988

Since the pioneering contributions made by Heck, Negishi, and Suzuki *et al.*,^{10,11} many efficient catalytic systems have been designed. A variety of electrophilic coupling partners, aryl, vinyl, and alkynyl halides and pseudo-halides, can be readily coupled.^{12,13} Conversely, alkyl halides, especially non-activated ones containing β -hydrogens, remain difficult substrates.¹⁴⁻¹⁶ Non-activated alkyl halides herein are considered to be those alkyl halides that are not functionalized with activating groups (such as benzyl, allyl, propargyl, cyclopropyl, alkoxy, carbonyl, and others) in the α -position.¹⁵ Based on the general catalytic cycle for cross coupling reactions of alkyl halides (Figure 1),¹⁷ there are three main steps in a catalytic cycle. They are (1) oxidative addition: the low-valent metal species reacts with alkyl halide to give a metal alkyl species; Generally the valence of the metal will be increased from M^n to M^{n+2} ; (2) transmetalation: metal alkyl species reacts with an organometallic reagent to give a diorgano-metal intermediate and inorganic metal salt; (3) reductive elimination: the diorgano-metal species gives the cross coupling product and regenerates the starting catalyst.

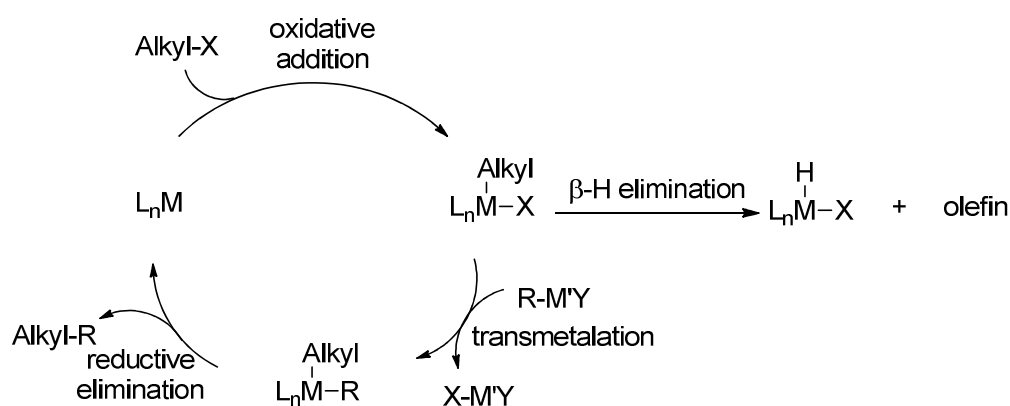


Figure 1. A general catalytic cycle for transition-metal-catalyzed C-C cross-coupling reactions of alkyl halides.

The two most frequently cited causes for the difficulty in the coupling of non-activated alkyl halides are: (a) alkyl electrophiles are more electron-rich compared to their aryl and vinyl counterparts, and therefore they have less tendency to undergo oxidative addition with a metal catalyst, and (b) If oxidative addition of alkyl halides occurs, the resulting metal alkyl intermediates are substantially less stable than an aryl or alkenyl metal species owing to a

lack of π electrons available to interact with the empty d orbitals of the metal center. These metal alkyl species are then prone to unproductive β -H elimination or hydrodehalogenation. The cross coupling is thus not efficient. For these reasons, the development of cross-coupling of non-activated alkyl halides has fallen behind those of the coupling of aryl and vinyl electrophiles.

Current progress in this area is mainly limited to alkyl-aryl/alkenyl coupling. The coupling of two sp^3 carbon atoms is even more difficult, because the reductive elimination between two sp^3 centers is slow compared to two sp^2 centers or a sp^3 and sp^2 center,¹⁸⁻²⁰ so a competitive exchange reaction between two alkyl groups may happen, which will form the symmetrical organometallic species (L_nMR_2), and produce the homocoupling product via reductive elimination. Moreover, the cross-coupling of secondary alkyl halides is an even more challenging task. The added steric hindrance of a secondary alkyl halide increases the energy barrier to oxidative addition, and also makes the resulting metal-alkyl species prone to β -H elimination. These factors make traditional transition-metal-catalyzed processes much more difficult. In the following sections, I will introduce the development of transition-metal-catalyzed alkyl-alkyl cross-coupling reactions.

1.2 Alkyl-alkyl Kumada-Corriu-Tamao coupling reactions

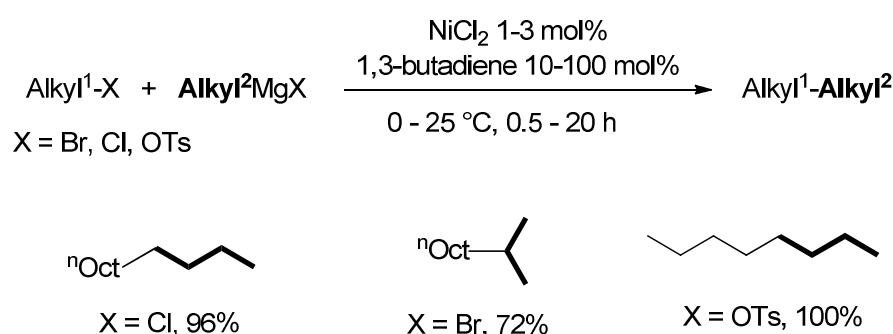
During the past 100 years, Grignard reagents have been perhaps the most widely used organometallic reagents because they are cheap, easy to synthesize, and commercially available.²¹ The reactions can be done in a short time under mild conditions (although atmospheric moisture and oxygen should be excluded).²²⁻²⁷ As early as 1972, Kumada *et al.*⁴ and Corriu and Masse²⁸ independently reported the cross-coupling reactions of Grignard reagents with alkenyl and aryl halides using nickel salts as catalysts.

In the past 30 years, there has been rapid development in the use of transition-metal catalysts in a variety of C-C bond formation reactions.^{29,30} Some reports have shown that Kumada-type reactions can overcome the difficulties of functional group tolerance, thus making such coupling reactions more widely applicable.^{31, 32} Examples of Kumada-type alkyl-alkyl cross-coupling reactions are introduced here.

In 1986, Widdowson *et al.* reported Pd-catalyzed alkyl-alkyl Kumada cross-coupling reactions.³³ By using $[Pd(dppf)]$ as catalyst (formed in situ from $[PdCl_2(dppf)]$ and diisobutylaluminum hydride (DIBAL); dppf = 1,1'-bis(diphenylphosphino)ferrocene), both primary and secondary alkyl iodides can be coupled with alkyl Grignard reagents and provide

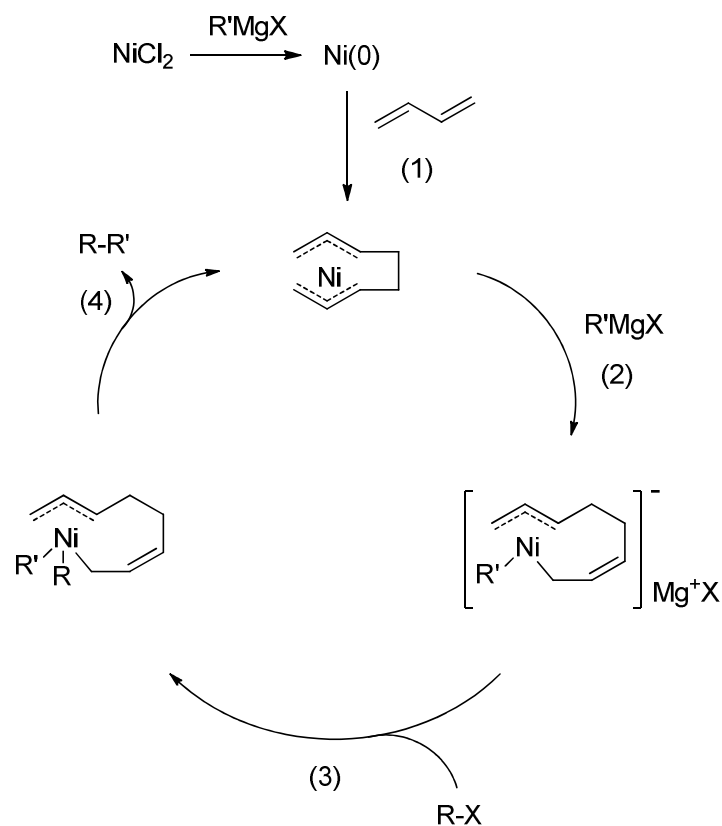
moderate to good yields. However, the reactions need be refluxed in THF. Furthermore, except for simple alkyl iodides, the results of alkyl bromide with functional groups were not shown in this paper.

In 2002, Kambe *et al.* reported the first efficient Ni-catalyzed Kumada-type cross-coupling reactions of primary and secondary Grignard reagents with primary alkyl chlorides, bromides, and tosylates under mild conditions (Scheme 1).³⁴ The use of 1,3-butadiene as a ligand is the key to attaining high yields of cross-coupling products. However, the functional compatibilities of the substrates were not explored, and secondary alkyl halides were not tested.



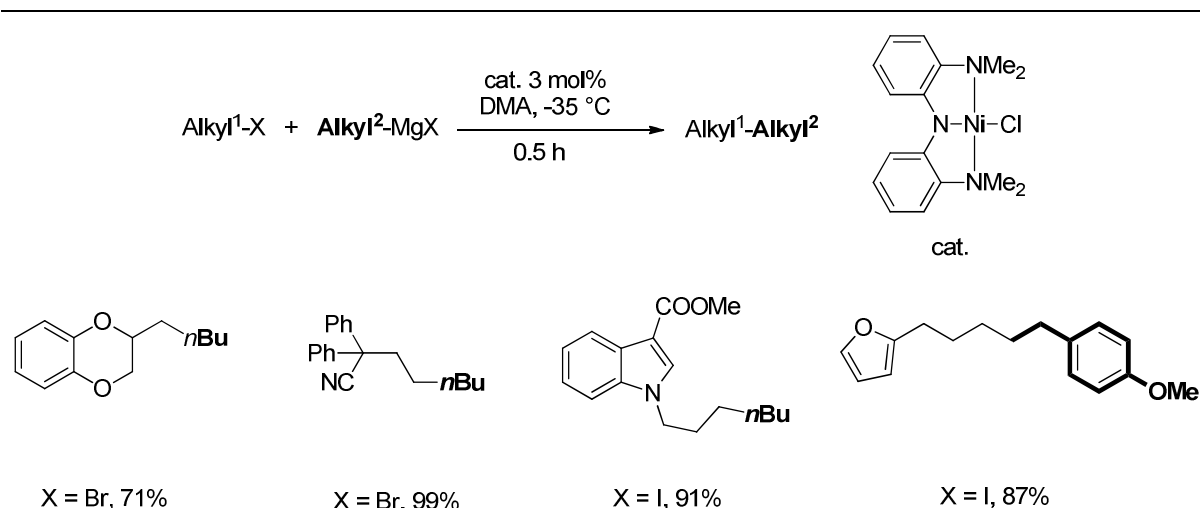
Scheme 1. Nickel-catalyzed cross-coupling reactions of alkyl halides and tosylates with alkyl Grignard reagents.

A radical clock experiment excluded the radical pathway. A plausible mechanism was also presented (Scheme 2). In step 1, Ni(0) (in situ generated from NiCl₂ and a Grignard reagent) reacts with 2 equiv. of 1,3-butadiene to afford a bis- π -allyl nickel complex. Then, the nickel allyl complex reacts with a Grignard reagent to form a η^1, η^3 -octadiene-diylnickelate complex. This latter complex then reacts with alkyl halide to form a dialkyl Ni complex (step 3). Reductive elimination then gives the coupling product and regenerates the bis- π -allyl nickel complex (step 4).



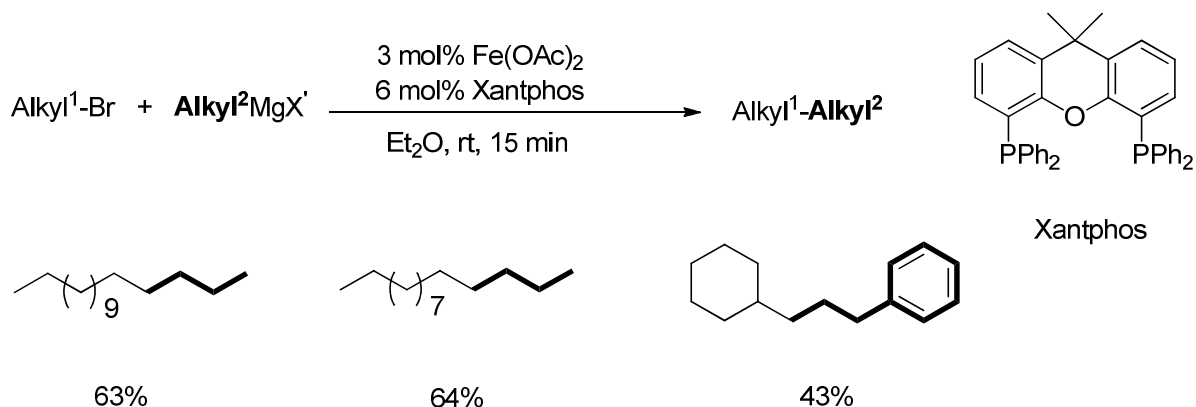
Scheme 2. A plausible reaction pathway of Ni-catalyzed Kumada coupling using 1,3-butadiene ligands.

Our group reported a nickel-catalyzed alkyl-alkyl Kumada coupling method in 2009 (Scheme 3).³⁵ By using a well-defined pincer nickel complex, $[(^{\text{Me}}\text{N}_2\text{N})\text{Ni}^{\text{II}}\text{Cl}]$, as pre-catalyst, non-activated and functionalized alkyl bromides and iodides can be coupled with alkyl Grignard reagents. A wide range of substrates can be used, and a very good functional group tolerance was achieved. Ester, amide, ether, acetal, nitrile, thioether and keto groups, as well as indole, pyrrole, and furan groups were tolerated. This work extends significantly the scope of cross-coupling reactions using Grignard nucleophiles, making these readily available reagents useful for the synthesis of organic molecules containing functional groups.



Scheme 3. Cross-coupling of non-activated and functionalized alkyl halides with alkyl Grignard reagents catalyzed by a Nickel complex with a pincer $\text{Me}_2\text{N}_2\text{N}$ Ligand.

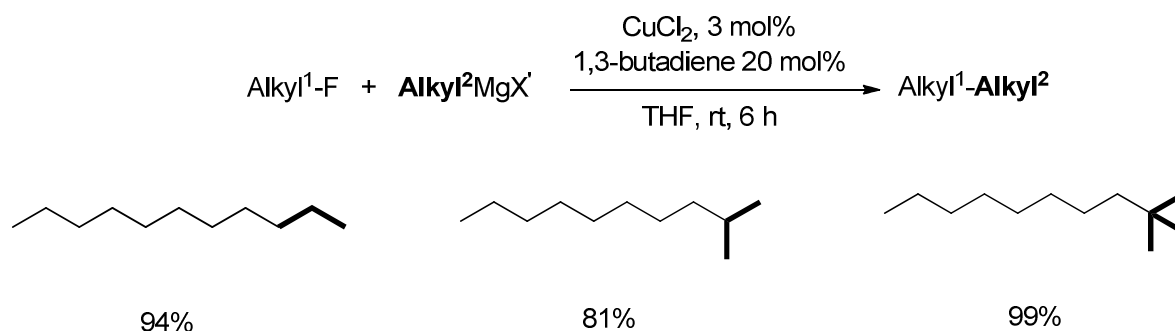
There are few efficient methods for iron-catalyzed Kumada-type $\text{C}(\text{sp}^3)\text{-C}(\text{sp}^3)$ coupling reactions. In 2006, Chai *et al.* found that $\text{Fe}(\text{OAc})_2$ in combination with Xantphos was effective in coupling alkyl halides with alkyl Grignard reagents.³⁶ The yields were generally low to medium. This was the first example of an iron-catalyzed $\text{sp}^3\text{-sp}^3$ cross-coupling reaction between Grignard reagents with unactivated alkyl halides (Scheme 4).



Scheme 4. Iron-catalyzed cross-coupling reactions of alkyl halides with alkyl Grignard reagents.

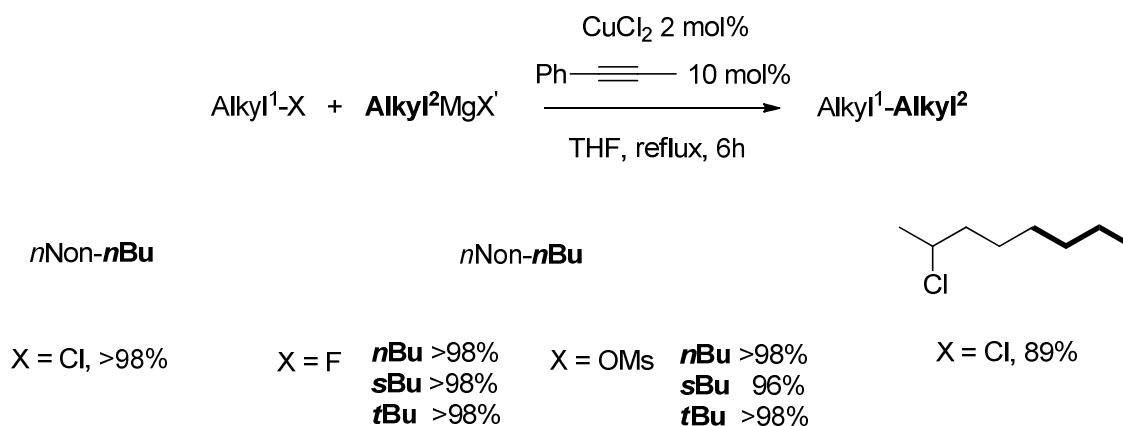
Copper-catalyzed cross-coupling reactions between alkyl halides and Grignard reagents were first reported by Kochi *et al.* in 1972.³⁷ More than 30 years later, a significant exploration was done by Kambe *et al.* Carbon-Fluorine bonds have been thought to be the strongest bond in organic compounds, and the cleavage of $\text{C}_{\text{sp}^3}\text{-F}$ bond is hard. Kambe *et al.* reported an efficient system for the cross-coupling reaction of alkyl fluorides with Grignard reagents catalyzed by simple NiCl_2 or CuCl_2 salts with 1,3-butadiene as the ligand (Scheme 5).³⁸ This protocol proceed efficiently between primary alkyl fluorides and various Grignard

reagents (primary, secondary, and tertiary alkyl and phenyl Grignard reagents) under mild conditions. The reactivity of alkyl halides was also examined and observed to be in the order chloride < fluoride < bromide. For the coupling of alkyl chloride, the yield was only 3%. The high reactivities of fluorides are originated from its conversion into bromides in the presence of MgBr_2 .³⁹



Scheme 5. Copper-catalyzed cross-coupling reactions of alkyl fluorides with alkyl Grignard reagents.

Four years later, in 2007, Kambe *et al.* overcame the difficulties for the coupling of alkyl chlorides (Scheme 6).⁴⁰ They described the first example of a Cu-catalyzed cross-coupling reaction of alkyl chlorides with alkyl Grignard reagents in the presence of 1-phenylpropyne as an additive. This method can be also used for alkyl fluorides and mesylates. It is worth to note that only simple alkyl halides such as octyl and decyl halides were used as the substrates in both of these two reports. The synthetic utility of these reactions was not fully demonstrated.

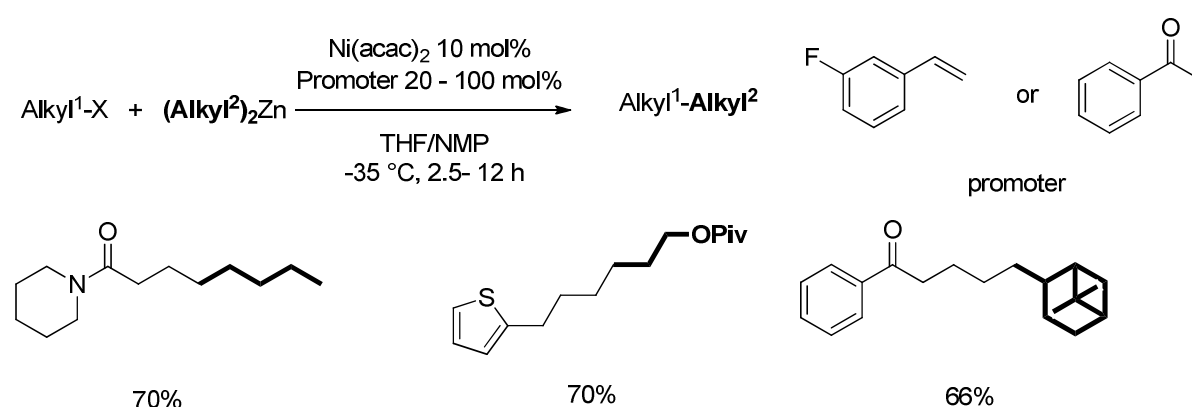


Scheme 6. Copper-catalyzed cross-coupling reactions of alkyl chlorides with alkyl Grignard reagents by using 1-phenylpropyne as an additive.

1.3 Alkyl-alkyl Negishi coupling reactions

The Negishi reaction results in the formation of a new C-C bond between an organozinc compound and an organohalide.⁴¹ Traditionally Pd and Ni-based catalysts are used.⁴²⁻⁴⁴ Recently, chemists found that iron catalysts can also achieve this task.^{45,46} Compared to Grignard reagents, organozinc compounds are milder nucleophiles. In principle, more functional groups are compatible.^{47,48} The coupling products may be obtained in good to excellent yields in a stereospecific manner.⁴⁹

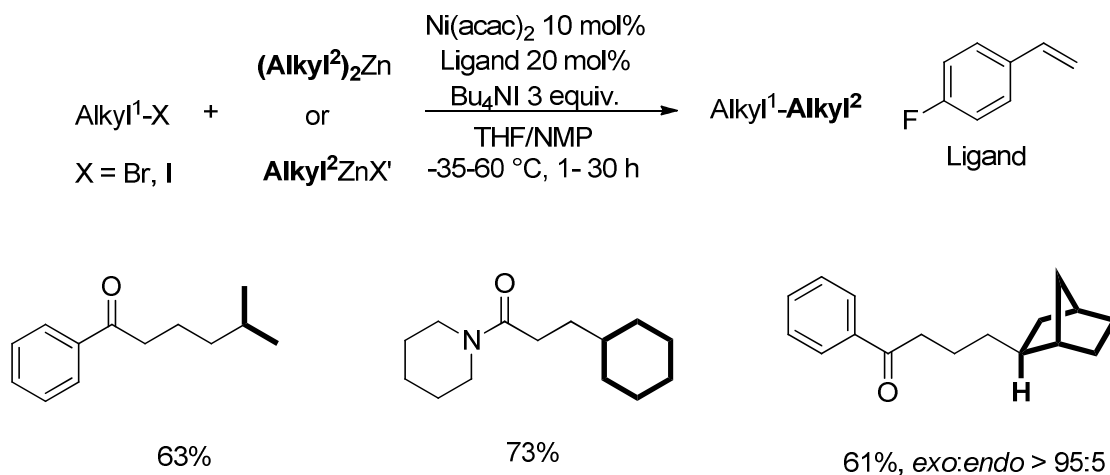
Knochel *et al.* pioneered the development of alkyl-alkyl Negishi cross-coupling reactions. In their first report, alkyl iodides could be coupled with dialkyl zinc reagents in the presence of stoichiometric quantities of $[\text{Me}_2\text{Cu}(\text{CN})(\text{MgCl})_2]$.⁵⁰ Later, they reported substrate-specific alkyl-alkyl cross coupling reactions catalyzed by nickel catalyst. Only alkyl halides containing double bonds at the 4- or 5- position as substrates could be coupled. It was suspected that the remote double bond could act as an additional ligand for Ni intermediates in the cross-coupling reactions.^{51,52} In 1998, the same group extended this methodology (Scheme 7).⁵³ Instead of using special alkyl halides containing double bond, they utilized *m*-trifluoromethylstyrene or acetophenone as a promoter. Functionalized primary iodoalkanes and primary diorganozinc compounds can be coupled efficiently. It is proposed that the main effect of these two promoters is that they facilitate the reductive elimination of the intermediate Ni(II) complex $(\text{Alkyl}^1)(\text{Alkyl}^2)\text{NiL}_n$ by removing electron density from the metal center.



Scheme 7. Nickel-catalyzed Negishi-type cross-coupling reactions of alkyl-alkyl cross-coupling reported by Knochel *et al.*

With these successes in hand, a similar catalytic system was later developed. Slight modifications of the reaction conditions by adding Bu_4NI , allowed efficient Ni-catalyzed

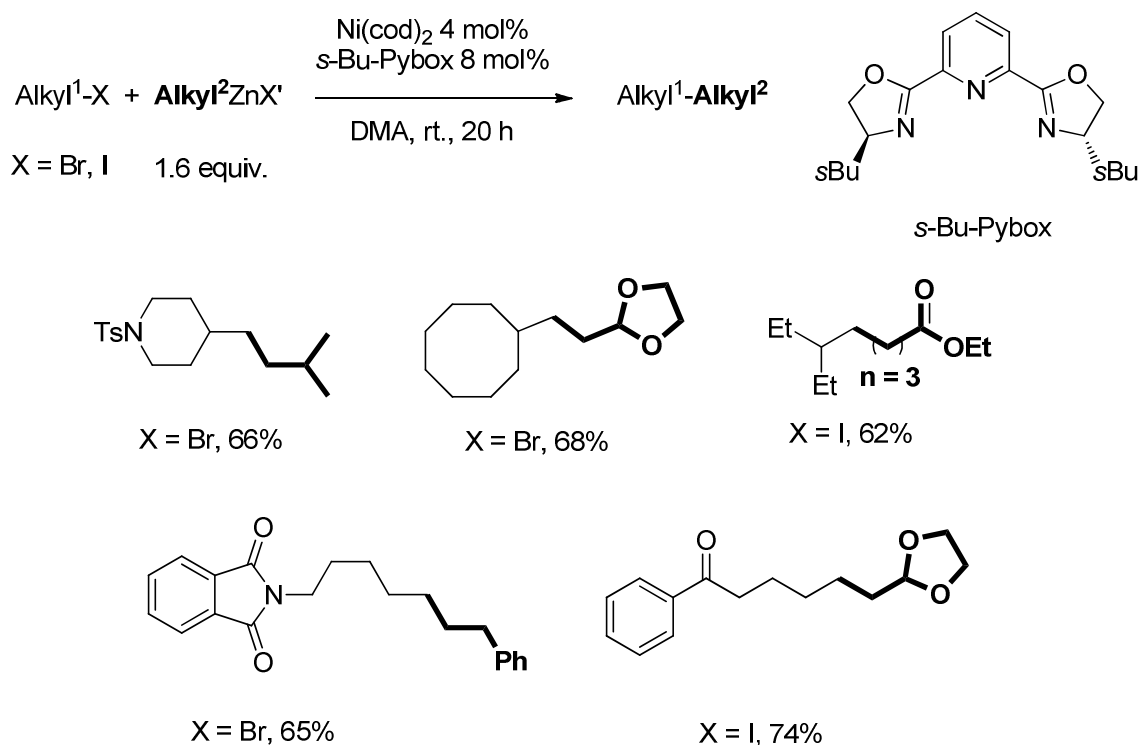
cross-coupling reactions between primary alkyl iodides and benzylzinc bromides.⁵⁴ This system can be also applied to the efficient coupling of primary and secondary organozinc reagents with primary alkyl halides (Scheme 8).⁵⁵ The possible role of Bu₄NI is that it enhances the ionic concentration of the medium, which promotes the cross-coupling reactions.



Scheme 8. Nickel-catalyzed Negishi-type cross-coupling reactions of alkyl halides with secondary alkylzinc reagents.

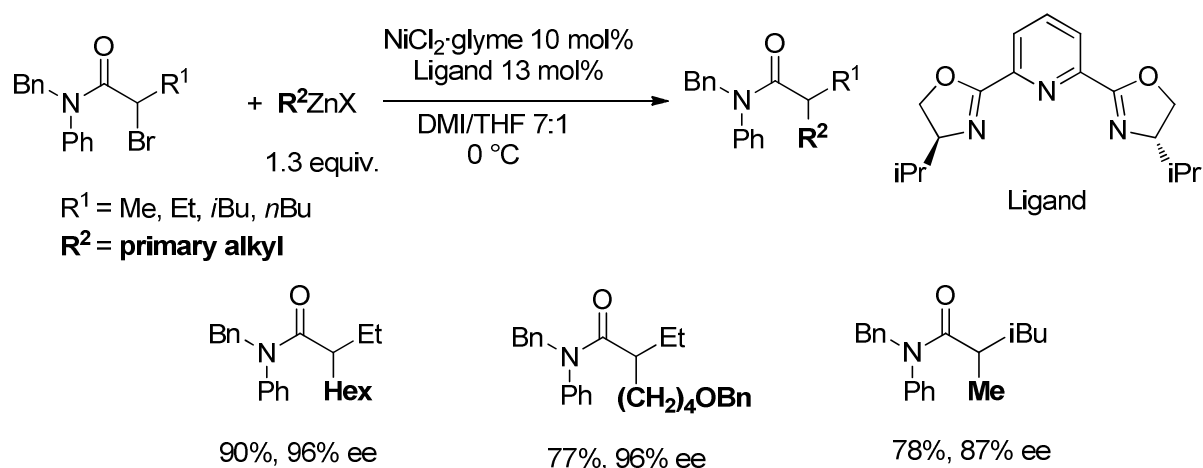
Fu's group also provided significant contributions in this field. With a combination of 2% Pd₂(dba)₃/8% PCyp₃/1.2 equiv. NMI in THF/NMP at 80 °C (Cyp = cyclopentyl, NMI = *N*-methylimidazole), a range of β-hydrogen-containing primary alkyl iodides, bromides, chlorides, and tosylates were coupled with an array of alkyl-, alkenyl-, and arylzinc halides in excellent yields.⁵⁶ The process is also compatible with a variety of functional groups, including esters, amides, imides, nitriles, and heterocycles. Additionally, Organ *et al.* also discovered the Pd-N-heterocyclic carbene (NHC) system that achieves room-temperature Negishi cross-coupling of non-activated primary bromides and alkyl organozinc reagents with a variety of functionality.^{57,58}

In 2003, Fu *et al.* reported that Ni(cod)₂ in the presence of (*s*-Bu)-Pybox in DMA catalyzed room temperature cross-coupling of secondary (and primary) alkyl bromides and iodides with alkylzinc halides in moderate to good yield with high functional group tolerance under mild conditions (Scheme 9).⁵⁹ This is the first example of the Negishi cross-coupling of non-activated, β-hydrogen-containing, secondary alkyl halides, which opened a new area of synthetic chemistry.



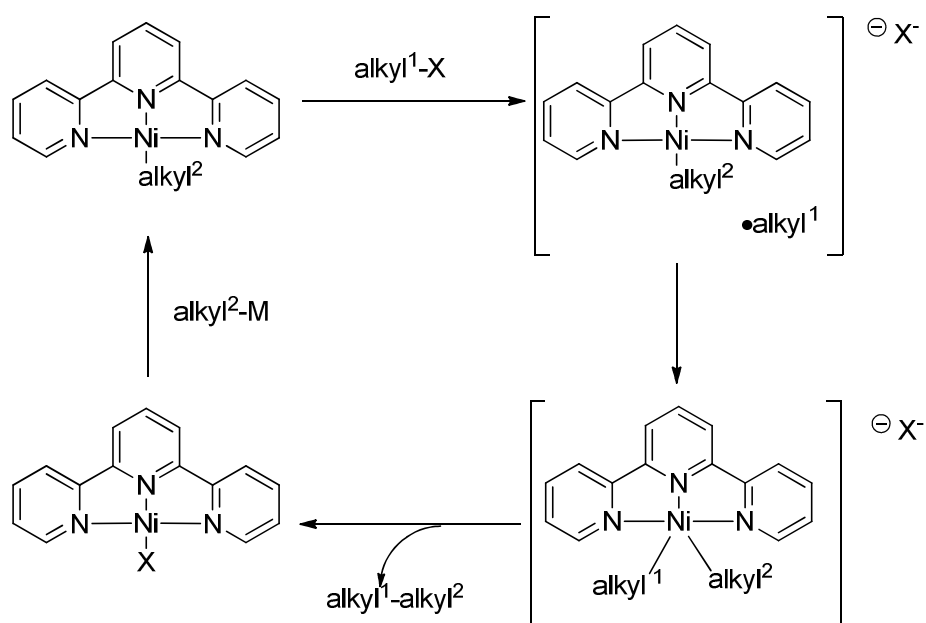
Scheme 9. Nickel-catalyzed Negishi-type cross-coupling reactions of secondary alkyl halides with alkylzinc reagents.

Later, Fu *et al.* expanded the method to asymmetric Negishi cross-couplings of α -bromo amides with organozinc reagents (Scheme 10).⁶⁰ The nickel-pybox combination was again very reactive for this medium. Furthermore, the polar solvent 1,3-dimethyl-2-imidazolidinone (DMI) and THF were crucial for this method. This is the first method that achieved catalytic asymmetric cross-couplings of alkyl electrophiles.



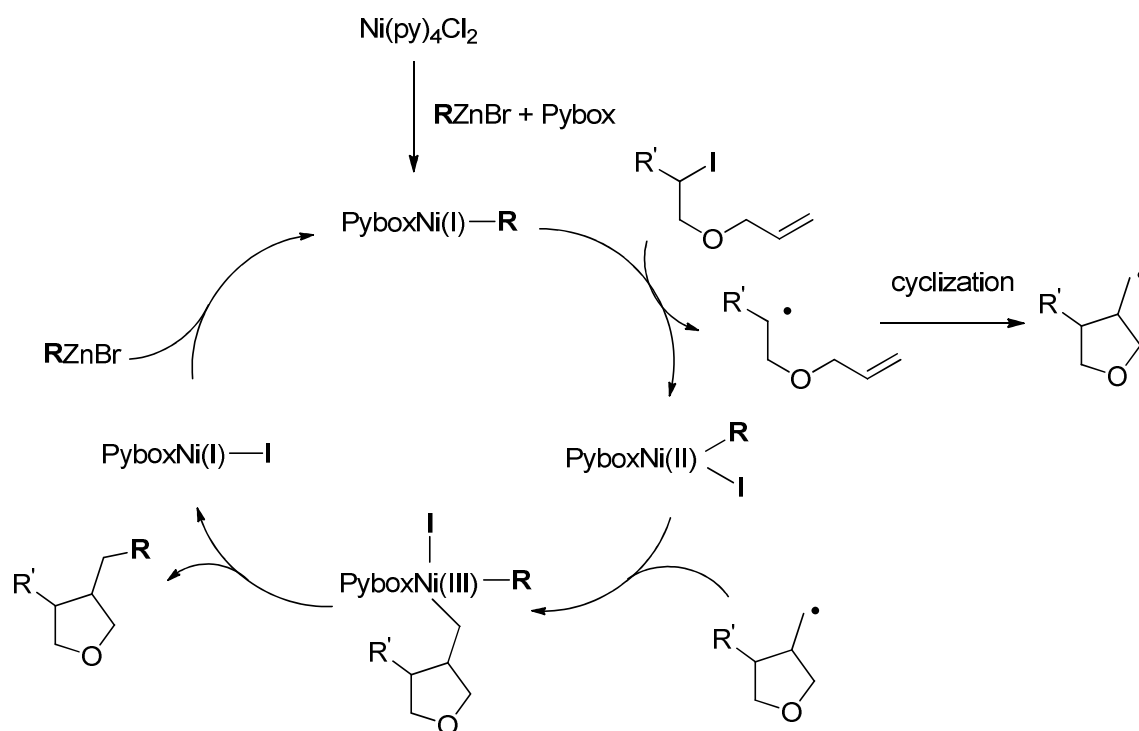
Scheme 10. First asymmetric Negishi coupling of secondary α -bromo amides with organozinc reagents.

Vicic *et al.* carried out an extensive study to probe the mechanism of Ni-catalyzed alkyl-alkyl cross-couplings (Scheme 11).⁶¹ The $[\text{Ni}(\text{terpy})(\text{CH}_3)]$ (terpy = terpyridine) complex was the first successfully isolated and structurally characterized catalyst. It was proposed that the $[\text{Ni}(\text{terpy})(\text{Alkyl}^2)]$ compound could activate alkyl halide to form $[\text{Ni}(\text{terpy})(\text{Alkyl}^2)]\text{X}$ and release an alkyl radical via single-electron-transfer. Then, recombination of the carbon radical with Ni gives $[\text{Ni}(\text{terpy})(\text{alkyl}^1)(\text{alkyl}^2)]$. Reductive elimination provides the coupling product and $[\text{Ni}(\text{terpy})\text{X}]$. Transmetalation of $[\text{Ni}(\text{terpy})\text{X}]$ within the alkyl nucleophile could regenerate Ni-alkyl species.



Scheme 11. Proposed catalytic cycle for alkyl-alkyl coupling by Ni-terpy complex.

Cárdenas *et al.* utilized the proposed intermediacy of alkyl radicals in the Ni/Pybox system,⁶² synthesizing the substituted cyclic ethers via cascade formation of C sp³-sp³ bonds. Alkyl iodides containing an alkene group first underwent intra-molecular ring-closing reactions before being coupled to alkylzinc halides (Scheme 12).

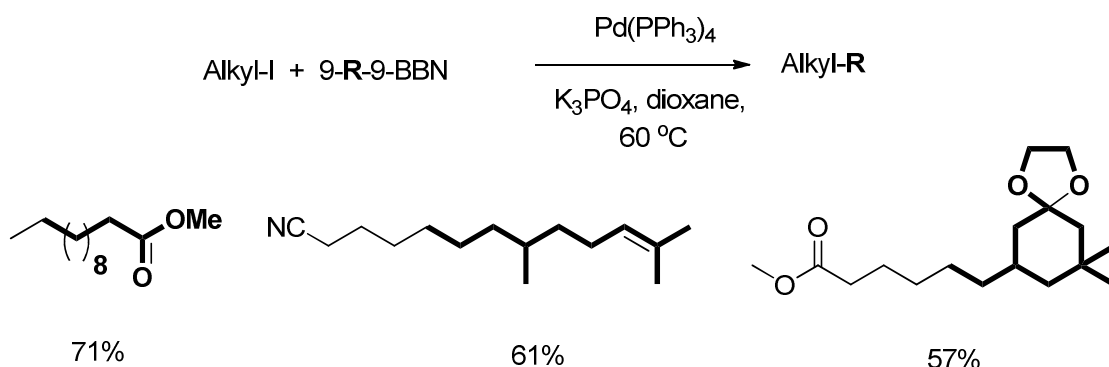


Scheme 12. Possible mechanistic pathways for the nickel-catalyzed cyclization/coupling reaction.

1.4 Alkyl-alkyl Suzuki-Miyaura coupling reactions

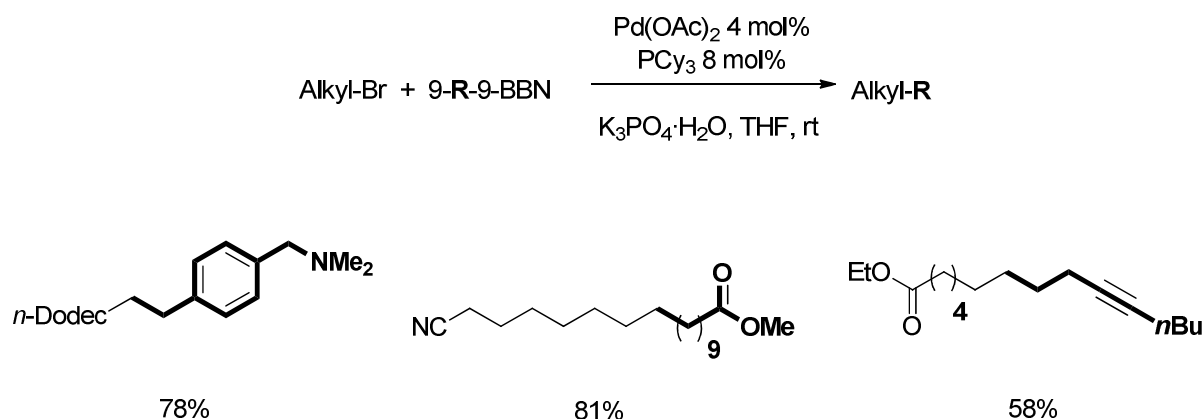
The Suzuki-Miyaura reaction couples organo (aryl- or vinyl-) boronic acids/esters with organo halides (aryl, vinyl or alkyl). It is one of the most versatile and widely used cross-coupling reactions because of the commercial availability and low toxicity of the starting materials, easy handling (relative air- and water-stable), and high functional-group tolerance.⁶³⁻⁶⁷ More importantly, the corresponding products could be obtained in good to excellent yields in a region- and stereospecific manner and nearly without steric hindrance problems.^{68,69} Originally, Pd acted as an efficient catalyst and dominated in this field for a long time.^{70,71} Recently, Fu *et al.* have extended this field by showing alkyl bromides and chlorides can be used as substrates using Ni catalysts.⁷² Significant contributions of alkyl-alkyl cross-coupling reactions are introduced in this section.

Suzuki *et al.* developed the first Pd-catalyzed Suzuki-type alkyl-alkyl cross-coupling reactions in 1992.⁷³ In the presence of Pd(PPh₃)₄ and K₃PO₄, alkyl iodide can react with 9-alkyl-9-BBN smoothly and provide moderate to good cross-coupling yields (Scheme 13). Functional 9-alkyl-9-BBN, aryl-BBN, and alkenyl BBN can be used as substrates, while alkyl bromides or secondary alkyl halides cannot be applied. The reaction was also identified as a radical process.



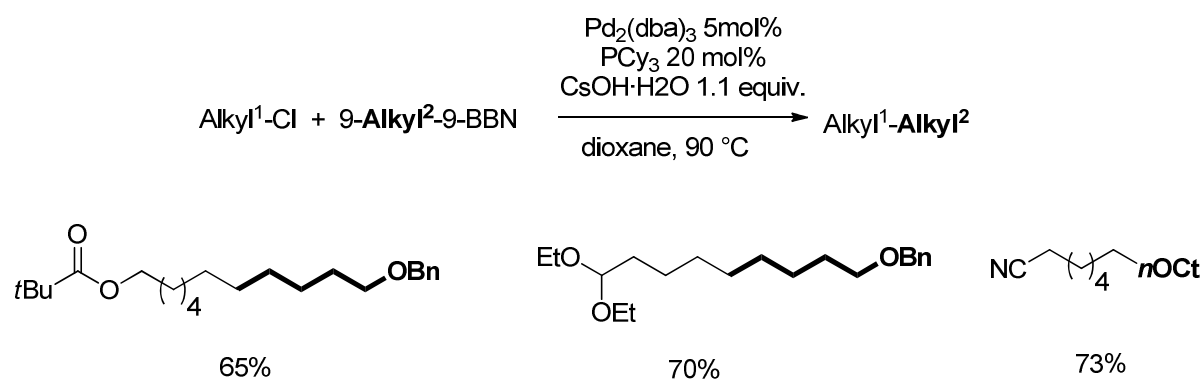
Scheme 13. The first Pd-catalyzed Suzuki-type alkyl-alkyl cross-coupling reactions.

Fu *et al.* established the first efficient Suzuki reactions of alkyl bromides that possess β -hydrogens.⁷⁴ This work represents a significant expansion in the scope of the Suzuki reaction. Under the system of $\text{Pd}(\text{OAc})_2/\text{PCy}_3$ (1:2) in the presence of $\text{K}_3\text{PO}_4 \cdot 3\text{H}_2\text{O}$, the non-activated alkyl halides (I or Br) coupled with B-alkyl-9-BBN at room temperature and gave good to excellent yields (Scheme 14). Additionally, Organ *et al.* first introduced the *N*-heterocyclic carbenes in Pd-catalyzed alkyl-alkyl Suzuki-Miyaura coupling reactions. Alkyl bromides can react with B-alkyl-9-BBN and provide modest yields.⁷⁵ Later, by using a modified carbene ligand, the system was improved and high yields can be obtained.^{76,77}



Scheme 14. Pd-catalyzed Suzuki-type alkyl-alkyl cross-coupling reactions with alkyl bromides.

Later, Fu *et al.* reported that with $\text{Pd}_2(\text{dba})_3$ and PCy_3 in the presence of $\text{CsOH} \cdot 3\text{H}_2\text{O}$, the more challenging alkyl chlorides could also be coupled with 9-alkyl-9-BBN at high temperature (90°C) in dioxane (Scheme 15).⁷⁸ The process is compatible with a variety of functional groups, including silyl ether, acetal, amine, nitriles and ester.

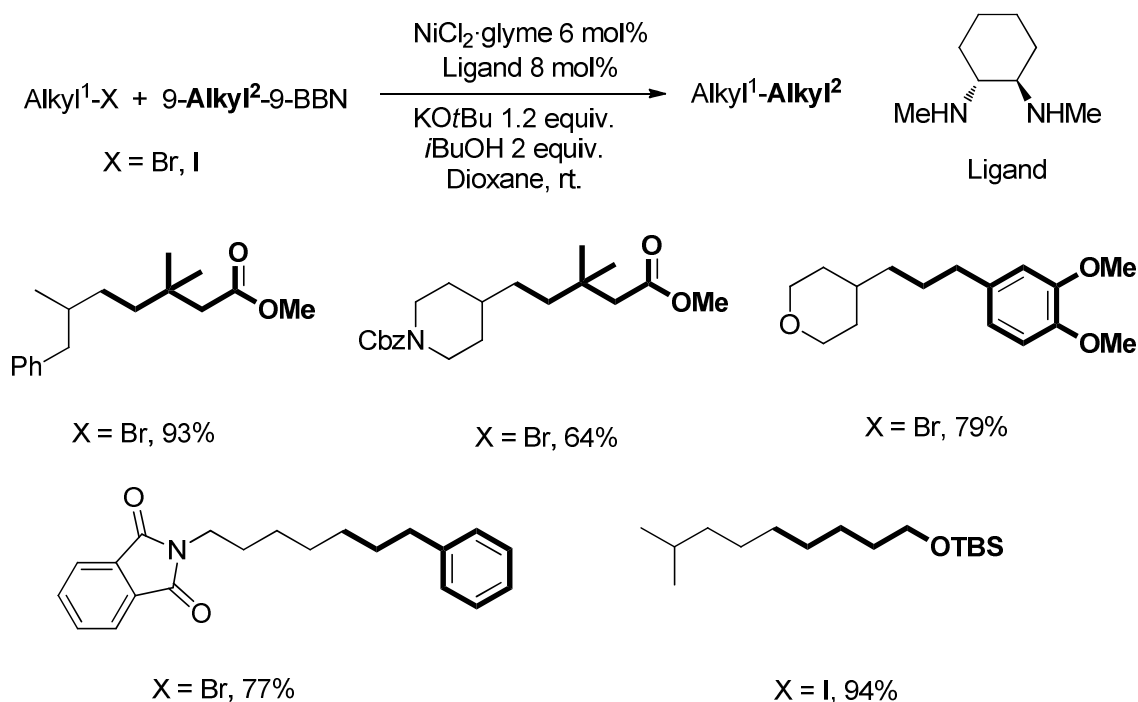


Scheme 15. Pd-catalyzed Suzuki-type alkyl-alkyl cross-coupling reactions with alkyl chlorides.

Subsequently, the same group tried to establish a method for the coupling of alkyl tosylates.⁷⁹ After a series of modification, they found that with $\text{P}^t\text{Bu}_2\text{Me}$, rather than PCy_3 , the coupling of B-alkyl-9-BBN with alkyl tosylates could be realized. A combination of $\text{Pd}(\text{OAc})_2$ and $\text{P}^t\text{Bu}_2\text{Me}$ in the presence of NaOH in dioxane at $50\text{ }^\circ\text{C}$ was the conditions employed. During the study, they found that the reaction was exceptionally sensitive toward the cone angle of the ligands employed. A bench-stable trialkyl phosphonium salt, $[\text{HP}^t\text{Bu}_2\text{Me}]\text{BF}_4$, was a good precursor to the phosphine ligand. The Capretta group also developed a series of phosphadamantane ligands. Combining these ligands with $\text{Pd}(\text{OAc})_2$, the resulting complexes were shown to work very well in Suzuki-type alkyl-alkyl cross-couplings.⁸⁰

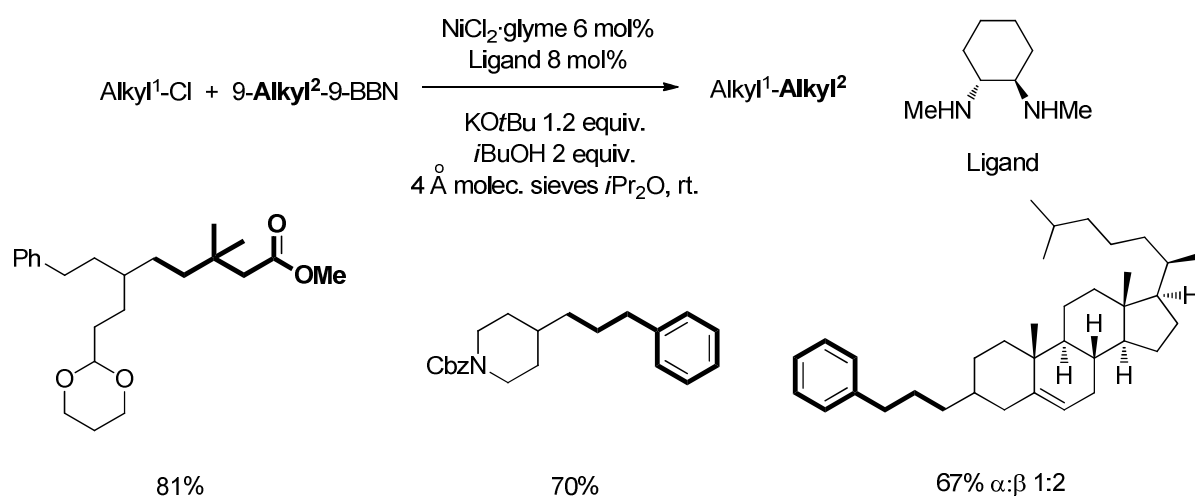
B-alkyl-9-BBN are useful substrates in Suzuki coupling reactions, yet we cannot ignore their drawbacks: they are not readily handled in air nor commercially available, and are less atom-economic. Boronic acids are desirable alternatives to be utilized in Suzuki coupling. Fu *et al.* explored a series of parameters, and discovered several efficient catalytic systems. They reported the first palladium-catalyzed protocols for the coupling of boronic acids and unactivated alkyl electrophiles (bromides) that bear $\beta\text{-H}$ functionality.⁸¹

In 2007, Fu *et al.* described the first method for achieving alkyl-alkyl Suzuki coupling of unactivated secondary alkyl halides with alkylboranes using a Ni/amine system (Scheme 16).⁸² The simple, readily available diamine ligands were the most effective. KO^tBu and $^i\text{BuOH}$ were also necessary. They proposed that the role of these basic species is to activate the alkylborane for transmetalation with nickel.



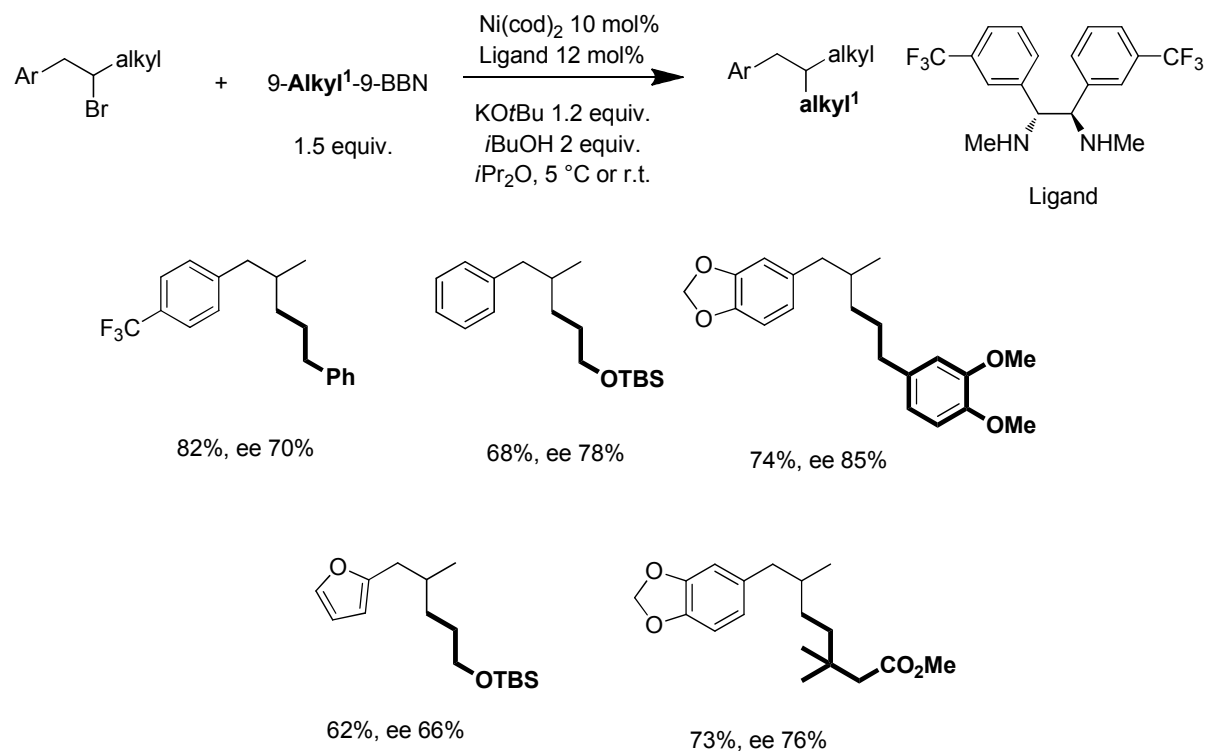
Scheme 16. Ni-catalyzed Suzuki-type alkyl-alkyl cross-coupling reactions of alkyl bromides and iodides.

In 2010, Fu *et al.* reported the first Ni-catalyzed alkyl-alkyl Suzuki reaction of unactivated secondary alkyl chlorides under a similar system (NiCl₂•glyme/dioxane to NiBr₂•glyme/ⁱPr₂O) (Scheme 17).⁸³ This protocol was very efficient in the coupling of functionalized alkyl electrophiles under mild conditions. More important, this catalytic system not only break the barrier associated with unreactive alkyl chlorides, but also could be applied to Suzuki coupling of secondary and primary alkyl bromides and iodides.



Scheme 17. Ni-catalyzed Suzuki-type cross-coupling reactions of secondary alkyl chlorides.

By using $\text{Ni}(\text{cod})_2$ /chiral diamine as catalyst, the system can be also applied to asymmetric cross-couplings of non-activated alkyl electrophiles. This was the first example of enantioselective Suzuki couplings of alkyl electrophiles (Scheme 18).⁸⁴



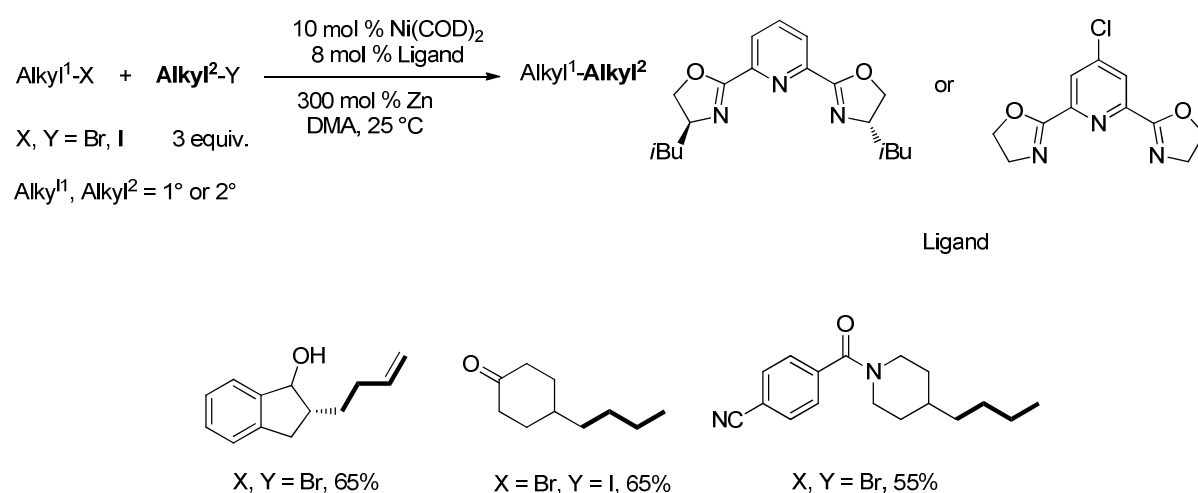
Scheme 18. Nickel-catalyzed Suzuki-type asymmetric cross-couplings of unactivated alkyl electrophiles.

1.5 Reductive alkyl-alkyl coupling reactions

Great progress has been achieved for the alkyl-alkyl cross-coupling reactions. An organometallic reagent is required in these reactions. In recent years, catalytic reductive coupling reactions of two electrophiles have become interesting. There has been some progress in reductive C-C aryl-alkyl cross-coupling,⁸⁵⁻⁸⁷ allyl-alkyl cross-coupling,^{88,89} and aryl acid chloride-alkyl cross-couplings reactions.⁹⁰

There are several advantages of this type method. First of all, the coupling partners can be used directly without preparing organometallic reagents, which means that there is less waste generated. Secondly, the procedure is easier to carry out compared to traditional methods using organometallic reagents. Unlike Grignard or organozinc reagents, the substrates are generally not air/moisture sensitive. They can be handled in ambient atmosphere. Solvents need not be rigorously dried. Special equipment and protection are not required. Third, direct reductive coupling might show a high degree of functional group tolerance. Functional

groups such as alcohol, carboxylic acid, N-Boc, or heteroaromatics are well tolerated. Thus, such coupling reactions may have potential application in organic synthesis. Gong *et al.* established the first effective cross-coupling of two alkyl halides via a Ni-catalyzed reductive process (Scheme 19).⁹¹ Pybox ligands are found to be necessary to suppress the homocoupling reactions. This protocol avoids the use of organometallic reagents, and exhibits a high functional group tolerance, including nitrogen heterocycles, keto, or even alcohol groups. They concluded that a non-Negishi process may be operative. The main problems of this method are the relative low coupling yields and the use of excess of one coupling partner (3 equiv.), which will limit its application in large scale production.



Scheme 19. Nickel-catalyzed reductive cross-couplings of non-activated alkyl halides using Pybox ligands.

1.6 Summary and Outlook

Transition-metal-catalyzed alkyl-alkyl cross coupling has been rapidly developed over the last years. High efficiency and good functional group tolerance have been demonstrated. However, there are still challenges remained in the field. The well-defined (pre)catalysts for cross coupling reactions are less developed. Moreover, the creation of tertiary and quaternary carbon centers is still a great challenge, as there are few reports for the coupling of secondary or even tertiary organometallic reagents with primary or secondary alkyl halides. Furthermore, the mechanism of the coupling reactions is still not clear, especially for first-row transition-metal-catalyzed processes.

1.7 References

- (1) de Meijere, A.; Diederich, F., Eds. *Metal-Catalyzed Cross-Coupling Reactions*, 2nd Completely Revised and Enlarged ed.; Wiley-VCH: Weinheim, Germany, **2004**.
- (2) Bolm, C. *J. Org. Chem.* **2012**, 77, 5221-5223.
- (3) Hartwig, J. *Organotransition metal chemistry : from bonding to catalysis*; University of Science Books, **2010**.
- (4) Tamao, K.; Sumitani, K.; Kumada, M. *J. Am. Chem. Soc.* **1972**, 94, 4374-4376.
- (5) Knochel, P.; Leuser, H.; Gong, L.-Z.; Perrone, S.; Kneisel, F. F. Polyfunctional zinc organometallics for organic synthesis. In *Handbook of Functionalized Organometallics: Applications in Synthesis*; Knochel, P., Ed.; Wiley-VCH: Weinheim, Germany, **2005**; Vol.1.
- (6) Tsuji, J. *Palladium in Organic Synthesis*; Topics in Organometallic Chemistry, Vol. 14; Springer: Berlin, **2005**.
- (7) Cahiez, G.; Moyeux, A. *Chem. Rev.* **2010**, 110, 1435-1462.
- (8) Franci , G.; Leitner, W. Organic synthesis with transition metal complexes using compressed carbon dioxide as reaction medium. *Transition Metals for Organic Synthesis: Building Blocks and Fine Chemicals*; Wiley: New York, **2004**; Vol. 2.
- (9) Spivey, A. C.; Gripton, C. J. G.; Hannah, J. P. *Curr. Org. Synth.* **2004**, 1, 211.
- (10) Negishi, E. *Angew. Chem., Int. Ed.* **2011**, 50, 6738-6764.
- (11) Suzuki, A. *Angew. Chem., Int. Ed.* **2011**, 50, 6722-6737.
- (12) Luh, T. Y.; Leung, M. K.; Wong, K. T. *Chem. Rev.* **2000**, 100, 3187-3204.
- (13) C rdenas, D. J. *Angew. Chem., Int. Ed.* **1999**, 38, 3018-3020.
- (14) Netherton, M. R.; Fu, G. C. *Adv. Synth & Catal.* **2004**, 346, 1525-1532.
- (15) Frisch, A. C.; Beller, M. *Angew. Chem., Int. Ed.* **2005**, 44, 674-688.
- (16) Rudolph, A.; Lautens, M. *Angew. Chem., Int. Ed.* **2009**, 48, 2656-2670.
- (17) Hu, X. *Chem. Sci.* **2011**, 2, 1867-1886.
- (18) Yuan, K.; Scott, W. J. *Tetrahedron Lett.* **1989**, 30, 4779-4782.
- (19) Yuan, K.; Scott, W. J. *J. Org. Chem.* **1990**, 55, 6188-6194.
- (20) Brown, J. M.; Cooley, N. A. *Chem. Rev.* **1998**, 88, 1031-1046.
- (21) Seyferth, D. *Organometallics*, **2009**, 28, 1598-1605.
- (22) Liu, N.; Wang, Z. X. *J. Org. Chem.* **2011**, 76, 10031-10038.
- (23) Joshi-Pangu, A.; Wang, C. Y.; Biscoe, M. R. *J. Am. Chem. Soc.* **2011**, 133, 8478-8481.
- (24) Ackermann, L.; Kapdi, A. R.; Schulzke, C. *Org. Lett.* **2010**, 12, 2298-2301.

-
- (25) Guan, B. T.; Lu, X. Y.; Zheng, Y.; Yu, D. G.; Wu, T.; Li, K. N.; Li, B. J.; Shi, Z. J. *Org. Lett.* **2010**, *12*, 396-399.
- (26) López-Pérez, A.; Adrio, J.; Carretero, J. C. *Org. Lett.* **2009**, *11*, 5514-5517.
- (27) Furstner, A.; Leitner, A. *Angew. Chem. Int. Ed.*, **2002**, *41*, 609-612.
- (28) Corriu, R. J. P.; Masse, J. P. *J. Chem. Soc., Chem. Commun.* **1972**, 144-144.
- (29) *Chemistry of Triple-Bonded Functional Groups* (Eds.: S. Patai), Wiley, New York, **1994**.
- (30) Chen, T.; Yang, L.; Li, L.; Huang, K. W. *Tetrahedron*, **2012**, *68*, 6152-6157.
- (31) Knochel, P. In *Grignard Reagents. New Developments*; Richey, H. G., Jr., Ed.; Wiley: Chichester, U.K., **2000**; Vol. 39.
- (32) Shinokubo, H.; Oshima, K.; *Eur. J. Org. Chem.* **2004**, 2081-2091.
- (33) Castle, P. L.; Widdowson, D. A. *Tetrahedron Lett.* **1986**, *27*, 6013-6016.
- (34) Terao, J.; Watanabe, H.; Ikumi, A.; Kuniyasu, H.; Kambe, N. *J. Am. Chem. Soc.* **2002**, *124*, 4222-4223.
- (35) Vechorkin, O.; Hu, X. L. *Angew. Chem. Int. Ed.* **2009**, *48*, 2937-2940.
- (36) Dongol, K. G.; Koh, H.; Sau, M.; Chai, C. L. L. *Adv. Synth. Catal.* **2007**, *349*, 1015-1018.
- (37) Tamura, M.; Kochi, J. K. *J. Organomet. Chem.* **1972**, *42*, 205-228.
- (38) Terao, J.; Ikumi, A.; Kuniyasu, H.; Kambe, N. *J. Am. Chem. Soc.* **2003**, *125*, 5646-5647.
- (39) Begum, S. A.; Terao, J.; Kambe, N. *Chem. Lett.* **2007**, *36*, 196-197.
- (40) Terao, J.; Todo, H.; Begum, S. A.; Kuniyasu, H.; Kambe, N. *Angew. Chem. Int. Ed.* **2007**, *46*, 2086-2089.
- (41) King, A. O.; Okukado, N.; Negishi, E. I. *J. Chem. Soc., Chem. Commun.* **1977**, 683-684.
- (42) Xi, Z.; Zhou, Y.; Chen, W. *J. Org. Chem.* **2008**, *73*, 8497-8501.
- (43) Milne, J. E.; Buchwald, S. L. *J. Am. Chem. Soc.* **2004**, *126*, 13028-13032.
- (44) Hadei, N.; Kantchev, E. A. B.; O'Brien, C. J.; Organ, M. G. *Org. Lett.* **2005**, *7*, 3805-3807.
- (45) Hatakeyama, T.; Nakagawa,.; Nakamura, M. *Org. Lett.* **2009**, *11*, 4496-4499.
- (46) Bedford, R. B.; Huwe, M.; Wilkinson, M. C. *Chem. Commun.* **2009**, 600-602.
- (47) Liu, J.; Deng, Y.; Wang, H.; Zhang, H.; Yu, G.; Wu, B.; Zhang, H.; Li, Q.; Marder, T. B.; Yang, Z.; Lei, A. *Org. Lett.* **2008**, *10*, 2661-2664.
- (48) Wunderlich, S.; Knochel, P. *Org. Lett.* **2008**, *10*, 4705-4707.
- (49) Krasovskiy, A.; Lipshutz, B. H. *Org. Lett.* **2011**, *13*, 3822-3825.

-
- (50) Tucker, C. E.; Knochel, P. *J. Org. Chem.* **1993**, *58*, 4781 – 4782.
- (51) Devasagayarak, A.; Stüdemann, T.; Knochel, P. *Angew. Chem., Int. Ed.* **1995**, *34*, 2723-2725.
- (52) Giovannini, R.; Stüdemann, T.; Devasagayarak, A.; Dussin, G.; Knochel, P. *J. Org. Chem.* **1999**, *64*, 3544-3553.
- (53) Giovannini, R.; Stüdemann, T.; Dussin, G.; Knochel, P. *Angew. Chem. Int. Ed.* **1998**, *37*, 2387-2390.
- (54) Piber, M.; Jensen, A. E.; Rottländer, M.; Knochel, P. *Org. Lett.* **1999**, *1*, 1323-1326.
- (55) Jensen, A. E.; Knochel, P. *J. Org. Chem.* **2002**, *67*, 79-85.
- (56) Zhou, J. R.; Fu, G. C. *J. Am. Chem. Soc.* **2003**, *125*, 12527-12530.
- (57) Hadei, N.; Kantchev, E. A. B.; O'Brien, C. J.; Organ, M. G. *Org. Lett.* **2005**, *7*, 3805-3807.
- (58) Hadei, N.; Kantchev, E. A. B.; O'Brien, C. J.; Organ, M. G. *J. Org. Chem.* **2005**, *70*, 8503-8507.
- (59) Zhou, J. R.; Fu, G. C. *J. Am. Chem. Soc.* **2003**, *125*, 17426-17427.
- (60) Fischer, C.; Fu, G. C. *J. Am. Chem. Soc.* **2005**, *127*, 4594-4595.
- (61) Jones, G. D.; Martin, J. L.; McFarland, C.; Allen, O. R.; Hall, R. E.; Haley, A. D.; Brandon, R. J.; Konovalova, T.; Desrochers, P. J.; Pulay, P.; Vicic, D. A. *J. Am. Chem. Soc.* **2006**, *128*, 13175-13183.
- (62) Phapale, V. B.; Bueuel, E.; Garcea-Iglesias, M.; Cardenas, D. J. *Angew. Chem. Int. Ed.* **2007**, *46*, 8790-8795.
- (63) Mora, M.; Jiménez-Sanchidrián, C.; Ruiz, J. R. *Curr. Org. Chem.* **2012**, *16*, 1128-1150.
- (64) Blakey, S. B.; MacMillan, D. W. C. *J. Am. Chem. Soc.* **2003**, *125*, 6046-6047.
- (65) Littke, A. F.; Fu, G. C. *Angew. Chem. Int. Ed.* **1999**, *37*, 3387-3388.
- (66) Wolfe, J. P.; Singer, R. A.; Yang, B. H.; Buchwald, S. L. *J. Am. Chem. Soc.* **1999**, *121*, 9550-9561;
- (67) Molander, G. A.; Biolatto, B. *J. Org. Chem.* **2003**, *68*, 4302-4314.
- (68) Altenhoff, G.; Goddard, R.; Lehmann, C. W.; Glorius, F. *Angew. Chem. Int. Ed.*, **2003**, *42*, 3690-3693.
- (69) Yin, J.; Rainka, M. P.; Zhang, X. X.; Buchwald, S. L. *J. Am. Chem. Soc.* **2002**, *124*, 1162-1163.
- (70) Oh, C. H.; Jung, H. H.; Kim, K. S.; Kim, N. *Angew. Chem. Int. Ed.* **2003**, *42*, 805-808.
- (71) Goossen, L. J.; Koley, D.; Hermann, H. L.; Thiel, W. *J. Am. Chem. Soc.* **2005**, *127*, 11102-11114.

- (72) Jana, R.; Pathak, T. P.; Sigman, M. S. *Chem. Rev.* **2011**, *111*, 1417-1492.
- (73) Ishiyama, T.; Abe, S.; Miyaura, N.; Suzuki, A. *Chem. Lett.* **1992**, 691-694.
- (74) Netherton, M. R.; Dai, C.; Neuschuetz, K.; Fu, G. C. *J. Am. Chem. Soc.* **2001**, *123*, 10099-10100.
- (75) Arentsen, K.; Caddick, S.; Cloke, F. G. N.; Herring, A. P.; Hitchcock, P. B. *Tetrahedron Letters* **2004**, *45*, 3511-3515.
- (76) Valente, C.; Baglione, S.; Candito, D.; O'Brien, C. J.; Organ, M. G. *Chem. Comm.* **2008**, 735-737;
- (77) Achonduh, G. T.; Hadei, N.; Valente, C.; Avola, S.; O'Brien, C. J.; Organ, M. G. *Chem. Comm.* **2010**, *46*, 4109-4111.
- (78) Kirchhoff, J. H.; Dai, C.; Fu, G. C. *Angew. Chem. Int. Ed.* **2002**, *41*, 1945-1947.
- (79) Netherton, M. R.; Fu, G. C. *Angew. Chem. Int. Ed.* **2002**, *41*, 3910-3912.
- (80) Brenstrum, T.; Gerristma, D. A.; Adjabeng, G. M.; Frampton, C. S.; Britten, J.; Robertson, A. J.; McNulty, J.; Capretta, A. *J. Org. Chem.* **2004**, *69*, 7635-7639.
- (81) Kirchhoff, J. H.; Netherton, M. R.; Hills, I. D.; Fu, G. C. *J. Am. Chem. Soc.* **2002**, *124*, 13662-13663.
- (82) Saito, B.; Fu, G. C. *J. Am. Chem. Soc.* **2007**, *129*, 9602-9603.
- (83) Lu, Z.; Fu, G. C. *Angew. Chem. Int. Ed.* **2010**, *49*, 6676-6678.
- (84) Arp, F. O.; Fu, G. C. *J. Am. Chem. Soc.* **2005**, *127*, 10482-10483.
- (85) Amatore, M.; Gosmini, C. *Chem. Eur. J.* **2010**, *16*, 5848-5852.
- (86) Everson, D. A.; Shrestha, R.; Weix, D. J. *J. Am. Chem. Soc.* **2010**, *132*, 920-921.
- (87) Everson, D. A.; Jones, B. A.; Weix, D. J. *J. Am. Chem. Soc.* **2012**, *134*, 6146-6159.
- (88) Qian, X.; Auffrant, A.; Felouat, A.; Gosmini, C. *Angew. Chem. Int. Ed.* **2011**, *50*, 10402-10405.
- (89) Dai, Y.; Wu, F.; Zang, Z.; You, H.; Gong, H. *Chem. Eur. J.* **2012**, *18*, 808-812.
- (90) Wu, F.; Lu, W.; Qian, Q.; Ren, Q.; Gong, H. *Org. Lett.* **2012**, *14*, 3044-3047.
- (91) Yu, X.; Yang, T.; Wang, S.; Xu, H.; Gong, H. *Org. Lett.* **2011**, *13*, 2138-2141.

Chapter 2

A Structure-Activity Study of Nickel-Catalyzed Alkyl-Alkyl Kumada Coupling. Improved Catalysts for Coupling of Secondary Alkyl Halides.*

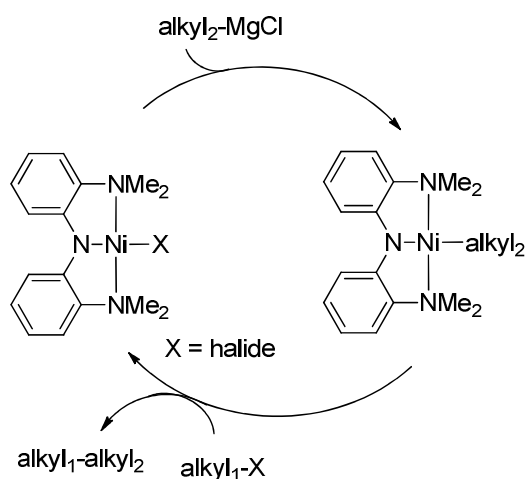
*Parts of the work presented in this chapter was published in:

Ren, P.; Vechorkin, O.; von Allmen, K.; Scopelliti, R.; Hu, X. L. *J. Am. Chem. Soc.* **2011**, *133*, 7084-7095.

2.1 Introduction

C-C cross coupling of non-activated alkyl halides and pseudo halides is one of the most actively pursued reactions in homogeneous catalysis.¹⁻⁶ The coupling of secondary alkyl halides is particularly interesting because it creates a tertiary carbon center that might be otherwise difficult to access.³ An asymmetric process would produce a stereogenic carbon center. Pioneering and remarkable work of Fu *et al.* demonstrated that this type of asymmetric catalysis could indeed be achieved starting from racemic activated and non-activated alkyl halides.⁷⁻¹³ However, non-activated secondary alkyl halides are very difficult to couple because of the increased steric hindrance of the substrates and the tendency of secondary alkyl halides to undergo base-mediated HX elimination (X = halide).³ Consequently, there are only a handful of catalysts known for alkyl-alkyl coupling of non-activated secondary alkyl electrophiles.^{7,8,14-21} And to the best of our knowledge, there are only two pre-formed and defined catalysts, including the one developed by our group.^{18,20,21}

We have focused on the development of well-defined (pre)catalysts for cross-coupling reactions.²² Our group recently reported a Ni^{II} pincer complex, [(^{Me}N₂N)NiCl] (**1**),^{20,22} that was an efficient catalyst for Kumada-Corriu-Tamao (Kumada) coupling of non-activated alkyl halides with Grignard reagents.^{20,21,23} Mechanistic study suggested that the catalysis started with the transmetalation of the Ni halide complex with an alkyl Grignard reagent to form a Ni alkyl species, which reacted with the alkyl halide to form the coupling product and regenerated the catalyst (Scheme 1).^{20,24} The catalysis has a wide substrate scope and a high functional group tolerance.^{21,23} As Grignard reagents are relatively cheap, easy to synthesize or purchase, this Ni-catalyzed Kumada coupling method is attractive for the synthesis of highly functionalized organic molecules. The scope of the coupling method, especially for secondary alkyl halides, however, remained to be expanded.^{20,21,23} In this chapter, I described a structure-activity study of nickel-catalyzed alkyl-alkyl Kumada coupling employing a series of isolated nickel complexes. It was possible to study some main factors governing the efficiency of the catalysis. Furthermore, catalysts much more efficient than complex **1** had been developed for the coupling of secondary alkyl halides.



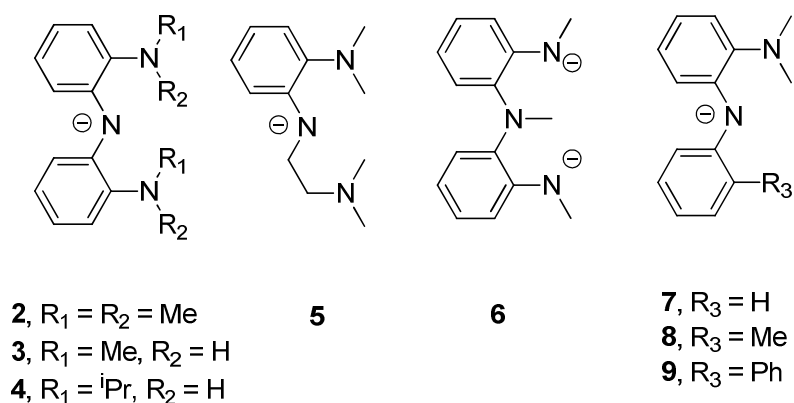
Scheme 1. The proposed catalytic cycle for alkyl-alkyl Kumada coupling by the pincer complex **1**.

2.2 Synthesis and structure of nickel catalysts

2.2.1 Ligand synthesis

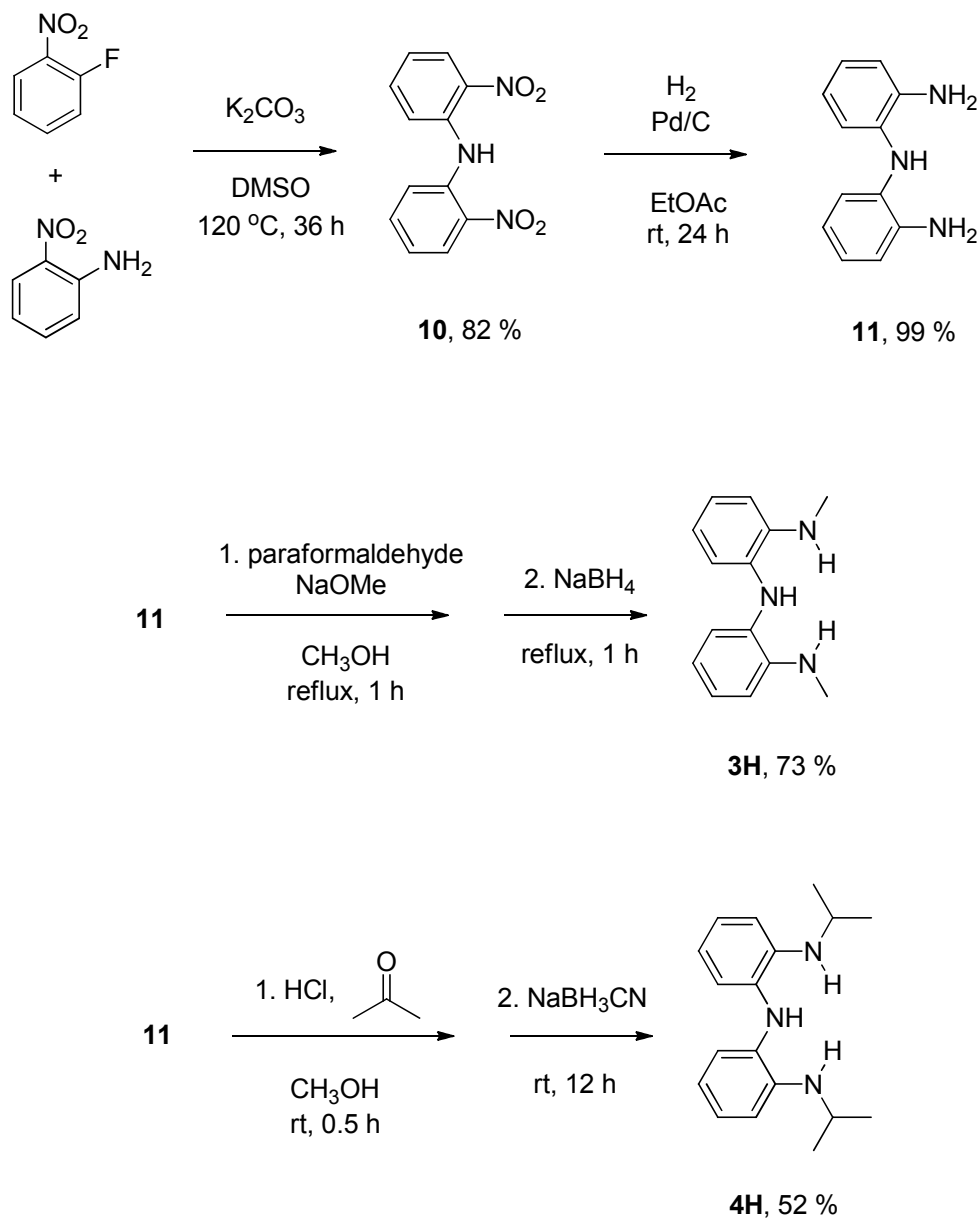
In addition to the pincer ligand $^{\text{Me}}\text{N}_2\text{N}$ (**2**),²² several new ligands (**3-9**) were employed in this study (Chart 1). An analogue of ligand **4** with electron-donating methoxy substituents was recently reported by Heyduk *et al.*²⁵

Chart 1.



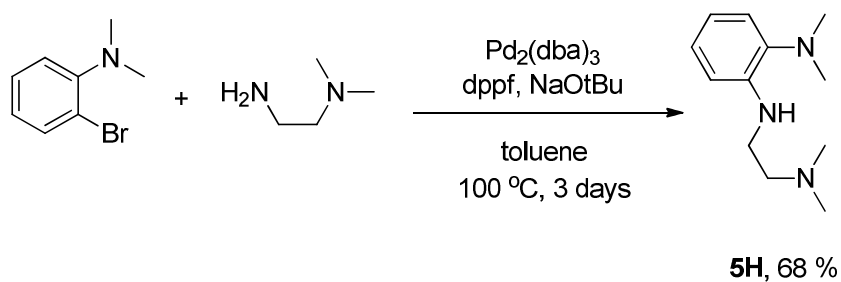
Protonated, neutral forms of these ligands were first prepared. Scheme 2 shows the synthesis of **3H** and **4H**. Coupling of 1-fluoro-2-nitrobenzene with 2-nitroaniline proceeded smoothly without a catalyst to give bis(2-nitrophenyl)amine (**10**) in a high yield. Reduction of **10** with H_2 using Pd/C catalyst gave bis(2-aminophenyl)amine (**11**) in a quantitative yield. Condensation of **9** with paraformaldehyde in the presence of a base, and subsequent reduction with NaBH_4 gave bis(2-methylaminophenyl)amine (**3H**) in a good yield. **11** was also reacted

with acetone in the presence of an acid, and then reduced with NaBH_3CN to give bis(2-isopropylaminophenyl)amine (**4H**) in a modest yield. The overall synthetic sequence is similar to those employed for the preparation of pincer and tripodal triamido ligands.^{25,26}

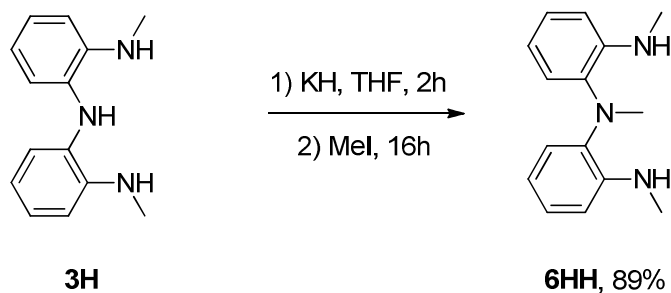


Scheme 2. Synthesis of pro-ligands **3H** and **4H**.

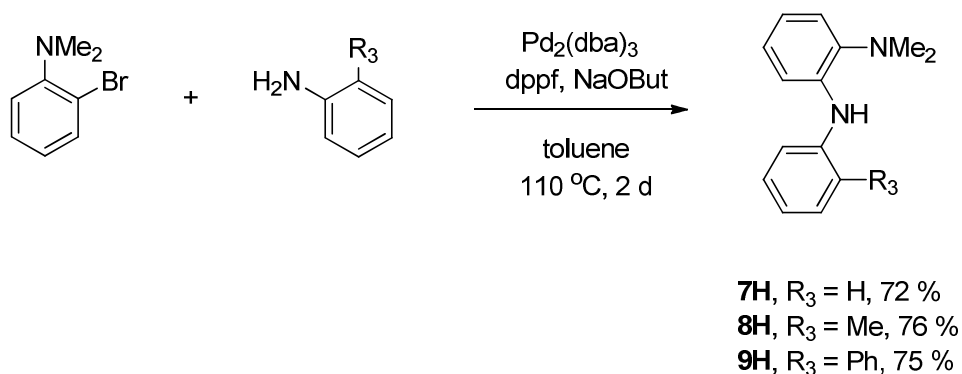
Schemes 3 and 5 show the synthesis of tridentate ligand **5H**, **7H**, **8H**, and **9H**. These compounds were prepared in high yields using Pd-catalyzed Buchwald-Hartwig C-N coupling method.^{27,28} Ligand **7H** was previously made by a different method.²⁹ The proton of diphenyl amino group is more acidic than that of methyl phenyl amino group, thus **6HH** could be prepared by selectively deprotonation of **3H** with potassium hydride, and then methylation (Scheme 4).



Scheme 3. Synthesis of pro-ligands **5H**.



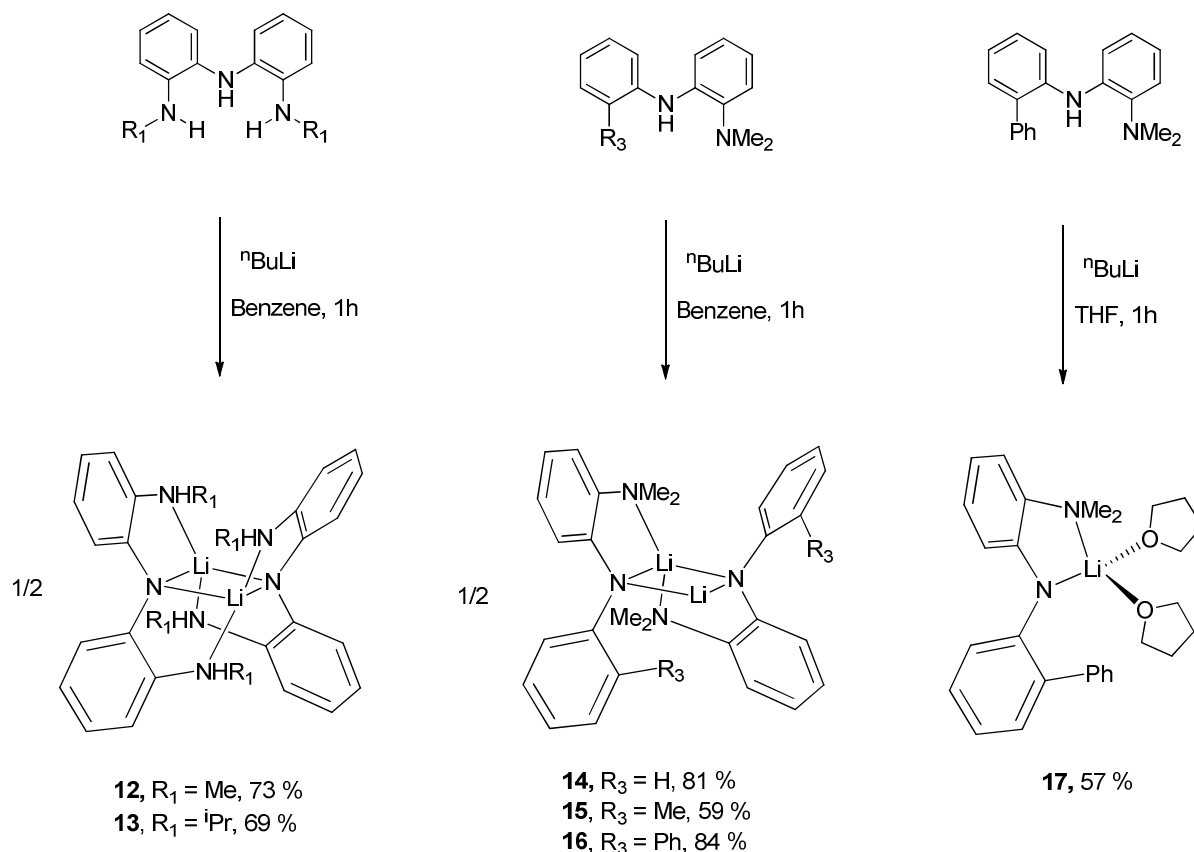
Scheme 4. Synthesis of pro-ligands **6HH**.



Scheme 5. Synthesis of pro-ligands **7H-9H**.

2.2.2 Metallation using organo lithium and magnesium reagents.

Our group showed earlier that Ni complex **1** could be synthesized by reaction of a Ni salt with the Li complex of ligand **2**.²² To access analogous Ni complexes with ligands **3-9**, the amine groups were deprotonated by ⁿBuLi to form the corresponding Li complexes.



Scheme 6. Lithiation of ligands **3**, **4**, **7-9**.

Lithiation occurred readily with $^n\text{BuLi}$ to give complexes **12-17** (Scheme 6). In a non-coordinating solvent such as benzene, the products should be dimeric $[\text{LLi}]_2$, similar to $[\text{Me}_2\text{N}_2\text{NLi}]_2$.²² For ligands **3** and **4**, only the proton on the bridging nitrogen atom was removed to form an anilido donor when one equivalent of $^n\text{BuLi}$ was used. The crystal structure of **13** was determined (Figure 1). The two Li ions have a similar coordination environment. The analogous complex **12** should have a similar structure. For ligand **8**, the resulting complex **15** also has a dimeric solid-state structure (Figure 2). The two Li ions are not equivalent. One Li center is coordinated to four nitrogen donors from two molecules of ligand **8**, in a distorted tetrahedral geometry. The other Li center is coordinated to two anilido donors, and has a weak interaction with a C-H bond of the ligand from another molecule. The Li-C and Li-H distances are 2.463 and 2.294 Å, respectively. This Li-CH interaction was responsible for the polymeric structure of complex **15** in the solid state. Due to the similarity of ligands **7-9**, complexes **14** and **16** may be expected to have structures similar to **15**.

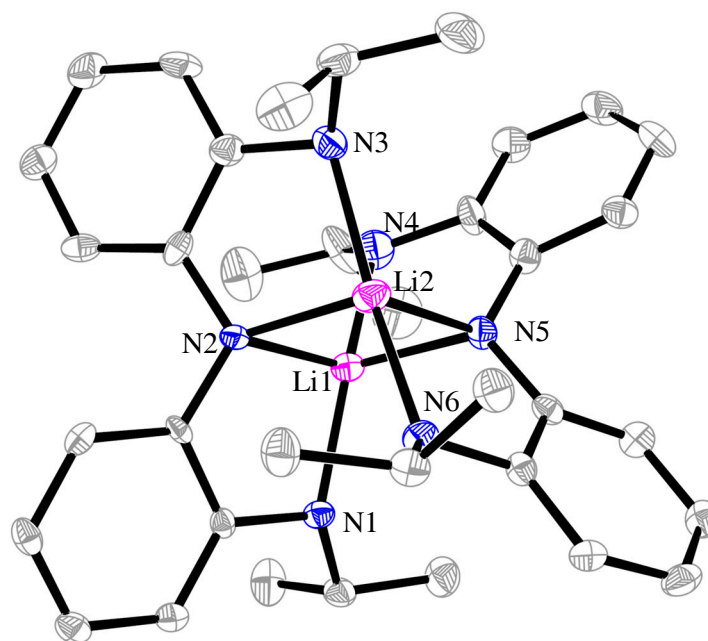


Figure 1. Crystal structure of complex **13**. The thermal ellipsoids are displayed in 50% probability. The following structures in this chapter are displayed at 50% probability which will not be illustrated any more. Selected bond lengths (Å): Li1-N1 2.049(9), Li1-N2 2.052(8), Li1-N4 2.042(9), Li1-N5 2.062(8), Li2-N2 2.039(9), Li2-N3 2.063(8), Li2-N5 2.022(8), Li2-N6 2.102(8).

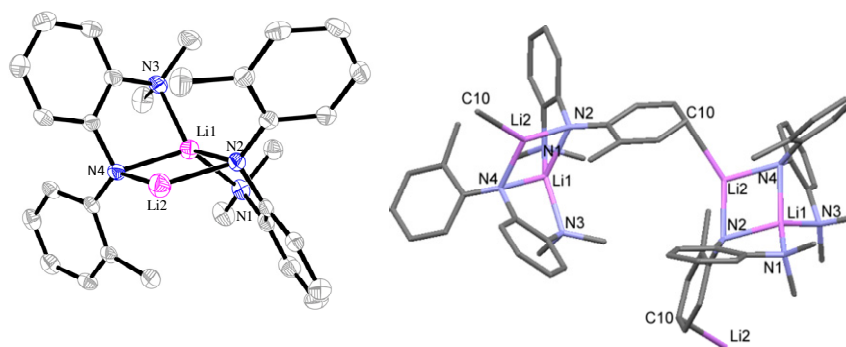


Figure 2. Left: Crystal structure of complex **15**. Selected bond lengths (Å): Li1-N1 2.051(4), Li1-N2 2.079(4), Li1-N3 2.045(4), Li1-N4 2.045(4), Li2-N2 2.034(4), Li2-N4 2.015(4), Li2-C10 2.464(4). Right: Line drawing presentations of the structures of complexes **15**. In the structure of **15**, a weak Li-CH interaction is shown as bond between Li2 and C10.

When ligand **9** was lithiated in THF, a monomeric complex **17** was formed. The structure of **17** shows that the Li ion is coordinated to one molecule of **9** and two molecules of THF, in a tetrahedral fashion (Figure 3). When the dimeric complex **16** was treated with THF, it was converted to **17**. Thus, the structures of these Li complexes depend on the solvents they were dissolved in. Donor solvents such as THF should favor monomeric forms.

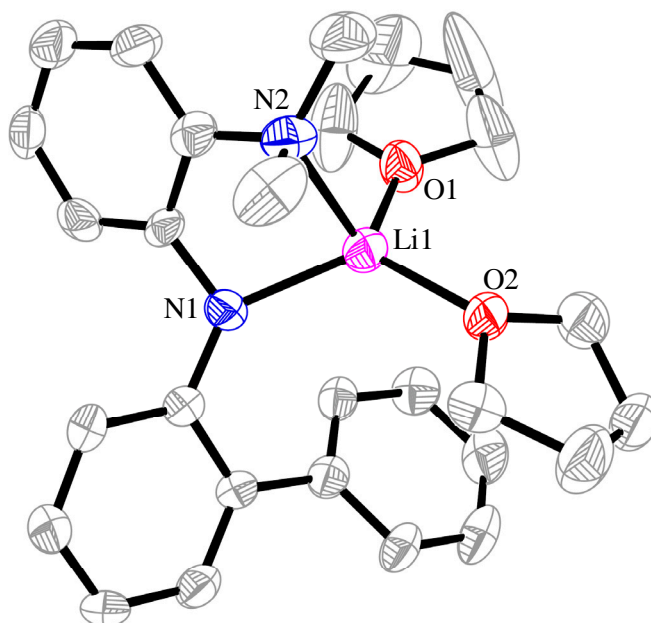
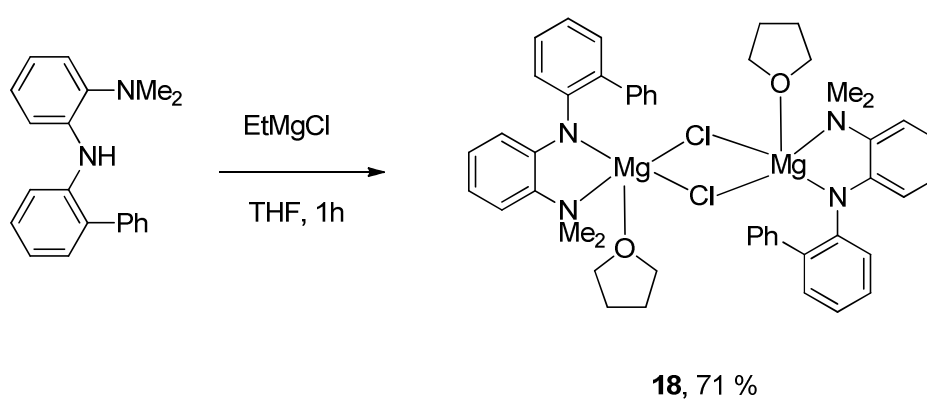


Figure 3. Crystal structure of complex **17**. Selected bond lengths (Å): Li1-N1 1.993(7), Li1-N2 2.179(8), Li1-O1 1.963(7), Li1-O2 1.924(7).

A magnesium complex was also synthesized as a potential transmetallation reagent. Reaction of **7** with EtMgCl in THF produced the dimeric compound **18** (Scheme 7). The structure of **18** was revealed by crystallography (Figure 4).



Scheme 7. Synthesis of Mg complex **18**.

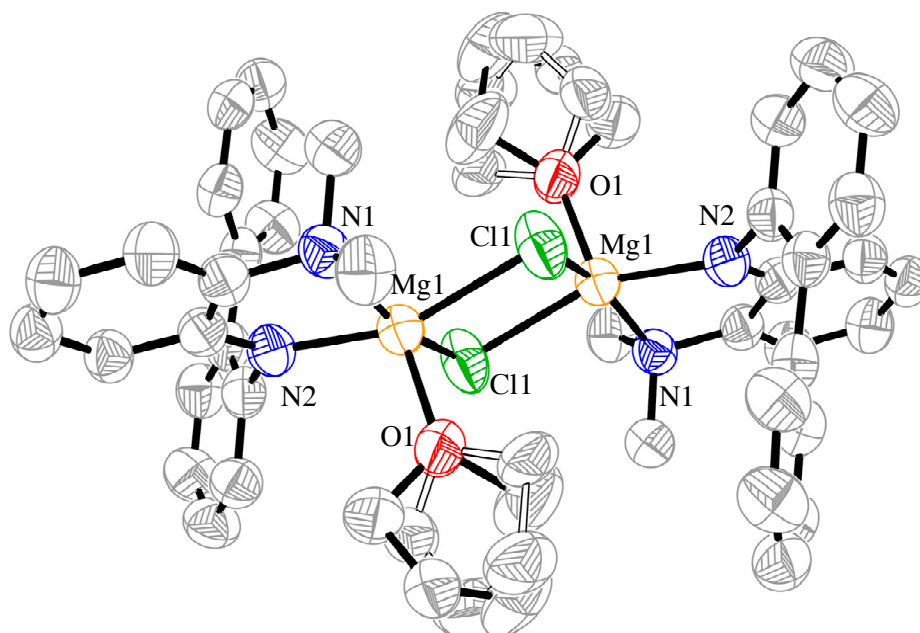
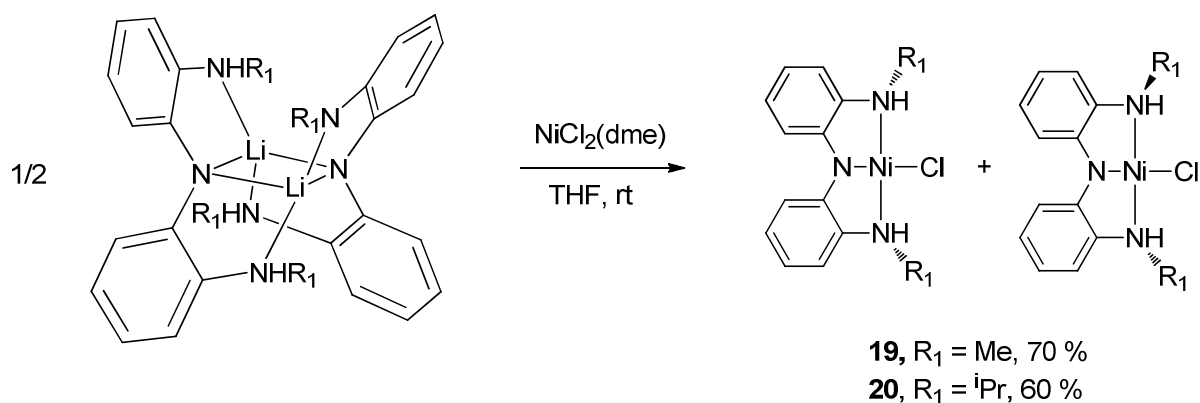


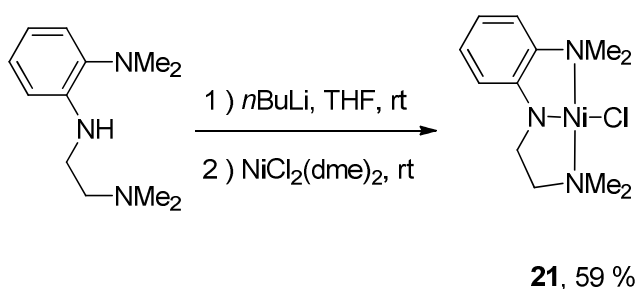
Figure 4. Crystal structure of complex **18**. Selected bond lengths (Å): Mg1-N1 2.231(3), Mg1-N2 2.036(3), Mg1-O1 2.029(3), Mg1-Cl1 2.4225(18).

2.2.3 Synthesis of nickel complexes of ligands 3-9

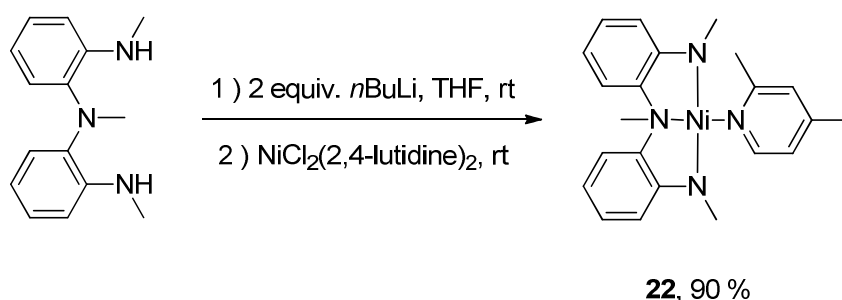
For tridentate ligands **3** and **4**, their Ni complexes could be easily prepared by reactions of the Li complexes with $\text{NiCl}_2(\text{dme})$ (dme = dimethoxyethane) in THF (Scheme 8). The resulting Ni complexes (**19** and **20**) are diamagnetic. Only the *rac*-isomer was observed in the solid state (vide infra). However, in the solution, both *rac* and *meso* isomers exist, as indicated by the ^1H and ^{13}C NMR spectra. The ratios of isomers are 1:1 for **19**, and 1:3 for **20**. The synthesis of Ni pincer complex **21** could be achieved by a similar route without isolating the lithium complex (Scheme 9). By adding 2 equivalents of $^n\text{BuLi}$ to form the corresponding lithium di-amide complex, it then could react with $\text{NiCl}_2(2,4\text{-lutidine})_2$ to produce Ni complex **22** in very high yield (Scheme 10).



Scheme 8. Synthesis of Ni pincer complexes **19** and **20**.



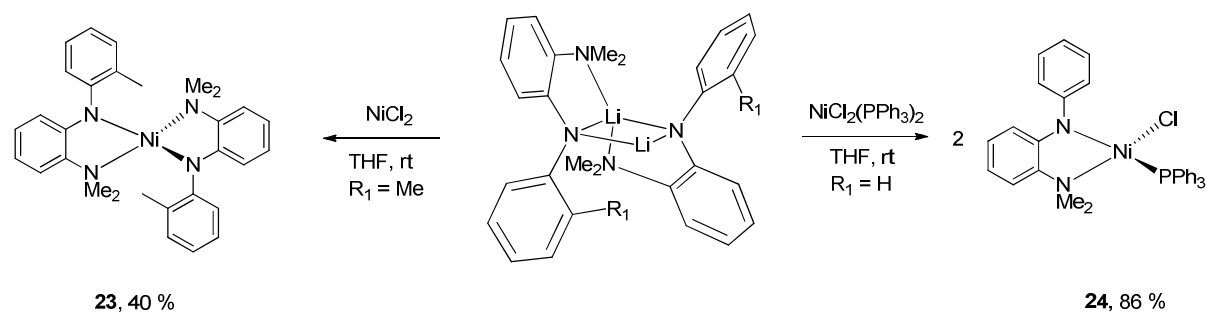
Scheme 9. Synthesis of Ni pincer complex **21** with hemilabile ligand.



Scheme 10. Synthesis of Ni pincer complex **22** with di-amide ligand.

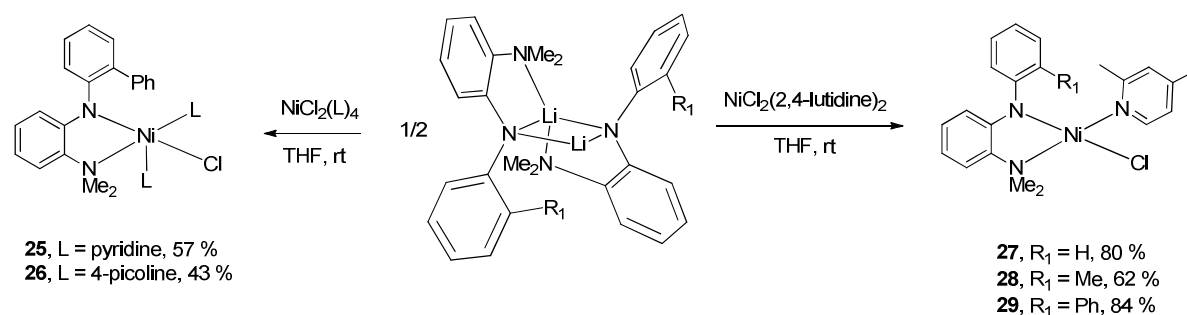
The synthesis of Ni complexes with bidentate ligands **7-9** proved to be more challenging. Reaction of Li complexes **14-16** with $\text{NiCl}_2(\text{dme})$ in THF or CH_3CN did not lead to the expected Ni complexes, but rather the formation of protonated ligands, **7H-9H**. The Mg complex **18**, on the other hand, failed to react with a Ni salt. The coordination chemistry of bidentate ligands was thoroughly studied employing various Ni precursors such as anhydrous NiCl_2 , NiBr_2 , NiI_2 , $\text{NiCl}_2(\text{THF})_{1.5}$, $\text{NiCl}_2(\text{PPh}_3)_2$, $\text{NiCl}_2(\text{Py})_4$, $\text{Ni}(\text{OAc})_2$, $\text{NiCl}_2(2,4\text{-lutidine})_2$, $\text{NiCl}_2(4\text{-picoline})_4$. Under most conditions, reactions of **14-16** with these Ni salts produced mostly protonated ligands and sometimes small quantities of paramagnetic compounds that could not be identified. Fortunately, after many struggles, I was able to prepare a series of Ni complexes with these ligands by judicious choice of Ni precursors and reaction conditions.

Reaction of Li complex **15** with anhydrous NiCl_2 in THF led to the formation of complex **23**, in which two molecules of ligand **8** coordinate to one Ni ion (Scheme 11). The complex is paramagnetic and its ^1H NMR spectrum shows chemical shifts from -40 to +40 ppm. Changing the stoichiometry of the reagents did not affect the outcome of this reaction. Reaction of Li complex **14** with $\text{NiCl}_2(\text{PPh}_3)_2$ in THF led to the paramagnetic complex **24** (Scheme 11). The Ni is bound to one molecule of **7**, Cl^- , and PPh_3 .

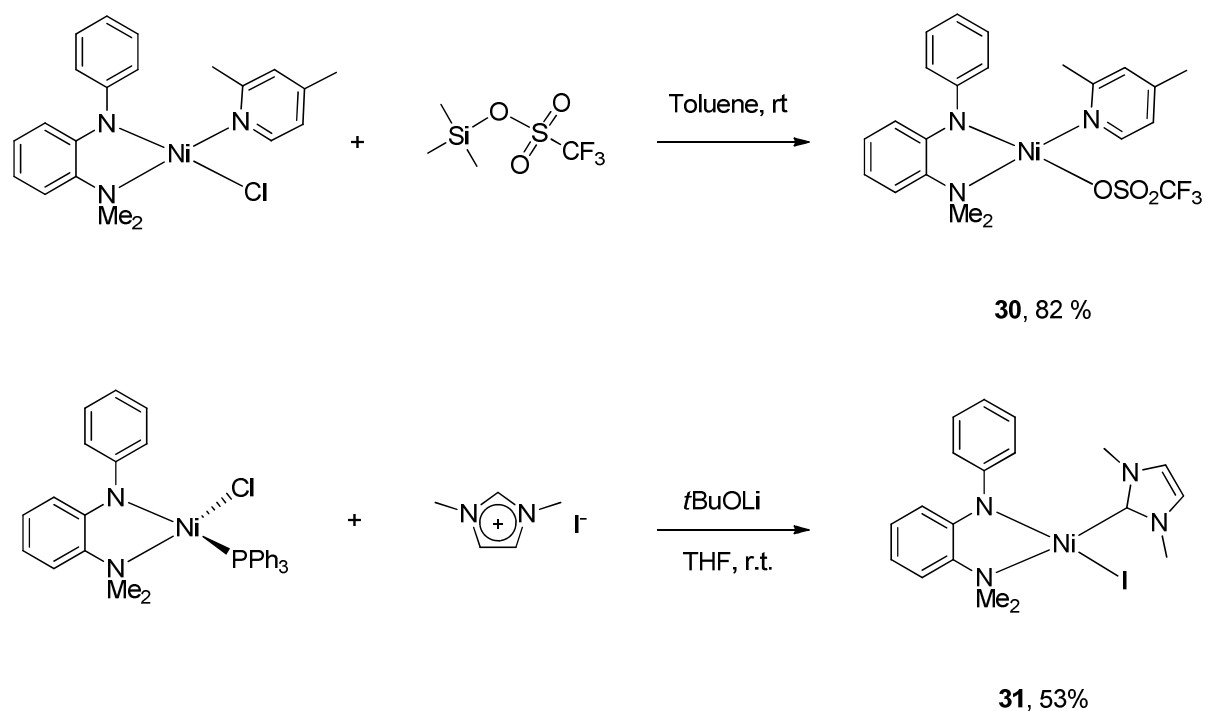


Scheme 11. Synthesis of complex **23** and **24**.

Reactions of Li complex **16** with $\text{NiCl}_2(\text{py})_2$ and $\text{NiCl}_2(4\text{-picoline})_4$ yielded five-coordinate Ni complexes **25** and **26** (Scheme 12). Both compounds are paramagnetic. Finally, four-coordinate and diamagnetic Ni complexes were prepared by reaction of **14-16** with $\text{NiCl}_2(2,4\text{-lutidine})_2$ (Scheme 12). The resulting complexes (**27-29**) have the formula of $[(^R\text{NN})\text{Ni}(2,4\text{-lutidine})(\text{Cl})]$. The diamagnetism is consistent with square-planar structures, which were confirmed by crystallography (section 2.2.4). The Cl^- in Ni complex **27** could be replaced by OTf, when **27** was reacted with TMSOTf. Similarly, the auxiliary ligand PPh_3 of complex **24** could be substituted with a carbene ligand 1,3-dimethylimidazolin-2-ylidene (dmiy) which was generated from the corresponding imidazolium iodide with base in situ (Scheme 13).



Scheme 12. Synthesis of complexes **25-29**.



Scheme 13. Synthesis of complexes **30** and **31**.

2.2.4 Structures of Ni complexes.

The solid-state structures of complexes **19–31** were determined by X-ray crystallography. The results confirmed the structural formula depicted in Schemes 8–13. The structures of **19** and **20** (Figures 5 and 6) resemble that of **1**. The pincer ligands coordinate in a meridional fashion. The larger substituents (Me and ⁱPr) on the amine adapt a *rac* orientation. The Ni–N distances in **19** and **20** are all comparable to **1**. The Ni (II) ions of **21** and **22** are in a square-planar geometry (Figures 7 and 8). The Ni–N (alkyl arm) distance is slightly shorter than the Ni–N (aryl arm).

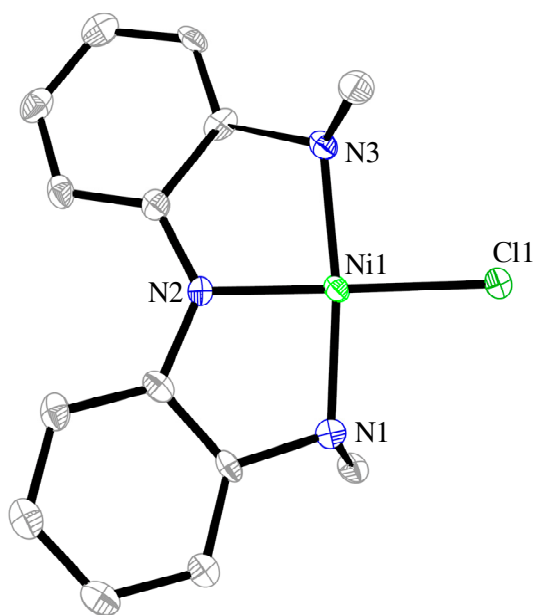


Figure 5. Crystal structure of complex $[(^{\text{HMe}}\text{N}_2\text{N})\text{NiCl}]$ (**19**). There are two independent molecules in the asymmetric unit, and only one of them is shown. The crystal contains half molecule of solvent (CH_2Cl_2) which is not shown.

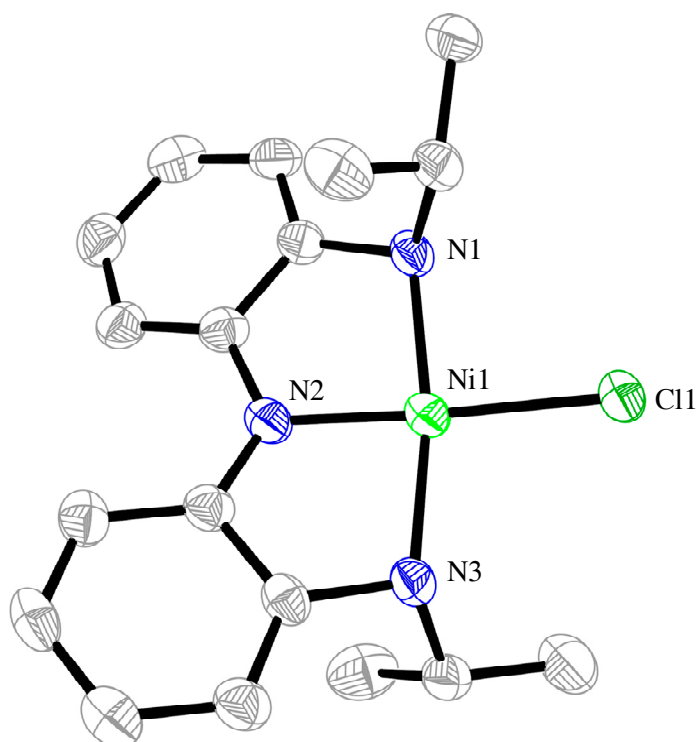


Figure 6. Crystal structure of $[(^{\text{HiPr}}\text{N}_2\text{N})\text{NiCl}]$ (**20**).

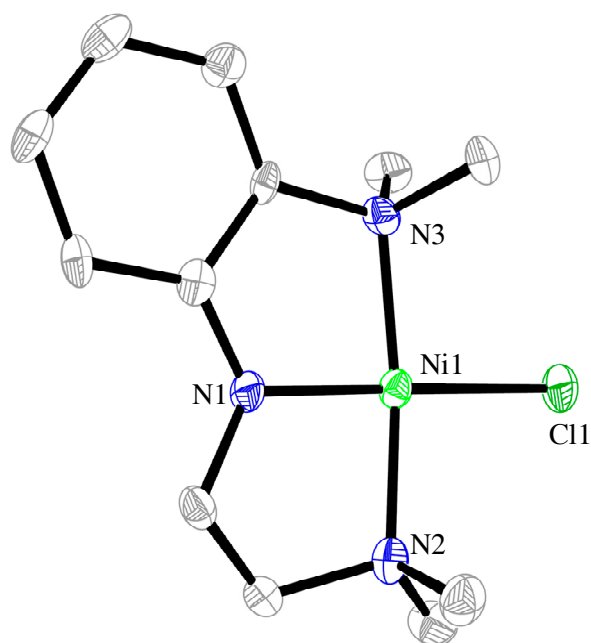


Figure 7. Crystal structure of complexes $[(^{\text{Me}}\text{N}^{\text{Me}}\text{NNiCl})]$ (**21**). There are two independent molecules in the asymmetric unit of **21**, and only one of them is shown.

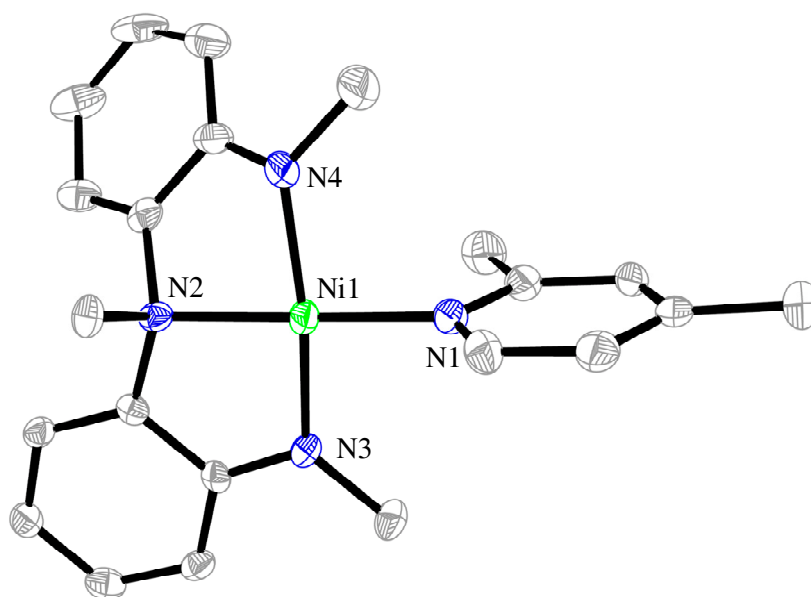


Figure 8. Crystal structure of complexes $[(^{\text{Me}}\text{N}_2^{\text{Me}}\text{NNi(lut)})]$ (**22**).

The structures of **23** and **24** (Figures 9 and 10) show that the Ni(II) ions are in a distorted tetrahedral coordination environment. The structures of **25** and **26** show the coordination geometry of Ni ions to be distorted square pyramidal (Figures 11 and 12). The two nitrogen atoms of ligand **9**, Cl⁻, and one pyridine/picoline nitrogen constitute the plane. The chloride anion occupies the position *trans* to the amido nitrogen. The second pyridine/picoline ligand occupies the axial position. The Ni-N distance for the axial pyridine/picoline ligand is slightly shorter, about 0.06 Å. The structures of **27**, **28**, and **29** (Figures 13-15) are similar, showing square-planar Ni(II) ions. Like **25** and **26**, the chloride anion occupies the position *trans* to the amido nitrogen. To minimize steric congestion, the 2-methyl group of the 2,4-lutidine ligand is *trans* to the R₁ (Me and Ph) group of the bidentate ligands in **28** and **29**. In all complexes of ligand **9** (**25**, **26**, **29**), the phenyl R₁ substituent is not co-planar with the parent aryl group in the solid-state. The structures of **30** and **31** resemble **27**, but OTf⁻ and I⁻ groups, respectively, occupy the position *trans* to the amido nitrogen (Figures 16 and 17).

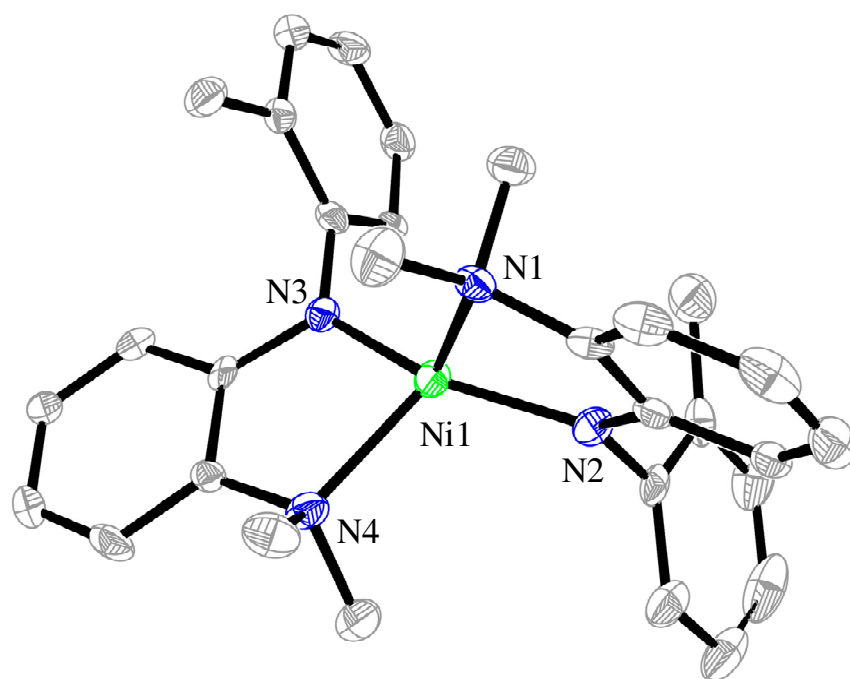


Figure 9. Crystal structure of complex [^{Me}NN)₂Ni] (**23**).

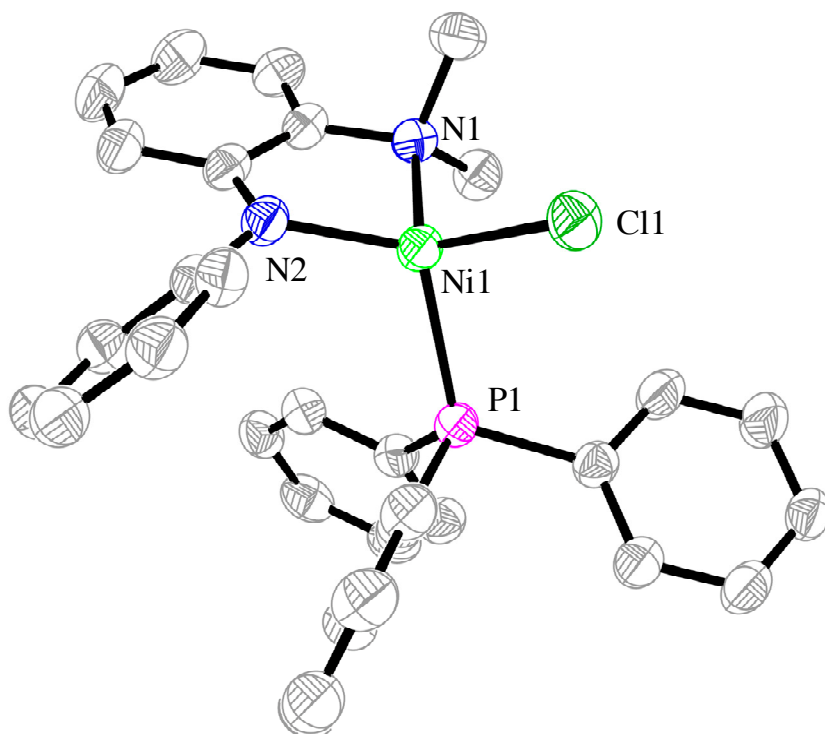


Figure 10. Crystal structure of complex $[(^H\text{NN})\text{Ni}(\text{PPh}_3)\text{Cl}]$ (**24**).

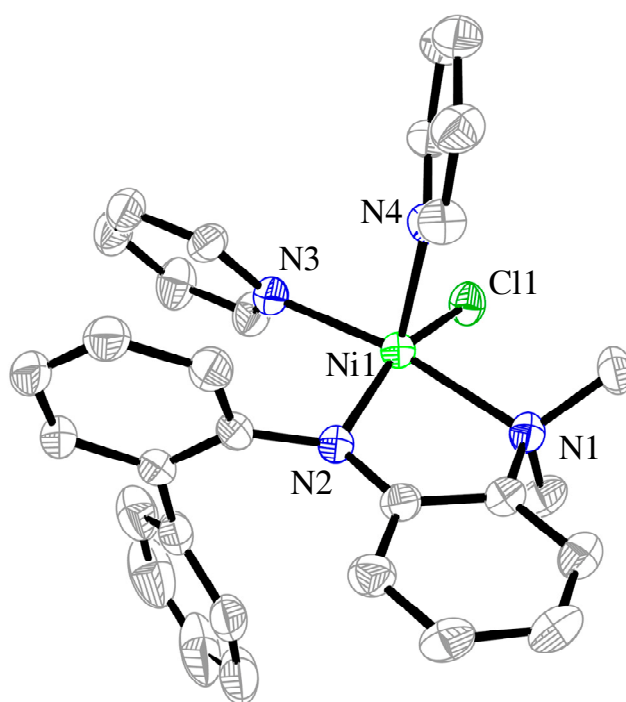


Figure 11. Crystal structure of complex $[(^{\text{Ph}}\text{NN})\text{Ni}(\text{Py})_2\text{Cl}]$ (**25**).

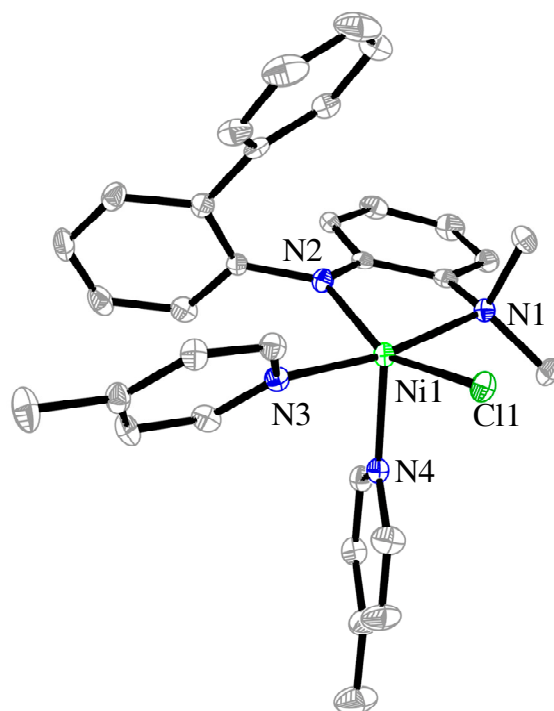


Figure 12. Crystal structure of complex $[(^{\text{Ph}}\text{NN})\text{Ni}(\text{4-Picoline})_2\text{Cl}]$ (**26**).

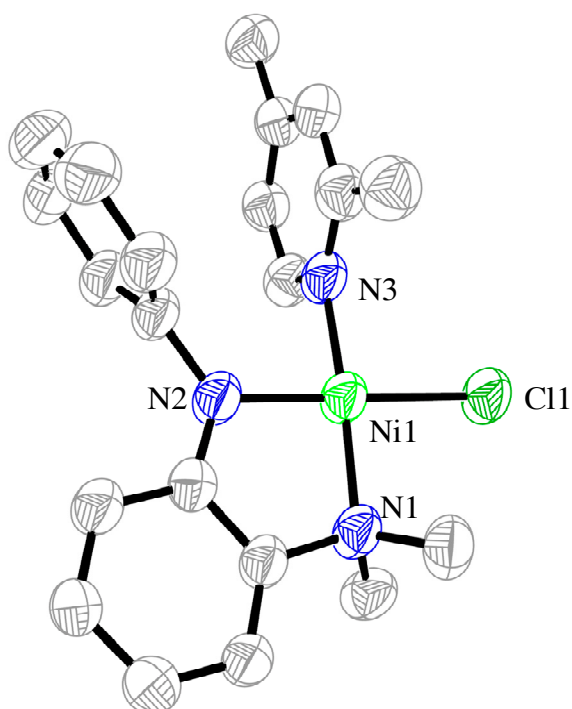


Figure 13. Crystal structure of complex $[(^{\text{H}}\text{NN})\text{Ni}(\text{2,4-lutidine})\text{Cl}]$ (**27**).

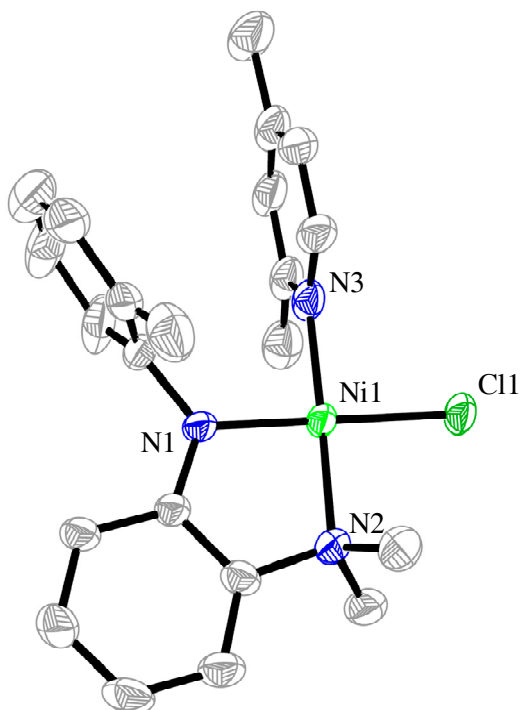


Figure 14. Crystal structure of complex $[(^{\text{Me}}\text{NN})\text{Ni}(\text{2,4-lutidine})\text{Cl}]$ (**28**).

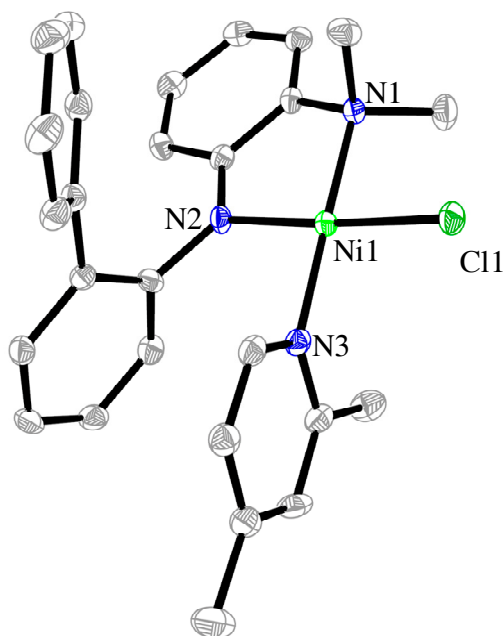


Figure 15. Crystal structure of complex $[(^{\text{Ph}}\text{NN})\text{Ni}(\text{2,4-lutidine})\text{Cl}]$ (**29**).

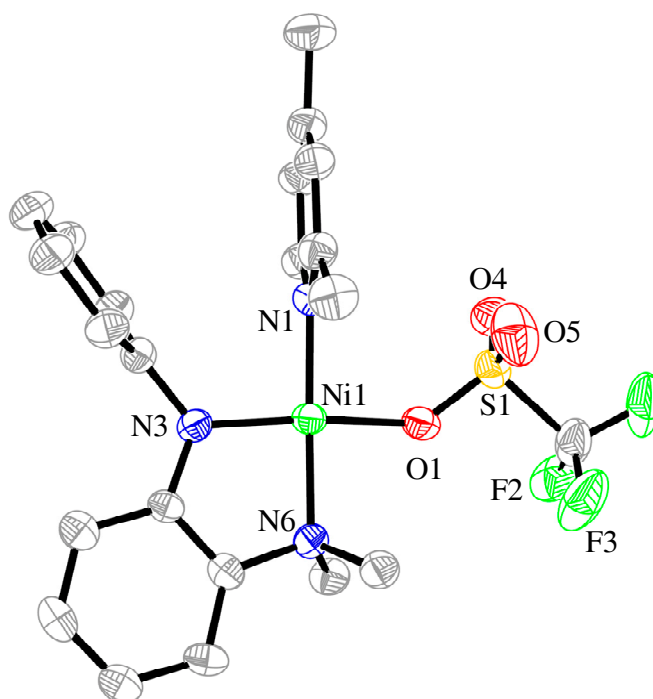


Figure 16. Crystal structure of complex $[(^H\text{NN})\text{Ni}(2,4\text{-lutidine})\text{OTf}]$ (**30**). There are two independent molecules in the asymmetric unit of **30**, and only one of them is shown. The unit cell of **30** contains one molecule of solvent (toluene) which is not shown.

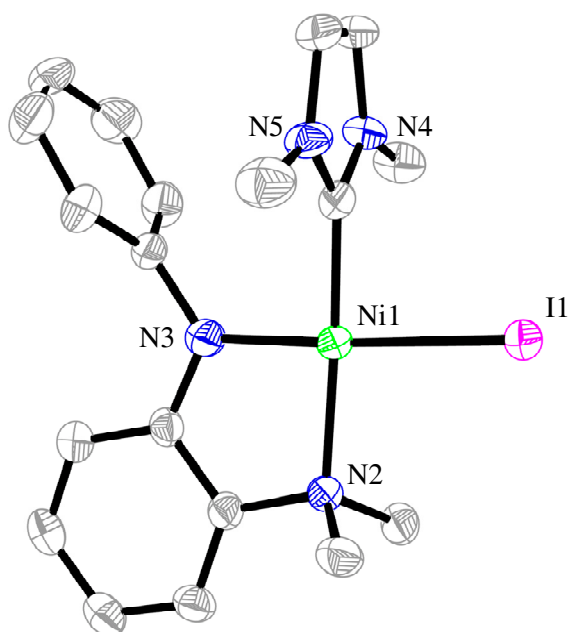


Figure 17. Crystal structure of complex $[(^H\text{NN})\text{Ni}(\text{dmiy})\text{I}]$ (**31**). The crystal of **31** contains one molecule of solvent (toluene) which is not shown.

Table 1 lists the selected Ni-L/X bond distances in complexes **19-31**. Several trends are noteworthy. In all complexes, the Ni-N(amide) bonds are significantly shorter than the Ni-N(amine) bonds. In general, low-spin and diamagnetic compounds have shorter Ni-L distances, and the bonds in five-coordinate, square-pyramidal complexes are noticeably longer than their counterparts in four-coordinate complexes.

Table 1. Selected bond distances in complexes **19-31**.^a

Complex	Ni-N (amide)	Ni-N (amine)	Ni-X	Ni-L (additional)	Geometry	Spin state
19	1.842(5)	1.932(5)	2.2051(16) Ni-Cl	-	Square-Planar	Dia
20	1.838(4)	1.943(3)	2.2156(12) Ni-Cl	-	Square-Planar	Dia
21	1.893(3)	1.983(3)	2.2217(11) Ni-Cl	1.966(4) L = N(alkyl)	Square-Planar	Dia
22	1.884(35)	1.938(3)	-	1.901(4) L = N(Lut)	Square-Planar	Dia
23	1.905(3)	2.090(4)	-	-	Tetrahedral	Para
24	1.906(2)	2.060(2)	2.2184(8) Ni-Cl	2.3256(8) L = P(PPh ₃)	Tetrahedral	Para
25	1.979(2)	2.174(2)	2.3597(8) Ni-Cl	2.076(2) L = N(Py)	Square-Pyramidal	Para
26	1.9754(16)	2.1625(15)	2.3635(6) Ni-Cl	2.0891(17) L = N(4-pico)	Square-Pyramidal	Para
27	1.877(4)	1.950(4)	2.2069(14) Ni-Cl	1.900(4) L = N(Lut)	Square-Planar	Dia
28	1.882(4)	1.981(4)	2.2198(13) Ni-Cl	1.913(4) L = N(Lut)	Square-Planar	Dia
29	1.887(2)	1.965(2)	2.2113(8) Ni-Cl	1.913(2) L = N(Lut)	Square-Planar	Dia
30	1.849(4)	1.954(4)	1.937(4) Ni-OTf	1.916(4) L = N(Lut)	Square-Planar	Dia
31	1.869(4)	2.020(4)	2.5323(9) Ni-I	2.5323(9) L = dmiy	Square-Planar	Dia

^a Distances are in Angstroms. Averaged bond distances were used in cases where there is more than one bond of the same given type. The geometry was approximated.

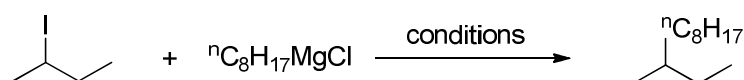
2.3 Kumada coupling of secondary alkyl halides using nickel complexes as catalysts

2.3.1 Test reactions

[(^{Ph}NN)Ni(2,4-lutidine)Cl] (**29**) was used as test catalyst to optimize the reaction conditions for coupling 2-iodobutane with octylMgCl. Screening of reaction conditions showed that these reactions were best run at -20 °C and in DMA (DMA =

dimethylacetoamide), and using 1 equivalent of Grignard reagent diluted in THF (Table 2). Slow addition of Grignard reagents was sometime beneficial and, in the best cases, gave 5 to 10 % better yields. The reactions generally finished within two hours. By changing the catalyst to **27** and **28**, the yield could be further improved to 74%. The coupling of 2-iodobutane with octylMgCl (eq. 1) and cyclohexyl iodide with butylMgCl (eq. 2) was chosen as a model reaction to test the performance of Ni complexes **19-31**. The catalysis using complex **1** was used as a reference.

Table 2. Optimizing conditions and control experiments.^a



Entry	Grignard	Cat. (mol%)	Solvent	Temp. (°C)	Time	Yield (%) ^[b]
1	1.2 equiv.	29 (3%)	DMA (0.75mL)	-20	0.5h	55
2	1.2 equiv.	29 (3%)	DMA (0.75mL)	r.t.	0.5h	21
3	1.2 equiv.	29 (3%)	DMA (0.75mL)	0	0.5h	42
4	1.2 equiv.	29 (3%)	DMA (0.75mL)	-10	0.5h	49
5	1.2 equiv.	29 (3%)	DMA (0.75mL)	-30	0.5h	16
6	1.2 equiv.	29 (9%)	DMA (0.75mL)	-20	0.5h	55
7	1.2 equiv.	-	DMA (0.75mL)	-20	0.5h	0
8	1.2 equiv.	29 (3%)	DMA (2mL)	-20	0.5h	37
9	2 equiv.	29 (3%)	DMA (0.75mL)	-20	0.5h	40
10 ^[c]	1.2 equiv.	29 (3%)	DMA (0.75mL)	-20	0.5h	24
11 ^[d]	1.2 equiv.	29 (3%)	DMA (0.75mL)	-20	0.5h	23
12 ^[e]	1.2 equiv.	29 (3%)	DMA (0.75mL)	-20	0.5h	25
13	1 equiv.	29 (3%)	DMA (0.75mL)	-20	0.5h	55
14	1.2 equiv.	29 (3%)	DMF (0.75mL)	-20	0.5h	10
15	1 equiv.	29 (3%)	NMP (0.75mL)	-20	0.5h	12
16	1 equiv.	29 (3%)	THF (0.75mL)	-20	0.5h	trace
17	1 equiv.	29 (3%)	Dioxane (0.75mL)	-20	0.5h	trace
18	1.2 equiv.	17 (3%)	DMA (0.75mL)	-20	0.5h	trace
19	1.2 equiv.	NiCl₂(2,4-lut)₂ (3 %)	DMA (0.75mL)	-20	0.5h	16
20	1.2 equiv.	1 (3 %)	DMA (0.75mL)	-20	0.5h	trace
21 ^[f]	1 equiv.	29 (3 %)	DMA (0.75mL)	-20	1h	66

Table 2. (Continued)

Entry	Grignard	Cat. (mol%)	Solvent	Temp. (°C)	Time	Yield (%) ^[b]
22 ^[f]	1 equiv.	29 (1 %)	DMA (0.75mL)	-20	1h	45
23 ^[f]	1 equiv.	29 (3 %)	DMA (0.5mL)	-20	1h	49
24 ^[f]	1 equiv.	27 (3 %)	DMA (0.5mL)	-20	1h	66
25 ^[f]	1 equiv.	27 (3 %)	DMA (0.75mL)	-20	2h	74
26 ^[f]	1 equiv.	28 (3 %)	DMA (0.75mL)	-20	2h	74
27 ^[f]	1 equiv.	27 (3 %)	DME (0.75mL)	-20	2h	10
28 ^[f]	1 equiv.	27 (3 %)	DCE (0.75mL)	-20	2h	15
29 ^[f]	1 equiv.	27 (3 %)	DEE (0.75mL)	-20	2h	6

^a ⁿOctylMgCl was added dropwise to a solution of 2-iodobutane (0.5 mmol) according to the conditions specified in Table 2. The reaction was allowed to proceed for a certain period of time. ^b GC yields relative to 2-iodobutane. ^c adding 30% TMEDA as additive, TMEDA = *N,N,N',N'*-tetramethylethylenediamine. ^d adding 60 % BDMAEE as additive, BDMAEE = bis[2-(*N,N*-dimethylaminoethyl)]ether. ^e adding 1 equiv. LiCl as additive. ^f 0.5 mmol (1 equiv.) of ⁿOctylMgCl was diluted in THF (3 mL), and then was added dropwise via a syringe pump (1 h).

Figure 18 and Table 3 summarize the results. The original pincer catalyst [^{Me}N₂N)NiCl] (**1**) was not efficient for coupling of 2-iodobutane (entry 1, Table 3), giving a 4 % coupling yield for equation 1. It gave a modest yield for the coupling of cyclohexyl iodide. Analogous pincer complexes with NHR donors [^{HMe}N₂N)NiCl] (**19**) and [^{HiPr}N₂N)NiCl] (**20**) were not at all active for the coupling (entries 2 and 3, Table 3). The catalytic behavior of pincer complex with a more labile NEt₂ side arm [^{Me}N^{Me}N)NiCl] (**21**) is similar to **1**, but the yield for coupling of cyclohexyl iodide was lower than **1** (entry 4, Table 3). Complex [^{Me}N₂^{Me}N)Ni(2,4-lutidine)] (**22**) with a dianionic pincer ligand was not active for the coupling reactions at all (entry 5, Table 3). [^HNN)₂Ni] complex (**23**) was also inactive (entry 6, Table 3). As shown in Table 4, most of the starting alkyl halides remained after the reactions using these precatalysts, and thus their inefficiency was due to the inability to activate alkyl halides. More encouraging results were obtained with [^HNN)Ni(PPh₃)Cl] (**24**). It was active for the coupling of both acyclic and cyclic secondary iodides, giving a yield of 68 % and 61 % for 2-butyl and cyclohexyl iodide, respectively (entry 7, Table 3). The five-coordinate complexes **25** [^{Ph}NN)Ni(Cl)(Py)₂] and **26** [^{Ph}NN)Ni(Cl)(4-Picoline)₂] were also active (entries 8 and 9, Table 3). The coupling yields for 2-butyl iodide were low, and for cyclohexyl iodide were modest. The square-planar complexes [^RNN)Ni(2,4-lutidine)Cl] (**27-29**) were the most active catalysts (entries 10-12, Table 3). Coupling yields between 62 % and 84 % were obtained. The coupling yields of [^HNN)Ni(2,4-lutidine)OTf] (**30**) were slightly lower than that of **27**. The Ni complex [^HNN)Ni(dmiy)I] (**31**) was not active. From

the experimental results, Ni Complex $[(^H\text{NN})\text{Ni}(2,4\text{-lutidine})\text{Cl}]$ (**27**) was the best catalyst, giving yields of 74 % and 84% for the coupling of 2-butyl and cyclohexyl iodide, respectively (entry 10, Table 3).

Table 3. Kumada coupling of secondary alkyl halides, test reactions.^a

$ \begin{array}{c} \text{I} \\ \\ \text{CH}_3\text{CH}_2\text{CH}_2\text{CH}_3 \end{array} + {}^n\text{C}_8\text{H}_{17}\text{MgCl} \xrightarrow[\text{DMA, -20 }^\circ\text{C}]{3 \text{ mol\% cat.}} \begin{array}{c} {}^n\text{C}_8\text{H}_{17} \\ \\ \text{CH}_3\text{CH}_2\text{CH}_2\text{CH}_3 \end{array} \quad (1) $				
$ \begin{array}{c} \text{I} \\ \\ \text{C}_6\text{H}_{11} \end{array} + {}^n\text{C}_4\text{H}_9\text{MgCl} \xrightarrow[\text{DMA, -20 }^\circ\text{C}]{3 \text{ mol\% cat.}} \begin{array}{c} {}^n\text{C}_4\text{H}_9 \\ \\ \text{C}_6\text{H}_{11} \end{array} \quad (2) $				
Entry	Catalyst	Formula	Yield (%) for reaction (1)	Yield (%) for reaction (2)
1	1		4	46
2	19		trace	1
3	20		trace	trace
4	21		1	27
5	22		2	5
6	23		1	1
7	24		68	61
8	25		20	54

Table 3. (Continued)

Entry	Catalyst	formula	Yield (%) for reaction (1)	Yield (%) for reaction (2)
9	26		16	57
10	27		74	84
11	28		74	77
12	29		62	80
13	30		64	80
14	31		0	0

^a 0.5 mmol (1 equiv.) of RMgCl was diluted in THF (3 mL), and then was added dropwise via a syringe pump during 1 h to a DMA solution containing the nickel catalyst (0.015 mmol, 3 %) and alkyl iodide (0.5 mmol) at -20 °C. After addition, the reaction mixture was further stirred for 1 h at -20 °C and then the solution was taken out from the cooling system and stirred for 1 h to warm up to room temperature.

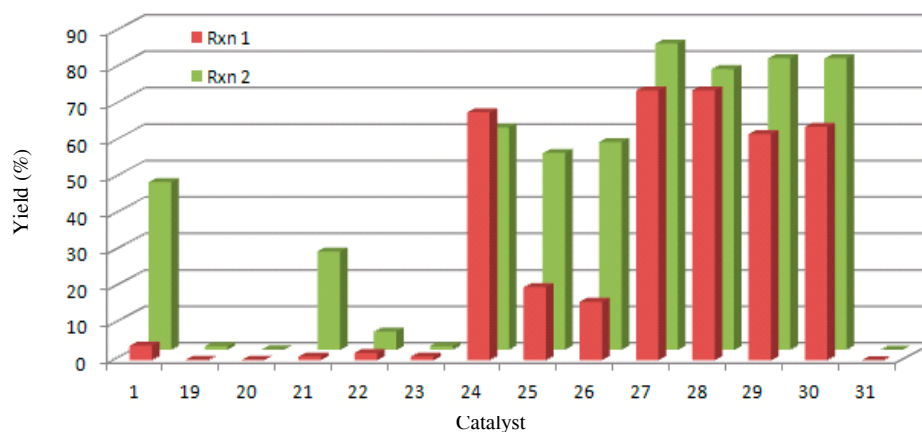


Figure 18. A graphical representation of the efficiency of various Ni catalysts for the test coupling reaction.

Table 4. Distribution of unreacted starting material and major side products for Kumada coupling of secondary alkyl Halides, test reactions^a

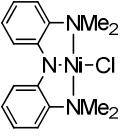
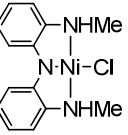
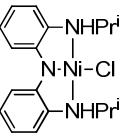

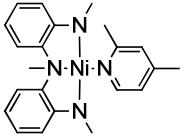
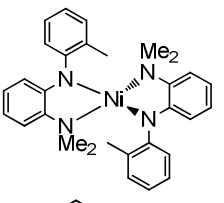
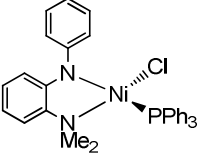
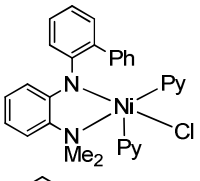
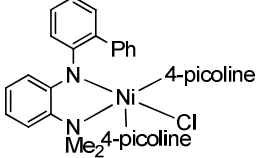
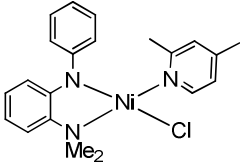
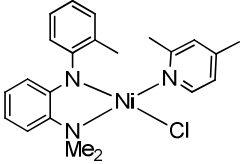
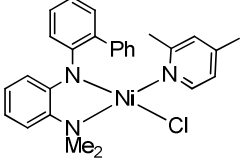
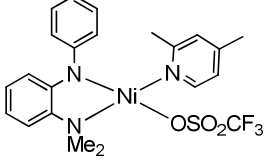
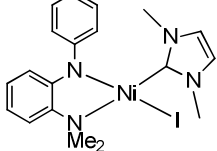
Entry	Catalyst	Formula	Amount (%) of alkyl halide left after reaction (1)	Major detectable side product and yield (%) for reaction (1)	Amount (%) of alkyl halide left after reaction (2)	Major detectable side product and yield (%) for reaction (2)
1	1		70	-	57	-
2	19		67	-	65	-
3	20		62	-	79	-
4	21		95	trace	-	Cyclohexyl-cyclohexyl (13%); Butyl-Butyl (4%)
5	22		8	Octyl-Octyl (3%)	-	Cyclohexyl-cyclohexyl (16%); Butyl-Butyl (6%)
6	23		48	-	88	-
7	24		10	Octyl-Octyl (10%)	-	Cyclohexyl-cyclohexyl (10%)
8	25		7	Octyl-Octyl (10%)	4	Cyclohexyl-cyclohexyl (10%)
9	26		49	Octyl-Octyl (5%)	12	Cyclohexyl-cyclohexyl (7%); Butyl-Butyl (8%)

Table 4. (Continued)

Entry	Catalyst	Formula	Amount (%) of alkyl halide left after reaction (1)	Major detectable side product and yield (%) for reaction (1)	Amount (%) of alkyl halide left after reaction (2)	Major detectable side product and yield (%) for reaction (2)
10	27		-	Octyl-Octyl (10%)	7	Cyclohexyl-cyclohexyl (6%); Butyl-Butyl (5%)
11	28		-	Octyl-Octyl (10%)	5	Cyclohexyl-cyclohexyl (10%); Butyl-Butyl (8%)
12	29		-	Octyl-Octyl (10%)	3	Cyclohexyl-cyclohexyl (8%); Butyl-Butyl (7%)
13	30		-	Octyl-Octyl (9%)	-	Cyclohexyl-cyclohexyl (9%); Butyl-Butyl (5%)
14	31		88	-	99	-

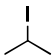
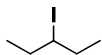
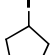
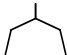
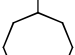

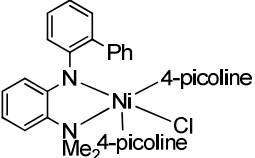
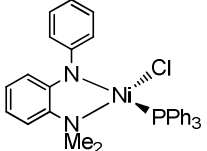
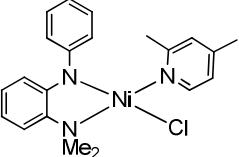
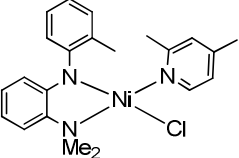
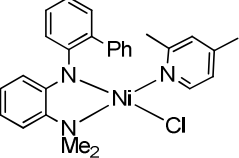
^a See Table 3 for conditions.

2.3.2 Ranking of catalysts

Complexes **1**, **24**, **26**, and **27-29** showed certain activity for reactions (1) and (2). They were further tested for the coupling of additional cyclic and acyclic secondary alkyl iodides. The results are summarized in Table 5 and Figure 19.

For coupling of cyclic alkyl iodides, the pincer complex **1** had a low efficiency for cyclopentyl iodide, and was inactive for cycloheptyl and cyclooctyl iodide. A similar trend was observed with 5-coordinate complex **26**. It had a modest efficiency for the coupling of cyclopentyl iodide, and a low efficiency for cycloheptyl and cyclooctyl iodide. Both **1** and **26** had low to no efficiency for the coupling of isopropyl and 3-pentyl iodide. The results were consistent with those shown in Table 3, and together, ranked complexes **1** and **26** as poor catalysts for coupling of secondary iodides. Table 6 showed that the low efficiency was largely due to the inability to activate secondary alkyl halides.

Table 5. Kumada coupling of secondary alkyl iodides, continued.^a

$\text{R}_1\text{CH}(\text{I})\text{R}_2 + {}^n\text{C}_8\text{H}_{17}\text{MgCl} \xrightarrow[\text{DMA, -20 } ^\circ\text{C}]{3 \text{ mol\% cat.}} \text{R}_1\text{CH}({}^n\text{C}_8\text{H}_{17})\text{R}_2 \quad (3)$					
$\text{Cycloalkyl-CH}_2\text{I} + {}^n\text{C}_4\text{H}_9\text{MgCl} \xrightarrow[\text{DMA, -20 } ^\circ\text{C}]{3 \text{ mol\% cat.}} \text{Cycloalkyl-CH}_2({}^n\text{C}_4\text{H}_9) \quad (4)$					
					
 (1)	8	trace	38	trace	0
 (26)	43	3	47	13	7
 (24)	58	50	43	65	52
 (27)	69	53	69	87	82
 (28)	75	38	68	81	61
 (29)	68	31	69	65	54

^a Same conditions as in Table 3.

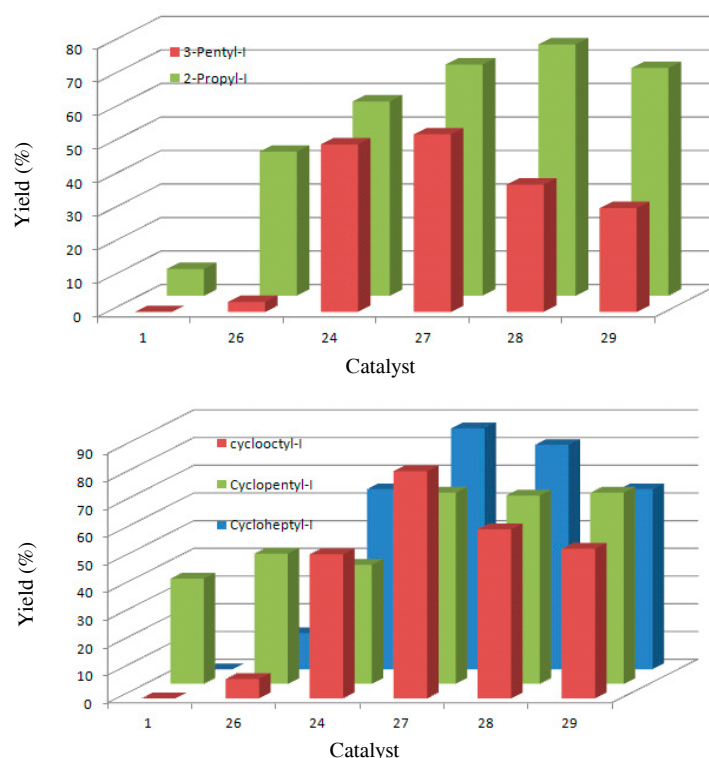

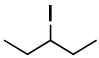
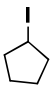
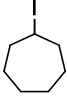
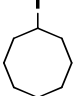

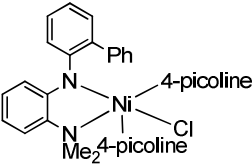
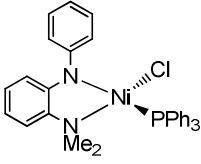
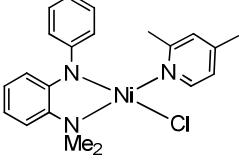
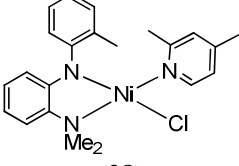
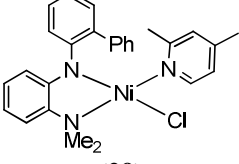


Figure 19. Graphical representation of the efficiency of various Ni catalysts for coupling reactions of secondary alkyl iodides.

Four-coordinate complexes **24** and **27-29** were much more efficient catalysts. Alkyl halides were readily activated (Table 6), and modest to high yields were obtained for the coupling of all substrates. For all but one coupling reaction, complex **24** was the least efficient among these four catalysts, giving coupling yields of about 20% lower than the best yields for cyclic substrates. Table 7 showed that more elimination products were produced using **24** as pre-catalyst. The exception is the coupling of 2-pentyl iodide for which it gave the second highest yield (50%). For the coupling of isopropyl and cyclopentyl iodide, complexes **27-29** were similarly efficient, having yields of about 70%. However, for coupling of 3-pentyl, cycloheptyl, and cyclooctyl iodide, the performance of **27-29** was noticeably different. Complex **27**, with the least bulky ligand **7**, was clearly the best catalyst. It gave yields of 53%, 87%, and 82% for these substrates. The efficiency dropped with **28**, and lowered furthermore with **29**.

Table 6. Distribution of unreacted starting material for Kumada coupling of secondary alkyl iodides.^a

					
 (1)	62	67	47	80	89
 (26)	14	67	22	52	64
 (24)	-	21	-	-	7
 (27)	-	13	-	-	-
 (28)	-	27	-	-	-
 (29)	-	10	-	-	-

^a Same conditions as in Table 3.**Table 7.** Distribution of major side products for Kumada coupling of secondary alkyl iodides.^a

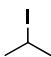
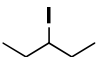
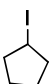
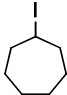
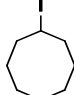

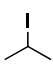
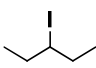
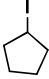
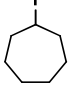
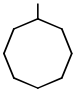
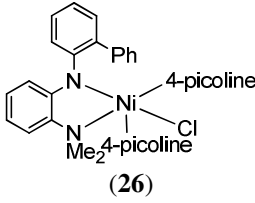
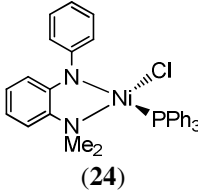
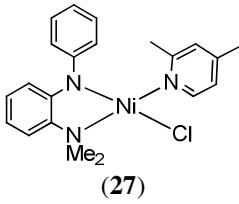
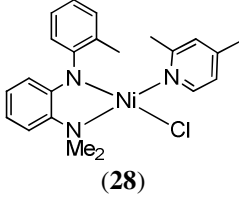
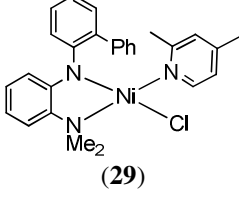
					
 (1)	-	-	-	-	-

Table 7. (Continued)

					
 (26)	Octyl-Octyl (7%) Octene (12%)	Octyl-Octyl (3%) Octylene (6%)	Butyl-Butyl (8%) Cyclopentyl-Cyclopentyl (9%)	Butyl-Butyl (4%) Cycloheptyl-Cycloheptyl (8%) Cycloheptene (14%)	Butyl-Butyl (3%) Cyclooctyl-Cyclooctyl (5%) Cyclooctane (7%) Cyclooctene (12%)
 (24)	Octyl-Octyl (9%) Octene (17%)	Octyl-Octyl (8%) Octylene (4%)	Butyl-Butyl (6%) Cyclopentyl-Cyclopentyl (7%)	Butyl-Butyl (9%) Cycloheptyl-Cycloheptyl (2%) Cycloheptene (36%)	Butyl-Butyl (7%) Cyclooctyl-Cyclooctyl (1%) Cyclooctane (26%) Cyclooctene (22%)
 (27)	Octyl-Octyl (12%)	Octyl-Octyl (9%) Octylene (8%)	Butyl-Butyl (11%) Cyclopentyl-Cyclopentyl (13%)	Butyl-Butyl (5%) Cycloheptyl-Cycloheptyl (7%) Cycloheptene (1%)	Butyl-Butyl (4%) Cyclooctyl-Cyclooctyl (4%) Cyclooctane (5%) Cyclooctene (8%)
 (28)	Octyl-Octyl (10%)	Octyl-Octyl (7%) Octylene (13%)	Butyl-Butyl (11%) Cyclopentyl-Cyclopentyl (13%)	Butyl-Butyl (6%) Cycloheptyl-Cycloheptyl (8%) Cycloheptene (2%)	Butyl-Butyl (6%) Cyclooctyl-Cyclooctyl (7%) Cyclooctane (9%) Cyclooctene (14%)
 (29)	Octyl-Octyl (13%)	Octyl-Octyl (8%) Octylene (22%)	Butyl-Butyl (12%) Cyclopentyl-Cyclopentyl (14%)	Butyl-Butyl (5%) Cycloheptyl-Cycloheptyl (10%) Cycloheptene (12%)	Butyl-Butyl (6%) Cyclooctyl-Cyclooctyl (11%) Cyclooctane (11%) Cyclooctene (15%)

^a Same conditions as in Table 3. ^b The elimination product of cyclopentyl iodide, cyclopentene, cannot be detected by GC because it comes out together with the solvent. ^c The elimination product of cycloheptyl iodide, cycloheptene, overlaps with cycloheptane in GC measurements. The yields of cycloheptene were approximately by the combined yields of cycloheptene and cycloheptane.

As complexes **24** and **27** gave a similar coupling yield for 2-pentyl iodide, they were further tested for the coupling of acyclic secondary alkyl iodides that are bulkier than 3-pentyl iodide. Modest yields of 42 – 65% were obtained (Table 8). Complex **24** was slightly more efficient than **27**, but the difference in yields was small, ranging from 2 % - 11%.

Table 8. Kumada coupling of bulky acyclic secondary alkyl iodides^a

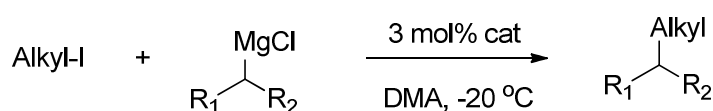
$\text{R}_1\text{CH}(\text{I})\text{R}_2 + {}^n\text{C}_8\text{H}_{17}\text{MgX} \xrightarrow[\text{DMA, -20 } ^\circ\text{C}]{3 \text{ mol\% } \mathbf{24} \text{ or } \mathbf{27}} \text{R}_1\text{CH}({}^n\text{C}_8\text{H}_{17})\text{R}_2$			
Entry	$\text{R}_1\text{CH}(\text{X})\text{R}_2$	Yield with 24 (%)	Yield with 27 (%)
1		65	54
2		51	45
3		46	44
4		51	42

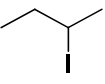
^a Same conditions as in Table 3.

Overall, the results in Tables 5 and 8 indicate that complex **27** is the best catalyst for the coupling of cyclic and non-bulky acyclic secondary alkyl iodides, and complex **24** is the best catalyst for the coupling of bulky acyclic secondary alkyl iodides.

The coupling with secondary alkyl Grignard reagents^{30, 31} was also attempted (Table 9). A very low yield was obtained for coupling of secondary alkyl iodide with a secondary alkyl Grignard reagent (entry 1, Table 9). The yields for coupling of primary alkyl iodides with secondary alkyl Grignard reagents were modest, and similar efficiencies were obtained for complexes **27-29**. Unlike pincer complex **1**,²⁴ no significant isomerization products were formed using these catalysts.

Table 9. Kumada Coupling of Secondary Alkyl Grignard Reagents^a



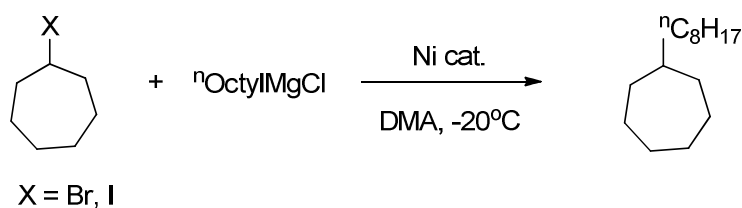
Entry	Alkyl-I	$\begin{array}{c} \text{MgCl} \\ \\ \text{R}_1 - \text{C} - \text{R}_2 \end{array}$	Cat.	Yield (%)
1		$\begin{array}{c} \text{MgCl} \\ \\ \text{Cyclohexyl} \end{array}$	29	7
2	n-C ₈ H ₁₇	$\begin{array}{c} \text{MgCl} \\ \\ \text{Cycloheptyl} \end{array}$	27	43
3	n-C ₈ H ₁₇	$\begin{array}{c} \text{MgCl} \\ \\ \text{Cycloheptyl} \end{array}$	28	51
4	n-C ₈ H ₁₇	$\begin{array}{c} \text{MgCl} \\ \\ \text{Cycloheptyl} \end{array}$	29	42
5	n-C ₄ H ₉	$\begin{array}{c} \text{MgCl} \\ \\ \text{Cycloheptyl} \end{array}$	27	45

^a Same conditions as in Table 3.

2.3.3 Probing the origin of the activity and efficiency for catalysts **1**, **24**, and **27**.

Here we define 'activity' as the reactivity of the catalyst toward alkyl halides, and it is correlated to the conversion of alkyl halides. 'Efficiency', on the other hand, is correlated to the selectivity and yield of the cross coupling product. A catalyst can be very active yet not efficient.

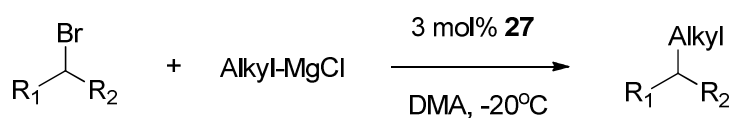
The coupling of cycloheptyl-I and cycloheptyl-Br was tested. The reaction time was set to 1 hour (addition of Grignard reagent) + 1 hour (further reaction) at -20 °C. The results are shown in Table 10. Catalyst **1** was not an active catalyst, and most of the starting cycloheptyl halides remained (entries 1 and 5, Table 10). Catalyst **24** was slightly more active, yet **27** was more efficient. For coupling of cycloheptyl-I, a high yield of 74 % was obtained with **27**; with **24**, the yield was 53 %, and the main side product was cycloheptene (entries 2 and 3, Table 10). The conversion was more than 90 % in both cases. For coupling of cycloheptyl-Br, yields of about 30 % were obtained with both catalysts (entries 6 and 7, Table 10). Catalyst **24** seems to be more active, giving a higher conversion. Yet more olefin was produced using **24**, and the overall efficiency was similar. When no catalyst was used, most alkyl halides remain unreacted, and a small amount of olefins were produced (entries 4 and 8, Table 10). Thus, the olefins observed in the coupling reactions using catalysts **24** and **27** should originate from metal-mediated β-H elimination.

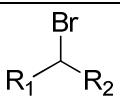
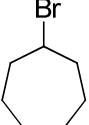
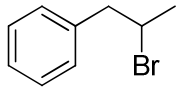
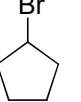
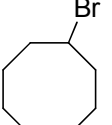
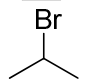
Table 10. Kumada coupling of secondary alkyl halides^a

Entry	X/ Catalyst	Octane	Octene	Cyclo- C ₇ H ₁₄	Cyclo- heptene	C ₇ H ₁₃ I or C ₇ H ₁₃ Br	Oct -Oct	C ₇ H ₁₃ - C ₇ H ₁₃	C ₇ H ₁₃ -Oct
1	I/1	99	0	0	7	76	<1	<1	<1
2	I/24	8	2	8	36	1	8	1	53
3	I/27	9	4	7	8	8	5	8	74
4	I/no	> 99	0	0	4	77	0	0	0
5	Br/1	95	0	0	6	97	<1	0	<1
6	Br/24	52	3	1	32	31	2	<1	38
7	Br/27	49	5	1	12	43	2	6	34
8	Br/no	86	0	0	2	92	0	0	0

^a Same conditions as in Table 3.

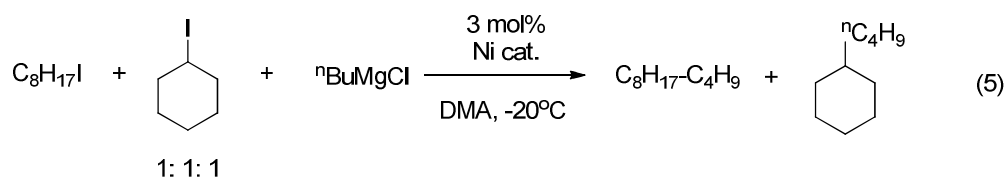
These results show that for coupling of cyclic secondary alkyl halides, catalyst **1** has little activity because alkyl halides could not react during catalysis. On the contrary, alkyl halides are activated employing catalysts **24** and **27**. Catalyst **24** seems to give the fastest alkyl halide activation, yet the catalysis is not very efficient due to β-H elimination which leads to olefinic products. The activation of alkyl bromide is slower than that of alkyl iodide. According to entry 7, Table 10, coupling of secondary alkyl bromide was fairly selective using **27** as the catalyst, although the conversion was low within the chosen reaction time. The coupling yields could be increased if a longer reaction time (2 h) was applied. Table 11 shows the results for some secondary alkyl bromides. Modest to good yields were obtained.

Table 11. Kumada Coupling of Secondary Alkyl Bromides^a

Entry		Alkyl	Yield (%)
1		n-C ₈ H ₁₇	69
2		n-C ₈ H ₁₇	52
3		n-C ₄ H ₉	75
4		n-C ₄ H ₉	60
5		n-C ₈ H ₁₇	64

^a 0.6 mmol (1.2 equiv.) of RMgCl was diluted in THF (3 mL), and then was added dropwise via a syringe pump during 1 h to a DMA solution containing the nickel catalyst (0.015 mmol, 3 %) and alkyl bromide (0.5 mmol) at -20 °C . After addition, the reaction mixture was further stirred for 2 h at -20 °C and then the solution was taken out from the cooling system and stirred for 10 min to warm up to room temperature.

We showed earlier that for catalyst **1**, coupling of primary alkyl halides was faster than secondary alkyl halides.²⁰ To determine whether this preference also holds for catalysts **24** and **27**, competition experiments were conducted using equal amounts of cyclohexyl and octyl iodides (eq. 5, Scheme 14 and table 12).



	Conversion:		Yields:	
catalyst 24 :	78 %	29 %	41 %	21 %
catalyst 27 :	73 %	31 %	33 %	20 %

Scheme 14. Competition experiment for primary and secondary alkyl iodides.

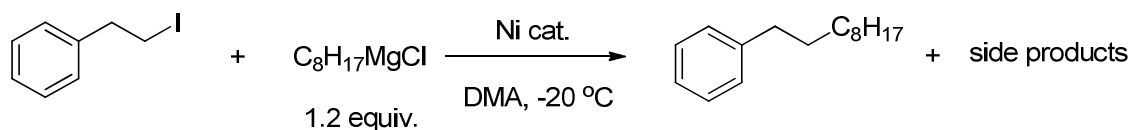
Table 12. Competition reaction primary and secondary alkyl iodides.^a

Catalyst	Quenching time	Conversion for C ₈ H ₁₇ I (%)	Conversion for cyclohexyl-I (%)	Yield for C ₈ H ₁₇ -C ₄ H ₉ (%)	Yield for Cyclohexyl-C ₄ H ₉ (%)
24	10 sec.	60	40	38	23
24	1 min.	62	38	41	23
24	2 min.	67	40	40	25
24	5 min.	63	38	40	26
27	10 sec.	60	44	35	14
27	1 min.	59	43	36	17
27	2 min.	64	43	36	20
27	5 min.	59	38	37	22

^a The typical procedure for coupling was used, except that the addition of Grignard reagents was done at once. The reactions were conducted in multiple trials, with different quenching times.

According to Scheme 14, with both catalysts **24** and **27**, the coupling of octyl iodide was faster than cyclohexyl iodide. The difference in reaction rate is modest, as the conversion of octyl iodide was more than 2 times higher than cyclohexyl iodide. These results suggest that activation of primary alkyl halides is also faster than secondary alkyl halides with the new catalysts.

Catalysts **24** and **27** were further studied for the coupling of primary alkyl halides. Unfortunately the yields were modest and generally lower than with catalyst **1**. Further experiments were conducted to probe the origin of this lowered efficiency for coupling of primary alkyl electrophiles. The coupling of 2-phenylethyl-I with octylMgCl was chosen so that all expected side products could be easily determined by GC and GC/MS. 1.2 equivalent of Grignard reagent was used to ensure a high conversion. The reaction time was 30 minutes. Table 13 shows the results.

Table 13. Kumada coupling of primary alkyl iodides^a

Entry	Catalyst	Octene	Ethyl-benzene	Styrene	Phenyl-ethyl-I	Phenyl-ethyl-Cl	Oct-Oct	(Phenyl-Ethyl) ₂	C ₆ H ₅ C ₂ H ₄ -Oct
1	no	0	0	27	3	58	0	0	0
2	1	7	2	2	0	0	4	7	85
3	24	5	0	20	0	23	13	16	29
4	27	12	3	7	0	<1	18	24	41

^a 0.6 mmol (1.2 equiv) of octyl-MgCl in THF (2 M) was added dropwise to a DMA (0.75 mL) solution of Ni Cat. (3 mol%) and the alkyl halide (0.5 mmol) at -20 °C. After addition, the reaction mixture was further stirred for 30 min at -20 °C and then the solution was taken out from the cooling system and stirred for 10 min to warm up to room temperature.

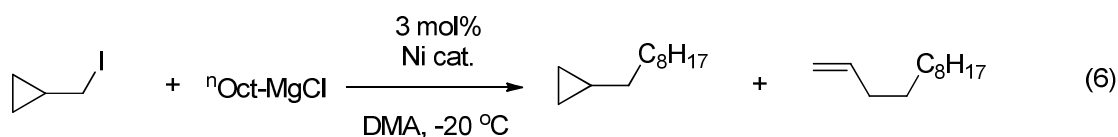
When the coupling was conducted without a catalyst, we found that 97 % of β -phenylethyl-I reacted (entry 1, Table 13). The main product was β -phenylethyl-Cl, possibly formed via a I/Cl exchange reaction with octyl-MgCl. Base-mediated elimination was severe, and 27 % of styrene was formed. These background reactions needed to be overcome for a successful cross coupling. With catalyst **1**, the productive cross coupling was rapid and efficient, and out-competed the non-catalytic side reactions (entry 2, Table 13). A 85 % coupling yield was achieved. With catalyst **24**, the cross coupling was not sufficiently rapid, and the non-catalytic side reactions were significant (entry 3, Table 13). The I/Cl exchange reaction was only partially attenuated, giving β -phenylethyl-Cl in a 23 % yield. Base-mediated elimination was also severe, and 20 % of styrene was formed. In addition, homo-coupling was noticeable. The yield of cross coupling was a low 29 %. With catalyst **27**, the cross coupling was fast enough to suppress the non-catalytic side reactions (entry 4, Table 13). However, homo-coupling marred the efficiency of cross coupling (41 %).

The results in table 13 show that for coupling of primary alkyl iodides, the activity has the order of **1** > **27** > **24**. Complex **24** was not active enough, and non-catalytic side reactions prevailed. Complex **27** was sufficiently active, but its efficiency suffers from significant homo-coupling. As a result, neither **24** nor **27** is a good catalyst for the coupling of primary alkyl halides. These two catalysts are thus best suited for coupling of secondary alkyl electrophiles. Fortunately, complex **1** is an excellent catalyst for the coupling of primary substrates. A combination of these three catalysts can cover a wide range of substrates.

2.4 Radical clock

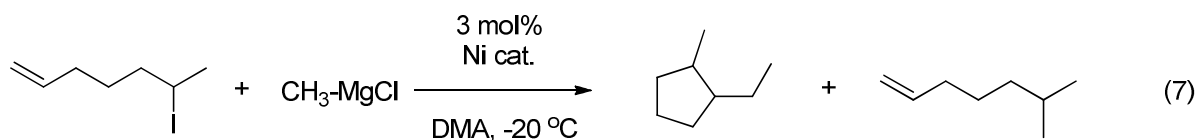
Our group reported earlier that activation of alkyl halides using catalyst **1** occurred via a radical mechanism. To ascertain that this is the case for catalysis using complex **24** and **27**,

we carried out coupling reactions using a radical clock, cyclopropylmethyl iodide (eq. 6, Scheme 15). Despite that the overall coupling yields for this primary alkyl iodide were again modest (*vide supra*), the distribution of coupling products gave insight into the activation process of the substrates. Both ring-closed and ring-opened products were observed with both catalysts, and the ring-opened products dominated. These results confirmed that the activation of primary alkyl halide takes place via an alkyl radical intermediate. The recombination of the primary carbon radical with the catalyst has a rate that is slightly lower than the ring-opening rearrangement of cyclopropyl-methyl radical, which has a first-order rate constant of about 10^8 s^{-1} .⁵⁸



Yields:

catalyst 24 : 8 %	32 %
catalyst 27 : 12 %	30 %



Yields:

catalyst 24 : 38 %	trace
catalyst 27 : 30 %	trace

Scheme 15. Alkyl-alkyl Kumada coupling reactions using radical clocks.

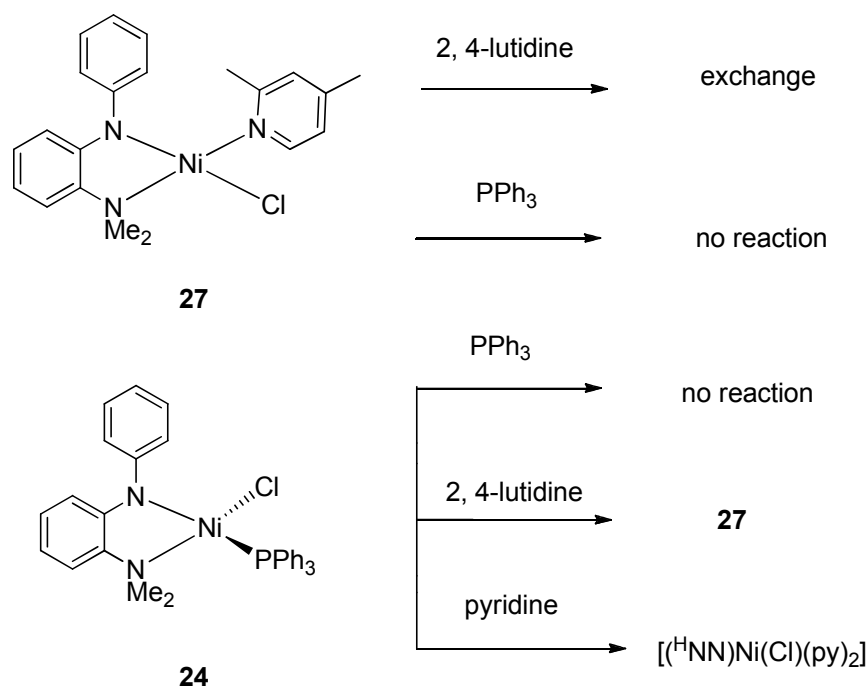
A similar radical clock reaction was carried out with a secondary alkyl halide, 6-iodohept-1-ene (eq. 7, Scheme 15). Using **24** or **27** as the catalyst, the coupling with CH_3MgCl yielded the ring-closed product, 1-ethyl-2-methylcyclopentane, in yield of about 30 %. The direct coupling product, 6-methylhept-1-ene, was produced in trace. Thus, the recombination of this acyclic secondary carbon radical with the catalyst is slower than the ring-closing rearrangement of the hept-6-en-2-radical, which has a first-order rate constant of about 10^5 s^{-1} .

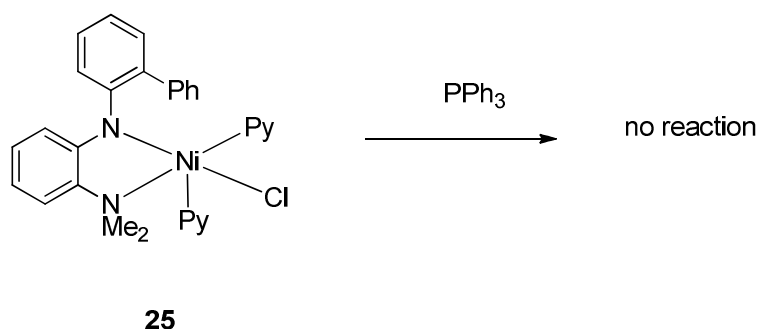
2.5 Substitution reactions for complexes **24**, **25**, and **27**

Precatalysts **24**, **25**, and **27** have tetrahedral, square-pyramidal, and square-planar structures, respectively. Unlike the pincer complex **1**, the pyridine, PPh₃, and lutidine ligands in these complexes might be subject to dissociation and ligand substitution during catalysis. To probe the stability of these complexes towards external donor ligands, substitution reactions were carried out.

The lutidine ligand in complex **27** could not be substituted by PPh₃, and the complex did not react with extra lutidine to form a 5-coordinate species (Scheme 16). However, the lutidine ligand could exchange with external lutidine. On the contrary, the PPh₃ ligand in **24** was prone to substitution (Scheme 16). It reacted with 2,4-lutidine to form **27** quantitatively. It also reacted with pyridine, likely forming a 5-coordinate complex like **25**, according to NMR. It either did not undergo exchange reaction with PPh₃ or the exchange was too slow to be observed by NMR. Complex **25**, on the other hand, did not react with PPh₃.

The substitution reactions showed that pyridine and lutidine ligands bind more strongly than PPh₃ for the Ni-bidentate ligand system. Because ligand substitution can occur either via associate or dissociate mechanism, the formation of 3-coordinate species from **24** and **27** in the substitution and exchanges reactions could not be definitely confirmed.



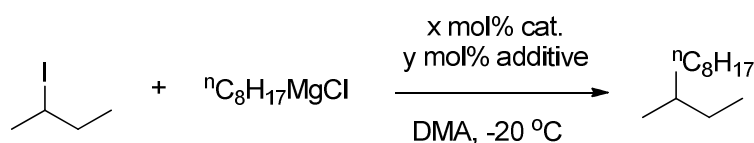


Scheme 16. Ligand substitution reactions of complexes **24**, **25**, and **27**.

2.6 Inhibition study for pre-catalysts **24** and **27**

As shown in Table 14, addition of an excess amount of PPh_3 or 2,4-lutidine decreased both the conversions and the coupling yields for precatalyst **24** and **27**. The more PPh_3 or 2,4-lutidine added, the lower the conversions and yields (compare entries 2 and 3, and 6 and 7, Table 14). These results suggest that PPh_3 and 2,4-lutidine ligands in **24** and **27** dissociate from the Ni centers to form species with lower coordination numbers during catalysis. Addition of PPh_3 or 2,4-lutidine decreases the concentrations of these species, and thus diminishes the efficiency of catalysis. The effect of this addition should be similar to that of decreasing the loading of the catalysts. Indeed, a lower loading of catalysts led to lower conversions and yields (entries 4 and 8, Table 14).

Table 14. Inhibition study for catalysis by **24** and **27**^a



Entry	Cat.	x	Additive	y	Conversion (%)	Yield (%)
1	24	3			100	77
2	24	3	PPh_3	15	96	42
3	24	3	PPh_3	30	60	37
4	24	0.6			41	12
5	27	3			100	62
6	27	3	2,4-lutidine	15	83	36

Table 14. (Continued)

Entry	Cat.	x	Additive	y	Conversion (%)	Yield (%)
7	27	3	2,4-lutidine	30	60	18
8	27	0.6			92	18

^a Same conditions as in Table 3, except that the Grignard reagent was added at once.

2.7 Discussion

2.7.1 Synthesis of Ni complexes

The earlier reported pincer complex **1** was not very efficient for the coupling of secondary alkyl halides. We hypothesized that it was due to the steric encumbrance of the pincer ligand **2** on a square-planar Ni(II) ion. Ligands **3** and **4** were therefore synthesized in aim to reduce the steric hindrance of the ligands. Ligand **5** was synthesized for the same purpose, assuming that the alkyl amine donor might be hemilabile. Their synthesis and metallation were straightforward, in accordance with the well-known excellent chelating properties of pincer-type ligands.³³ While **3** and **4** could serve as trianionic ligands, they were purposely employed as a mono-anionic bis(amino)amide ligand via selective lithiation. The corresponding Ni complexes **19**, **20** and **21** have structures similar to **1**. Ligand **6** is di-anionic amino-amide system. By changing the ligand's electronic and steric properties, the resulting Ni complex may bring some new insight into the coupling reactions.

We thought that in ligands **2-6**, the electronic property was dictated by both amino and amido donors. Bidentate ligands **7-9** were then prepared as a new class of mixed amine-amide ligands. Combining them with another mono-dentate ligand could lead to a wider control in the steric and electronic properties of ligands, while mimicking the main characters of pincer ligands **2**. However, it turned out that metallation of bidentate ligands was not trivial, and the originally targeted products, square-planar Ni(II) complexes, could only be accessed employing NiCl₂(2,4-lutidine)₂ as the Ni precursor. The use of other Ni salts resulted in various Ni complexes with tetrahedral or square pyramidal geometries.

2.7.2 Alkyl-alkyl Kumada coupling using preformed Ni complexes

Having many defined and structurally characterized Ni complexes in hand, we carried out a structure-activity study for alkyl-alkyl Kumada coupling reactions. As complex **1** was efficient for the coupling of primary but not secondary alkyl halides, we focused on the

coupling of secondary alkyl iodides. Two representative reactions, coupling of 2-butyl iodide with octylMgCl (Table 3, eq 1), and coupling of cyclohexyl iodide with butylMgCl (Table 3, eq 2), were used as test reactions for Ni complexes **1**, **19-31**. Pincer complex **1** and **21** had a low efficiency, and **19**, **20**, **22** and **31** had no efficiency. Most of the substrates remained intact after the reactions. Complexes **19** and **20** have protons as substituents on the amino donors which might be cleaved upon addition of basic Grignard reagents, leading to decomposition of the complexes. This might explain why they were completely inactive. The structure of complex **21** is similar to **1**, and its skeleton is potentially more flexible and hemilabile, however its coupling yield of cyclohexyl iodide is slightly lower than **1**. The coupling of octyl iodide was also tested, the yield was similar to **1**.³⁴ This suggests that the alkyl amine side arm remains coordinated during catalysis. Complex **22** contains di-anionic ligand with 2,4-lutidine occupying the fourth position. Complex **23** is tetrahedral and has a Ni center coordinated by two molecules of bidentate ligand **8**. Compound **22** and **23** were not catalytically active. We showed earlier that transmetalation of an alkyl group from the Grignard reagent to the Ni-halide was a key step in alkyl-alkyl coupling by catalyst **1** (Scheme 1). The inactivity of **22** and **23** might be attributed to the lack of a site for transmetallation. Complexes **24-30** all have such a site and they were indeed active for the cross coupling reactions. As shown in Table 3 and Figure 18, they performed better than complex **1** in the test reactions. The catalytic efficiency is slightly different between the chloride complex **27** and the triflate complex **30**, but the origin of the difference is hard to clarify. The carbene complex **31** [$(^H\text{NN})\text{Ni}(\text{dmly})\text{I}$] was not active even though it had a Ni-I bond that was amenable for transmetalation. This was probably due to a significant change in the electronic and steric property of the nickel complex resulted from coordination of the carbene ligand. Such a complex is no longer active for the alkyl-alkyl Kumada coupling reactions of secondary alkyl halides, highlighting the importance of ligand electronic and steric properties for these coupling reactions.

Selected catalysts (**1**, **24**, **26-29**) were further tested for the coupling of a wide range of secondary alkyl halides (Tables 3, 5, 8 and 11). Analysis of the results shown in Tables 3 and 5 indicates that coordination number has a noticeable influence on the performance of these catalysts. Five-coordinate complexes **25** and **26** were less efficient than four-coordinate complexes **24** and **27-29**, indicated by lower conversion of the substrates. This could be explained considering that even if one pyridine ligand in **25** and **26** dissociates, the resulting 4-coordinate species are still less active than the 3-coordinate species from **27-29**. On the other hand, spin-state of the precatalysts has at most a small influence. Paramagnetic catalyst

24 is only slightly inferior to the diamagnetic catalysts **27-29** and is significantly more active than diamagnetic **1**.

Complexes **27-29** differ only in the substituents on the bidentate ligands. It was then possible to examine the electro-steric effects of the ligands using these complexes. The bulk of the ligands is in the order of **27** < **28** < **29**, but the efficiency of the catalysis follows the opposite order, **27** > **28** > **29**. Thus, a less bulky ligand is better for the coupling of secondary alkyl halides. Considering on the other hand the donor property of ligands, the Ni center in **28** is more electron rich than in **27** which is more electron rich than in **29**. This is not the order of catalytic efficiency. Therefore, steric instead of electronic factor dictates the performance of catalysts **27-29**. The efficiency of the catalysts correlates inversely with the yields of elimination products (Tables 7). Assuming that such products arise from metal-mediated beta-H elimination, the results suggest that a bulkier ligand favors β -H elimination through steric pressure.

Precatalysts **24** and **27** differ in one ligand (PPh₃ versus 2,4-lutidine), coordination geometry (tetrahedral versus squareplanar), and spin state (paramagnetic versus diamagnetic). Despite these differences, their catalytic efficiencies are similar. The ligand substitution reactions, and particularly the inhibition studies, showed that the PPh₃ and lutidine ligands dissociated from the Ni centers to form the same active catalyst. The small difference in catalytic performance is then attributed to the different reaction rates and equilibrium constants for ligand dissociation. Also, complex **31** was successfully synthesized through the substitution of PPh₃ with carbene ligand dmiy from complex **24**. However, **31** had no efficiency for coupling of secondary alkyl halides and low efficiency for primary alkyl halides.³⁵ It is possible that the carbene ligand bonds to the nickel so well that it cannot dissociate from the nickel center to form the active three-coordinate Ni intermediate. And compared to the NMe₂ arm of **2** (^{Me}N₂N), the dimy ligand is bigger. As a result, **31** had no efficiency for the coupling of secondary alkyl halides and low efficiency for coupling of primary alkyl halides.

Compared to pincer complex **1**, complexes **24** and **27** are less efficient for coupling of primary alkyl halides, but much more efficient for coupling of secondary alkyl halides. The origin of this contrast in efficiency is probably related to the fact that with complex **1**, no ligand dissociates from the Ni center; with complexes **24** and **27**, the PPh₃ and lutidine ligands dissociate readily during catalysis.

For primary alkyl iodides, a main challenge for cross coupling is the noncatalytic side reactions such as I/Cl exchange and base-mediated elimination (Table 13). These side

reactions are rapid, and to be efficient, a catalyst needs to activate the substrate quickly. The 4-coordinate catalytically active species from **1** is electron-rich, and has a high activity toward primary alkyl halides. For complexes **24** and **27**, the *in situ* generated 3-coordinate active species are less electron-rich, and react more slowly with primary alkyl halides. Using precatalyst **24**, the activation of alkyl halides is not fast enough to compete with noncatalytic side reactions. For catalyst **27**, the activation of alkyl halides is sufficiently fast, but homocoupling is severe and the overall efficiency drops. As the coupling takes place via an alkyl radical, the homocoupling products probably originate from bimolecular combination of the radicals.

The situation is different for the coupling of secondary alkyl halides. Activation of secondary substrates is slower than for primary substrates due to steric constraints. However, noncatalytic side reactions are no longer a problem (Table 10). Furthermore, bimolecular combination of secondary alkyl radicals is slow, so homocoupling does not present a problem. Likely for steric reason, complex **1** has a very low activity for secondary substrates and is therefore not a good catalyst. For complexes **24** and **27**, after the PPh₃ and 2,4-lutidine ligands dissociate, the resulting 3-coordinate species can activate secondary substrates in an appreciable rate (albeit slower than with primary substrates). The various Ni alkyl species involved in the coupling now suffer more from β -H elimination due to a more open Ni center. In these cases, some olefinic products were formed. For precatalyst **24**, β -H elimination appears to be more facile and a substantial amount of olefin is produced. For this reason, **24** gives a cross-coupling yield of 50-70% for secondary substrates. Fortunately, a good compromise was found in precatalyst **27** so that only a small amount of olefin is produced in the coupling reactions. It thus becomes a very good catalyst.

Dissociation of PPh₃ and lutidine from precatalysts **24** and **27** gives the same 3-coordinate Ni-Cl species. Yet, the catalytic performance of **24** and **27** is sometimes quite different. This difference might be attributed to the different reaction rates and equilibrium constants for ligand dissociation. Similar observations have been made in a series of Pd-PEPPSI complexes.³⁶ Some of the complexes differ only in the fourth pyridinyl ligand, which is shown to dissociate during catalysis. The catalytic performance of these complexes varies.³⁴ The overall catalytic cycle for reactions catalyzed by **24** and **27** should be similar to the one shown in Scheme 1. Transmetalation of a 3-coordinate Ni-halide species produces the corresponding Ni alkyl species, which reacts with an alkyl halide to give the coupling product. The results from coupling reactions of radical probe type-substrates indicate that the activation of alkyl halide occurs via a radical mechanism.

2.8 Conclusions

In summary, we describe here a structure-activity study for Ni-catalyzed alkyl-alkyl Kumada coupling. A large number of Ni(II) complexes with tridentate and bidentate mixed amino-amide ligands were prepared and structurally characterized. The complexes of the bidentate ligands span a wide range of coordination numbers, geometries, and spin states. The rich coordination chemistry of Ni with these bidentate ligands points to the difficulty in identifying catalytically active species in many Ni catalyzed cross coupling reactions, where the catalysts are mixtures of Ni salts and ligands. Such problems can be alleviated by using pre-formed and well-defined coordination compounds as catalysts.

Compared to the previously reported pincer complex, $[(^{\text{Me}}\text{N}_2\text{N})\text{NiCl}]$ (**1**), the newly prepared Ni complexes with the bidentate ligands are better catalysts for the coupling of secondary alkyl halides, as long as they contain one transmetalation site. Four-coordinate compounds are more efficient than five-coordinate compounds. Within the same series of compounds, the efficiency of the catalysis improves with a more open Ni center. Coordination geometry and spin state seem to have little influence.

For Kumada coupling of secondary alkyl halides, two excellent catalysts have been developed. Tetrahedral complex $[(^{\text{H}}\text{NN})\text{Ni}(\text{PPh}_3)\text{Cl}]$ (**24**) is the best catalyst for coupling of bulky acyclic secondary alkyl iodides, with yields of 46 – 65 %. Square-planar complex $[(^{\text{H}}\text{NN})\text{Ni}(\text{2,4-lutidine})\text{Cl}]$ (**27**) is the best catalyst for coupling of cyclic and less bulky acyclic secondary alkyl iodides and bromides. A wide scope has been achieved using this catalyst, with typical yields of 60 - 87 %. The origin of the efficiency was thoroughly probed and was related to the steric property of the catalysts. To the best of our knowledge, these two complexes are the most efficient catalysts for alkyl-alkyl Kumada coupling of non-activated secondary alkyl halides.

2.9 Experimental section

2.9.1 Chemicals and Reagents

All manipulations were carried out under an inert $\text{N}_2(\text{g})$ atmosphere using standard Schlenk or glovebox techniques. Solvents were purified using a two-column solid-state purification system (Innovative Technology, NJ, USA) and transferred to the glove box without exposure to air. Deuterated solvents were purchased from Cambridge Isotope Laboratories, Inc., and were degassed and stored over activated 3 Å molecular sieves. Unless otherwise noted, all other reagents and starting materials were purchased from commercial

sources and used without further purification. Liquid compounds were degassed by standard freeze-pump-thaw procedures prior to use. Ligand $^{\text{Mc}}\text{NN}_2\text{H}$ and complex $[(^{\text{Mc}}\text{NN}_2)\text{NiCl}]$ (**1**) were prepared as described previously.²² The following chemicals were prepared according to literature procedures: $\text{NiCl}_2(2,4\text{-lutidine})_2$,³⁷ $\text{NiCl}(\text{THF})_{1.5}$,³⁸ $\text{NiCl}_2(\text{PPh}_3)_2$,³⁹ $\text{NiCl}_2(\text{py})_4$, $\text{NiCl}_2(4\text{-picoline})_4$,⁴⁰ 3-iodopentane,¹⁴ iodocycloheptane,⁴¹ 6-iodo-1-heptene.⁴²

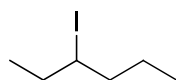
2.9.2 Physical methods

The ^1H and ^{13}C NMR spectra were recorded at 293 K on a Bruker Avance 400 spectrometer. ^1H NMR chemical shifts were referenced to residual solvent as determined relative to Me_4Si ($\delta = 0$ ppm). The $^{13}\text{C}\{^1\text{H}\}$ chemical shifts were reported in ppm relative to the carbon resonance of CDCl_3 (77.0 ppm), C_6D_6 (128.0 ppm), CD_3CN (1.3 ppm) or $\text{THF-}d_8$ (25.3 ppm). GC-MS measurements were conducted on a Perkin-Elmer Clarus 600 GC equipped with Clarus 600T MS. GC measurement was conducted on a Perkin-Elmer Clarus 400 GC with a FID detector. HRESI-MS measurements were conducted at the EPFL ISIC Mass Spectrometry Service with a Micro Mass QTOF Ultima spectrometer. Elemental analyses were performed on a Carlo Erba EA 1110 CHN instrument at EPFL. The temperature of reactions below room temperature was regulated by a Julabo FT-902 chiller. X-ray diffraction studies were carried out in the EPFL Crystallographic Facility. Data collections were performed at low temperature using four-circle kappa diffractometers equipped with CCD detectors. Data were reduced and then corrected for absorption.⁴³ Solution, refinement and geometrical calculations for all crystal structures were performed by SHELXTL.⁴⁴

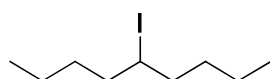
2.9.3 Synthetic methods

General procedure for preparing substrates

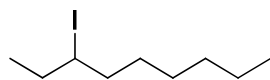
Triphenylphosphine (1.4 equiv) and imidazole (1.4 equiv) were dissolved in dry dichloromethane (200 mL). This solution was cooled with ice-water bath, and iodine (1.4 equiv) was added per small portions. Then the alcohol was added dropwise to the above solution. The mixture was allowed to warm to room temperature, and it was stirred overnight. Next, hexane was added, and the solids were removed by passing the mixture through silica gel (hexane washing). The solvent was removed on a rotary evaporator, and the residue was purified by flash chromatography using hexane as eluant.



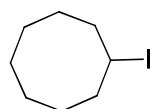
3-Iodohexane. This compound was prepared according to the general procedure from 3-hexanol (100 mmol, 10.22 g). The product was obtained as a colorless oil (13.22 g, 62 %). ^1H NMR (400 MHz, CDCl_3): 4.05-4.16 (m, 1H), 1.70-1.95 (m, 3H), 1.49-1.69 (m, 2H), 1.31-1.48 (m, 1H), 1.02 (t, $J = 6.8$ Hz, 3H), 0.92 (t, $J = 6.8$ Hz, 3H). ^{13}C NMR (100 MHz, CDCl_3): 42.4, 42.3, 33.7, 22.8, 14.1, 13.2.⁴⁵



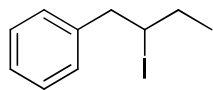
5-Iodononane. This compound was prepared according to the general procedure from 5-nonanol (100 mmol, 14.43 g). The product was obtained as a colorless oil (19.11 g, 75 %). ^1H NMR (400 MHz, CDCl_3): 4.05-4.16 (m, 1H), 1.78-1.92 (m, 2H), 1.60-1.72 (m, 2H), 1.42-1.53 (m, 2H), 1.20-1.42 (m, 6H), 0.90 (t, $J = 6.4$ Hz, 6H). ^{13}C NMR (100 MHz, CDCl_3): 40.4, 40.3, 31.6, 21.9, 13.9.



3-Iodononane. This compound was prepared according to the general procedure from 3-nonanol (100 mmol, 14.43 g). The product was obtained as a colorless oil (21.76 g, 86 %). ^1H NMR (400 MHz, CDCl_3): 4.02-4.13 (m, 1H), 1.61-1.95 (m, 4H), 1.20-1.55 (m, 8H), 1.01 (t, $J = 7.2$ Hz, 3H), 0.88 (t, $J = 7.6$ Hz, 3H). ^{13}C NMR (100 MHz, CDCl_3): 42.6, 40.3, 33.7, 31.7, 29.5, 28.5, 22.6, 14.1, 14.0.



Iodocyclooctane. This compound was prepared according to the general procedure from cyclooctanol (100 mmol, 12.82 g). The product was obtained as colorless oil (17.38 g, 73 %). ^1H NMR (400 MHz, CDCl_3): 4.51-4.63 (m, 1H), 2.17-2.31 (m, 4H), 1.40-1.72 (m, 10H). ^{13}C NMR (100 MHz, CDCl_3): 38.2, 37.9, 27.4, 26.6, 25.1.



(2-iodobutyl)benzene. This compound was prepared according to the general procedure from 1-phenyl-2-butanol (20 mmol, 3.00 g). The product was obtained as colorless oil (4.00 g, 77 %). ^1H NMR (400 MHz, CDCl_3): 7.22-7.43 (m, 5H), 4.25-4.42 (m, 1H), 3.17-3.42 (m, 2H), 1.78-1.88 (m, 2H), 1.12 (t, $J = 6.8$ Hz, 3H). ^{13}C NMR (100 MHz, CDCl_3): 139.8, 128.9, 128.4, 126.7, 47.1, 40.8, 32.5, 14.2.

Synthesis of bis(2-methylaminophenyl)amine ($^{\text{HMe}}\text{N}_2\text{NH}$), **3H**:

To a mixture of bis(2-aminophenyl)amine **9** (4.98 g, 0.025 mol) and paraformaldehyde (7.50 g, 0.246 mol) in MeOH (300 mL) was added a solution of NaOMe (15 mL, 28 wt% in MeOH) dropwise at 0 °C. The mixture was stirred under reflux for 1 h. After addition of NaBH_4 (10.25 g, 0.271 mol), the solution was heated under reflux for 1 h. The reaction mixture was cooled to room temperature. To this mixture, 1 M NaOH (100 mL) was added followed by extraction with DCM (3 \times 200 mL). The combined organic phase was dried over Na_2SO_4 and was filtered. The solvent was removed under vacuum, resulting in a dark liquid which was purified by column chromatography (SiO_2 , hexane:DCM 3:1). Yield: 5.2 g, 73 %. ^1H NMR (400 MHz, CDCl_3): 7.04 (t, $J = 5.8$ Hz, 2H), 6.69-6.74 (m, 6H), 4.86 (br. s, 1H), 3.75 (br. s, 2H), 2.87 (s, 6H). ^{13}C NMR (100 MHz, CDCl_3): 141.8, 130.7, 123.7, 119.7, 117.9, 110.7, 30.8. HR-MS (ESI): calculated for ($\text{C}_{14}\text{H}_{17}\text{N}_3$, $\text{M}+\text{H}$), 228.1501; found, 228.1498. Anal. Calcd for $\text{C}_{14}\text{H}_{17}\text{N}_3$: C, 73.98; H, 7.54; N, 18.49. Found: C, 73.76; H, 7.65; N, 18.41.

Synthesis of bis(2-isopropylaminophenyl)amine ($^{\text{HiPr}}\text{N}_2\text{NH}$), **4H**:

A solution of bis(2-aminophenyl)amine (3.47 g, 17 mmol) was prepared in degassed MeOH (90 mL) under an inert atmosphere. Acetone (2.4 mL, 34 mmol) and HCl (2.8 mL, 37 %) was added. The reaction mixture turned green during the addition of HCl. It was stirred for 30 min at room temperature, followed by careful addition of NaBH_3CN (4.50 g, 72 mmol), then the solution turned red. It was stirred for further 12 h at room temperature. The solvent was removed and the resulting residue was taken up in dichloromethane (400 mL). It was washed with an aqueous solution of sodium dithionite (2 \times 400 mL, 1M), and an aqueous solution of sodium bicarbonate (2 \times 400 mL, 1M). The aqueous phase was extracted with dichloromethane (2 \times 300 mL). The combined organic layers were dried over NaSO_4 and the solvent was removed under vacuum. The brown oil was purified by column chromatography on SiO_2 (Hexane/EtOAc 3:1). Bis(2-isopropylphenyl)amine was obtained as a yellow oil

(2.57 g, 52 %). ^1H NMR (400 MHz, CDCl_3): 7.00 (t, $J = 6.8$ Hz, 2H), 6.75 (t, $J = 8$ Hz, 4H), 6.68 (t, $J = 7.6$ Hz, 2H), 4.94 (br. s, 1H), 3.66 (sept. $J = 6.4$ Hz, 2H), 3.56 (br.s, 2H), 1.21 (d, $J = 6.0$ Hz, 12H). ^{13}C NMR (100 MHz, CDCl_3): 139.86, 131.39, 123.42, 120.36, 117.77, 112.56, 44.24, 23.04. HR-MS (ESI): calculated for ($\text{C}_{18}\text{H}_{25}\text{N}_3$, $\text{M}+\text{H}$), 284.2127; found, 284.2135. Anal. Calcd for $\text{C}_{18}\text{H}_{25}\text{N}_3$: C, 76.28; H, 8.89; N, 14.83. Found: C, 76.41; H, 8.99; N, 15.02.

Synthesis of 2-(2-(dimethylamino)ethyl)-*N,N*-dimethylaniline ($^{\text{Me}}\text{N}^{\text{Me}}\text{N}'\text{NH}$), **5H**:

A 250 mL reaction vessel was charged with $\text{Pd}_2(\text{dba})_3$ (1.36 g, 1.49 mmol), bis(diphenylphosphino)-ferrocene (DPPF) (1.65 g, 2.97 mmol), NaO^tBu (9.84 g, 98 mmol) and toluene (100 mL) under a dinitrogen atmosphere. 2-Bromo-*N,N*-dimethylaniline (14.60 g, 73 mmol) and 2-(dimethylamino)ethylamine (6.42 g, 73 mmol) were added to the reaction mixture. The resulting brown solution was vigorously stirred for 3 days at 100 °C. The solution was then cooled to room temperature and filtered through Celite. Removal of the solvent yielded a black liquid which was then purified by flash chromatography (silica-gel, acetone), and then was distilled under vacuum to afford the product as a light yellow oil. Yield: 9.50 g, 68%. ^1H NMR (400 MHz, CDCl_3): 6.98-7.04 (m, 2H), 6.68 (dt, $J = 7.6$, 1.2 Hz, 1H), 6.62 (d, $J = 8.0$ Hz, 1H), 4.95 (br. s, 1H), 3.21 (q, $J = 6.4$ Hz, 2H), 2.65 (s, 6H), 2.59 (t, $J = 6.4$ Hz, 2H), 2.28 (s, 6H). ^{13}C NMR (100 MHz, CDCl_3): 143.1, 140.3, 124.5, 118.8, 116.3, 109.8, 58.6, 45.5, 43.8, 41.6. HR-MS (ESI): calculated for ($\text{C}_{12}\text{H}_{21}\text{N}_3$, $\text{M}+\text{H}$), 208.1814; found, 208.1810. Anal. Calcd for $\text{C}_{12}\text{H}_{21}\text{N}_3$: C, 69.52; H, 10.21; N, 20.27. Found: C, 69.73; H, 10.21; N, 20.09.

Synthesis of *N,N*-bis(2-methylaminophenyl)methylamine ($^{\text{HMe}}\text{N}_2^{\text{Me}}\text{N}$), **6HH**:

A THF solution (150 mL) of **3H** (9.092 g, 40.0 mmol) was added to KH (1.604 g, 40.0 mmol) by portion. The reaction mixture was stirred for 2 hours at room temperature. After MeI (11.360 g, 80.0 mmol) was added to the above solution and stirred for overnight at room temperature. After removal of the solvent, the residue was added 100 mL water, and extracted with 100 mL \times 3 CH_2Cl_2 . Removal of the solvent yielded the crude product which was then purified by flash chromatography (silica-gel, hexane/ EtOAc 30:1) to afford the product as a white solid. Yield: 8.560 g, 89%. ^1H NMR (400 MHz, CDCl_3): 7.09 (dt, $J = 7.6$, 1.2 Hz, 2H), 7.03 (dd, $J = 7.6$, 1.2 Hz, 2H), 6.63-6.73 (m, 4H), 4.24 (br. s, 2H), 3.03 (s, 3H), 2.85 (d, $J = 5.2$ Hz, 6H). ^{13}C NMR (100 MHz, CDCl_3): 143.3, 136.2, 125.2, 121.6, 116.8, 110.1, 40.6, 30.6. HR-MS (ESI): calculated for ($\text{C}_{15}\text{H}_{19}\text{N}_3$, $\text{M}+\text{H}$), 242.1657; found,

242.1655. Anal. Calcd for $C_{15}H_{19}N_3$: C, 74.65; H, 7.94; N, 17.41. Found: C, 75.02; H, 7.82; N, 17.51.

Synthesis of N^1,N^1 -dimethyl- N^2 -phenylbenzene-1,2-diamine (H NNH), **7H**:

A 250 mL reaction vessel was charged with $Pd_2(dba)_3$ (1.36 g, 1.49 mmol), bis(diphenylphosphino)-ferrocene (DPPF) (1.65 g, 2.97 mmol), NaO^tBu (9.84 g, 98 mmol) and toluene (100 mL) under a dinitrogen atmosphere. 2-Bromo- N,N -dimethylaniline (14.60 g, 73 mmol) and aniline (6.80 g, 73 mmol) were added to the reaction mixture. The resulting brown solution was vigorously stirred for 2 days at 110 °C. The solution was then cooled to room temperature and filtered through Celite. Removal of the solvent yielded a black liquid which was then purified by flash chromatography (silica-gel, hexane/ EtOAc 30:1) to afford the product as a light yellow oil. Yield: 11.23 g, 72%. 1H NMR (400 MHz, $CDCl_3$): 7.34 (d, J = 7.6 Hz, 1H), 7.24 (t, J = 6.6 Hz, 2H), 6.99-7.13 (m, 3H), 6.97 (t, J = 6.8 Hz, 1H), 6.84-6.95 (m, 2H), 6.57 (br. s, 1H), 2.63 (s, 6H). ^{13}C NMR (100 MHz, $CDCl_3$): 142.8, 142.3, 137.8, 129.4, 123.9, 120.6, 119.8, 119.4, 118.0, 114.3, 43.9. HR-MS (ESI): calculated for ($C_{14}H_{16}N_2$, M+H), 213.1392; found, 213.1396. Anal. Calcd for $C_{14}H_{16}N_2$: C, 79.21; H, 7.60; N, 13.20. Found: C, 79.12; H, 8.11; N, 13.55.

Synthesis of N^1,N^1 -dimethyl- N^2 -(*o*-tolyl)benzene-1,2-diamine (Me NNH), **8H**:

It was synthesized in a procedure similar to the one described for (**5**) except that the *o*-toluidine (7.82 g, 73 mmol) instead of aniline was used. Yield 12.50 g, 76%. 1H NMR (400 MHz, $CDCl_3$): 7.33 (d, J = 7.6 Hz, 1H), 6.98-7.21 (m, 4H), 6.84-6.97 (m, 2H), 6.83 (t, J = 7.2 Hz, 1H), 6.42 (br. s, 1H), 2.69 (s, 6H), 2.28 (s, 3H). ^{13}C NMR (100 MHz, $CDCl_3$): 142.1, 141.1, 138.6, 130.8, 128.8, 126.6, 124.0, 121.7, 119.4, 119.3, 118.9, 114.3, 44.0, 17.9. HR-MS (ESI): calculated for ($C_{15}H_{18}N_2$, M+H), 227.1548; found, 227.1540. Anal. Calcd for $C_{15}H_{18}N_2$: C, 79.61; H, 8.02; N, 12.38. Found: C, 79.72; H, 8.18; N, 12.62.

Synthesis of N^1 -([1,1'-biphenyl]-2-yl)- N^2,N^2 -dimethylbenzene-1,2-diamine (Ph NNH), **9H**:

It was synthesized in a procedure similar to the one described for (**7**) except that the 2-aminobiphenyl (12.35 g, 73 mmol) instead of aniline. Yield 15.86 g, 75%. 1H NMR (400 MHz, $CDCl_3$): 7.52 (d, J = 8.0 Hz, 1H), 7.28-7.46 (m, 7H), 6.98-7.06 (m, 3H), 6.84 (t, J = 7.2 Hz, 1H), 6.69 (br.s, 1H), 2.50 (s, 6H). ^{13}C NMR (100 MHz, $CDCl_3$): 142.6, 140.0, 139.3, 138.2, 132.4, 130.8, 129.2, 128.5, 128.1, 127.2, 124.0, 121.0, 119.7, 119.7, 118.1, 114.3,

43.8. HR-MS (ESI): calculated for ($C_{20}H_{20}N_2$, M+H), 289.1705; found, 289.1709. Anal. Calcd for $C_{20}H_{20}N_2$: C, 83.30; H, 8.99; N, 9.71. Found: C, 83.43; H, 7.11; N, 9.11.

Synthesis of Bis(2-nitrophenyl)amine, **10**:

A solution of 1-fluoro-2-nitrobenzene (10.00 g, 70.9 mmol, 1.0 eq), 2-nitroaniline (9.79 g, 70.9 mmol, 1.0 eq.) and K_2CO_3 (11.80 g, 85.1 mmol, 1.2 eq.) was prepared in DMSO (200 mL). The reaction mixture was stirred at 120 °C for 36 h. H_2O was added (100 mL) and the mixture was extracted with DCM (3 x 300 mL). The combined organic layer was washed with a solution of NaCl (4 x 200 mL, 15 %). Bis(2-nitrophenyl)amine was obtained as an orange solid (15.1 g, 82 %). The 1H NMR and ^{13}C NMR data of the product were identical to those described in the literature.⁴⁶

Synthesis of Bis(2-aminophenyl)amine, **11**:

A solution of bis(2-nitrophenyl)amine, **8** (7.50 g, 28.9 mmol, 1.0 eq.) was prepared in EtOAc (80 mL). After catalyst Pd/C (570 mg, 7.6 mol %) was added, the reaction mixture was stirred under a hydrogen atmosphere (1 atm) at room temperature for 24 h. The solution was filtered under a nitrogen atmosphere and the solvent was removed under vacuum. The resulting residue was dissolved in dichloromethane and filtered over Celite under a nitrogen atmosphere. The solvent was removed and bis-(2-aminophenyl)amine was obtained as a light yellow solid (5.78 g, 99 %). The 1H NMR data of the product were identical to those described in the literature.⁴⁷

Synthesis of $^{HMe}N_2NLi$, **12**:

A solution of bis(2-methylaminophenyl)amine (0.640 g, 2.82 mmol) was prepared in benzene (20 mL) under an inert atmosphere. A solution of nBuLi (1.6 M in hexane, 1.76 mL, 2.82 mmol) was added carefully. The solution turned green. The reaction mixture was stirred for 1 h at room temperature, followed by the removal of the solvent under vacuum. Yields: 0.468 g, 73 %. 1H NMR (400 MHz, C_6D_6): 7.38 (d, $J = 7.6$ Hz, 2H), 7.14 (s, 2H), 7.02 (t, $J = 5.6$ Hz, 2H), 6.65-6.70 (m, 4H), 2.03 (s, 6H). The as-prepared sample contains a small amount of unidentified impurities that are difficult to remove, but it can be used without further purification to make the Ni complex.

Synthesis of ^{HiPr}N₂NLi, **13**:

A solution of bis(2-isopropylaminophenyl)amine (0.952 g, 3.36 mmol) was prepared in toluene (15 mL) under an inert atmosphere. A solution of ⁿBuLi (1.6 M in hexane, 2.20 mL, 3.52 mmol) was added carefully. The solution turned green. The reaction mixture was stirred for 16 h at room temperature, followed by removal of the solvent under vacuum. Pentane was added (15 mL) to dissolve the impurities. The product was filtered and dried under vacuum. The lithium salt was obtained as light green solid (0.672 g, 69%). X-ray quality crystals were obtained by slow evaporation of a concentrated benzene solution. ¹H NMR (400 MHz, C₆D₆): 7.32 (d, *J* = 7.6 Hz, 2H), 7.02 (t, *J* = 6.8 Hz, 2H), 6.86 (t, *J* = 7.2 Hz, 2H), 6.65 (t, *J* = 6.8 Hz, 2H), 2.97-3.17 (m, 2H), 2.24 (br.s, 2H), 0.75 (d, *J* = 4.8 Hz, 12H). Anal. Calcd for C₃₆H₄₈Li₂N₆: C, 74.72; H, 8.36; N, 14.52. Found: C, 74.45; H, 8.55; N, 14.65.

Synthesis of ^HNNLi, **14**:

A solution of **7H** (4.246 g, 20.0 mmol) was prepared in benzene (60 mL) under an inert atmosphere. A solution of ⁿBuLi (1.6 M in hexane, 13.1 mL, 21.0 mmol) was added carefully. The reaction mixture was stirred for 1 h at room temperature, followed by partial removal of solvent under vacuum. Pentane was added (15 mL) to precipitate the product. The product was filtered and dried under vacuum (3.530 g, 81%). ¹H NMR (400 MHz, CD₃CN): 7.16 (d, *J* = 8 Hz, 1H), 6.75-6.95 (m, 5H), 6.68 (t, *J* = 6.8 Hz, 1H), 6.12-6.32 (m, 2H), 2.53 (s, 6H). ¹³C NMR (100 MHz, CD₃CN): 157.9, 153.2, 144.6, 129.6, 126.1, 119.9, 119.1, 114, 6, 113.3, 112.3, 45.3. Anal. Calcd for C₂₈H₃₀Li₂N₄: C, 77.05; H, 6.93; N, 12.84. Found: C, 77.48; H, 7.02; N, 12.40.

Synthesis of ^{Me}NNLi, **15**:

It was synthesized in a procedure similar to the one described for **14** except that the following quantities of reagents were used: **8H** (4.266g, 18.9 mmol), ⁿBuLi (1.6 M in hexane, 12.4 mL, 19.8 mmol), benzene (53 mL). Yield: 2.603g (59%). Diffusion of pentane into a benzene solution of **13** afforded colourless crystals suitable for X-ray analysis. ¹H NMR (400 MHz, CD₃CN): 6.95-7.10 (m, 2H), 6.93 (d, *J* = 7.2 Hz, 1H), 6.85 (t, *J* = 6.8 Hz, 1H), 6.76 (d, *J* = 7.2 Hz, 1H), 6.67 (t, *J* = 7.2 Hz, 1H), 6.36 (t, *J* = 6.8 Hz, 1H), 6.17 (t, *J* = 6.8 Hz, 1H), 2.60 (s, 6H), 2.12 (s, 3H). ¹³C NMR (100 MHz, CD₃CN): 157.2, 154.4, 143.8, 131.1, 129.2, 127.0, 126.2, 119.5, 114.8, 114.6, 110.9, 45.2, 19.8. Anal. Calcd for C₃₀H₃₀Li₂N₄: C, 77.57; H, 7.38; N, 12.06. Found: C, 77.55; H, 8.05; N, 12.08.

Synthesis of $^{\text{Ph}}\text{NNLi}$, **16**:

It was synthesized in a procedure similar to the one described for **14** except that the following quantities of reagents were used: **9H** (3.071 g, 10.7 mmol), $^n\text{BuLi}$ (1.6 M in hexane, 7.0 mL, 11.2 mmol), benzene (30 mL). Yield: 2.650 g (84%). ^1H NMR (400 MHz, CD_3CN): 7.49 (d, $J = 7.2$ Hz, 2H), 7.29 (t, $J = 7.2$ Hz, 2H), 7.05-7.20 (m, 2H), 7.02 (d, $J = 7.2$ Hz, 1H), 6.96 (d, $J = 8$ Hz, 1H), 6.80-6.92 (m, 2H), 6.67 (t, $J = 7.2$ Hz, 1H), 6.40 (t, $J = 6.8$ Hz, 1H), 6.16 (t, $J = 6.8$ Hz, 1H), 2.41 (s, 6H). ^{13}C NMR (100 MHz, CD_3CN): 156.7, 154.6, 144.8, 144.6, 133.1, 131.7, 130.1, 129.0, 128.8, 126.2, 126.1, 119.4, 119.0, 115.9, 114.5, 111.9, 45.1. Anal. Calcd for $\text{C}_{40}\text{H}_{38}\text{Li}_2\text{N}_4$: C, 81.62; H, 6.51; N, 9.52. Found: C, 82.15; H, 6.59; N, 9.03.

Synthesis of $[(^{\text{Ph}}\text{NN})\text{Li}(\text{THF})_2]$, **17**:

A solution of **9H** (0.288 g, 1.0 mmol) was prepared in THF (3 mL) under an inert atmosphere. A solution of $^n\text{BuLi}$ (1.6 M in hexane, 0.7 mL, 1.1 mmol) was added carefully. The reaction mixture was stirred for 1 h at room temperature, followed by removal of the solvent under vacuum. The solid residue was recrystallized from THF/pentane (1:6) at -26 $^{\circ}\text{C}$. Yield: 0.250 g, 57 %. Alternatively, dissolution of complex **16** in THF produced the same product, as shown by NMR. And Diffusion of pentane into a THF solution of **16** at -26 $^{\circ}\text{C}$ afforded colourless crystals of **17** suitable for X-ray analysis. ^1H NMR (400 MHz, $\text{THF}-d_8$): 7.56 (d, $J = 7.6$ Hz, 2H), 7.15 (t, $J = 7.6$ Hz, 2H), 7.08 (t, $J = 9.2$ Hz, 2H), 7.01 (t, $J = 7.6$ Hz, 1H), 6.91 (d, $J = 8$ Hz, 1H), 6.78-6.83 (m, 2H), 6.64 (t, $J = 7.2$ Hz, 1H), 6.40 (t, $J = 7.2$ Hz, 1H), 6.09 (t, $J = 7.6$ Hz, 1H), 2.48 (s, 6H). ^{13}C NMR (100 MHz, $\text{THF}-d_8$): 157.6, 155.6, 145.3, 143.6, 133.4, 131.6, 129.9, 128.4, 128.2, 126.4, 125.5, 121.9, 118.4, 116.5, 115.3, 111.1, 68.3, 45.3, 26.4. Anal. Calcd for $\text{C}_{28}\text{H}_{35}\text{LiN}_2\text{O}_2$: C, 76.69; H, 8.04; N, 6.39. Found: C, 76.79; H, 8.14; N, 6.59.

Synthesis of $[(^{\text{Ph}}\text{NN})\text{MgCl}(\text{THF})_2]$, **18**:

A 2.0 M solution of EtMgCl in THF (1.0 mL, 2.0 mmol) was added to a solution of **9H** (0.577g, 2.0 mmol) in THF (10 mL) under stirring. After 1 h, the solvent was evaporated and the solid residue was dissolved in a minimum quantity of benzene and filtered. Pentane was added to the filtrate and a precipitate was formed. The precipitate was collected, washed with pentane, and dried under vacuum (0.597 g, 71%). Diffusion of pentane into a benzene solution of **16** afforded colourless crystals suitable for X-ray analysis. ^1H NMR (400 MHz, C_6D_6): 7.50-7.70 (m, 4H), 7.20-7.40 (m, 2H), 6.92-7.07 (m, 4H), 6.84 (d, $J = 7.2$ Hz, 1H),

6.73 (t, $J = 7.6$ Hz, 1H), 6.43 (t, $J = 7.2$ Hz, 1H), 3.61 (br.s, 4H), 2.46 (br.s, 6H), 1.23 (br.s, 4H). The as-prepared sample contains a small amount of THF that was difficult to remove.

Synthesis of [$(^{\text{HMe}}\text{N}_2\text{N})\text{NiCl}$], **19**:

$^n\text{BuLi}$ (2.5 mmol, 1.6 M in hexane) was slowly added to a THF solution (20 mL) of the ligand $\text{H}^{\text{HMe}}\text{N}_2\text{N}$ (0.569 g, 2.5 mmol) at room temperature. The reaction mixture was stirred for 1 h, and then this solution was added into a solution of $\text{NiCl}_2(\text{dme})$ (0.550 g, 2.5 mmol, dme = dimethoxyethane) in THF (10 mL). The resulting solution was stirred overnight and then evaporated in vacuum. The residue was extracted with CH_2Cl_2 (20 mL), and then was concentrated to *ca.* 5 mL. Addition of pentane (20 mL) afforded a green precipitate, which was filtered, washed with additional pentane, and dried *in vacuo*. Yield: 0.630g (70%). Diffusion of pentane into a dichloromethane solution of **19** afforded green needle crystals suitable for X-ray analysis. ^1H NMR (400 MHz, CDCl_3): 7.27 (d, $J = 8.0$ Hz, 1H), 7.01 (t, $J = 7.2$ Hz, 1H), 6.96 (d, $J = 8.4$ Hz, 1H), 6.84-6.90 (m, 2H), 6.77 (d, $J = 7.6$ Hz, 1H), 6.39-6.50 (m, 2H), 5.30 (s, 1H), 3.28-3.39 (m, 1H), 3.01-3.13 (m, 1H), 2.76-2.86 (m, 16H). ^{13}C NMR (100 MHz, CDCl_3): 149.01, 148.66, 140.26, 139.75, 128.35, 127.93, 123.76, 123.34, 115.58, 115.28, 113.89, 113.42, 42.22, 41.02. Anal. Calcd for $\text{C}_{14.5}\text{H}_{15}\text{Cl}_2\text{N}_3\text{Ni}$: C, 48.26; H, 4.19; N, 11.64. Found: C, 48.15; H, 4.54; N, 11.53.

Synthesis of [$(^{\text{HiPr}}\text{N}_2\text{N})\text{NiCl}$], **20**:

A THF solution (10 mL) of **13** (0.132 g, 0.6 mmol) was added to a THF suspension (2 mL) of $\text{NiCl}_2(\text{dme})$ (0.174 g, 0.6mmol). The reaction mixture was stirred overnight at room temperature. After removal of solvent, the residue was extracted with CH_2Cl_2 (10 mL), and then was concentrated to *ca.* 5 mL. Addition of pentane (30 mL) afforded a green precipitate, which was filtered, washed with additional pentane, and dried *in vacuo*. Yield: 0.136g (60 %). Diffusion of pentane into a dichloromethane solution of **20** afforded green needle crystals suitable for X-ray analysis. ^1H NMR (400 MHz, CDCl_3): 7.22 (d, $J = 8.4$ Hz), 7.14 (d, $J = 8$ Hz)] (total 2H), 6.94-6.98 (m, 2H), 6.76 (d, $J = 7.2$ Hz, 2H), [6.42 (t, $J = 6.8$ Hz), 6.35 (t, $J = 7.2$ Hz)] (total 2H), [3.91 (sept., $J = 6.4$ Hz), 3.66 (sept., $J = 6$ Hz)] (total 2H), [3.04 (s), 2.85 (s)] (total 2H), [1.78 (d, $J = 6.4$ Hz), 1.73 (d, $J = 6.4$ Hz)] (total 6H), [1.54 (d, $J = 6.4$ Hz), 1.33 (d, $J = 6.4$ Hz)] (total 6H). ^{13}C NMR (100 MHz, CDCl_3): 151.63, 150.25, 135.92, 134.89, 128.15, 127.96, 125.47, 125.42, 114.56, 114.53, 113.94, 112.83, 54.99, 23.18, 22.31, 19.89. Anal. Calcd for $\text{C}_{18}\text{H}_{24}\text{ClN}_3\text{Ni}$: C, 57.41; H, 6.42; N, 11.16. Found: C, 57.18; H, 6.69; N, 11.02.

Synthesis of $[(^{\text{Me}}\text{N}^{\text{Me}}\text{N}'\text{N})\text{NiCl}]$, **21**:

$^n\text{BuLi}$ (16 mmol, 1.6 M in hexane) was slowly added to a THF solution (150 mL) of the ligand HNNN^{Et} (3.317 g, 16 mmol) at room temperature. The reaction mixture was stirred for 1 h, and then this solution was added into a solution of $\text{NiCl}_2(\text{dme})$ (3.516 g, 16 mmol, dme = dimethoxyethane) in THF (50 mL). The resulting solution was stirred overnight and then evaporated in vacuum. The residue was extracted with CH_2Cl_2 (100 mL), and then was concentrated to *ca.* 20 mL. Addition of pentane (100 mL) afforded a green precipitate, which was filtered, washed with additional pentane, and dried *in vacuo*. Yield: 2.850 g (59%). Diffusion of pentane into a dichloromethane solution of **21** afforded brown crystals suitable for X-ray analysis. ^1H NMR (400 MHz, CDCl_3): 6.86 (dt, $J = 7.8, 1.2$ Hz, 1H), 6.78 (dd, $J = 8.0, 0.8$ Hz, 1H), 6.15-6.25 (m, 2H), 2.80 (s, 6H), 2.62 (t, $J = 6.0$ Hz, 2H), 2.50 (s, 6H), 2.37 (t, $J = 6.0$ Hz, 2H). ^{13}C NMR (100 MHz, CDCl_3): 153.6, 144.2, 128.4, 119.3, 111.6, 109.5, 66.8, 50.6, 49.1, 44.1. Anal. Calcd for $\text{C}_{12}\text{H}_{20}\text{ClN}_3\text{Ni}$: C, 47.97; H, 6.71; N, 13.99 Found: C, 47.93; H, 6.82; N, 14.15.

Synthesis of $[(^{\text{Me}}\text{N}_2^{\text{Me}}\text{N})\text{Ni}(\text{lut})]$, **22**:

$^n\text{BuLi}$ (32 mmol, 1.6 M in hexane) was slowly added to a THF solution (150 mL) of the ligand $^{\text{Me}}\text{NN}^{\text{HMe}}_2$ **6HH** (3.856 g, 16 mmol) at room temperature. The reaction mixture was stirred for 1 h, and then this solution was added into a solution of $\text{NiCl}_2(2,4\text{-lutidine})_2$ (5.502 g, 16 mmol) in THF (50 mL). The resulting solution was stirred overnight and then evaporated in vacuum. The residue was extracted with benzene (100 mL), and then was concentrated to *ca.* 20 mL. Addition of pentane (100 mL) afforded a green precipitate, which was filtered, washed with additional pentane, and dried *in vacuo*. Yield: 5.810 g (90%). Diffusion of pentane into a benzene solution of **22** afforded brown crystals suitable for X-ray analysis. ^1H NMR (400 MHz, C_6D_6): 8.36 (br. s, 1H), 7.48 (dd, $J = 8.0, 1.2$ Hz, 2H), 7.23-7.32 (m, 2H), 6.49 (d, $J = 8.0$ Hz, 2H), 6.43 (dt, $J = 7.6, 0.8$ Hz, 2H), 6.21 (s, 1H), 6.11 (d, $J = 5.2$ Hz, 1H), 3.62 (br. s, 3H), 3.59 (s, 3H), 1.69 (s, 6H), 1.59 (s, 3H). ^{13}C NMR (100 MHz, C_6D_6): 160.5, 159.6, 150.7, 148.7, 141.0, 129.1, 125.9, 122.9, 121.6, 110.3, 109.5, 53.5, 33.1, 25.5, 20.2. Anal. Calcd for $\text{C}_{22}\text{H}_{26}\text{N}_4\text{Ni}$: C, 65.22; H, 6.47; N, 13.83. Found: C, 65.54; H, 6.43; N, 13.66.

Synthesis of $[(^{\text{Me}}\text{NN})_2\text{Ni}]$, **23**:

A THF solution (5 mL) of **13** (0.0879 g, 0.38 mmol) was added to a THF suspension (2 mL) of NiCl_2 (0.025 g, 0.19 mmol). The reaction mixture was stirred overnight at room

temperature. After removal of solvent, the residue was extracted with benzene (10 mL). The solvent was evaporated to give a purple solid which was washed with pentane and dried *in vacuo*. Yield: 0.039 g (40 %). ^1H NMR (400 MHz, C_6D_6): 34.44, 34.19, 26.44, 24.64, 10.40, -16.54, -23.36, -34.81, -37.82. X-ray quality crystals were obtained by slow evaporation of a concentrated acetonitrile solution. Anal. Calcd for $\text{C}_{30}\text{H}_{34}\text{N}_4\text{Ni}$: C, 70.75; H, 6.73; N, 11.00. Found: C, 69.80; H, 6.54; N, 10.76.

Synthesis of $[(^{\text{H}}\text{NN})\text{Ni}(\text{Cl})(\text{PPh}_3)]$, **24**:

A THF solution (20 mL) of **14** (0.460 g, 2.1 mmol) was added to a THF suspension (10 mL) of $\text{NiCl}_2(\text{PPh}_3)_2$ (1.253 g, 1.9 mmol). The reaction mixture was stirred overnight at room temperature. After removal of the solvent, the residue was extracted with CH_2Cl_2 (20 mL), and then was concentrated to *ca.* 5 mL. Addition of pentane (30 mL) afforded the desired product, which was filtered, washed with additional pentane, and dried *in vacuo*. Yield: 0.882 g (81 %). Diffusion of pentane into a benzene solution of **24** afforded violet crystals suitable for X-ray analysis. ^1H NMR (400 MHz, C_6D_6): 41.76, 33.83, 18.02, 15.27, -1.82, -4.39, -46.66, -51.66, -54.70. Anal. Calcd for $\text{C}_{32}\text{H}_{30}\text{ClN}_2\text{PNi}$: C, 67.70; H, 5.33; N, 4.93. Found: C, 67.71; H, 5.63; N, 4.70.

Synthesis of $[(^{\text{Ph}}\text{NN})\text{Ni}(\text{Cl})(\text{Py})_2]$, **25**:

A THF solution (30 mL) of **16** (1.470 g, 5.0 mmol) was added to a THF suspension (20 mL) of $\text{NiCl}_2(\text{Py})_4$ (2.230 g, 5.0 mmol). The reaction mixture was stirred overnight at room temperature. After removal of solvent, the residue was washed with pentane and dried under vacuum, 20 mL CH_2Cl_2 was added to dissolve the solid. Addition of pentane (40 mL) led to a white precipitate. The solution was filtered through Celite, concentrated to *ca.* 5 mL. Additional of pentane (30 mL) afforded the desired product, which was filtered, washed with additional pentane, and dried *in vacuo*. Yield: 1.530 g (57 %). Diffusion of pentane into a toluene solution of **25** afforded purple crystals suitable for X-ray analysis. ^1H NMR (400 MHz, C_6D_6): 34.06, 22.22, 21.04, 19.36, 18.93, 13.78, 5.98, 4.39, 4.24, -10.52, -13.76, -14.97. Anal. Calcd for $\text{C}_{30}\text{H}_{29}\text{ClN}_4\text{Ni}$: C, 66.76; H, 5.42; N, 10.38. Found: C, 66.50; H, 5.49; N, 10.32.

Synthesis of $[(^{\text{Ph}}\text{NN})\text{Ni}(\text{Cl})(4\text{-Picoline})_2]$, **26**:

It was synthesized in a procedure similar to the one described for **25** except that the following quantities of reagents were used: **16** (1.470 g, 5.0 mmol), $\text{NiCl}_2(4\text{-Picoline})_4$

(2.510 g, 5.0 mmol). Yield: 1.210 g (43 %). Diffusion of pentane into a toluene solution of **26** afforded brown crystals suitable for X-ray analysis. ^1H NMR (400 MHz, C_6D_6): 32.64, 21.98, 21.05, 18.99, 10.38, 7.94, 6.80, 4.38, 4.24, -6.95, -10.00, -13.85, -14.30, -22.01. Anal. Calcd for $\text{C}_{32}\text{H}_{33}\text{ClN}_4\text{Ni}$: C, 67.69; H, 5.86; N, 9.87. Found: C, 67.18; H, 5.82; N, 9.69.

Synthesis of $[(^{\text{H}}\text{NN})\text{Ni}(2,4\text{-lutidine})\text{Cl}]$, **27**:

A THF solution (50 mL) of **14** (1.669 g, 7.7 mmol) was added to a THF suspension (25 mL) of $\text{NiCl}_2(2,4\text{-lutidine})_2$ (2.614 g, 7.6 mmol). The reaction mixture was stirred overnight at room temperature. After removal of solvent, the residue was extracted with benzene (40 mL), and then was concentrated to *ca.* 20 mL. Addition of pentane (60 mL) afforded the desired product, which was filtered, washed with additional pentane, and dried *in vacuo*. Yield: 2.503 g (80 %). Diffusion of pentane into a dichloromethane solution of **27** afforded brown crystals suitable for X-ray analysis. ^1H NMR (400 MHz, CDCl_3): 9.98 (br. s, 1H), 7.44 (t, $J = 6.4$ Hz, 2H), 7.34 (br. s, 1H), 7.14 (d, $J = 8$ Hz, 1H), 7.04 (t, $J = 7.2$ Hz, 1H), 6.87 (br. s, 1H), 6.21 (d, $J = 7.2$ Hz, 2H), 6.13 (br. s, 6H), 5.96 (t, $J = 6.8$ Hz, 1H), 5.41 (t, $J = 6.4$ Hz, 1H), 4.95 (d, $J = 8$ Hz, 1H), 3.92 (br. s, 3H), 1.97 (br. s, 3H). Anal. Calcd for $\text{C}_{21}\text{H}_{24}\text{ClN}_3\text{Ni}$: C, 61.13; H, 5.86; N, 10.18. Found: C, 61.30; H, 6.09; N, 9.88.

Synthesis of $[(^{\text{Me}}\text{NN})\text{Ni}(2,4\text{-lutidine})\text{Cl}]$, **28**:

It was synthesized in a procedure similar to the one described for **27** except that the following quantities of reagents were used: **15** (0.978 g, 4.2 mmol), $\text{NiCl}_2(2,4\text{-lutidine})_2$ (1.437 g, 4.2 mmol). Yield: 1.120 g (62 %). Diffusion of pentane into a dichloromethane solution of **28** afforded brown crystals suitable for X-ray analysis. ^1H NMR (400 MHz, C_6D_6): 8.66 (br. s, 1H), 6.98 (br. s, 1H), 6.78 (br. s, 1H), 6.63 (br. s, 3H), 6.40 (br. s, 1H), 6.08 (br. s, 1H), 6.00 (br. s, 1H), 5.77 (br. s, 2H), 3.90 (br. s, 3H), 3.32 (br. s, 6H), 2.67 (br. s, 3H), 1.32 (br. s, 3H). Anal. Calcd for $\text{C}_{22}\text{H}_{26}\text{ClN}_3\text{Ni}$: C, 61.94; H, 6.14; N, 9.85. Found: C, 62.28; H, 6.47; N, 9.79.

Synthesis of $[(^{\text{Ph}}\text{NN})\text{Ni}(2,4\text{-lutidine})\text{Cl}]$, **29**:

It was synthesized in a procedure similar to the one described for **27** except that the following quantities of reagents were used: **16** (2.251 g, 7.6 mmol), $\text{NiCl}_2(2,4\text{-lutidine})_2$ (2.614 g, 7.6 mmol). Yield: 3.120 g, 84%. Diffusion of pentane into a dichloromethane solution of **29** afforded brown crystals suitable for X-ray analysis. ^1H NMR (400 MHz, C_6D_6): 8.38 (br. s, 1H), 7.61 (br. s, 2H), 7.23 (br. s, 3H), 7.09 (br. s, 2H), 6.94 (br. s, 1H),

6.84 (br. s, 1H), 6.64 (br. s, 2H), 6.11 (br. s, 1H), 6.02 (br. s, 2H), 5.80 (br. s, 1H), 3.59 (br. s, 3H), 3.36 (br. s, 6H), 1.35 (br. s, 3H). Anal. Calcd for C₂₇H₂₈ClN₃Ni: C, 66.36; H, 5.78; N, 8.60. Found: C, 65.91; H, 5.92; N, 8.45

Synthesis of [(^HNN)Ni(2,4-lutidine)(OTf)], **30**:

A trimethylsilyl triflate (0.445 g, 2.0 mmol) was added to a toluene (40 mL) solution of **24** (0.825 g, 2.0 mmol). The reaction mixture was stirred overnight at room temperature. After removal of solvent, the residue was extracted with Et₂O (40 mL), and then the solution was evaporated to form the solid, washed with additional pentane, and dried *in vacuo* afforded the desired product. Yield: 0.860 g (82%). Diffusion of pentane into a toluene solution of **30** afforded brown crystals suitable for X-ray analysis. ¹H NMR (400 MHz, C₆D₆): 8.83 (s, 1H), 6.65-6.72 (m, 3H), 6.55-6.62 (m, 3H), 6.42-6.49 (m, 1H), 5.89-6.11 (m, 4H), 3.87 (s, 3H), 2.93 (s, 6H), 1.31 (s, 3H). Anal. Calcd for C₂₂H₂₄F₃N₃NiO₃S: C, 50.22; H, 4.60; N, 7.49. Found: C, 50.43; H, 4.67; N, 7.86.

Synthesis of [(^HNN)Ni(dmiy)I], **31**:

A THF solution (30 mL) containing **24** (1.135 g, 2.0 mmol), 1,3-dimethylimidazolium iodide (0.448 g, 2.0 mmol) and LiOtBu (0.160 g, 2.0 mmol) was stirred for 5 hours at room temperature. After removal of solvent, the residue was extracted with benzene (40 mL), and then was concentrated to *ca.* 5 mL. Addition of pentane (60 mL) afforded the desired product, which was filtered, washed with additional pentane, and dried *in vacuo*. Yield: 0.428 g (43 %). Diffusion of pentane into a toluene solution of **31** afforded green crystals suitable for X-ray analysis. ¹H NMR (400 MHz, CDCl₃): 6.97-7.05 (m, 3H), 6.76-6.88 (m, 3H), 6.51-6.70 (m, 1H), 6.40 (s, 2H), 6.24-6.30 (m, 1H), 5.98 (dd, *J* = 8.0, 1.2 Hz, 1H), 4.21 (s, 6H), 3.23 (s, 6H). ¹³C NMR (100 MHz, CDCl₃): 161.4, 156.5, 153.6, 140.2, 128.6, 128.1, 127.8, 122.6, 122.3, 120.4, 113.4, 111.4, 51.6, 37.9. Anal. Calcd for C₁₉H₂₃IN₄Ni: C, 46.29; H, 4.70; N, 11.36. Found: C, 46.26; H, 4.59; N, 11.27.

2.9.4 Crystallographic Details

(1) Complex 13 (ov-kim1)

A total of 21893 reflections ($-10 \leq h \leq 11$, $-11 \leq k \leq 11$, $-23 \leq l \leq 23$) were collected at *T* = 140(2) K in the range of 3.41 to 25.00° of which 5614 were unique (*R*_{int} = 0.0998); MoK α radiation (λ = 0.71073 Å). The structure was solved by the direct methods. All non-hydrogen atoms were refined anisotropically, and hydrogen atoms were placed in calculated idealized

positions. The residual peak and hole electron densities were 0.837 and -0.368 eÅ^{-3} , respectively. The absorption coefficient was 0.068 mm^{-1} . The least squares refinement converged normally with residuals of $R(F) = 0.0862$, $wR(F^2) = 0.1509$ and a GOF = 1.112 ($I > 2\sigma(I)$). $\text{C}_{36}\text{H}_{48}\text{Li}_2\text{N}_6$, Mw = 578.68, space group $P-1$, Triclinic, $a = 9.425(10)$, $b = 9.633(7)$, $c = 19.58(2) \text{ Å}$, $\alpha = 101.90(7)^\circ$, $\beta = 98.01(7)^\circ$, $\gamma = 103.41(6)^\circ$, $V = 1660(3) \text{ Å}^3$, $Z = 2$, $\rho_{\text{calcd}} = 1.158 \text{ Mg/m}^3$.

(2) Complex 15 (rp300452)

A total of 16461 reflections ($-13 \leq h \leq 13$, $-13 \leq k \leq 12$, $-24 \leq l \leq 24$) were collected at $T = 140(2) \text{ K}$ in the range of 2.91 to 25.03° of which 4565 were unique ($R_{\text{int}} = 0.0846$); $\text{MoK}\alpha$ radiation ($\lambda = 0.71073 \text{ Å}$). The structure was solved by the direct methods. All non-hydrogen atoms were refined anisotropically, and hydrogen atoms were placed in calculated idealized positions. The residual peak and hole electron densities were 0.173 and -0.168 eÅ^{-3} , respectively. The absorption coefficient was 0.069 mm^{-1} . The least squares refinement converged normally with residuals of $R(F) = 0.0440$, $wR(F^2) = 0.0728$ and a GOF = 0.843 ($I > 2\sigma(I)$). $\text{C}_{30}\text{H}_{34}\text{Li}_2\text{N}_4$, Mw = 464.49, space group $P2_1/c$, Monoclinic, $a = 11.6380(14)$, $b = 10.9616(13)$, $c = 20.954(3) \text{ Å}$, $\beta = 102.795(13)^\circ$, $V = 2606.7(5) \text{ Å}^3$, $Z = 4$, $\rho_{\text{calcd}} = 1.184 \text{ Mg/m}^3$.

(3) Complex 17 (rp300551)

A total of 11731 reflections ($-11 \leq h \leq 11$, $-9 \leq k \leq 11$, $-25 \leq l \leq 25$) were collected at $T = 140(2) \text{ K}$ in the range of 2.81 to 25.02° of which 4211 were unique ($R_{\text{int}} = 0.0548$); $\text{MoK}\alpha$ radiation ($\lambda = 0.71073 \text{ Å}$). The structure was solved by the direct methods. All non-hydrogen atoms were refined anisotropically, and hydrogen atoms were placed in calculated idealized positions. The residual peak and hole electron densities were 0.248 and -0.172 eÅ^{-3} , respectively. The absorption coefficient was 0.072 mm^{-1} . The least squares refinement converged normally with residuals of $R(F) = 0.0548$, $wR(F^2) = 0.0957$ and a GOF = 0.944 ($I > 2\sigma(I)$). $\text{C}_{28}\text{H}_{35}\text{LiN}_2\text{O}_2$, Mw = 438.52, space group $P3_1$, Trigonal, $a = 9.9517(6)$, $b = 9.9517(6)$, $c = 21.757(2) \text{ Å}$, $V = 1866.0(2) \text{ Å}^3$, $Z = 3$, $\rho_{\text{calcd}} = 1.171 \text{ Mg/m}^3$.

(4) Complex 18 (rp400091)

A total of 6947 reflections ($-13 \leq h \leq 13$, $-16 \leq k \leq 16$, $-16 \leq l \leq 16$) were collected at $T = 140(2) \text{ K}$ in the range of 2.36 to 24.45° of which 3599 were unique ($R_{\text{int}} = 0.0474$); $\text{MoK}\alpha$

radiation ($\lambda = 0.71073 \text{ \AA}$). The structure was solved by the direct methods. All non-hydrogen atoms were refined anisotropically, and hydrogen atoms were placed in calculated idealized positions. The residual peak and hole electron densities were 0.199 and -0.256 e\AA^{-3} , respectively. The absorption coefficient was 0.219 mm^{-1} . The least squares refinement converged normally with residuals of $R(F) = 0.0693$, $wR(F^2) = 0.1559$ and a GOF = 1.136 ($I > 2\sigma(I)$). $\text{C}_{48}\text{H}_{54}\text{Cl}_2\text{Mg}_2\text{N}_4\text{O}_2$, Mw = 838.47 , space group $P2_1/n$, Monoclinic, $a = 11.674(2)$, $b = 14.028(3)$, $c = 14.417(3) \text{ \AA}$, $\beta = 110.70(3)^\circ$, $V = 2208.5(8) \text{ \AA}^3$, $Z = 2$, $\rho_{\text{calcd}} = 1.261 \text{ Mg/m}^3$.

(5) Complex 19 (rp500152)

A total of 7061 reflections ($-12 \leq h \leq 12$, $-16 \leq k \leq 14$, $-10 \leq l \leq 19$) were collected at $T = 140(2) \text{ K}$ in the range of 3.06 to 27.50° of which 7061 were unique ($R_{\text{int}} = 0.0000$); $\text{MoK}\alpha$ radiation ($\lambda = 0.71073 \text{ \AA}$). The structure was solved by the direct methods. All non-hydrogen atoms were refined anisotropically, and hydrogen atoms were placed in calculated idealized positions. The residual peak and hole electron densities were 3.048 and -2.234 e\AA^{-3} , respectively. The absorption coefficient was 1.595 mm^{-1} . The least squares refinement converged normally with residuals of $R(F) = 0.0724$, $wR(F^2) = 0.2213$ and a GOF = 1.103 ($I > 2\sigma(I)$). $\text{C}_{14.5}\text{H}_{17}\text{Cl}_2\text{N}_3\text{Ni}$ (including $0.5 \text{ CH}_2\text{Cl}_2$), Mw = 362.92 , space group $P-1$, Triclinic, $a = 9.9490(8)$, $b = 12.5384(19)$, $c = 14.8903(16) \text{ \AA}$, $\alpha = 113.657(10)^\circ$, $\beta = 110.70(3)^\circ$, $\gamma = 111.582(8)^\circ$, $V = 1545.7(3) \text{ \AA}^3$, $Z = 4$, $\rho_{\text{calcd}} = 1.559 \text{ Mg/m}^3$.

(6) Complex 20 (rp500011)

A total of 5251 reflections ($-29 \leq h \leq 29$, $-10 \leq k \leq 10$, $-17 \leq l \leq 17$) were collected at $T = 140(2) \text{ K}$ in the range of 2.46 to 24.39° of which 2763 were unique ($R_{\text{int}} = 0.0478$); $\text{MoK}\alpha$ radiation ($\lambda = 0.71073 \text{ \AA}$). The structure was solved by the direct methods. All non-hydrogen atoms were refined anisotropically, and hydrogen atoms were placed in calculated idealized positions. The residual peak and hole electron densities were 0.360 and -0.396 e\AA^{-3} , respectively. The absorption coefficient was 1.244 mm^{-1} . The least squares refinement converged normally with residuals of $R(F) = 0.0520$, $wR(F^2) = 0.1098$ and a GOF = 1.120 ($I > 2\sigma(I)$). $\text{C}_{18}\text{H}_{24}\text{ClN}_3\text{Ni}$, Mw = 376.56 , space group $C2/c$, Monoclinic, $a = 25.079(5)$, $b = 8.7830(18)$, $c = 16.494(3) \text{ \AA}$, $\beta = 101.76(3)^\circ$, $V = 3556.9(12) \text{ \AA}^3$, $Z = 8$, $\rho_{\text{calcd}} = 1.406 \text{ Mg/m}^3$.

(6) Complex 21 (rp700491)

A total of 28546 reflections ($-19 \leq h \leq 18$, $-9 \leq k \leq 11$, $-21 \leq l \leq 20$) were collected at $T = 100(2)$ K in the range of 3.13 to 24.99° of which 4626 were unique ($R_{\text{int}} = 0.0771$); $\text{MoK}\alpha$ radiation ($\lambda = 0.71073$ Å). The structure was solved by the direct methods. All non-hydrogen atoms were refined anisotropically, and hydrogen atoms were placed in calculated idealized positions. The residual peak and hole electron densities were 0.393 and -0.378 eÅ⁻³, respectively. The absorption coefficient was 1596 mm⁻¹. The least squares refinement converged normally with residuals of $R(F) = 0.0370$, $wR(F^2) = 0.0624$ and a GOF = 1.093 ($I > 2\sigma(I)$). $\text{C}_{10}\text{H}_{20}\text{ClN}_3\text{Ni}$, Mw = 300.47 , space group $Pca2_1$, Orthorhombic, $a = 16.1973(14)$, $b = 9.2551(7)$, $c = 18.251(2)$ Å, $V = 2736.0(4)$ Å³, $Z = 8$, $\rho_{\text{calcd}} = 1.459$ Mg/m³.

(6) Complex 22 (rp700466)

A total of 33427 reflections ($-10 \leq h \leq 10$, $-18 \leq k \leq 18$, $-18 \leq l \leq 17$) were collected at $T = 100(2)$ K in the range of 3.13 to 25.00° of which 3515 were unique ($R_{\text{int}} = 0.1201$); $\text{MoK}\alpha$ radiation ($\lambda = 0.71073$ Å). The structure was solved by the direct methods. All non-hydrogen atoms were refined anisotropically, and hydrogen atoms were placed in calculated idealized positions. The residual peak and hole electron densities were 0.980 and -0.505 eÅ⁻³, respectively. The absorption coefficient was 0.980 mm⁻¹. The least squares refinement converged normally with residuals of $R(F) = 0.0603$, $wR(F^2) = 0.1062$ and a GOF = 1.128 ($I > 2\sigma(I)$). $\text{C}_{22}\text{H}_{26}\text{N}_4\text{Ni}$, Mw = 405.18 , space group $P2_1/n$, Monoclinic, $a = 8.4828(9)$, $b = 15.428(5)$, $c = 15.348(4)$ Å, $\beta = 91.847(17)^\circ$, $V = 2007.6(8)$ Å³, $Z = 4$, $\rho_{\text{calcd}} = 1.341$ Mg/m³.

$P2(1)/n$

(7) Complex 23 (rp300461)

A total of 18331 reflections ($-30 \leq h \leq 30$, $-15 \leq k \leq 15$, $-10 \leq l \leq 11$) were collected at $T = 140(2)$ K in the range of 2.87 to 26.72° of which 4901 were unique ($R_{\text{int}} = 0.0951$); $\text{MoK}\alpha$ radiation ($\lambda = 0.71073$ Å). The structure was solved by the direct methods. All non-hydrogen atoms were refined anisotropically, and hydrogen atoms were placed in calculated idealized positions. The residual peak and hole electron densities were 0.650 and -0.458 eÅ⁻³, respectively. The absorption coefficient was 0.782 mm⁻¹. The least squares refinement converged normally with residuals of $R(F) = 0.0486$, $wR(F^2) = 0.0815$ and a GOF = 0.906 ($I > 2\sigma(I)$). $\text{C}_{30}\text{H}_{34}\text{N}_4\text{Ni}$, Mw = 509.32 , space group $Pna2_1$, Orthorhombic, $a = 24.052(3)$, $b = 12.1888(18)$, $c = 8.7468(12)$ Å, $V = 2564.2(6)$ Å³, $Z = 4$, $\rho_{\text{calcd}} = 1.319$ Mg/m³.

(8) Complex 24 (rp500073)

A total of 13288 reflections ($-18 \leq h \leq 18$, $-14 \leq k \leq 14$, $-26 \leq l \leq 26$) were collected at $T = 140(2)$ K in the range of 2.13 to 27.67° of which 7094 were unique ($R_{\text{int}} = 0.0518$); $\text{MoK}\alpha$ radiation ($\lambda = 0.71073$ Å). The structure was solved by the direct methods. All non-hydrogen atoms were refined anisotropically, and hydrogen atoms were placed in calculated idealized positions. The residual peak and hole electron densities were 0.623 and -0.663 eÅ⁻³, respectively. The absorption coefficient was 0.755 mm⁻¹. The least squares refinement converged normally with residuals of $R(F) = 0.0542$, $wR(F^2) = 0.1226$ and a GOF = 0.995 ($I > 2\sigma(I)$). $\text{C}_{38}\text{H}_{36}\text{ClN}_2\text{NiP}$, Mw = 645.82, space group $P2_1/n$, Monoclinic, $a = 14.755(3)$, $b = 10.848(2)$, $c = 20.482(4)$ Å, $\beta = 95.92(3)^\circ$, $V = 3260.9(11)$ Å³, $Z = 4$, $\rho_{\text{calcd}} = 1.315$ Mg/m³.

(9) Complex 25 (rp500091)

A total of 6164 reflections ($-11 \leq h \leq 11$, $-14 \leq k \leq 14$, $-33 \leq l \leq 33$) were collected at $T = 140(2)$ K in the range of 2.72 to 27.48° of which 6164 were unique ($R_{\text{int}} = 0.0000$); $\text{MoK}\alpha$ radiation ($\lambda = 0.71073$ Å). The structure was solved by the direct methods. All non-hydrogen atoms were refined anisotropically, and hydrogen atoms were placed in calculated idealized positions. The residual peak and hole electron densities were 0.525 and -0.770 eÅ⁻³, respectively. The absorption coefficient was 0.842 mm⁻¹. The least squares refinement converged normally with residuals of $R(F) = 0.0423$, $wR(F^2) = 0.1040$, and a GOF = 1.112 ($I > 2\sigma(I)$). $\text{C}_{30}\text{H}_{29}\text{ClN}_4\text{Ni}$, Mw = 539.73, space group $P2_12_12_1$, Orthorhombic, $a = 9.2090(18)$, $b = 11.415(2)$, $c = 25.719(5)$ Å, $V = 2703.6(9)$ Å³, $Z = 4$, $\rho_{\text{calcd}} = 1.326$ Mg/m³.

(10) Complex 26 (rp400696)

A total of 51271 reflections ($-14 \leq h \leq 14$, $-17 \leq k \leq 17$, $-25 \leq l \leq 25$) were collected at $T = 140(2)$ K in the range of 3.05 to 27.50° of which 6842 were unique ($R_{\text{int}} = 0.0542$); $\text{MoK}\alpha$ radiation ($\lambda = 0.71073$ Å). The structure was solved by the direct methods. All non-hydrogen atoms were refined anisotropically, and hydrogen atoms were placed in calculated idealized positions. The residual peak and hole electron densities were 0.235 and -0.256 eÅ⁻³, respectively. The absorption coefficient was 0.764 mm⁻¹. The least squares refinement converged normally with residuals of $R(F) = 0.0306$, $wR(F^2) = 0.0568$ and a GOF = 1.091 ($I > 2\sigma(I)$). $\text{C}_{32}\text{H}_{33}\text{ClN}_4\text{Ni}$, Mw = 567.78, space group $P2_12_12_1$, Orthorhombic, $a = 11.3515(5)$, $b = 13.3682(12)$, $c = 19.724(2)$ Å, $V = 2993.2(4)$ Å³, $Z = 4$, $\rho_{\text{calcd}} = 1.260$ Mg/m³.

(11) Complex 27 (rp400172)

A total of 6939 reflections ($-10 \leq h \leq 10$, $-16 \leq k \leq 16$, $-22 \leq l \leq 22$) were collected at $T = 140(2)$ K in the range of 3.05 to 26.37° of which 3943 were unique ($R_{\text{int}} = 0.0417$); $\text{Mo}_{\text{K}\alpha}$ radiation ($\lambda = 0.71073$ Å). The structure was solved by the direct methods. All non-hydrogen atoms were refined anisotropically, and hydrogen atoms were placed in calculated idealized positions. The residual peak and hole electron densities were 0.552 and -0.752 eÅ⁻³, respectively. The absorption coefficient was 1.104 mm⁻¹. The least squares refinement converged normally with residuals of $R(F) = 0.0735$, $wR(F^2) = 0.1793$ and a GOF = 1.143 ($I > 2\sigma(I)$). $\text{C}_{21}\text{H}_{24}\text{ClN}_3\text{Ni}$, Mw = 412.59 , space group $P2_1/n$, Monoclinic, $a = 8.6520(17)$, $b = 13.343(3)$, $c = 17.759(4)$ Å, $\beta = 100.48(3)^\circ$, $V = 2016.0(7)$ Å³, $Z = 4$, $\rho_{\text{calcd}} = 1.359$ Mg/m³.

(12) Complex 28 (rp400242)

A total of 32840 reflections ($-13 \leq h \leq 13$, $-32 \leq k \leq 32$, $-16 \leq l \leq 16$) were collected at $T = 140(2)$ K in the range of 3.03 to 25.03° of which 7321 were unique ($R_{\text{int}} = 0.0834$); $\text{Mo}_{\text{K}\alpha}$ radiation ($\lambda = 0.71073$ Å). The structure was solved by the direct methods. All non-hydrogen atoms were refined anisotropically, and hydrogen atoms were placed in calculated idealized positions. The residual peak and hole electron densities were 0.842 and -0.753 eÅ⁻³, respectively. The absorption coefficient was 1.056 mm⁻¹. The least squares refinement converged normally with residuals of $R(F) = 0.0655$, $wR(F^2) = 0.1600$ and a GOF = 1.170 ($I > 2\sigma(I)$). $\text{C}_{22}\text{H}_{26}\text{ClN}_3\text{Ni}$, Mw = 426.62 , space group $P2_1/n$, Monoclinic, $a = 11.049(3)$, $b = 27.593(3)$, $c = 13.867(3)$ Å, $\beta = 92.802(15)^\circ$, $V = 4222.6(15)$ Å³, $Z = 8$, $\rho_{\text{calcd}} = 1.342$ Mg/m³.

(13) Complex 29 (rp400173)

A total of 77139 reflections ($-19 \leq h \leq 19$, $-20 \leq k \leq 20$, $-25 \leq l \leq 25$) were collected at $T = 140(2)$ K in the range of 3.05 to 27.50° of which 5545 were unique ($R_{\text{int}} = 0.0955$); $\text{Mo}_{\text{K}\alpha}$ radiation ($\lambda = 0.71073$ Å). The structure was solved by the direct methods. All non-hydrogen atoms were refined anisotropically, and hydrogen atoms were placed in calculated idealized positions. The residual peak and hole electron densities were 0.791 and -0.528 eÅ⁻³, respectively. The absorption coefficient was 0.931 mm⁻¹. The least squares refinement converged normally with residuals of $R(F) = 0.0502$, $wR(F^2) = 0.0906$ and a GOF = 1.236 ($I > 2\sigma(I)$). $\text{C}_{27}\text{H}_{28}\text{ClN}_3\text{Ni}$, Mw = 488.68 , space group $Pbca$, Orthorhombic, $a = 15.2003(16)$, $b = 16.024(3)$, $c = 19.873(4)$ Å, $V = 4840.4(13)$ Å³, $Z = 8$, $\rho_{\text{calcd}} = 1.341$ Mg/m³.

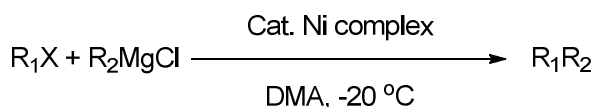
(14) Complex 30 (rp600366)

A total of 22872 reflections ($-15 \leq h \leq 15$, $-27 \leq k \leq 27$, $-27 \leq l \leq 27$) were collected at $T = 140(2)$ K in the range of 2.17 to 27.67° of which 11825 were unique ($R_{\text{int}} = 0.0714$); $\text{MoK}\alpha$ radiation ($\lambda = 0.71073$ Å). The structure was solved by the direct methods. All non-hydrogen atoms were refined anisotropically, and hydrogen atoms were placed in calculated idealized positions. The residual peak and hole electron densities were 0.618 and -0.573 eÅ⁻³, respectively. The absorption coefficient was 0.853 mm⁻¹. The least squares refinement converged normally with residuals of $R(F) = 0.0645$, $wR(F^2) = 0.1454$ and a GOF = 0.987 ($I > 2\sigma(I)$). $\text{C}_{25.50}\text{H}_{28}\text{F}_3\text{N}_3\text{NiO}_3\text{S}$, Mw = 572.28 , space group $P2_1/n$, Monoclinic, $a = 12.306(4)$, $b = 21.035(4)$, $c = 21.091(6)$ Å, $\beta = 100.604(17)^\circ$, $V = 5366(3)$ Å³, $Z = 8$, $\rho_{\text{calcd}} = 1.417$ Mg/m³.

(15) Complex 31 (rp600571)

A total of 18022 reflections ($-14 \leq h \leq 14$, $-14 \leq k \leq 14$, $-28 \leq l \leq 28$) were collected at $T = 140(2)$ K in the range of 2.24 to 27.48° of which 10800 were unique ($R_{\text{int}} = 0.0376$); $\text{MoK}\alpha$ radiation ($\lambda = 0.71073$ Å). The structure was solved by the direct methods. All non-hydrogen atoms were refined anisotropically, and hydrogen atoms were placed in calculated idealized positions. The residual peak and hole electron densities were 1.171 and -1.754 eÅ⁻³, respectively. The absorption coefficient was 1.946 mm⁻¹. The least squares refinement converged normally with residuals of $R(F) = 0.0496$, $wR(F^2) = 0.1496$ and a GOF = 1.154 ($I > 2\sigma(I)$). $\text{C}_{26}\text{H}_{31}\text{IN}_4\text{Ni}$, Mw = 585.16 , space group $P-1$, Triclinic, $a = 10.892(2)$, $b = 11.176(2)$, $c = 22.147(4)$ Å, $\alpha = 100.07(3)^\circ$, $\beta = 98.76(3)^\circ$, $\gamma = 94.04(3)^\circ$, $V = 2610.3(9)$ Å³, $Z = 4$, $\rho_{\text{calcd}} = 1.489$ Mg/m³.

2.9.5 Typical procedure for the alkyl-alkyl Kumada coupling



0.5 mmol (1 equiv.) of RMgCl was diluted in THF (3 mL), and then was added dropwise via a syringe pump during 1 h to a DMA solution containing the nickel catalyst (0.015 mmol, 3 %) and alkyl iodide (0.5 mmol) at -20°C . After addition, the reaction mixture was further stirred for 1 h at -20°C and then the solution was taken out from the cooling system and stirred for 1h to warm up to room temperature. A mixture of distilled water (15 mL), hydrochloric acid (25%, 1 mL), and dodecane (internal standard, 60 µL, 0.265 mmol) or

decane (internal standard, 60 μ L, 0.310 mmol) was added to the reaction mixture. The resulting solution was extracted with diethyl ether (3×10 mL) and the organic phase was separated, dried over MgSO_4 , and filtered. The organic products were identified by GC-MS, and the yields were determined by GC with decane or dodecane as the internal standard.

2.9.6 Coupling of radical clocks

The cross coupling reaction in eq. 6 was carried out following the protocol described in Table 11. The reaction in eq. 7 was carried out following the protocol described in Table 3. The products were identified by GC, GC-MS and NMR for eq. 6, and GC and GC-MS for eq. 7. The yields were determined by GC relative to the organic halides. The ^1H NMR of the ring-opened⁴⁸ and ring-closed⁴⁹ products of eq. 6 were identical to those reported in the literatures. The MS spectra of the ring-opened and ring-closed products of eq. 7 were identical to those reported in the MS database of the instrument (see 2.11 GC-MS spectra of products). For the ring-closed products, both cis- and trans-isomers were produced, and the yields are referred to the overall yields of both isomers.

2.10 References and Notes

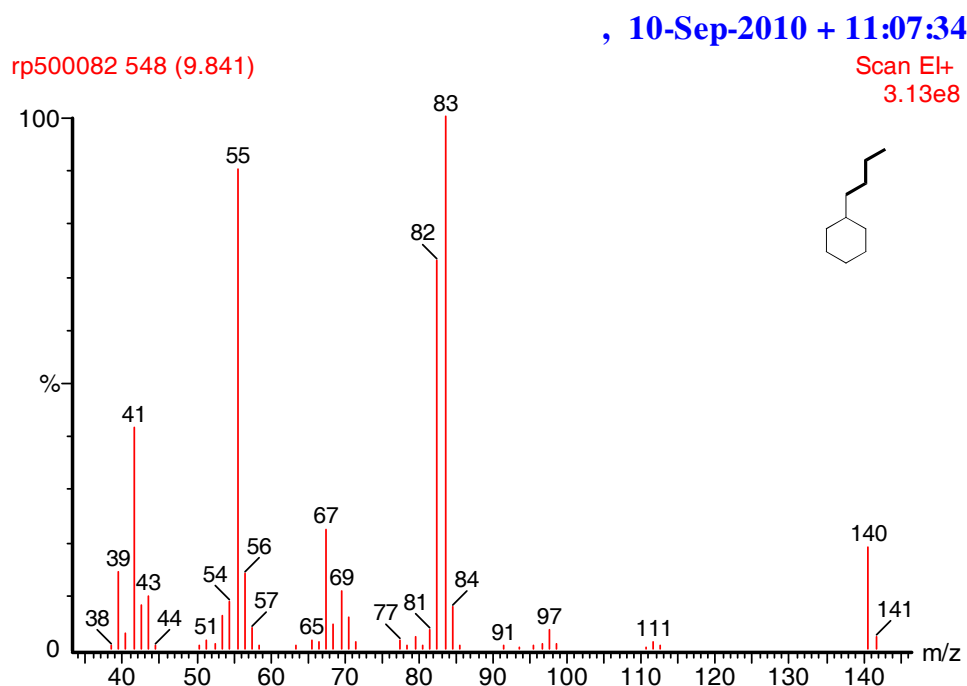
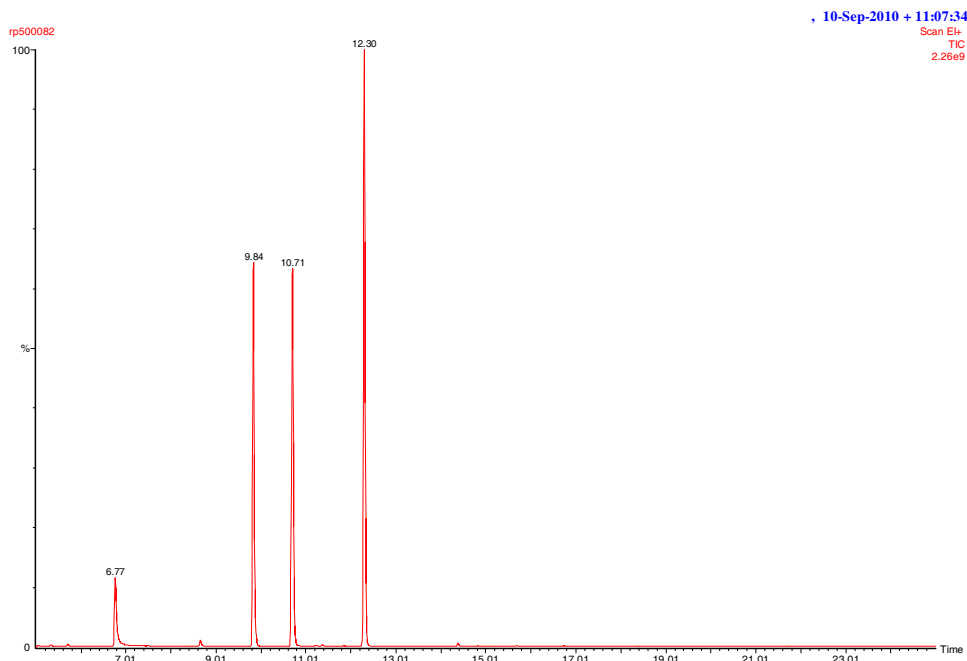
- (1) Netherton, M. R.; Fu, G. C. *Adv. Synth. Catal.* **2004**, *346*, 1525-1532.
- (2) Frisch, A. C.; Beller, M. *Angew. Chem., Int. Ed.* **2005**, *44*, 674-688.
- (3) Rudolph, A.; Lautens, M. *Angew. Chem., Int. Ed.* **2009**, *48*, 2656-2670.
- (4) Terao, J.; Kambe, N. *Acc. Chem. Res.* **2008**, *41*, 1545-1554.
- (5) Cardenas, D. J. *Angew. Chem., Int. Ed.* **2003**, *42*, 384-387.
- (6) Glorius, F. *Angew. Chem., Int. Ed.* **2008**, *47*, 8347-8349.
- (7) Saito, B.; Fu, G. C. *J. Am. Chem. Soc.* **2008**, *130*, 6694-6695.
- (8) Owston, N. A.; Fu, G. C. *J. Am. Chem. Soc.* **2010**, *132*, 11908-11909.
- (9) Fischer, C.; Fu, G. C. *J. Am. Chem. Soc.* **2005**, *127*, 4594-4595.
- (10) Smith, S. W.; Fu, G. C. *J. Am. Chem. Soc.* **2008**, *130*, 12645-12647.
- (11) Son, S.; Fu, G. C. *J. Am. Chem. Soc.* **2008**, *130*, 2756-2757.
- (12) Lundin, P. M.; Esquivias, J.; Fu, G. C. *Angew. Chem., Int. Ed.* **2009**, *48*, 154-156.
- (13) Dai, X.; Strotman, N. A.; Fu, G. C. *J. Am. Chem. Soc.* **2008**, *130*, 3302-3303.
- (14) Zhou, J. R.; Fu, G. C. *J. Am. Chem. Soc.* **2003**, *125*, 14726-14727.
- (15) Zhou, J.; Fu, G. C. *J. Am. Chem. Soc.* **2004**, *126*, 1340-1341.
- (16) Saito, B.; Fu, G. C. *J. Am. Chem. Soc.* **2007**, *129*, 9602-9603.

-
- (17) Lu, Z.; Fu, G. C. *Angew. Chem., Int. Ed.* **2010**, *49*, 6676-6678.
- (18) Anderson, T. J.; Jones, G. D.; Vicic, D. A. *J. Am. Chem. Soc.* **2004**, *126*, 8100-8101.
- (19) Phapale, V. B.; Bunuel, E.; Garcia-Iglesias, M.; Cardenas, D. J. *Angew. Chem., Int. Ed.* **2007**, *46*, 8790-8795.
- (20) Vechorkin, O.; Csok, Z.; Scopelliti, R.; Hu, X. L. *Chem.-Eur. J.* **2009**, *15*, 3889-3899.
- (21) Vechorkin, O.; Hu, X. L. *Angew. Chem., Int. Ed.* **2009**, *48*, 2937-2940.
- (22) Csok, Z.; Vechorkin, O.; Harkins, S. B.; Scopelliti, R.; Hu, X. L. *J. Am. Chem. Soc.* **2008**, *130*, 8156-8157.
- (23) Vechorkin, O.; Proust, V.; Hu, X. L. *J. Am. Chem. Soc.* **2009**, *131*, 9756-9766.
- (24) Breitenfeld, J.; Vechorkin, O.; Corminboeuf, C.; Scopelliti, R.; Hu, X. L. *Organometallics* **2010**, *29*, 3686-3689.
- (25) Nguyen, A. I.; Blackmore, K. J.; Carter, S. M.; Zarkesh, R. A.; Heyduk, A. F. *J. Am. Chem. Soc.* **2009**, *131*, 3307-3316.
- (26) Jones, M. B.; MacBeth, C. E. *Inorg. Chem.* **2007**, *46*, 8117-8119.
- (27) Wolfe, J. P.; Wagaw, S.; Marcoux, J. F.; Buchwald, S. L. *Acc. Chem. Res.* **1998**, *31*, 805-818.
- (28) Hartwig, J. F. *Acc. Chem. Res.* **1998**, *31*, 852-860.
- (29) Earley, R. A.; Gallagher, M. J. *J. Organomet. Chem.* **1969**, *20*, 117-127.
- (30) Wang, H. B.; Liu, J.; Deng, Y.; Min, T. Y.; Yu, G. X.; Xu, X. J.; Yang, Z.; Lei, A. W. *Chem.-Eur. J.* **2009**, *15*, 1499-1507.
- (31) Liu, J.; Wang, H. B.; Zhang, H.; Wu, X. J.; Zhang, H.; Deng, Y.; Yang, Z.; Lei, A. W. *Chem.-Eur. J.* **2009**, *15*, 4437-4445.
- (32) Fossey, J. S.; Lefort, D.; Sorba, J. *Free radicals in organic chemistry*; Wiley, **1995**.
- (33) *The chemistry of pincer compounds* Morales-Morales, D.; Jensen, C. M., Eds.; Elsevier: Amsterdam, **2007**.
- (34) **21** was tested for octyl iodide and butylMgCl coupling under the conditions of table 10. The yield was 60%, and conversion was 100%.
- (35) **31** was tested for octyl iodide and butylMgCl coupling under the conditions of table 10. The yield was 35%, and conversion was 100%.
- (36) Nasielski, J.; Hadei, N.; Achonduh, G.; Kantchev, E. A. B.; O'Brien, C. J.; Lough, A.; Organ, M. G. *Chem.-Eur. J.* **2010**, *16*, 10844-10853.
- (37) Wiencko, H. L.; Kogut, E.; Warren, T. H. *Inorg. Chim. Acta* **2003**, *345*, 199-208.
- (38) Eckert, N. A.; Bones, E. M.; Lachicotte, R. J.; Holland, P. L. *Inorg. Chem.* **2003**, *42*, 1720-1725.

- (39) Venanzi, L. M. *J. Chem. Soc.* **1958**, 719-724.
- (40) Long, G. J; Clarke, P. J. *Inorg. Chem.* **1978**, *17*, 1394-1401.
- (41) Laughrey, Z. R.; Upton, T. G.; Gibb, B. C. *Chem. Commun.* **2006**, 970-972.
- (42) Meyer, C.; Marek, I.; Courtemanche, G.; Normant, J. F. *Tetrahedron* **1994**, *50*, 11665-11692.
- (43) Blessing, R. H. *Acta Crystallogr. A* **1995**, *51*, 33-38.
- (44) Sheldrick, G. M. *SHELXTL* release 6.1.4 ed.; Bruker AXS Inc.: Madison, Wisconsin, 53719, USA, **2003**.
- (45) Montoro, R.; Wirth, T. *Synthesis* **2005**, 1473-1478.
- (46) Tietze, M.; Iglesias, A.; Merisor, E.; Conrad, J.; Klaiber, I.; Beifuss, U. *Org. Lett.* **2005**, *7*, 1549-1552.
- (47) Schrock, R. R.; Lee, J.; Liang, L. C.; Davis, W. M. *Inorg. Chim. Acta* **1998**, *270*, 353-362.
- (48) Terao, J.; Naitoh, Y.; Kuniyasu, H.; Kambe, N. *Chem. Commun.* **2007**, 825-827.
- (49) Kobayashi, T.; Ohmiya, H.; Yorimitsu, H.; Oshima, K. *J. Am. Chem. Soc.* **2008**, *130*, 11276-11277.

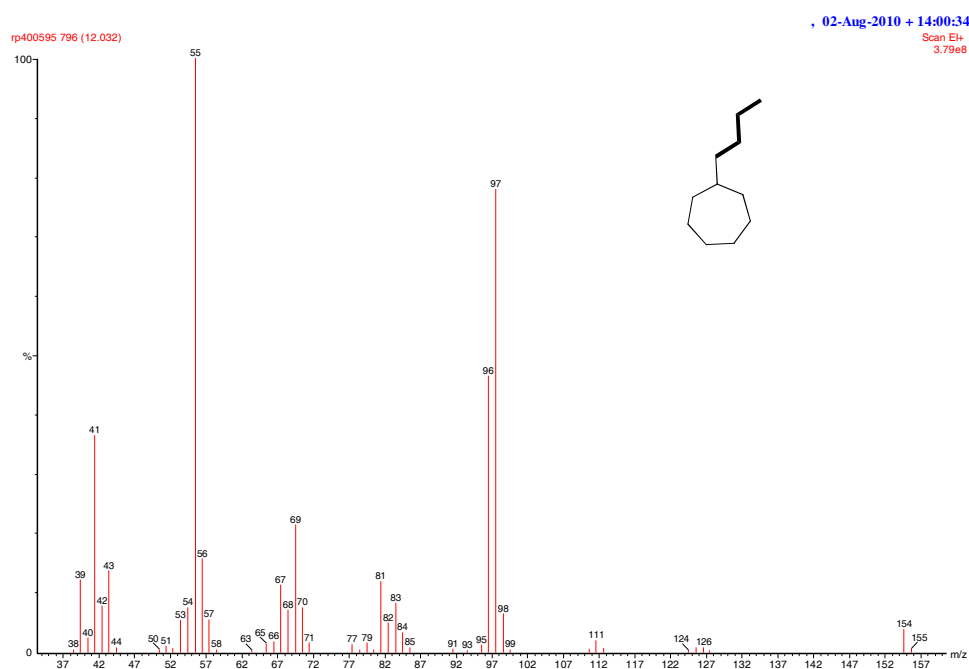
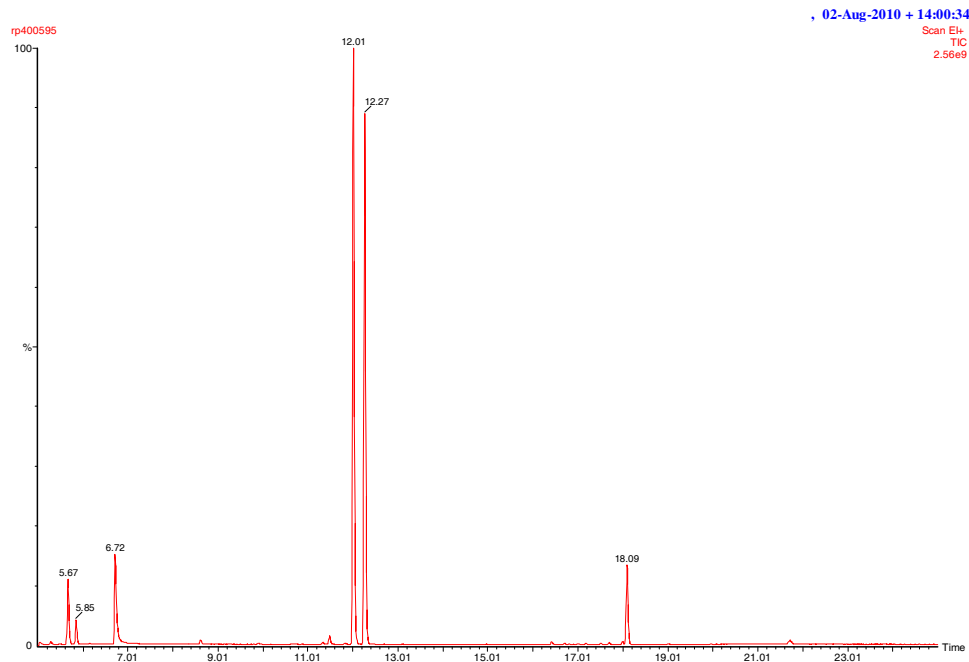
2.11 GC-MS spectra of products

Dodecane internal standard $R_t = 12.30$ min. Butylcyclohexane $R_t = 9.84$ min.

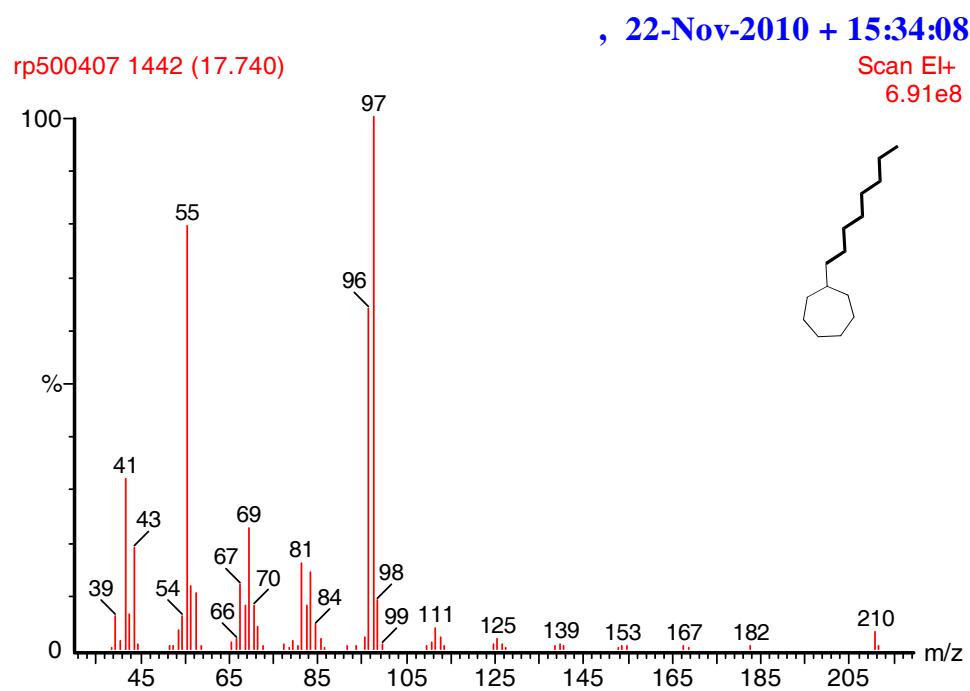
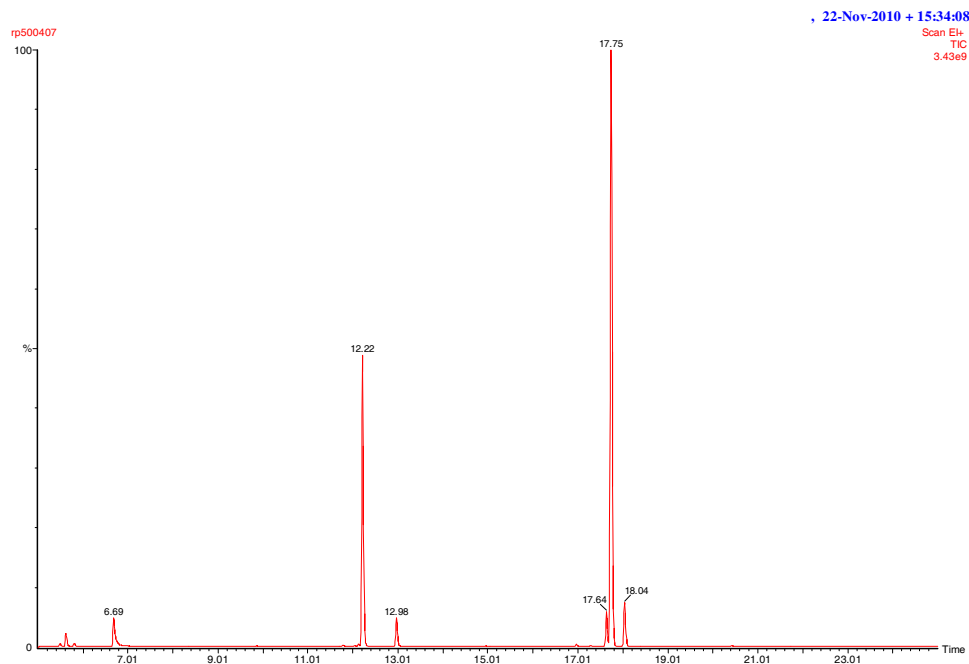


Chapter Two

Dodecane internal standard $R_t = 12.27$ min. Butylcycloheptane, $R_t = 12.01$ min.

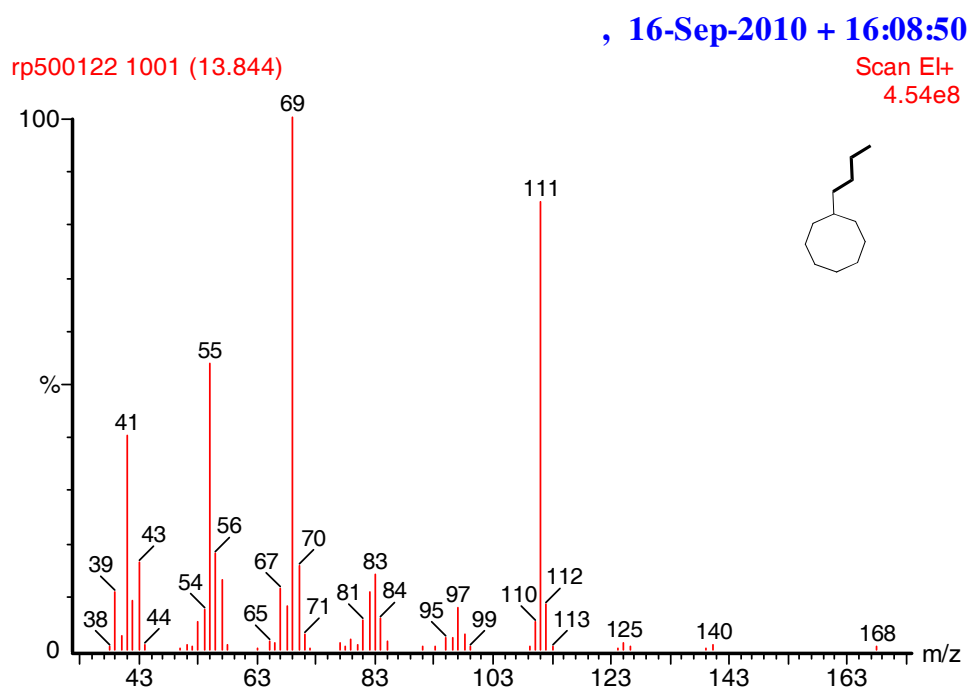
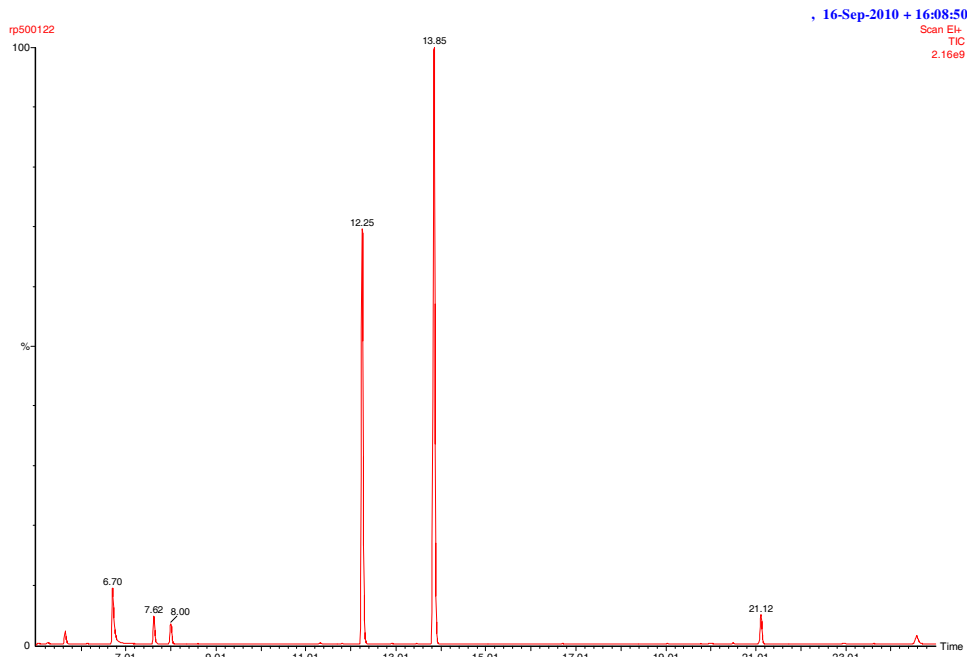


Dodecane internal standard $R_t = 12.22$ min. Octylcycloheptane $R_t = 17.75$ min.

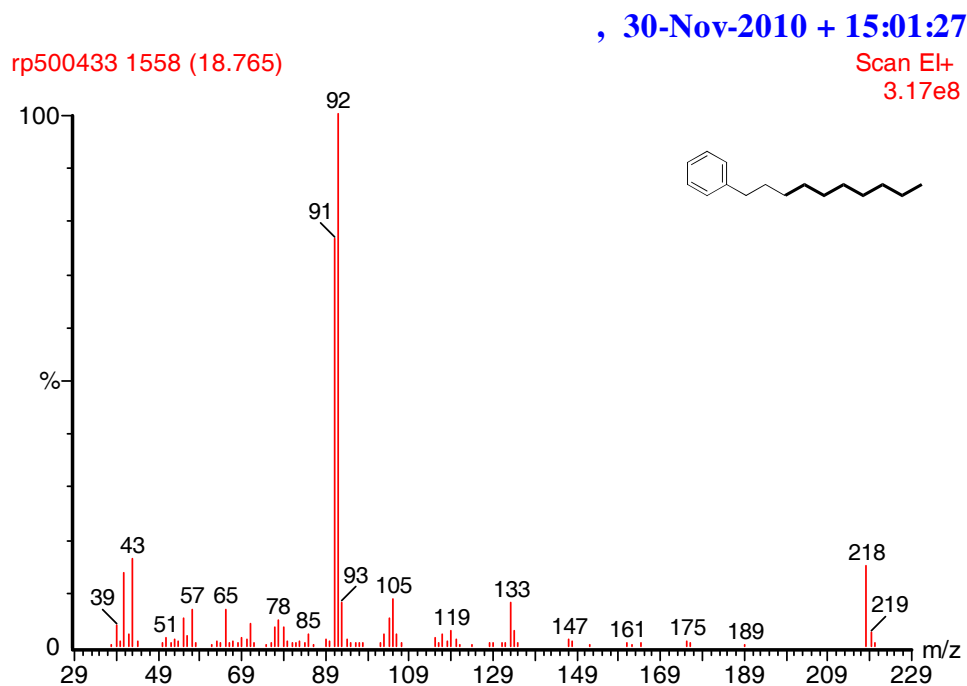
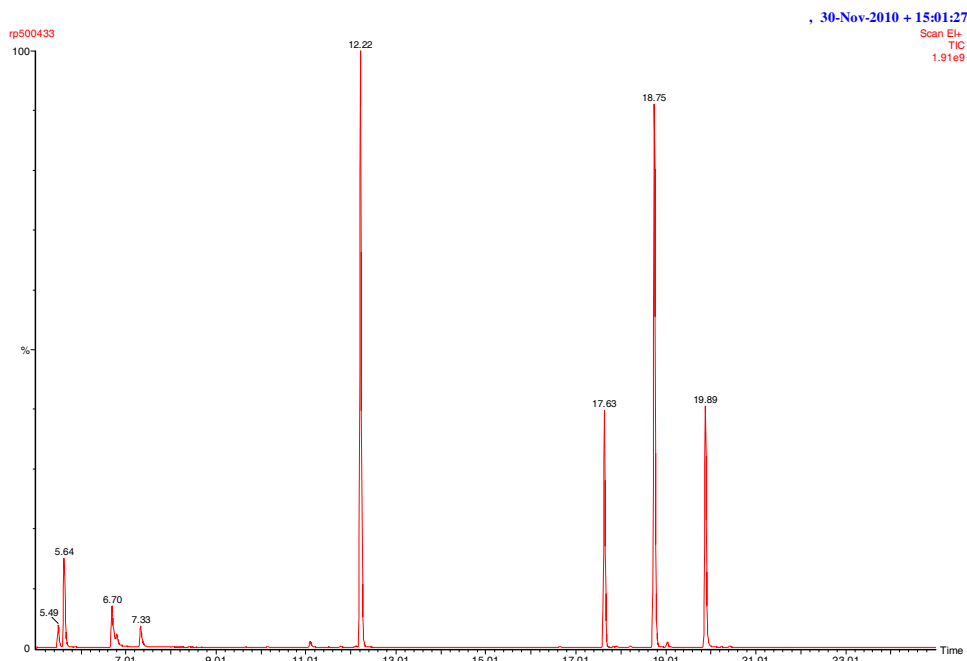


Chapter Two

Dodecane internal standard $R_t = 12.22$ min. Butylcyclooctane $R_t = 13.85$ min.

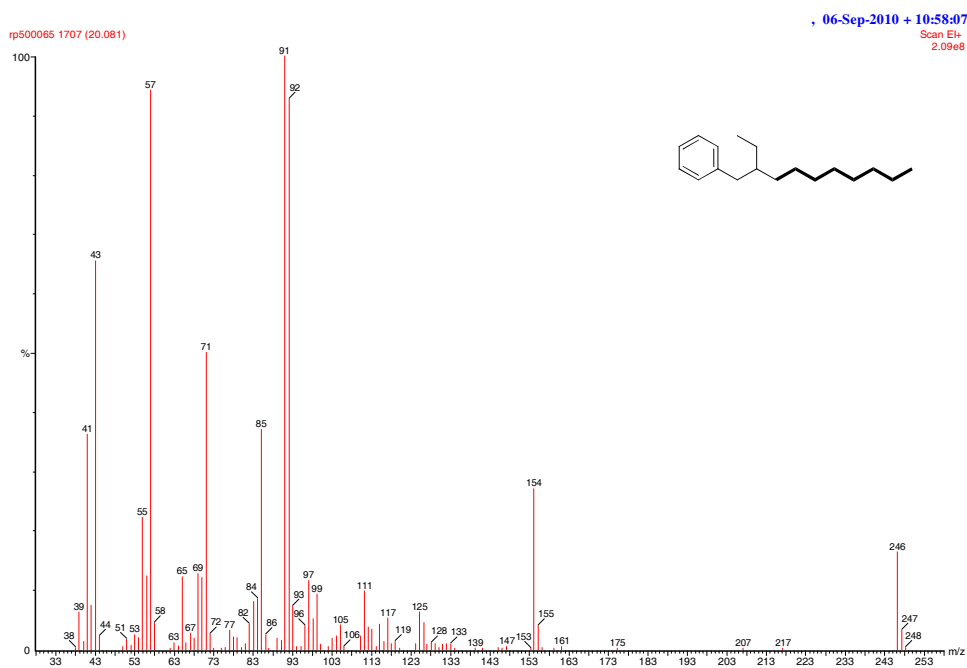
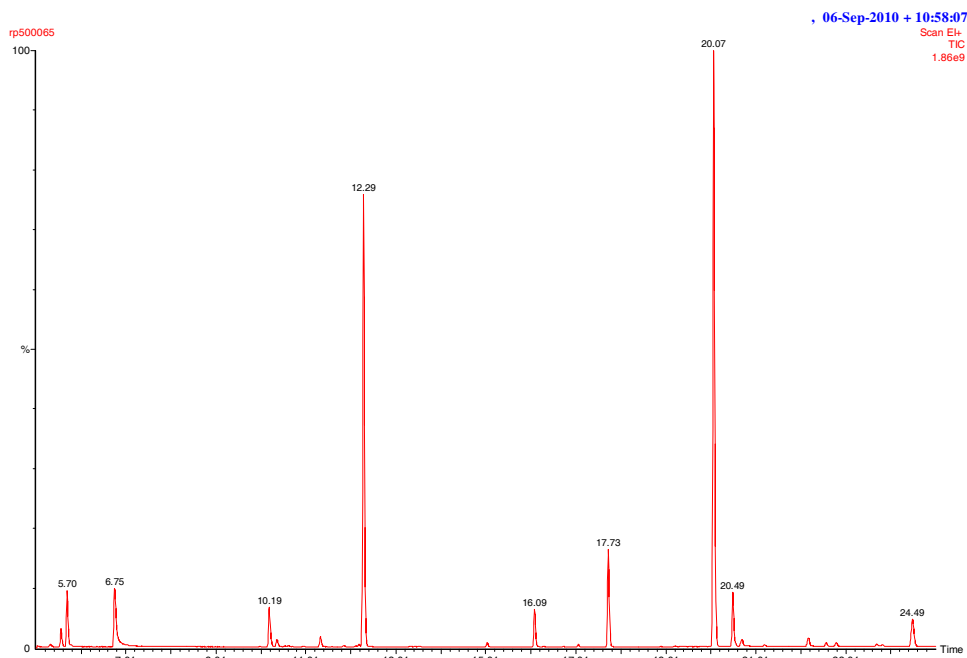


Dodecane internal standard $R_t = 12.22$ min. Decylbenzene $R_t = 18.75$ min.

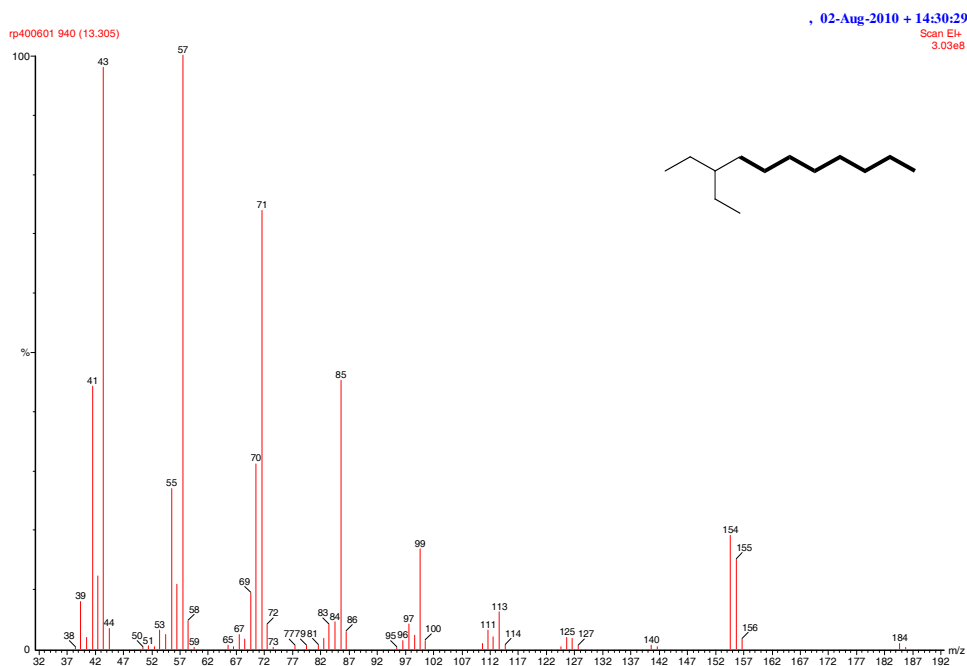
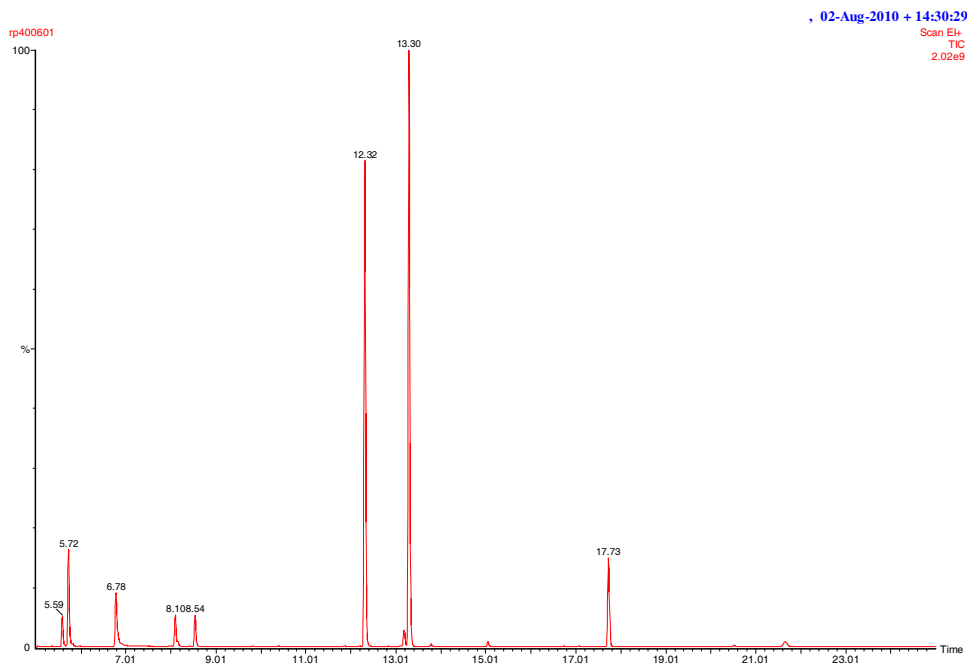


Chapter Two

Dodecane internal standard $R_t = 12.29$ min. (2-ethyldecyl)benzene $R_t = 20.07$ min.

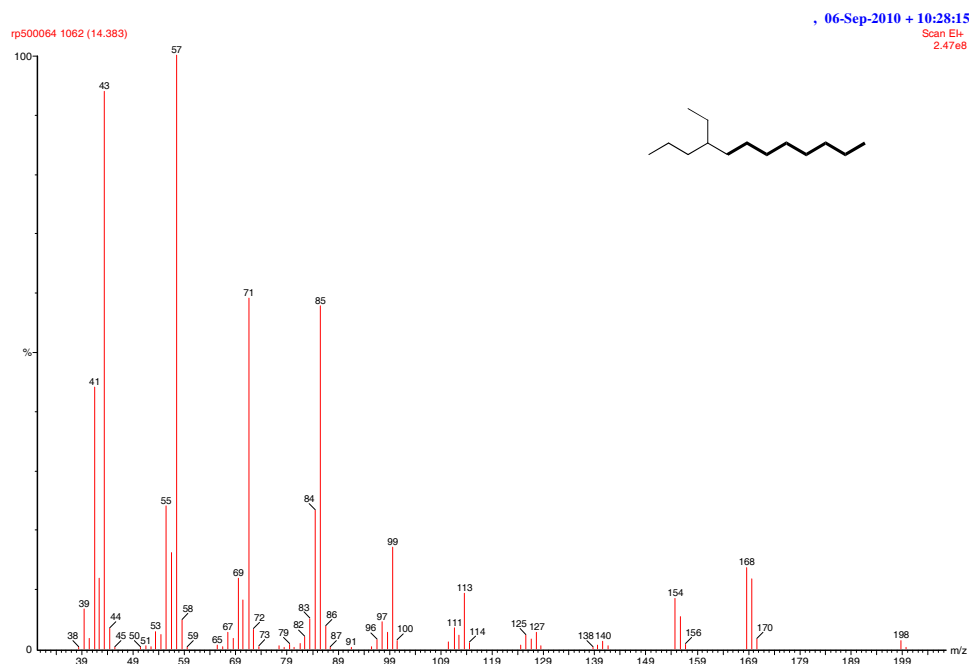
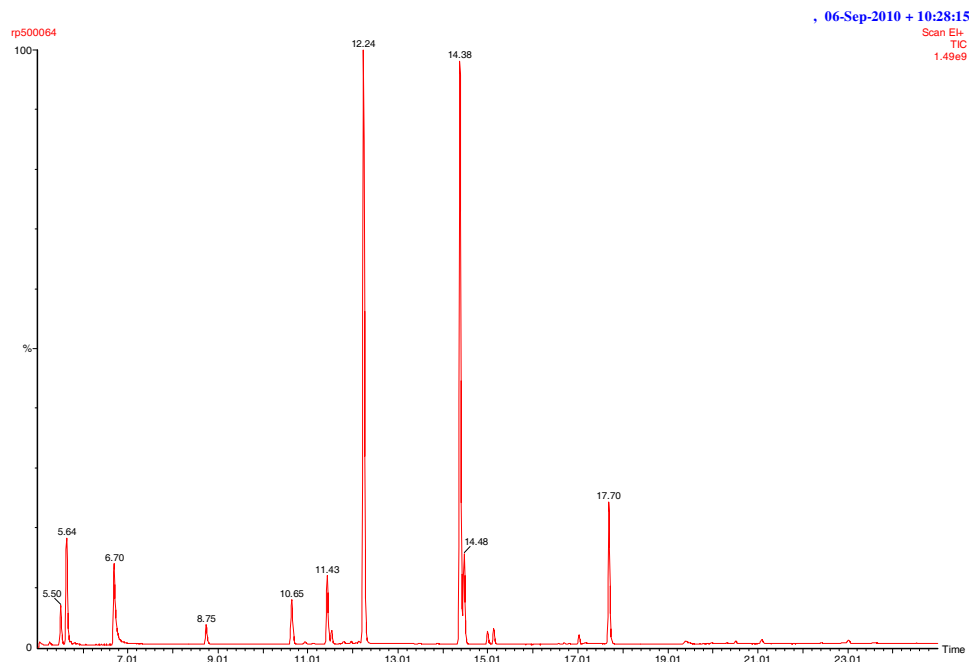


Dodecane internal standard $R_t = 12.32$ min. 3-Ethylundecane $R_t = 13.30$ min.

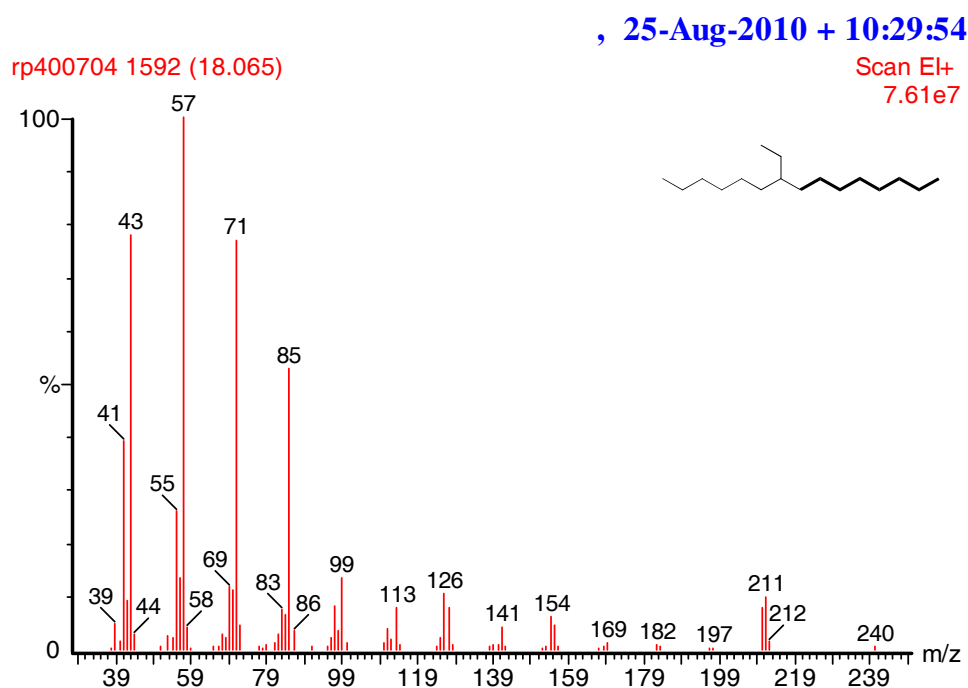
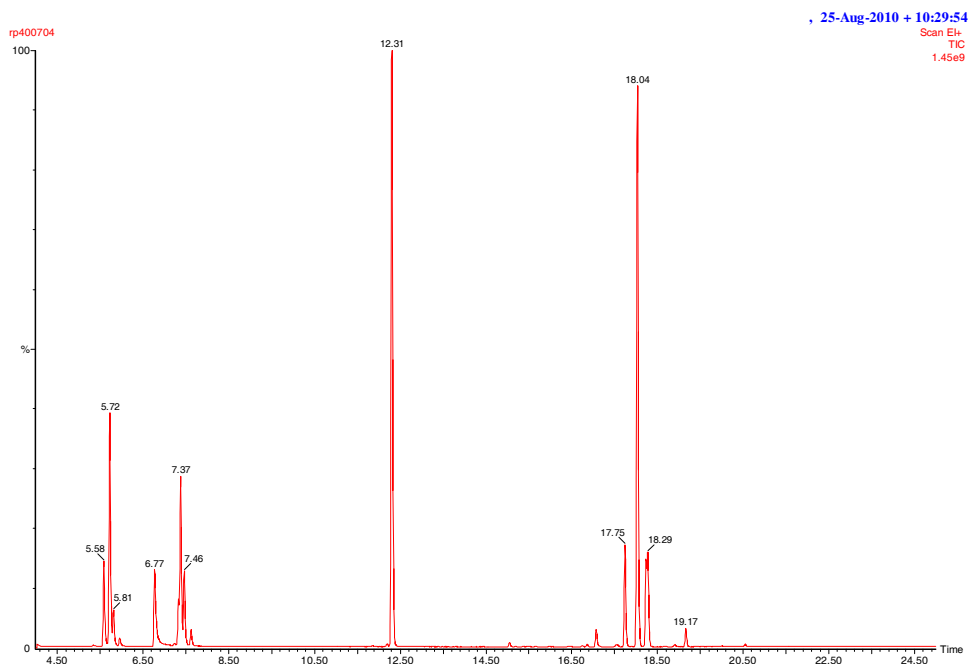


Chapter Two

Dodecane internal standard $R_t = 12.24$ min. 4-Ethyldecane $R_t = 14.38$ min.

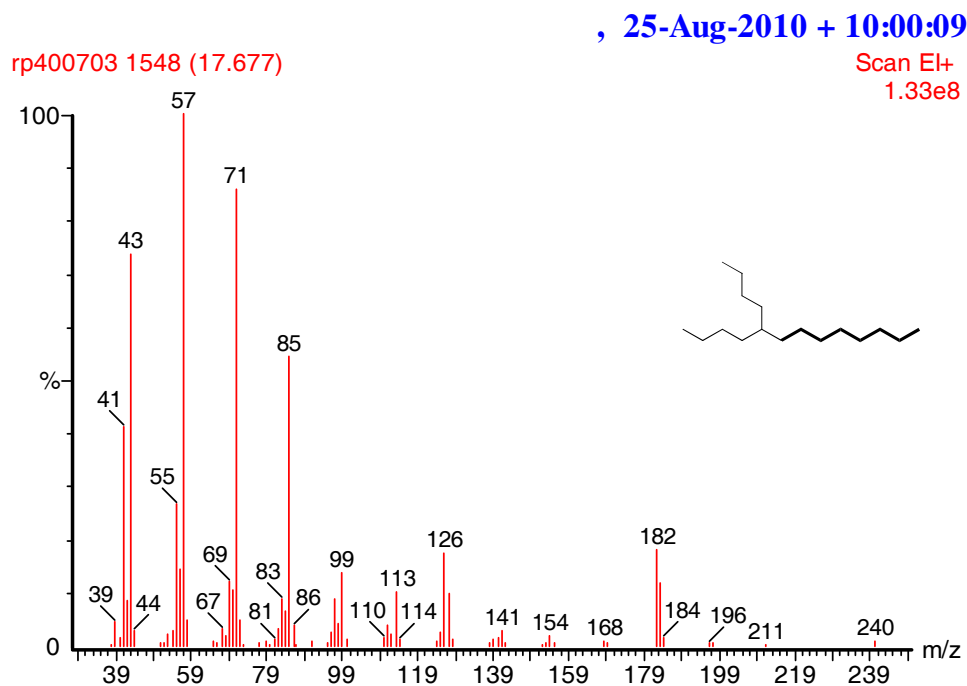
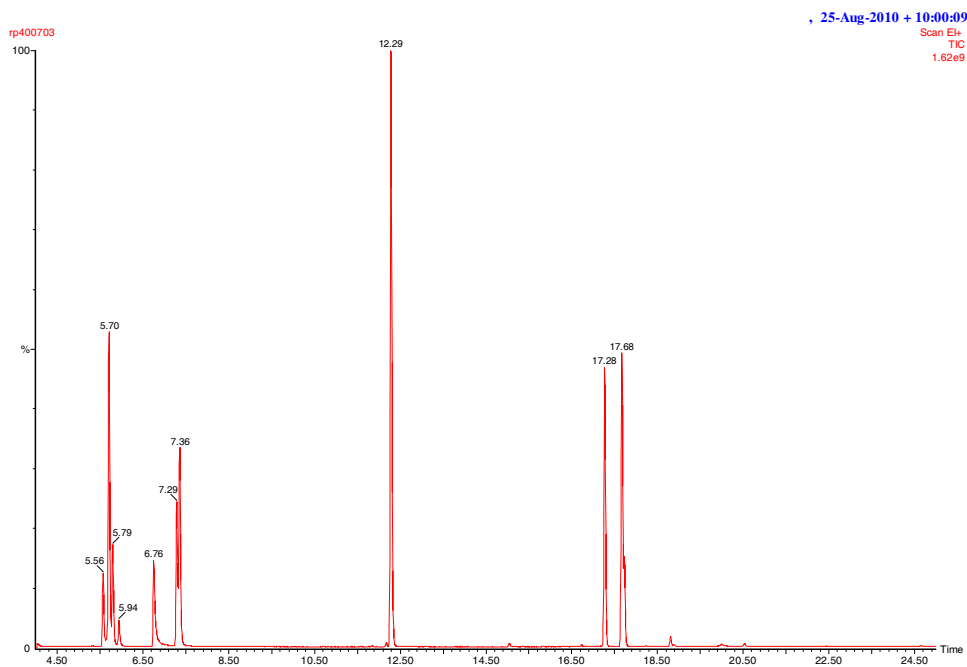


Dodecane internal standard $R_t = 12.31$ min. 7-Ethylpentadecane $R_t = 18.04$ min.

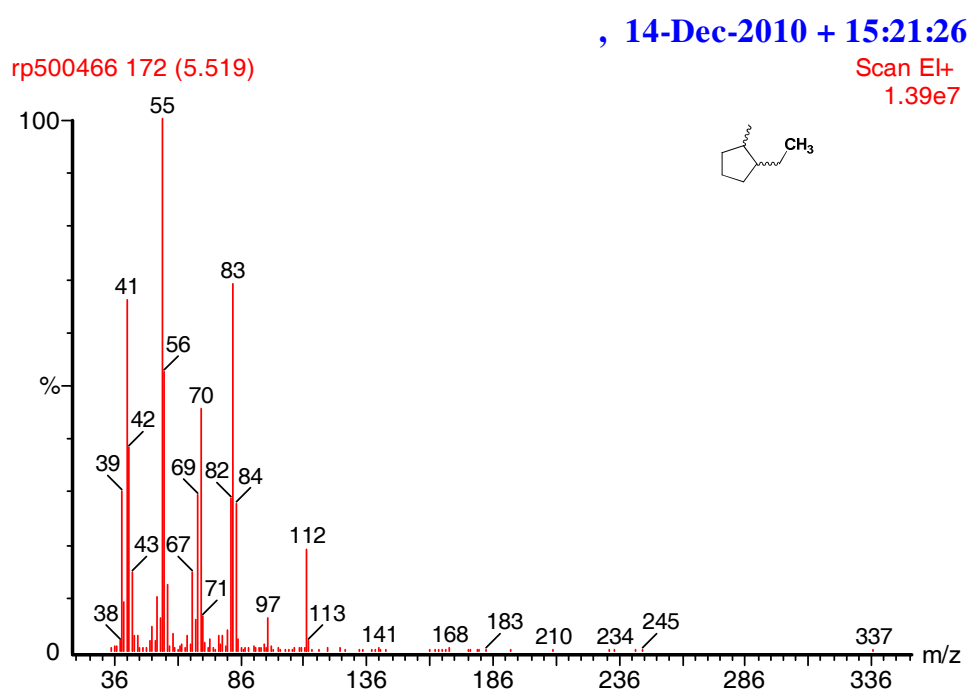
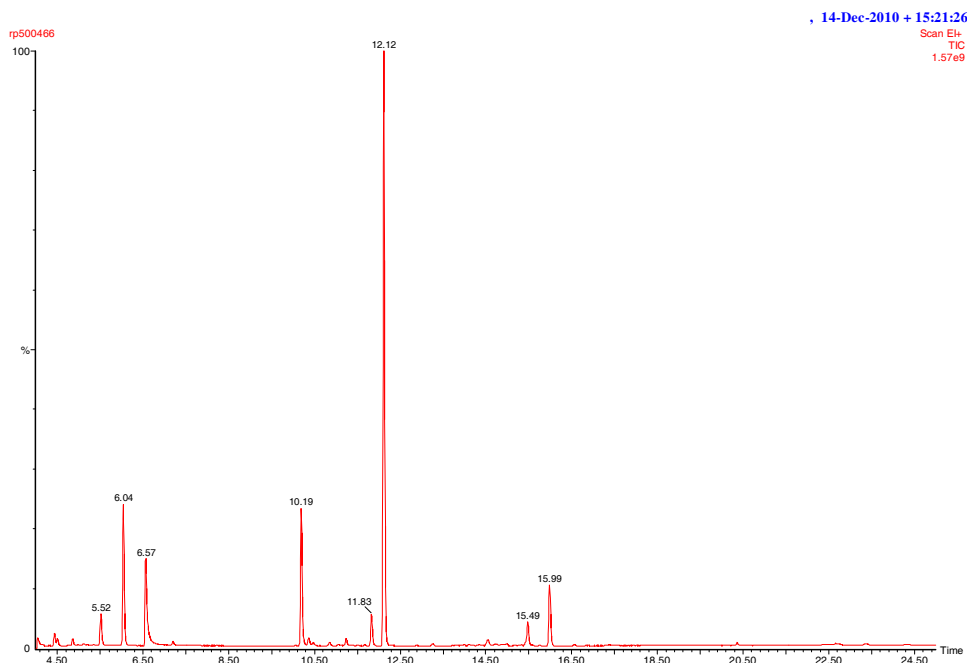


Chapter Two

Dodecane internal standard $R_t = 12.29$ min. 5-Butyltridecane $R_t = 17.68$ min.

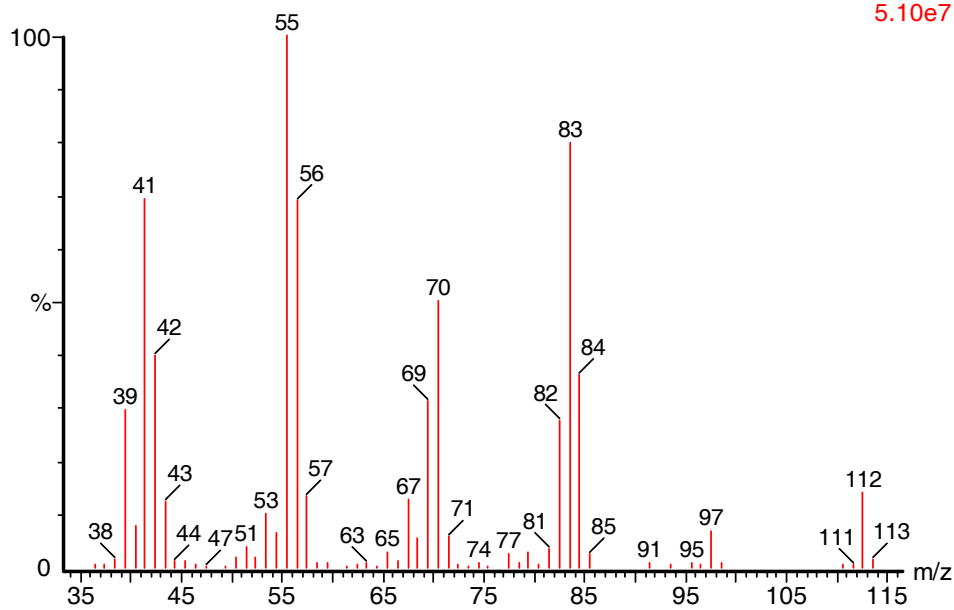


Dodecane internal standard $R_t = 12.12$ min. 1-ethyl-2-methylcyclopentane $R_t = 5.52$ and 6.04 min (cis and trans).

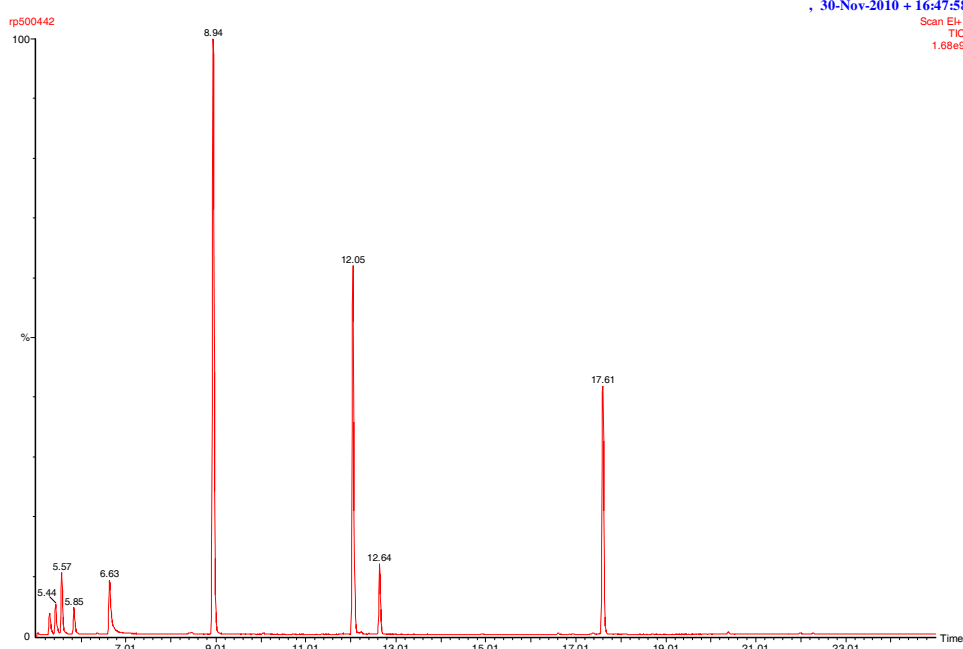


, 14-Dec-2010 + 15:21:26

rp500466 232 (6.049)

Scan EI+
5.10e7

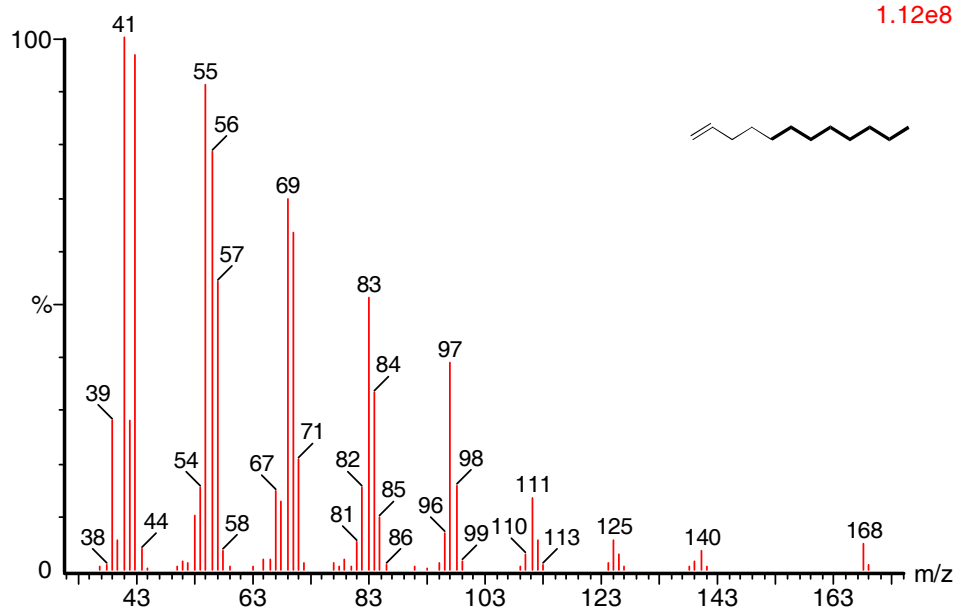
Decane internal standard $R_t = 8.94$ min. Dodec-1-ene $R_t = 12.05$ min, nonylcyclopropane $R_t = 12.64$ min.



, 30-Nov-2010 + 16:47:58

rp500442 798 (12.050)

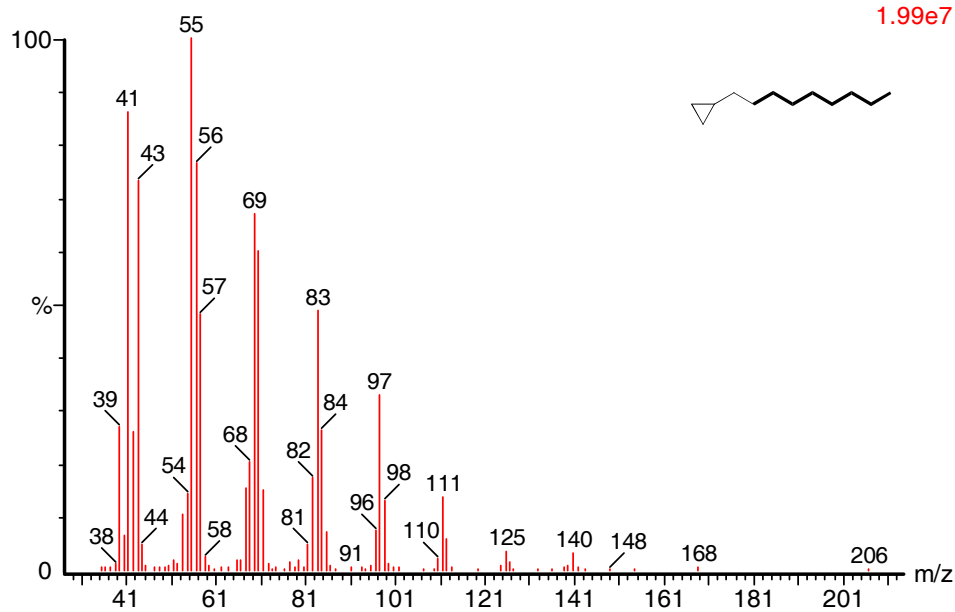
Scan EI+
1.12e8



, 30-Nov-2010 + 16:47:58

rp500442 866 (12.651)

Scan EI+
1.99e7



Chapter 3

Copper-Catalyzed Cross-Coupling of Functionalized Alkyl Halides and Tosylates with Secondary and Tertiary Alkyl Grignard Reagents*

*The results presented in this chapter were published in:

Ren, P.; Stern, L. A.; Hu, X. L. *Angew. Chem., Int. Ed.* **2012**, *51*, 9110-9113.

3.1 Introduction

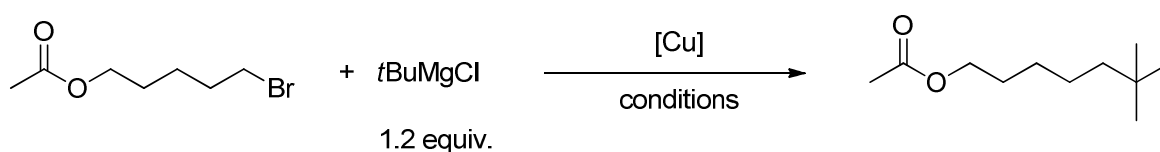
Efficient alkyl-alkyl cross-coupling reactions have historically been difficult to achieve, due to the reluctance of alkyl electrophiles to undergo oxidative addition, and due to the propensity of metal alkyl intermediates for β -H elimination.¹⁻⁷ Recent work shows that these problems can be circumvented by judicious choices of catalysts, ligands, and conditions.⁸⁻²⁷ The previous chapter demonstrated how secondary alkyl halides could couple with primary Grignard reagents in high yields using nickel catalysts. However, the complementary process, that is, the coupling of non-activated alkyl electrophiles with secondary and tertiary alkyl nucleophiles, is still challenging. This is due to the difficulty in transmetallation from sterically encumbered nucleophiles, and because isomerization of metal alkyl species is generally facile and will lead to undesired products.²⁸⁻³⁷ As a result, these potentially valuable coupling reactions have not been systematically investigated and only sporadic examples have been reported.^{10-13, 38-42} In this context, the work of Cahiez *et al.* and Kambe *et al.* on copper catalysis deserves special attention.^{12, 13, 38, 39} They showed that non-activated alkyl halides could be coupled to secondary and tertiary alkyl Grignard reagents in high yields in the presence of a copper salt, with or without a diene or alkyne ligand. These studies provide important proofs of concept. However, only simple alkyl halides such as octyl and decyl halides were used as the substrates. The synthetic utility of these reactions was not fully demonstrated, given the high reactivity of alkyl Grignard reagents towards functional groups. Following our group's earlier work in functional group-tolerant Kumada coupling of non-activated alkyl halides,^{26,43,44} we decided to study the copper-catalyzed coupling reactions using functionalized alkyl electrophiles as the coupling partners. In this chapter, I describe a copper-based method that is efficient for the coupling of secondary and tertiary Grignard reagents with alkyl halides and tosylates containing important and sensitive functional groups. The high activity, broad scope, and high functional group tolerance of the copper catalysis showcase its value in preparative and synthetically useful reactions.

3.2 Optimization of the reaction conditions for coupling of 5-bromopentyl acetate with ^tBuMgCl

The coupling of 5-bromopentyl acetate with ^tBuMgCl (1.0 M in THF) was used as the test reaction (Table 1). Without a catalyst, no coupling product was formed. In the presence of a simple copper salt such as CuCl, the coupling proceeded smoothly at room temperature. The yields were over 90% for reactions in THF, toluene, or ether, but lower for reactions in DMF

or NMP. A loading of 0.5 mol% was sufficient to give a yield of 94%. The coupling reaction could be catalyzed by a soluble Cu(I) complex such as $[\text{Cu}(\text{PPh}_3)\text{Cl}]_4$, or $[\text{Cu}(\text{Phen})(\text{PPh}_3)_2]\text{NO}_3$ in a similar yield. CuCl_2 and $\text{CuCl}_2 \cdot 2\text{H}_2\text{O}$ were also suitable pre-catalysts. It appears that Cu-catalyzed cross-coupling of 5-bromopentyl acetate with $t\text{BuMgCl}$ is highly efficient under very simple conditions such as a small loading of CuCl , room temperature, in THF, and with no additives.

Table 1. Entries for the optimization of conditions for the coupling of 5-bromopentyl acetate with $t\text{BuMgCl}$.



Entry	Cat. (loading)	Solvent	T[°C]	Yield (%) ^a
1	CuCl (3 mol%)	THF	r.t.	94
2	CuCl (3 mol%)	THF	-20	39
3	CuCl (3 mol%)	THF	-60	29
4	CuCl (1 mol%)	THF	r.t.	95 ^b
5	CuCl (0.5 mol%)	THF	r.t.	94 ^b
6	No cat.	THF	r.t.	Trace
7	CuCl_2 (3 mol%)	THF	r.t.	89
8	$\text{Cu}(\text{PPh}_3)\text{Cl}$ (3 mol%)	THF	r.t.	97
9	$[\text{Cu}(\text{Phen})(\text{PPh}_3)_2]\text{NO}_3$ (3 mol%)	THF	r.t.	90
10	$\text{Cu}(\text{CH}_3\text{CN})_4\text{PF}_6$ (3 mol%)	THF	r.t.	11

Table 1. (Continued)

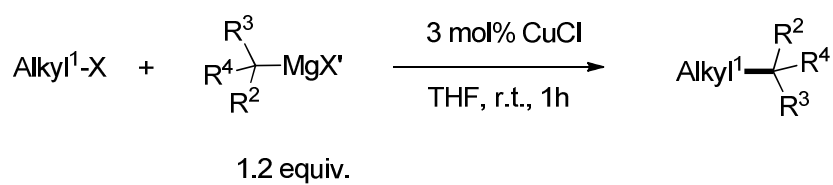
Entry	Cat. (loading)	Solvent	T[°C]	Yield (%) ^a
11	CuCl ₂ •2H ₂ O (3 mol%)	THF	r.t.	90
12	CuCl (3 mol%)	Et ₂ O	r.t.	93
13	CuCl (3 mol%)	DMF	r.t.	60
14	CuCl (3 mol%)	Toluene	r.t.	94
15	CuCl (3 mol%)	Pentane	r.t.	88
16	CuCl (3 mol%)	Dioxane	r.t.	Trace
17	CuCl (3 mol%)	DMA	r.t.	43
18	CuCl (3 mol%)	NMP	r.t.	38

^a GC yields. ^b Reaction performed on scale 10 times larger than given in the general reaction condition.

3.3 Scope of Kumada-Corriu-Tamao coupling of functionalized alkyl halides with alkyl Grignard reagents

Having demonstrated that the copper catalysis could be applied for the coupling of a functionalized alkyl halide with a tertiary alkyl Grignard reagent, we decided to explore the scope of this catalysis. For the convenience of experimental manipulation, the reactions were carried out in THF, at room temperature, and with 3 mol % CuCl as catalyst. As shown in Table 2, a large number of functionalized alkyl electrophiles could be coupled to secondary and tertiary alkyl Grignard reagents in high isolated yields. The coupling was generally completed within 1 h.

Table 2. Scope of Cu-catalyzed alkyl-alkyl coupling.^a

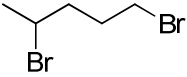
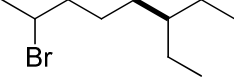
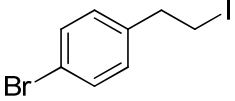
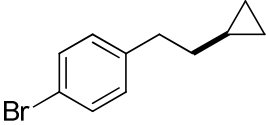
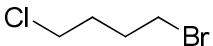
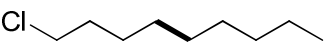
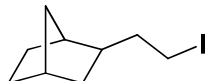
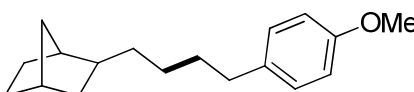
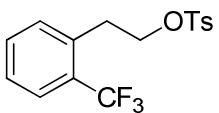
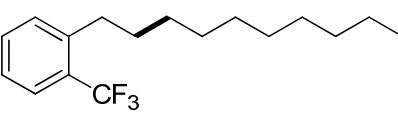


Entry	Alkyl-X	Product	Yield ^b (%)
1			82
2			77
3			75
4			73
5			76 ^c
6			91 ^c
7			81
8			82
9			90
10			80

Table 2. (Continued)

Entry	Alkyl-X	Product	Yield ^b (%)
11			82
12			75
13			86
14			82
15			84
16			84
17			83
18			87
19			74
20			75 ^d
21			93
22			85

Table 2. (Continued)

Entry	Alkyl-X	Product	Yield ^b (%)
23			76
24			94
25			90
26			93
27			78

^a See experimental part. ^b Isolated yield. ^c 2.2 equiv. of Grignard reagent was used. ^d 4 equiv. of NMP was used as additive.

Ester and amide groups were readily tolerated (entries 1-4, Table 2). A substrate containing a carboxylic acid group was successfully coupled when more than 2 equiv. of a Grignard reagent was applied (entry 5, Table 2). Presumably the first equivalent of the Grignard reagent deprotonated the carboxylic acid group to form a carboxylate group, which however did not interfere with the cross coupling. Likewise, a substrate containing an alcohol group was coupled in a high yield under similar conditions (entry 6, Table 2). As expected, the more robust ether and thioether groups were tolerated (entries 7-10, Table 2). Nitrile-containing substrates were coupled as well (entries 11 and 12, Table 2). Acetal group was also tolerated, which could lead to useful aldehyde-containing compounds after deprotection (entry 13, Table 2). Gratifyingly, substrates containing important heterocyclic groups such as indole, furan, piperidine, thiophene, and pyridine groups were coupled in high yields (entries 14-19, Table 2). The coupling of ketone-containing substrates was more challenging. Under the standard conditions, the yields were about 30-50% (entries 1 and 2, Table 3). Decreasing the Grignard or increasing the catalyst loading was not helpful. However, it was found that NMP (NMP = *N*-methylpyrrolidone) promoted the coupling of ketone-containing substrates. For example, with 4 equiv. of NMP as additive, the yield of a substrate containing an aliphatic ketone moiety was increased to 75% (entry 20, Table 1).

Table 3. Coupling of ketone-containing substrate.

Entry	Cat. (loading)	Conditions	Yield (%) ^a
1	CuCl (5 mol%)	ⁱ PrMgCl 1.2 equiv., r.t., THF	42
2	CuCl (5 mol%)	^t BuMgCl 1.2 equiv., r.t., THF	51
3	CuCl (5 mol%)	^t BuMgCl 1.2 equiv., -20 °C, THF	30
4	CuCl (5 mol%)	^t BuMgCl 1.2 equiv., r.t., THF, 4 equiv. NMP	75
5	CuCl (10 mol%)	^t BuMgCl 1.2 equiv., r.t., THF	71
6	CuBrS(CH ₃) ₂ (5 mol%)	^t BuMgCl 1.2 equiv., r.t., THF	68
7	CuCl (5 mol%)	^t BuMgCl 1.0 equiv., -20 °C, THF	30
8	CuCl (5 mol%)	^t BuMgCl 1.0 equiv., r.t., THF	29

^a GC yields.

Importantly, not only alkyl iodides and bromides, but also alkyl tosylates could be coupled (entries 18 and 19, Table 2). Because tosylates are often easily prepared from the corresponding alcohols, this success significantly increases the synthetic utility of the present coupling method. Alkyl-Cl could not be coupled under these conditions. Thus, selective coupling of an alkyl bromide in the presence of an alkyl-Cl group was achieved (entry 21, Table 2). Likewise, because secondary alkyl halide could not be coupled under these conditions, the coupling of primary alkyl bromide is selective in the presence of a secondary alkyl-Br moiety (entries 22-23, Table 2). Interestingly, the coupling of alkyl electrophile is selective in the presence of an aryl-Br moiety (entry 24, Table 2). This feature can be useful for sequential and selective functionalization of alkyl and aryl electrophiles.

The nucleophilic coupling partners are not limited to ⁱPrMgCl or ^tBuMgCl. Various acyclic and cyclic Grignard reagents could be used. While the present work focuses on the coupling of secondary and tertiary alkyl Grignard reagents, the same method could be used for the coupling of primary alkyl Grignard reagents with high yields (entries 25-27, Table 2).

The limit of the group tolerance of the coupling method was also probed, which indicated that aldehyde, nitro, and succinimide groups were not compatible with this method (Table 4). Probably these functional groups were too reactive towards Grignard reagents.

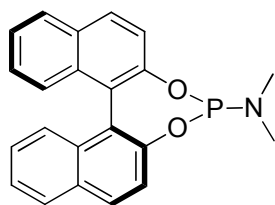
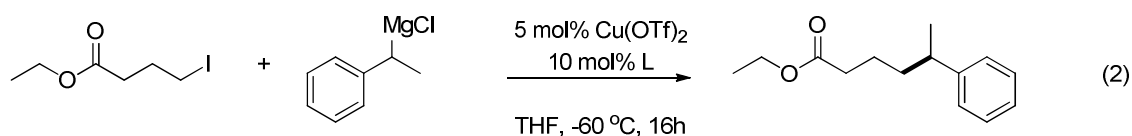
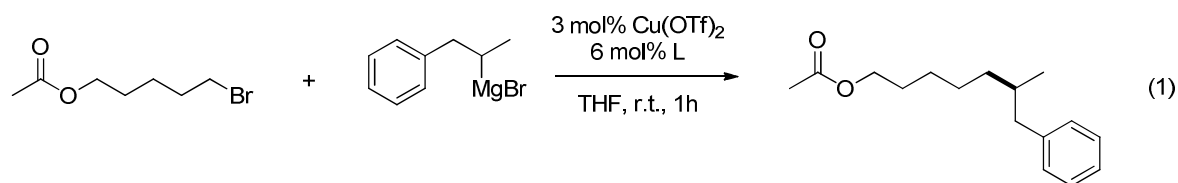
Table 4. Limitations of the coupling method.

$\text{Alkyl}^1\text{-X} + \begin{array}{c} \text{R}^3 \\ \\ \text{R}^4 - \text{C} - \text{MgX}' \\ \\ \text{R}^2 \end{array} \xrightarrow[\text{THF, r.t., 1h}]{5 \text{ mol\% CuCl}} \text{Alkyl}^1 - \begin{array}{c} \text{R}^2 \\ \\ \text{R}^4 - \text{C} \\ \\ \text{R}^3 \end{array}$			
1.2 equiv.			
Entry	Alkyl-X	Grignard	Yield (%) ^a
1		ⁱ PrMgCl	0
2		^t BuMgCl	0
3		ⁱ PrMgCl	trace
4		^t BuMgCl	16
5		^t BuMgCl	0

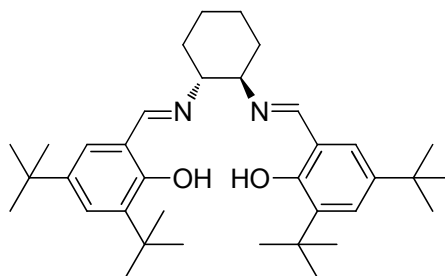
^a GC yields.

3.4 Attempts at asymmetric catalysis of alkyl-alkyl Kumada-Coriu-Tamao coupling

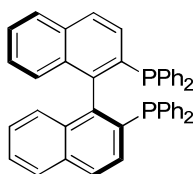
Since a tertiary or quaternary carbon center is produced by the cross coupling of a primary alkyl electrophile with a secondary or tertiary alkyl Grignard reagent, this reaction may provide the chance to create a stereogenic center via an asymmetric process. Thus, we attempted to develop enantioselective coupling reactions of this type using a chiral copper catalyst. Two test reactions were investigated (eq. 1 and 2, Scheme 1). Five chiral ligands commonly used for copper catalysis were applied in conjunction with a soluble Cu salt- $\text{Cu}(\text{OTf})_2$. Upon addition of a ligand to a solution of $\text{Cu}(\text{OTf})_2$, the color of the solution changed instantaneously, indicating the formation of a soluble copper complex. As shown in Scheme 1, the yields of the coupling reactions were high regardless of the ligands employed. However, none of the five ligands gave rise to an enantiomeric excess, even at $-60\text{ }^\circ\text{C}$. It is possible that the copper complexes with these ligands cannot differentiate between the two substituents of the secondary alkyl Grignard reagents. It is also possible that the active catalyst is an organocopper species without the chiral ligand attached. Further work is warranted to probe the origin of the non-enantioselectivity, and to eventually develop an enantioselective coupling method.



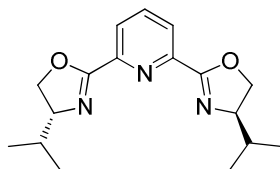
rxn. 1: yield: 82%, e.e.: ~ 0%
rxn. 2: yield: 74%, e.e.: ~ 0%



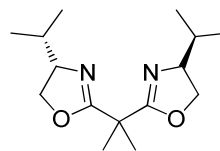
rxn. 1: yield: 73%, e.e.: ~ 0%
rxn. 2: yield: 67%, e.e.: ~ 0%



rxn. 1: yield: 68%, e.e.: ~ 0%
rxn. 2: yield: 88%, e.e.: ~ 0%



rxn. 1: yield: 83%, e.e.: ~ 0%
rxn. 2: yield: 75%, e.e.: ~ 0%

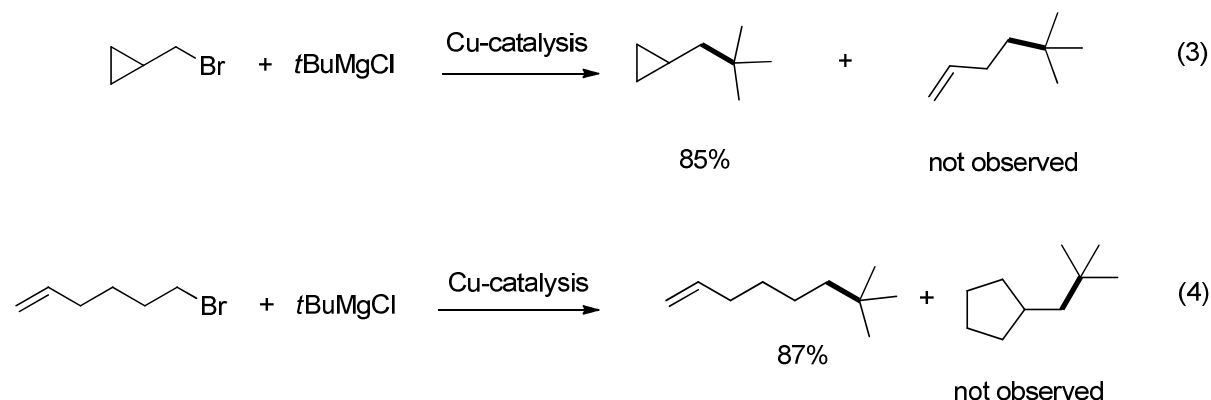


rxn. 1: yield: 84%, e.e.: ~ 0%
rxn. 2: yield: 75%, e.e.: ~ 0%

Scheme 1. Cross coupling reactions employing chiral ligands. Yields were determined by GC.

3.5 Mechanistic investigations

A few experiments were conducted to probe the mechanism of the coupling reactions. The Cu-catalyzed coupling of **1** with $t\text{BuMgCl}$ had the same yields in the absence and presence of excess (100 equiv.) amount of Hg. This result suggests that homogeneous copper species, rather than heterogeneous copper particles, are the active catalysts. The coupling of cyclopropyl methyl bromide with $t\text{BuMgCl}$ yielded only neopentylcyclopropane, but not 5,5-dimethylhex-1-ene (eq. 3, Scheme 2). The coupling of 6-bromo-1-hexene with $t\text{BuMgCl}$ yielded only 7,7-dimethyloct-1-ene, but not neopentylcyclopentane (eq. 4, Scheme 2). These results indicate that the activation of alkyl electrophile does not occur via a radical mechanism. Given that alkyl tosylates can be coupled in high yields, a $\text{S}_{\text{N}}2$ mechanism is more likely, which is consistent with the work of Kambe *et al.* on similar reactions.¹²



Scheme 2. Cross coupling reactions using radical probes. Yields were determined by GC.

3.6 Conclusions

In conclusion, we have developed a highly efficient method for the cross coupling of non-activated and functionalized alkyl halides and tosylates with secondary and tertiary alkyl Grignard reagents. The copper-based method is remarkably simple and general. The wide scope, and especially the tolerance to a large number of important yet sensitive functional groups, makes this method attractive for the preparation of functional molecules.⁴⁵

3.7 Experimental section

3.7.1 Chemicals and Reagents

All manipulations were carried out under an inert N₂(g) atmosphere using standard Schlenk or glovebox techniques. Solvents were purified using a two-column solid-state purification system (Innovative Technology, NJ, USA) and transferred to the glove box without exposure to air. Deuterated solvents were purchased from Cambridge Isotope Laboratories, Inc., and were degassed and stored over activated 3 Å molecular sieves. Unless otherwise noted, all other reagents and starting materials were purchased from commercial sources and used without further purification. Liquid compounds were degassed by standard freeze-pump-thaw procedures prior to use. The list of the references and procedures for the synthesis of the following starting materials can be found in our group previous publications:^{43,44,46,47} *N,N*-diethyl-6-bromohexanamide (table 2, entry 2), ethyl 4-iodobutanoate (table 2, entry 4), (3-bromopropoxy)benzene (table 2, entry 7), 6-iodo-2,2-diphenylhexanenitrile (table 2, entry 11), (3-bromopropyl)(phenyl)sulfane (table 2, entry 8), methyl 1-(3-iodopropyl)-1H-indole-3-carboxylate (table 2, entry 14), 1-(3-iodopropyl)-3-methyl-1H-indole (table 2, entry 15), 2-(3-iodopropyl)furan (table 2, entry 16), tert-butyl 4-(iodomethyl)piperidine-1-carboxylate (table 2, entry 17), 1-iodooctan-4-one (table 2, entry 20), 1-bromo-4-(2-iodoethyl)benzene (table 2, entry 24), 2-(2-iodoethyl)bicyclo[2.2.1]heptanes (table 2, entry 26). 2-(thiophen-2-yl)ethyl 4-methylbenzenesulfonate (table 2, entry 18), 2-(pyridin-2-yl)ethyl 4-methylbenzenesulfonate (table 2, entry 19), 2-(trifluoromethyl)phenethyl 4-methylbenzenesulfonate (table 2, entry 27) were prepared from the corresponding alcohol by standard methods.^{48,49} *Tert*-butylmagnesium chloride (1.0 M solution in THF), isopropylmagnesium chloride (2.0 M solution in THF), cyclopentylmagnesium chloride (2.0 M solution in diethyl ether), cyclopropylmagnesium bromide (0.5 M solution in THF), cycloheptylmagnesium bromide (2.0 M solution in diethyl ether), cyclohexylmagnesium chloride (2.0 M solution in diethyl

ether), 3-pentylmagnesium bromide (2.0 M solution in diethyl ether), pentylmagnesium chloride (2.0 M solution in THF), 4-methoxyphenethylmagnesium chloride (0.5 M solution in THF), octylmagnesium chloride (2 M solution in THF) were purchased from Aldrich. (1-phenylpropan-2-yl)magnesium bromide and (1-phenylethyl)magnesium chloride were prepared from their corresponding bromide or chloride in THF using general literature procedure.^{50,51} Concentration of Grignard reagents was determined using literature procedure.⁵²

3.7.2 Physical methods

The ^1H and ^{13}C NMR spectra were recorded at 293 K on a Bruker Avance 400 spectrometer. ^1H NMR chemical shifts were referenced to residual solvent as determined relative to Me_4Si ($\delta = 0$ ppm). The $^{13}\text{C}\{^1\text{H}\}$ chemical shifts were reported in ppm relative to the carbon resonance of CDCl_3 (77.0 ppm), $[\text{D}_6]\text{DMSO}$ (39.5 ppm). GC measurement was conducted on a Perkin-Elmer Clarus 400 GC with a FID detector. HRESI-MS measurements were conducted at the EPFL ISIC Mass Spectrometry Service with a Micro Mass QTOF Ultima spectrometer. APPI-MS experiments were performed on a hybrid linear ion trap Fourier transform ion cyclotron resonance mass spectrometer (LTQ FT-ICR MS, Thermo Scientific, Bremen, Germany) equipped with a 10 T superconducting magnet (Oxford Instruments Nanoscience, Abingdon, UK). Samples were dissolved at a concentration of 0.1 mg/mL in toluene and analysed using the atmospheric pressure photoionization (APPI) ion source at a flow rate of 10 $\mu\text{L}/\text{min}$. The nebulizer temperature was set to 300 $^\circ\text{C}$. Mass measurements were performed with a resolution of 100'000 at m/z 400, with 50 to 100 scans averaging. Data analysis was carried out using XCalibur software (Thermo Scientific, Bremen, Germany). Elemental analyses were performed on a Carlo Erba EA 1110 CHN instrument at EPFL. HPLC analyses were carried out on an Agilent 1260 system with CHIRALPACK[®] IB column for 6-methyl-7-phenylheptyl acetate and CHIRALCEL[®] OB-H column for ethyl 5-phenylhexanoate in hexane/isopropanol mixtures.

3.7.3 General procedures for the entries reported in Table 1, 3, 4

A 1.0 M solution of *tert*-butylmagnesium chloride (commercially available, 0.6 mL, 0.6 mmol) was added to a 1.5 mL of THF solution containing CuCl (1.5 mg, 0.015 mmol) and 5-bromopentyl acetate (83 μL , 0.5 mmol) (slow addition is not necessary and the Grignard reagent could be added at once). The reaction mixture was stirred at room temperature for 1 h. It was quenched by the addition of 10 mL of saturated NH_4Cl aqueous solution. The

organic phase in the resulting solution mixture was extracted with ether (3 times, 10 mL each), dried over Na₂SO₄, filtered, and subject to GC analysis. 60 µL of dodecane was used as an internal standard.

3.7.4 General procedures for the entries reported in Table 2

A solution of alkyl Grignard reagent (1.8 mmol) was added to a 4.5 mL of THF solution containing CuCl (4.5 mg, 0.045 mmol) and alkyl halide (1.5 mmol) (slow addition is not necessary and the Grignard reagent could be added at once). The reaction mixture was stirred at room temperature for 1 h. It was quenched by the addition of 20 mL of saturated NH₄Cl aqueous solution. The organic phase in the resulting solution mixture was extracted with ether (3 times, 20 mL each), dried over Na₂SO₄, filtered, and finally evaporated under a reduced pressure. The residue was purified by flash chromatography (silica-gel) to afford the product. For the new compounds, their ¹H and ¹³C data were reported together with high resolution mass spectrometric data and/or elemental analysis.

3.7.5 General procedures for cross coupling reactions employing chiral ligands in scheme 1

Cu(OTf)₂ (0.015 mmol) and chiral ligand (0.030 mmol) were stirred in THF (1.5 ml) at room temperature for 20 min. Then, 5-bromopentyl acetate (83 µL, 0.5 mmol) was added and the resulting solution was cooled to -60 °C. (1-phenylpropan-2-yl)magnesium bromide (0.6 mmol) was added, and the solution was stirred for 1h under -60 °C. The reaction was quenched by the addition of 10 mL of saturated NH₄Cl aqueous solution. The organic phase in the resulting solution mixture was extracted with ether (3 times, 10 mL each), dried over Na₂SO₄, filtered. The yield was determined by GC, 60 µL of dodecane was used as an internal standard. The e.e. value was determined by HPLC with chiral column. Similar procedure was used for the reaction shown in scheme 1, equation 2 except the condition details shown in the equation.

3.7.6 Hg-test experiment

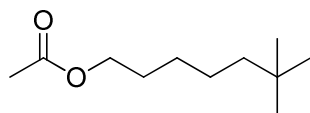
The reaction condition was the same as 3.7.3 except 100 equiv. Hg relative to CuCl was added in the beginning of the reaction.

3.7.7 Radical probe experiments

The cross coupling reactions in scheme 2 were carried out following the protocol described in part 3.7.3. The products were identified by GC, GC-MS and NMR. Particularly

the protons on the double bond of the product or starting materials are easy to identify by NMR.

3.7.8 Detailed descriptions for products



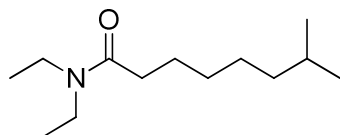
6,6-dimethylheptyl acetate (table 2, entry 1):

Eluated from the column with hexane-diethyl ether (10:1) in 82% yield as a colorless liquid.

^1H NMR (400 MHz, CDCl_3): 4.05 (t, $J = 6.4$ Hz, 2H), 2.04 (s, 3H), 1.65-1.56 (m, 2H), 1.38-1.20 (m, 4H), 1.20-1.12 (m, 2H), 0.86 (s, 9H).

^{13}C NMR (100 MHz, CDCl_3): 170.9, 64.5, 44.0, 30.1, 29.3, 28.6, 26.8, 24.1, 20.8.

HRESI-MS: calculated for ($\text{C}_{11}\text{H}_{23}\text{O}_2$, $\text{M}+\text{H}$), 187.1698; found, 187.1704.



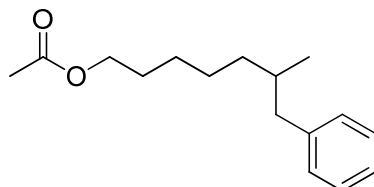
N,N-diethyl-7-methyloctanamide (table 2, entry 2):

Eluated from the column with hexane-diethyl ether (1:1) in 77% yield as a colorless liquid.

^1H NMR (400 MHz, CDCl_3): 3.28 (q, $J = 7.2$ Hz, 2H), 3.22 (q, $J = 7.2$ Hz, 2H), 2.19 (t, $J = 7.6$ Hz, 2H), 1.59-1.52 (m, 2H), 1.48-1.36 (m, 1H), 1.26-1.17 (m, 4H), 1.10-1.06 (m, 5H), 1.01 (t, $J = 7.2$ Hz, 3H), 0.77 (d, $J = 6.8$ Hz, 6H).

^{13}C NMR (100 MHz, CDCl_3): 172.0, 41.7, 39.8, 38.6, 32.9, 29.6, 27.7, 27.0, 25.3, 22.4, 14.2, 12.9.

HRESI-MS: calculated for ($\text{C}_{13}\text{H}_{28}\text{NO}$, $\text{M}+\text{H}$), 214.2171; found, 214.2170.



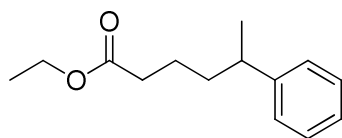
6-metyl-7-phenylheptyl acetate (table 2, entry 3):

Eluated from the column with hexane-diethyl ether (1:1) in 77% yield as a colorless liquid.

^1H NMR (400 MHz, CDCl_3): 7.33-7.28 (m, 2H), 7.26-7.17 (m, 3H), 4.09 (t, $J = 6.8$ Hz, 2H), 2.71-2.64 (m, 1H), 2.45-2.35 (m, 1H), 2.08 (s, 3H), 1.83-1.70 (m, 1H), 1.70-1.62 (m, 2H), 1.51-1.29 (m, 5H), 1.28-1.15 (m, 1H), 0.89 (d, $J = 6.4$ Hz, 3H).

^{13}C NMR (100 MHz, CDCl_3): 171.1, 141.1, 129.1, 128.0, 125.5, 64.5, 43.6, 36.4, 34.9, 28.5, 26.7, 26.1, 20.9, 19.3.

HRESI-MS: calculated for ($\text{C}_{16}\text{H}_{25}\text{O}_2$, $\text{M}+\text{H}$), 249.1855; found, 249.1852.

**Ethyl 5-phenylhexanoate (table 2, entry 4):⁵³**

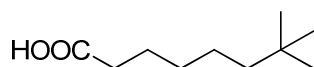
Eluated from the column with hexane-diethyl ether (100:0 to 10:1) in 73% yield as a colorless liquid.

¹H NMR (400 MHz, CDCl₃): 7.34-7.28 (m, 2H), 7.21-7.17 (m, 3H), 4.11 (q, *J* = 7.2 Hz, 2H), 2.78-2.65 (m, 1H), 2.27 (t, *J* = 6.8 Hz, 2H), 1.67-1.44 (m, 4H), 1.27-1.21 (m, 6H).

¹³C NMR (100 MHz, CDCl₃): 173.6, 147.1, 128.3, 126.9, 125.9, 60.1, 39.7, 37.7, 34.3, 23.1, 22.2, 14.2.

HRESI-MS: calculated for (C₁₄H₂₁O₂, M+H), 221.1542; found, 221.1552.

Elemental analysis: Anal. Calcd for C₁₄H₂₀O₂: C, 76.33; H, 9.15. Found: C, 76.69; H, 9.37.

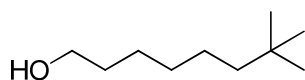
**7,7-dimethyloctanoic acid (table 2, entry 5):**

Queched with 30 ml H₂O and 1 ml 25% HCl instead of saturated NH₄Cl solution. Eluated from the column with hexane-diethyl ether (2:1) containing 1% HOAc in 76% yield as a colorless liquid.

¹H NMR (400 MHz, [D₆]DMSO): 11.99 (br.s, 1H), 2.18 (t, *J* = 7.2 Hz, 2H), 1.56-1.45 (m, 2H), 1.30-1.05 (m, 6H), 0.85 (s, 9H).

¹³C NMR (100 MHz, [D₆]DMSO): 174.5, 43.6, 33.7, 30.1, 29.6, 29.3, 24.6, 23.8.

HRESI-MS: calculated for (C₁₀H₁₉O₂, M-H), 171.1385; found, 171.1377.

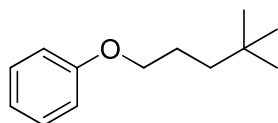
**7,7-dimethyloctan-1-ol (table 2, entry 6):**

Eluated from the column with hexane-diethyl ether (3:1) in 91% yield as a colorless liquid.

¹H NMR (400 MHz, CDCl₃): 3.64 (t, *J* = 6.4 Hz, 2H), 1.61-1.48 (m, 2H), 1.38-1.13 (m, 9H), 0.86 (s, 9H).

¹³C NMR (100 MHz, CDCl₃): 63.1, 44.2, 32.8, 30.3, 30.3, 29.4, 25.8, 24.5.

Elemental analysis: Anal. Calcd for C₁₀H₂₂O: C, 75.88; H, 14.01. Found: C, 75.54; H, 13.73.

**((4,4-dimethylpentyl)oxy)benzene (table 2, entry 7):**

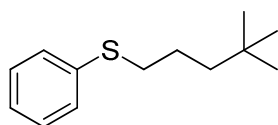
Eluated from the column with hexane-diethyl ether (60:1) in 81% yield as a colorless liquid.

¹H NMR (400 MHz, CDCl₃): 7.34-7.26 (m, 2H), 6.98-6.90 (m, 3H), 3.95 (t, *J* = 6.8 Hz, 2H), 1.86-1.72 (m, 2H), 1.41-1.28 (m, 2H), 0.95 (s, 9H).

¹³C NMR (100 MHz, CDCl₃): 159.1, 129.4, 120.4, 114.5, 68.7, 40.1, 30.2, 29.3, 24.7.

HRESI-MS: calculated for (C₁₃H₂₁O, M+H), 193.1592; found, 193.1600.

Elemental analysis: Anal. Calcd for C₁₃H₂₀O: C, 81.20; H, 10.48. Found: C, 80.97; H, 10.48.

**((4,4-dimethylpentyl)sulfanyl)benzene (table 2, entry 8):**

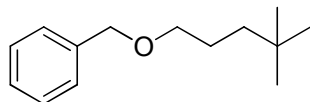
Eluated from the column with hexane in 82% yield as a colorless liquid.

¹H NMR (400 MHz, CDCl₃): 7.44-7.31 (m, 4H), 7.21 (t, *J* = 6.8 Hz, 1H), 2.95 (t, *J* = 7.2 Hz, 2H), 1.72-1.59 (m, 2H), 1.40-1.33 (m, 2H), 0.93 (s, 9H).

¹³C NMR (100 MHz, CDCl₃): 137.0, 128.7, 128.7, 125.5, 43.3, 34.4, 30.3, 29.3, 24.4.

HRESI-MS: calculated for (C₁₃H₂₁S, M+H), 209.1364; found, 209.1365.

Elemental analysis: Anal. Calcd for C₁₃H₂₁S: C, 74.94; H, 9.67. Found: C, 74.56; H, 9.45.



((4,4-dimethylpentyl)oxyl)methylbenzene (table 2, entry 9):

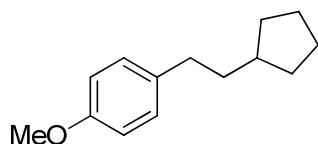
Eluted from the column with hexane-diethyl ether (50:1) in 90% yield as a colorless liquid.

¹H NMR (400 MHz, CDCl₃): 7.38-7.35 (m, 4H), 7.35-7.27 (m, 1H), 4.53 (s, 2H), 3.48 (t, *J* = 6.4 Hz, 2H), 1.68-1.59 (m, 2H), 1.28-1.24 (m, 2H), 0.92 (s, 9H).

¹³C NMR (100 MHz, CDCl₃): 138.6, 128.3, 127.6, 127.4, 72.8, 71.4, 40.2, 30.1, 29.3, 25.0.

HRESI-MS: calculated for (C₁₄H₂₃O, M+H), 207.1749; found, 207.1747.

Elemental analysis: Anal. Calcd for C₁₃H₂₀S: C, 81.50; H, 10.75. Found: C, 81.40; H, 10.85.



1-(2-cyclopentylethyl)-4-methoxybenzene (table 2, entry 10):

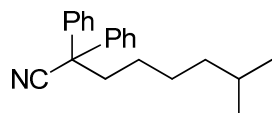
Eluted from the column with hexane-diethyl ether (40:1 to 10:1) in 80% yield as a colorless liquid.

¹H NMR (400 MHz, CDCl₃): 7.19 (d, *J* = 7.6 Hz, 2H), 6.92 (d, *J* = 8.0 Hz, 2H), 3.86 (s, 3H), 2.66 (t, *J* = 7.6 Hz, 2H), 1.88-1.80 (m, 3H), 1.80-1.54 (m, 6H), 1.31-1.22 (m, 2H).

¹³C NMR (100 MHz, CDCl₃): 157.5, 135.0, 129.1, 113.5, 55.1, 39.5, 38.4, 34.1, 32.6, 25.2.

HRESI-MS: calculated for (C₁₄H₂₁O, M+H), 205.1592; found, 205.1596.

Elemental analysis: Anal. Calcd for C₁₃H₂₀S: C, 81.50; H, 10.75. Found: C, 81.40; H, 10.85.



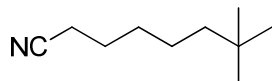
7-methyl-2,2-diphenyloctanenitrile (table 2, entry 11):

Eluted from the column with hexane-diethyl ether (10:1) in 82% yield as a colorless liquid.

¹H NMR (400 MHz, CDCl₃): 7.48-7.20 (m, 10H), 2.39-2.28 (m, 2H), 1.56-1.23 (m, 5H), 1.20-1.06 (m, 2H), 0.84 (d, *J* = 6.4 Hz, 6H).

¹³C NMR (100 MHz, CDCl₃): 140.3, 128.8, 127.7, 126.8, 122.5, 51.8, 39.7, 38.5, 27.8, 27.2, 25.8, 22.5.

HRESI-MS: calculated for (C₂₁H₂₆N, M+H), 292.2065; found, 292.2060.



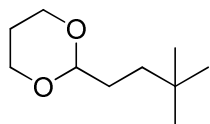
7,7-dimethyloctanenitrile (table 2, entry 12):

Eluted from the column with hexane-diethyl ether (10:1) in 75% yield as a colorless liquid.

¹H NMR (400 MHz, CDCl₃): 2.32 (t, *J* = 7.2 Hz, 2H), 1.69-1.62 (m, 2H), 1.44-1.35 (m, 2H), 1.32-1.20 (m, 2H), 1.20-1.14 (m, 2H), 0.85 (s, 9H).

¹³C NMR (100 MHz, CDCl₃): 119.8, 43.8, 30.2, 29.5, 29.3, 25.3, 23.7, 17.1.

HRESI-MS: calculated for (C₁₀H₂₀N, M+H), 154.1596; found, 154.1591.

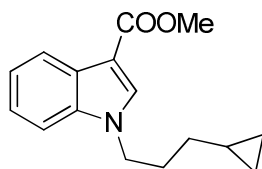
**2-(3,3-dimethylbutyl)-1,3-dioxane (table 2, entry 13):**

Eluated from the column with pentane-diethyl ether (10:1) in 86% yield as a colorless liquid.

^1H NMR (400 MHz, CDCl_3): 4.47 (t, $J = 5.2$ Hz, 1H), 4.14-4.07 (m, 2H), 3.80-3.72 (m, 2H), 2.15-2.00 (m, 1H), 1.62-1.52 (m, 2H), 1.36-1.28 (m, 1H), 1.28-1.24 (m, 2H), 0.87 (s, 9H).

^{13}C NMR (100 MHz, CDCl_3): 103.1, 66.9, 37.8, 30.6, 29.8, 29.2, 25.8.

HRESI-MS: calculated for ($\text{C}_{10}\text{H}_{21}\text{O}_2$, $\text{M}+\text{H}$), 173.1542; found, 173.1546.

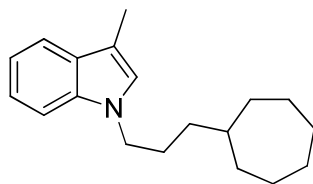
**Methyl 1-(3-cyclopropylpropyl)-1H-indole-3-carboxylate (table 2, entry 14):**

Eluated from the column with hexane-diethyl ether (9:2) in 82% yield as a colorless liquid.

^1H NMR (400 MHz, CDCl_3): 8.24-8.20 (m, 1H), 7.83 (s, 1H), 7.38-7.31 (m, 1H), 7.31-7.27 (m, 2H), 4.12 (t, $J = 7.2$ Hz, 2H), 3.93 (s, 3H), 2.02-1.92 (m, 2H), 1.29-1.20 (m, 2H), 0.72-0.61 (m, 1H), 0.50-0.41 (m, 2H), 0.07-0.00 (m, 2H).

^{13}C NMR (100 MHz, CDCl_3): 165.3, 136.3, 134.0, 126.5, 122.4, 121.6, 121.5, 109.9, 106.6, 50.8, 46.5, 31.6, 29.7, 10.2, 4.3.

HRESI-MS: calculated for ($\text{C}_{16}\text{H}_{20}\text{NO}_2$, $\text{M}+\text{H}$), 258.1494; found, 258.1497.

**1-(3-cycloheptylpropyl)-3-methyl-1H-indole (table 2, entry 15):**

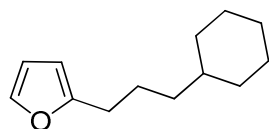
Eluated from the column with hexane in 84% yield as a colorless liquid.

^1H NMR (400 MHz, CDCl_3): 7.65 (d, $J = 7.6$ Hz, 1H), 7.37 (d, $J = 8.0$ Hz, 1H), 7.36-7.26 (m, 1H), 7.19-7.16 (m, 1H), 6.93 (s, 1H), 4.10 (t, $J = 7.2$ Hz, 2H), 2.43 (s, 3H), 1.98-1.82 (m, 2H), 1.82-1.45 (m, 11H), 1.40-1.19 (m, 4H).

^{13}C NMR (100 MHz, CDCl_3): 136.3, 128.7, 125.5, 121.2, 119.0, 118.4, 110.0, 109.2, 46.5, 39.0, 35.4, 34.5, 28.5, 28.3, 26.5, 9.7.

HRESI-MS: calculated for ($\text{C}_{19}\text{H}_{28}\text{N}$, $\text{M}+\text{H}$), 270.2222; found, 270.2212.

Elemental analysis: Anal. Calcd for $\text{C}_{19}\text{H}_{27}\text{N}$: C, 84.70; H, 10.10; N, 5.20. Found: C, 84.55; H, 10.48; N, 5.14.

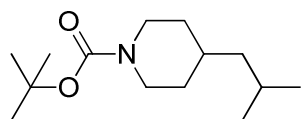
**2-(3-cyclohexylpropyl)furan (table 2, entry 16):**

Eluated from the column with hexane in 84% yield as a colorless liquid.

^1H NMR (400 MHz, CDCl_3): 7.30 (dd, $J = 2.0, 0.8$ Hz, 1H), 6.29-6.28 (m, 1H), 5.99-5.98 (m, 1H), 2.60 (t, $J = 7.6$ Hz, 2H), 1.79-1.60 (m, 7H), 1.18-1.33 (m, 6H), 0.92-0.80 (m, 2H).

^{13}C NMR (100 MHz, CDCl_3): 156.6, 140.6, 110.0, 104.4, 37.4, 37.0, 33.3, 28.3, 26.7, 26.4, 25.3.

Elemental analysis: Anal. Calcd for C₁₃H₂₀O: C, 81.20; H, 10.48. Found: C, 81.31; H, 10.63.



tert-butyl 4-isobutylpiperidine-1-carboxylate (table 2, entry 17):

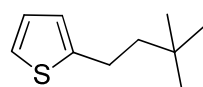
Eluated from the column with hexane-diethyl ether (10:1) in 83% yield as a colorless liquid.

¹H NMR (400 MHz, CDCl₃): 4.06 (br.s, 2H), 2.74-2.61 (m, 2H), 1.72-1.54 (m, 3H), 1.45 (s, 9H), 1.42-1.48(m, 1H, overlap), 1.11-0.98 (m, 4H), 0.86 (d, *J* = 6.4 Hz, 6H).

¹³C NMR (100 MHz, CDCl₃): 154.7, 78.9, 45.9, 43.9 (br), 33.4, 32.3, 28.4, 24.4, 22.7.

HRESI-MS: calculated for (C₁₄H₂₈NO₂, M+H), 242.2120; found, 242.2112.

Elemental analysis: Anal. Calcd for C₁₄H₂₇NO₂: C, 69.66; H, 11.27; N, 5.80. Found: C, 69.47; H, 11.27; N, 5.74.



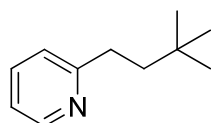
2-(3,3-dimethylbutyl)thiophene (table 2, entry 18):

Eluated from the column with pentane in 87% yield as a colorless liquid.

¹H NMR (400 MHz, CDCl₃): 7.13-7.09 (m, 1H), 6.94-6.90 (m, 1H), 6.81-6.78 (m, 1H), 2.85-2.79 (m, 2H), 1.66-1.58 (m, 2H), 0.97 (s, 9H).

¹³C NMR (100 MHz, CDCl₃): 146.5, 126.6, 123.5, 122.6, 46.2, 30.5, 29.2, 25.3.

HRESI-MS: calculated for (C₁₀H₁₇S, M+H), 169.1051; found, 169.1060.



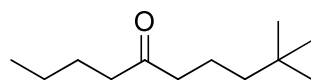
2-(3,3-dimethylbutyl)pyridine (table 2, entry 19):⁵⁴

Eluated from the column with pentane-diethyl ether (3:1) in 74% yield as a colorless liquid.

¹H NMR (400 MHz, CDCl₃): 8.54-8.49 (m, 1H), 7.55 (td, *J* = 7.6, 1.6 Hz, 1H), 7.13 (d, *J* = 8.0 Hz, 1H), 7.07-7.04 (m, 1H), 2.78-2.69 (m, 2H), 1.61-1.57 (m, 2H), 0.96 (s, 9H).

¹³C NMR (100 MHz, CDCl₃): 163.1, 149.1, 136.2, 122.5, 120.7, 44.3, 33.9, 30.5, 29.3.

HRESI-MS: calculated for (C₁₁H₁₈N, M+H), 164.1439; found, 164.1434.



9,9-dimethyldecan-5-one (table 2, entry 20):

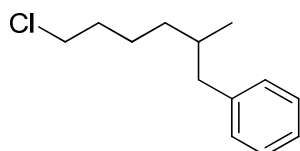
Eluated from the column with hexane-diethyl ether (60:1) in 75% yield as a colorless liquid.

¹H NMR (400 MHz, CDCl₃): 2.40-2.30 (m, 4H), 1.58-1.47 (m, 4H), 1.34-1.23 (m, 2H), 1.14-1.10 (m, 2H), 0.88 (t, *J* = 7.2 Hz, 3H), 0.85 (s, 9H).

¹³C NMR (100 MHz, CDCl₃): 211.6, 43.7, 43.6, 42.5, 30.3, 29.3, 26.0, 22.4, 19.1, 13.8.

HRESI-MS: calculated for (C₁₂H₂₅O, M+H), 185.1905; found, 185.1907.

Elemental analysis: Anal. Calcd for C₁₂H₂₄O: C, 78.20; H, 13.12. Found: C, 78.09; H, 13.21.

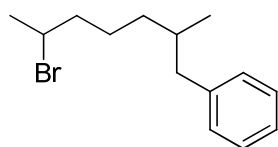
**(6-chloro-2-methylhexyl)benzene (table 2, entry 21):**

Eluated from the column with hexane in 93% yield as a colorless liquid containing 10% 2,3-dimethyl-1,4-diphenylbutane which cannot be separated from chromatography column.

^1H NMR (400 MHz, CDCl_3): 7.34-7.25 (m, 2H), 7.23-7.12 (m, 3H), 3.55 (t, $J = 6.4$ Hz, 2H), 2.64 (dd, $J = 13.6, 6.4$ Hz, 1H), 2.40 (dd, $J = 13.2, 8.0$ Hz, 1H), 1.84-1.69 (m, 3H), 1.62-1.32 (m, 3H), 1.25-1.12 (m, 1H), 0.88 (d, $J = 6.8$ Hz, 3H).

^{13}C NMR (100 MHz, CDCl_3): 141.4, 129.2, 128.2, 125.7, 45.2, 43.6, 35.8, 34.9, 32.9, 24.4, 19.4.

APPI-MS: calculated for $\text{C}_{13}\text{H}_{19}\text{Cl}$, 210.11698; Found, 210.11707.

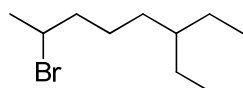
**(6-bromo-2-methylheptyl)benzene (table 2, entry 22):**

Eluated from the column with hexane in 85% yield as a colorless liquid containing 11% 2,3-dimethyl-1,4-diphenylbutane which cannot be separated from chromatography column.

^1H NMR (400 MHz, CDCl_3): 7.32-7.26 (m, 2H), 7.25-7.14 (m, 3H), 4.21-4.14 (m, 1H), 2.77-2.62 (m, 1H), 2.49-2.36 (m, 1H), 1.89-1.14 (m, 10H), 0.86-0.96 (m, 3H).

^{13}C NMR (100 MHz, CDCl_3): 141.3, 129.1, 128.1, 125.6, 51.8, 43.7, 43.5, 41.4, 41.3, 35.9, 35.8, 34.9, 34.8, 26.5, 26.4, 25.3, 25.2, 19.4, 19.3.

APPI-MS: calculated for $\text{C}_{14}\text{H}_{21}\text{Br}$, 268.08211; found, 268.08221.

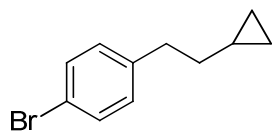
**2-bromo-6-ethyloctane (table 2, entry 23):**

Eluated from the column with hexane in 76% yield as a colorless liquid.

^1H NMR (400 MHz, CDCl_3): 4.20-4.09 (m, 1H), 1.90-1.67 (m, 5H), 1.52-1.13 (m, 9H), 0.84 (t, $J = 7.6$ Hz, 6H).

^{13}C NMR (100 MHz, CDCl_3): 52.0, 41.6, 40.2, 32.0, 26.5, 25.4, 25.3, 25.0, 10.9, 10.8.

Elemental analysis: Anal. Calcd for $\text{C}_{10}\text{H}_{21}\text{Br}$: C, 54.30; H, 9.57. Found: C, 54.25; H, 9.73.

**1-bromo-4-(2-cyclopropylethyl)benzene (table 2, entry 24):**

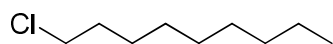
Eluated from the column with hexane in 94% yield as a colorless liquid.

^1H NMR (400 MHz, CDCl_3): 7.43-7.38 (m, 2H), 7.10-7.07 (m, 2H), 2.69 (t, $J = 7.6$ Hz, 2H), 1.56-1.48 (m, 2H), 0.77-0.63 (m, 1H), 0.49-0.39 (m, 2H), 0.10-0.04 (m, 2H).

^{13}C NMR (100 MHz, CDCl_3): 141.5, 131.2, 130.2, 119.2, 36.5, 35.4, 10.6, 4.5.

APPI-MS: calculated for $\text{C}_{11}\text{H}_{13}\text{Br}$, 224.01951; found, 224.01957.

Elemental analysis: Anal. Calcd for $\text{C}_{11}\text{H}_{13}\text{Br}$: C, 58.69; H, 5.82. Found: C, 58.44; H, 5.79.

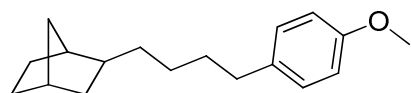


1-chlorononane (table 2, entry 25):²⁶

Eluated from the column with hexane in 90% yield as a colorless liquid.

¹H NMR (400 MHz, CDCl₃): 3.52 (t, *J* = 6.8 Hz, 2H), 1.82-1.70 (m, 2H), 1.48-1.34 (m, 2H), 1.34-1.20 (m, 10H), 0.88 (t, *J* = 6.8 Hz, 3H).

¹³C NMR (100 MHz, CDCl₃): 45.1, 32.7, 31.8, 29.4, 29.2, 28.9, 26.9, 22.7, 14.1.



2-(4-(4-methoxyphenyl)butyl)bicyclo[2.2.1]heptane (table 2, entry 26):

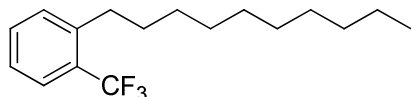
Eluated from the column with hexane in 93% yield as a colorless liquid.

¹H NMR (400 MHz, CDCl₃): 7.11-7.06 (m, 2H), 6.84-6.80 (m, 2H), 3.79 (s, 3H), 2.59-2.49 (m, 2H), 2.19-2.12 (m, 1H), 1.97-1.88 (m, 1H), 1.62-0.91 (m, 15H).

¹³C NMR (100 MHz, CDCl₃): 157.6, 135.1, 129.2, 113.6, 55.3, 42.2, 41.1, 38.3, 36.8, 36.5, 35.2, 35.1, 31.9, 30.2, 28.9, 27.5.

HRESI-MS: calculated for C₁₈H₂₇O, 259.2062; found, 259.2061.

Elemental analysis: Anal. Calcd for C₁₈H₂₆O: C, 83.67; H, 10.14. Found: C, 83.56; H, 10.26.



1-decyl-2-(trifluoromethyl)benzene (table 2, entry 27):⁵⁵

Eluated from the column with hexane in 93% yield as a colorless liquid.

¹H NMR (400 MHz, CDCl₃): 7.61 (d, *J* = 8.0 Hz, 1H), 7.49-7.42 (m, 1H), 7.33 (d, *J* = 7.6 Hz, 1H), 7.29-7.23 (m, 1H), 2.81-2.75 (m, 2H), 1.69-1.56 (m, 2H), 1.47-1.25 (m, 14H), 0.90 (t, *J* = 6.8 Hz, 2H).

¹³C NMR (100 MHz, CDCl₃): 141.8, 131.6, 130.9, 128.3 (²*J*_{C-F} = 30.1 Hz), 125.8 (³*J*_{C-F} = 5.8 Hz), 125.6, 124.7 (¹*J*_{C-F} = 272.1 Hz), 32.7, 31.9, 31.8, 29.7, 29.6, 29.6, 29.4, 29.4, 22.7, 14.1.

3.8 References and Notes

- (1) Luh, T. Y.; Leung, M. K.; Wong, K. T. *Chem. Rev.* **2000**, *100*, 3187-3204.
- (2) Netherton, M. R.; Fu, G. C. *Adv. Synth. Catal.* **2004**, *346*, 1525-1532.
- (3) Frisch, A. C.; Beller, M. *Angew. Chem., Int. Ed.* **2005**, *44*, 674-688.
- (4) Terao, J.; Kambe, N. *Acc. Chem. Res.* **2008**, *41*, 1545-1554.
- (5) Kambe, N.; Iwasaki, T.; Terao, J. *Chem. Soc. Rev.* **2011**, *40*, 4937-4947.
- (6) Rudolph, A.; Lautens, M. *Angew. Chem., Int. Ed.* **2009**, *48*, 2656-2670.
- (7) Hu, X. L. *Chem. Sci.* **2011**, *2*, 1867-1886.
- (8) Devasagayaraj, A.; Studemann, T.; Knochel, P. *Angew. Chem., Int. Ed.* **1995**, *34*, 2723-2725.
- (9) Giovannini, R.; Studemann, T.; Dussin, G.; Knochel, P. *Angew. Chem., Int. Ed.* **1998**, *37*, 2387-2390.

-
- (10) Terao, J.; Watanabe, H.; Ikumi, A.; Kuniyasu, H.; Kambe, N. *J. Am. Chem. Soc.* **2002**, *124*, 4222-4223.
- (11) Terao, J.; Todo, H.; Watanabe, H.; Ikumi, A.; Kambe, N. *Angew. Chem., Int. Ed.* **2004**, *43*, 6180-6182.
- (12) Terao, J.; Todo, H.; Begum, S. A.; Kuniyasu, H.; Kambe, N. *Angew. Chem., Int. Ed.* **2007**, *46*, 2086-2089.
- (13) Cahiez, G.; Chaboche, C.; Jezequel, M. *Tetrahedron* **2000**, *56*, 2733-2737.
- (14) Cahiez, G.; Chaboche, C.; Duplais, C.; Giulliani, A.; Moyeux, A. *Adv. Synth. Catal.* **2008**, *350*, 1484-1488.
- (15) Jones, G. D.; Martin, J. L.; McFarland, C.; Allen, O. R.; Hall, R. E.; Haley, A. D.; Brandon, R. J.; Konovalova, T.; Desrochers, P. J.; Pulay, P.; Vicic, D. A. *J. Am. Chem. Soc.* **2006**, *128*, 13175-13183.
- (16) Valente, C.; Baglione, S.; Candito, D.; O'Brien, C. J.; Organ, M. G. *Chem. Commun.* **2008**, 735-737.
- (17) Netherton, M. R.; Dai, C. Y.; Neuschutz, K.; Fu, G. C. *J. Am. Chem. Soc.* **2001**, *123*, 10099-10100.
- (18) Zhou, J. R.; Fu, G. C. *J. Am. Chem. Soc.* **2003**, *125*, 14726-14727.
- (19) Saito, B.; Fu, G. C. *J. Am. Chem. Soc.* **2007**, *129*, 9602-9603.
- (20) Saito, B.; Fu, G. C. *J. Am. Chem. Soc.* **2008**, *130*, 6694-6695.
- (21) Lu, Z.; Fu, G. C. *Angew. Chem., Int. Ed.* **2010**, *49*, 6676-6678.
- (22) Owston, N. A.; Fu, G. C. *J. Am. Chem. Soc.* **2010**, *132*, 11908-11909.
- (23) Lu, Z.; Wilsily, A.; Fu, G. C. *J. Am. Chem. Soc.* **2011**, *133*, 8154-8157.
- (24) Zultanski, S. L.; Fu, G. C. *J. Am. Chem. Soc.* **2011**, *133*, 15362-15364.
- (25) Wilsily, A.; Tramutola, F.; Owston, N. A.; Fu, G. C. *J. Am. Chem. Soc.* **2012**, *2012*, 5794-5797.
- (26) Vechorkin, O.; Hu, X. L. *Angew. Chem., Int. Ed.* **2009**, *48*, 2937-2940.
- (27) Ren, P.; Vechorkin, O.; von Allmen, K.; Scopelliti, R.; Hu, X. L. *J. Am. Chem. Soc.* **2011**, *133*, 7084-7095.
- (28) Jana, R.; Pathak, T. P.; Sigman, M. S. *Chem. Rev.* **2011**, *111*, 1417-1492.
- (29) *For representative examples of cross coupling reactions of secondary and tertiary alkyl nucleophiles with aryl and alkynyl electrophiles, see refs. 30-37.*
- (30) Hintermann, L.; Xiao, L.; Labonne, A. *Angew. Chem., Int. Ed.* **2008**, *47*, 8246-8250.
- (31) Smith, S. W.; Fu, G. C. *Angew. Chem., Int. Ed.* **2008**, *47*, 9334-9336.
- (32) Han, C.; Buchwald, S. L. *J. Am. Chem. Soc.* **2009**, *131*, 7532-7533.

-
- (33) Sandrock, D. L.; Jean-Gerard, L.; Chen, C. Y.; Dreher, S. D.; Molander, G. A. *J. Am. Chem. Soc.* **2010**, *132*, 17108-17110.
- (34) Joshi-Pangu, A.; Wang, C. Y.; Biscoe, M. R. *J. Am. Chem. Soc.* **2011**, *133*, 8478-8481.
- (35) Lohre, C.; Droge, T.; Wang, C. Y.; Glorius, F. *Chem.-Eur. J.* **2011**, *17*, 6052-6055.
- (36) Seel, S.; Thaler, T.; Takatsu, K.; Zhang, C.; Zipse, H.; Straub, B. F.; Mayer, P.; Knochel, P. *J. Am. Chem. Soc.* **2011**, *133*, 4774-4777.
- (37) Thaler, T.; Haag, B.; Gavryushin, A.; Schober, K.; Hartmann, E.; Gschwind, R. M.; Zipse, H.; Mayer, P.; Knochel, P. *Nature Chem.* **2010**, *2*, 125-130.
- (38) Cahiez, G.; Gager, O.; Buendia, J. *Synlett* **2010**, 299-303.
- (39) Terao, J.; Ikumi, A.; Kuniyasu, H.; Kambe, N. *J. Am. Chem. Soc.* **2003**, *125*, 5646-5647.
- (40) Burns, D. H.; Miller, J. D.; Chan, H. K.; Delaney, M. O. *J. Am. Chem. Soc.* **1997**, *119*, 2125-2133.
- (41) Donkervoort, J. G.; Vicario, J. L.; Jastrzebski, J.; Gossage, R. A.; Cahiez, G.; van Koten, G. *J. Organomet. Chem.* **1998**, *558*, 61-69.
- (42) Breitenfeld, J.; Vechorkin, O.; Corminboeuf, C.; Scopelliti, R.; Hu, X. L. *Organometallics* **2010**, *29*, 3686-3689.
- (43) Vechorkin, O.; Proust, V.; Hu, X. L. *J. Am. Chem. Soc.* **2009**, *131*, 9756-9766.
- (44) Vechorkin, O.; Godinat, A.; Scopelliti, R.; Hu, X. L. *Angew. Chem., Int. Ed.* **2011**, *50*, 11777-11781.
- (45) Dufour, J.; Neuville, L.; Zhu, J. P. *Chem.-Eur. J.* **2010**, *16*, 10523-10534.
- (46) Vechorkin, O.; Barmaz, D.; Proust, V.; Hu, X. L. *J. Am. Chem. Soc.* **2009**, *131*, 12078-12079.
- (47) Vechorkin, O.; Proust, V.; Hu, X. L. *Angew. Chem., Int. Ed.* **2011**, *49*, 3061-3064.
- (48) Ferraboschi, P.; Mieri, M. D.; Galimberti, F. *Tetrahedron : Asymmetry* **2010**, *21*, 2136-2141.
- (49) Cheng, K.; Kim, I. J.; Lee, M. J.; Adah, S. A.; Raymond, T. J.; Bilsky, E. J.; Aceto, M. D.; May, E. L.; Harris, L. S.; Coop, A.; Dersch, C. M.; Rothman, R. B.; Jacobson, A. E.; Rice, K. C. *Org. Biomol. Chem.* **2007**, *5*, 1177-1190.
- (50) Conejo-García, A.; Pisani, L.; del Carmen Núñez, M.; Catto, M.; Nicolotti, O.; Leonetti, F.; Campos, J. M.; Gallo, M. A.; Espinosa, A.; Carotti, A. *J. Med. Chem.* **2011**, *54*, 2627-2645.
- (51) Draoli, D. R.; Burdett, M. T.; Ellman, J. A. *J. Am. Chem. Soc.* **2001**, *123*, 10127-10128.
- (52) Love, B. E.; Jones, E. G. *J. Org. Chem.* **1999**, *64*, 3755-3756.

- (53) Kitano, M.; Ohashi, N. PCT Int. Appl., WO 9961414 A1 19991202, **1999**.
- (54) Lewis, J. C.; Bergman, R. G.; Ellman, J. A. *J. Am. Chem. Soc.* **2007**, *129*, 5332–5333.
- (55) Herve, A.; Rodriguez, A. L.; Fouquet, E. *J. Org. Chem.* **2005**, *70*, 1953-1956.

Chapter 4

Synthesis of Copper Complexes with Hemilabile Ligands; Copper-Catalyzed Direct Alkylation of Benzoxazoles Using Secondary Alkyl Halides*

*Parts of the work presented in this chapter was published in:

Ren, P.; Salihu, I.; Scopelliti, R.; Hu, X. *L.Org. Lett.* **2012**, *14*, 1748-1751.

4.1 Introduction

The synthesis of aromatic heterocycles has been actively investigated because these molecules often exhibit interesting biological, pharmaceutical, and materials functions.¹⁻³ Subsequently, direct C-H functionalization has emerged as one of the most straightforward and efficient methods for the derivatization of aromatic heterocycles. Significant progress has been made in direct arylation, alkenylation, and alkynylation.⁴⁻¹⁷ Direct alkylation has proved to be the most challenging, especially if the alkyl groups contain β -hydrogens.¹⁸⁻²⁵ This is likely due to the tendency of metal alkyl intermediates to undergo unproductive β -H elimination.²⁶⁻³⁰

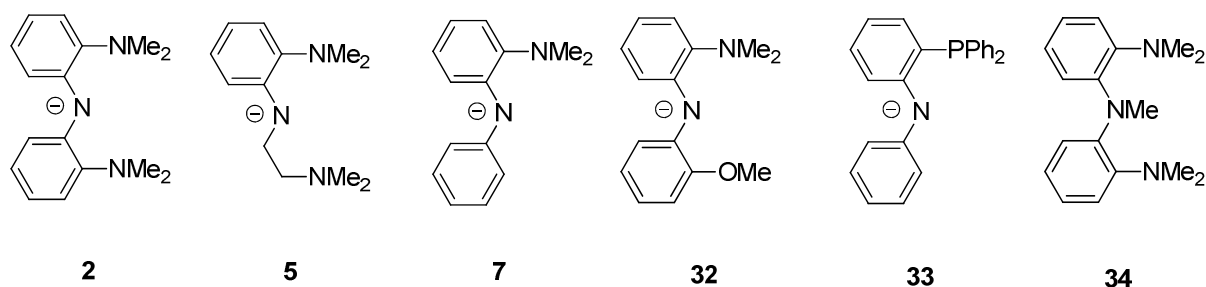
Several approaches are now available for direct alkylation of aromatic heterocycles, including Friedel-Crafts,³¹ radical alkylation,³²⁻³⁴ insertion of C-H bond into olefins,³⁵⁻⁴² coupling of heterocycles with tosylhydrazones,^{43,44} and coupling of heterocycles with alkyl electrophiles.⁴⁵⁻⁵⁰ Most reported methods only introduce a primary alkyl groups. Metal-catalyzed hydroarylation of olefins is, in principle, an effective way to incorporate a secondary alkyl group into heterocycles, yet current success is largely limited to the introduction of activated alkyl (e.g., benzyl and allyl) groups.³⁵⁻⁴¹ Wang *et al.* pioneered Cu-catalyzed direct benzylation and allylation of azoles with *N*-tosylhydrazones.⁴³ Miura *et al.* then reported Ni- and Co-catalyzed alkylation of azoles with *N*-tosylhydrazones, which was the first general method to couple non-activated secondary alkyl groups with azoles.⁴⁴ Our group and others recently developed metal-catalyzed direct alkylation of azoles and thiazoles using non-activated alkyl halides.^{43, 46, 47, 50} Unfortunately, only primary alkyl halides could be used. Earlier work from our group showed that a Ni pincer complex, $[(^{\text{Me}}\text{N}_2\text{N})\text{NiCl}]$,^{51, 52} was an active pre-catalyst for cross coupling of non-activated alkyl halides,⁵³⁻⁵⁵ and direct C—H alkylation.^{46,56} This result led to investigation in the chemistry of the analogous Cu complexes. In this chapter, several copper complexes with hemilabile ligands including $^{\text{Me}}\text{N}_2\text{N}$ were successfully synthesized, and their applications as catalysts in direct alkylation of azoles using secondary alkyl halides were studied. An important additive is also identified.

4.2 Copper complexes

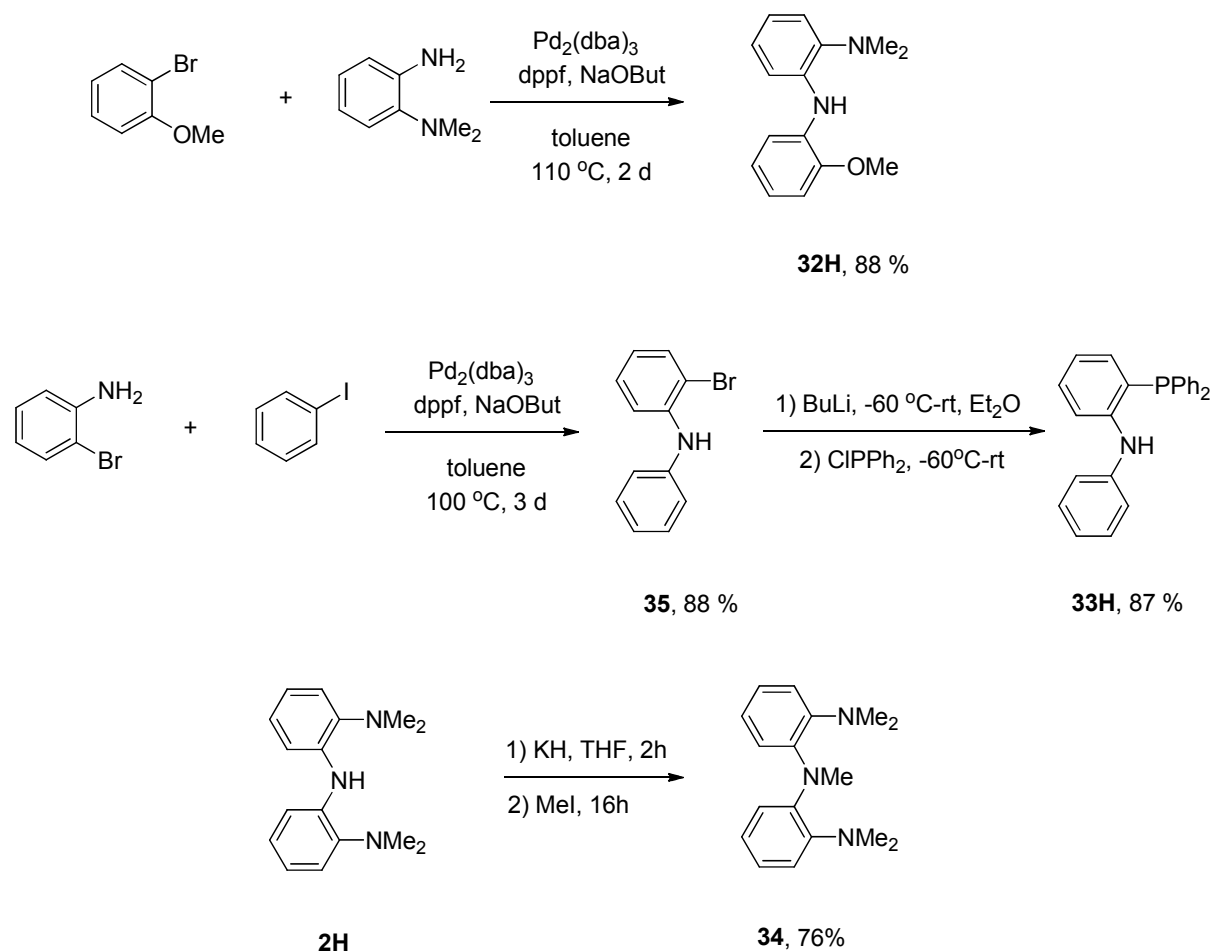
4.2.1 Ligand synthesis

In addition to the pincer ligands $^{\text{Me}}\text{N}_2\text{N}$ (**2**), $^{\text{Me}}\text{N}^{\text{Me}}\text{N}'\text{N}$ (**5**), and bidentate ligand $^{\text{H}}\text{NN}$ (**7**), which were discussed in Chapter 2, several new ligands (**32-34**) were employed in this study (Chart 1).

Chart 1.



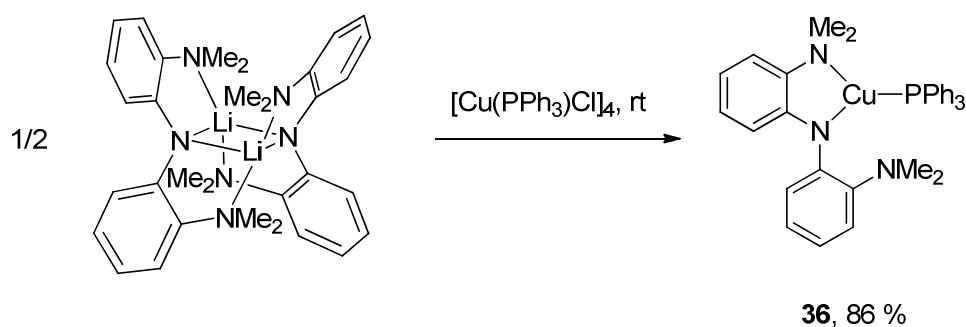
Protonated, neutral forms of ligands **32** and **33** were first prepared. **32H** and **35** were prepared in high yield using the Pd-catalyzed Buchwald-Hartwig C-N coupling method (Scheme 1), which is the same procedure used for the preparation of **2H**, **5H** and **7H** (Chapter 2). Phosphorylation of **35** using 2 equiv. of ⁿBuLi and ClPPh₂ and subsequent aqueous HCl workup led to isolation of **33H** in high yield. **34** was prepared by deprotonation with potassium hydride, and methylation with MeI (Scheme 1).



Scheme 1. Synthesis of ligands **32H**, **33H**, and **34**.

4.2.2 Synthesis and structures of copper complexes

Initially, **2** ($^{\text{Me}}\text{N}_2\text{N}$) was used as test ligand for the synthesis of copper complexes. The anionic bis(amino)amide ligand N_2N alone was not sufficient to stabilize the Cu(I) ion. The reactions of $[(^{\text{Me}}\text{N}_2\text{N})\text{Li}]_2^{51}$ with a Cu(I) precursor (e.g., CuI, CuCl, $[\text{Cu}(\text{CH}_3\text{CN})_4]\text{PF}_6$) led to the formation of copper mirror and protonated ligand $^{\text{Me}}\text{N}_2\text{NH}$. Triphenylphosphine, however, could be used as a co-ligand to form a stable Cu(I) complex. Thus, reaction of $[(^{\text{Me}}\text{N}_2\text{N})\text{Li}]_2$ with $[\text{Cu}(\text{PPh}_3)\text{Cl}]_4$ yielded $[(^{\text{Me}}\text{N}_2\text{N})\text{Cu}(\text{PPh}_3)]$ (**36**) (Scheme 2). The solid-state molecular structure of **36** was established by X-ray crystallography (Figure 1). The Cu ion is in a distorted trigonal planar ligand environment. The N_2N ligand is bidentate, with one of the amine donors being non-coordinating ($\text{N3-Cu1} = 3.290(2) \text{ \AA}$). The Cu-N (amide) distance ($1.9406(16) \text{ \AA}$) is significantly shorter than the Cu-N (amine) distance ($2.1339(16) \text{ \AA}$).



Scheme 2. Synthesis of the complex $[(^{\text{Me}}\text{N}_2\text{N})\text{Cu}(\text{PPh}_3)]$ (**36**).

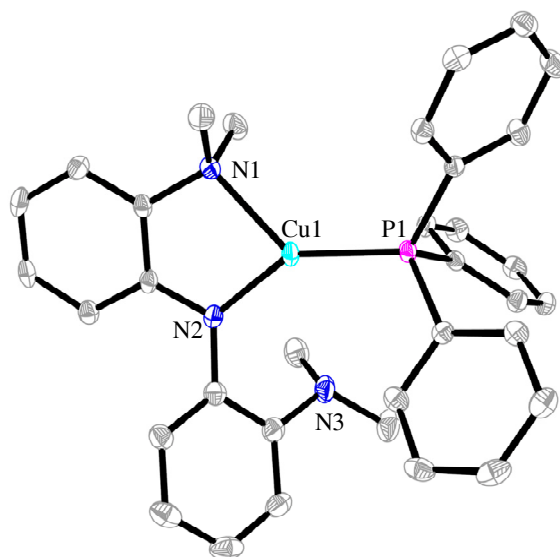
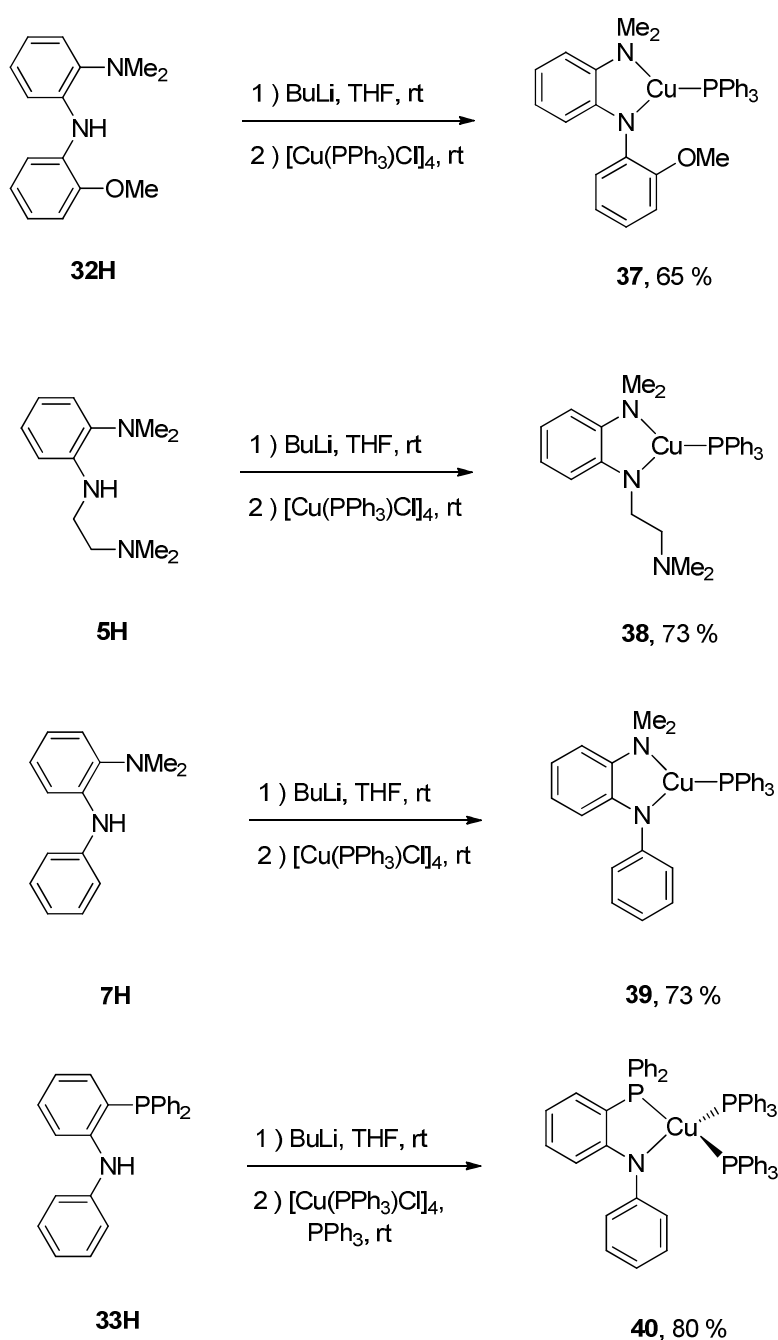


Figure 1. Crystal structure of **36**. The thermal ellipsoids are displayed in 50% probability. The following structures in this chapter are displayed at 50% probability which will not be illustrated any more.

After establishing the synthesis method of copper amino amide complex **36**, other amino amide ligands **5**, **7**, **32**, and **33** could be metallated with copper by a similar procedure. The protonated ligands were first deprotonated by 1 equiv. $^n\text{BuLi}$, then reacted with $[\text{Cu}(\text{PPh}_3)\text{Cl}]_4$ to yield corresponding copper complexes **37-40** (Scheme 3). For **40**, an additional 1 equiv. PPh_3 was needed to obtain high yield due to each copper complex unit containing two PPh_3 ligands. The structures of **37**, **38**, and **39** resemble **36**, in which copper is three coordinate. The Cu ion of **40** is in a tetrahedral ligand environment (Figure 2-5).



Scheme 3. Synthesis of the copper complexes **37-40**.

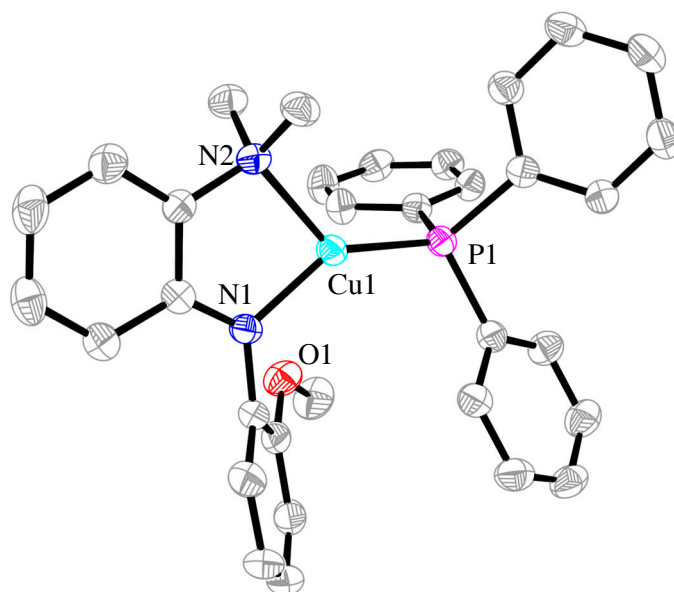


Figure 2. Crystal structure of complex $[(\text{NNO})\text{Cu}(\text{PPh}_3)]$ (**37**). There are two independent molecules in the asymmetric unit of **37**, and only one of them is shown. The unit cell of **37** contains one molecule of solvent (toluene) which is not shown.

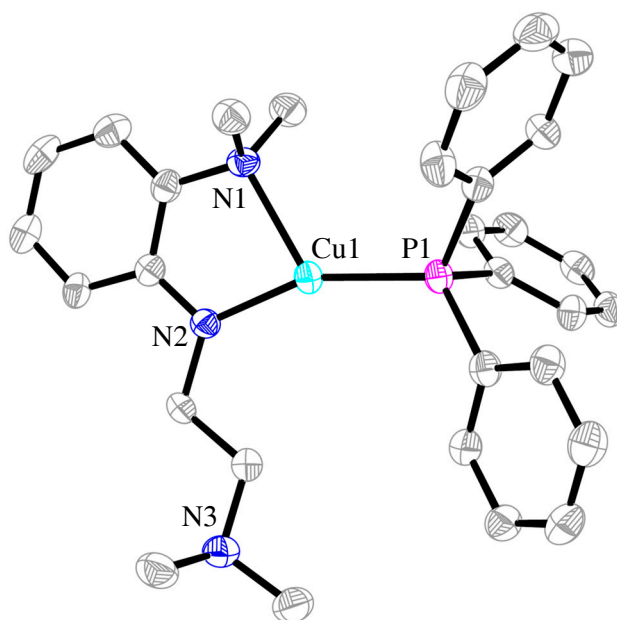


Figure 3. Crystal structure of complex $[(^{\text{Me}}\text{N}^{\text{Me}}\text{N}'\text{N})\text{Cu}(\text{PPh}_3)]$ (**38**).

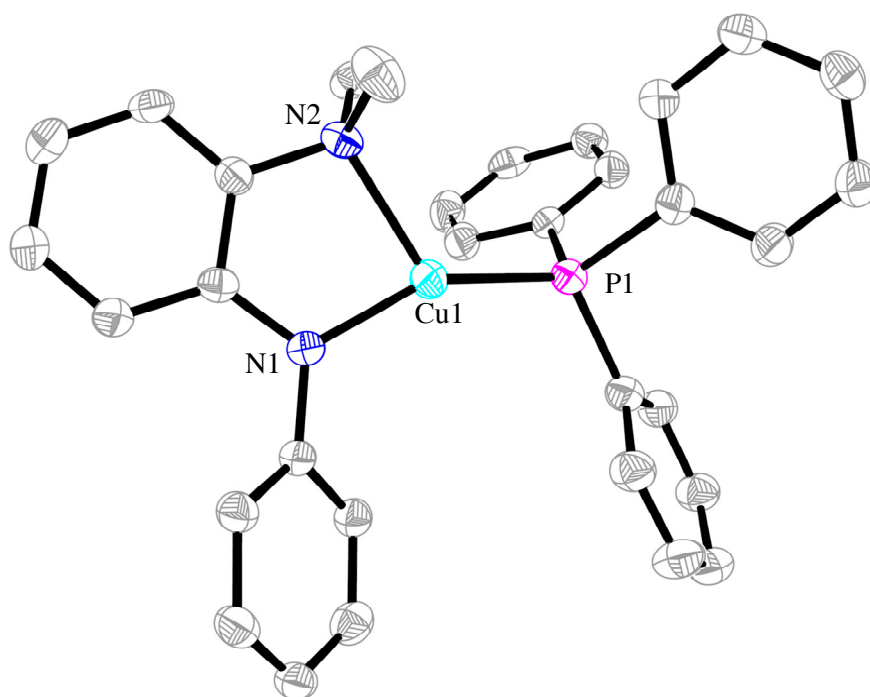


Figure 4. Crystal structure of complex $[(^H\text{NN})\text{Cu}(\text{PPh}_3)]$ (**39**).

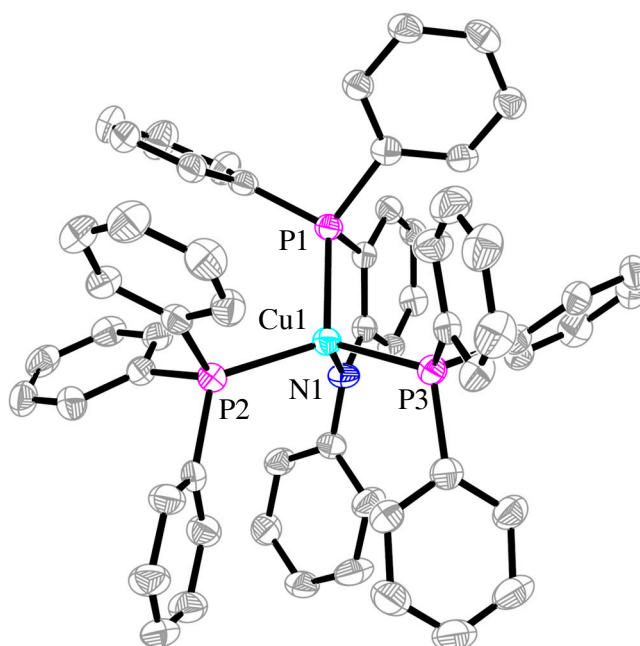
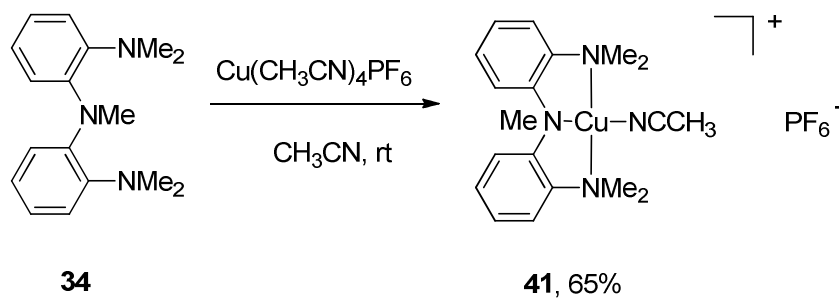


Figure 5. Crystal structure of complex $[(\text{NP})\text{Cu}(\text{PPh}_3)_2]$ (**40**). The unit cell of **40** contains 0.4 molecule of THF and 0.6 molecule of pentane which is not shown.

The neutral ligand **34** was reacted with $\text{Cu}(\text{CH}_3\text{CN})_4\text{PF}_6$ in acetonitrile at room temperature to yield cationic complex **41** (Scheme 4). The copper complex **41** is a tetrahedral structure with PF_6 as the counter anion (Figure 6). The ^1H NMR signal for bound CH_3CN in **41** was observed at 2.24 ppm in CD_2Cl_2 , 0.27 ppm downfield from free CH_3CN .



Scheme 4. Synthesis of the complex $[(^{\text{Me}}\text{N}_2^{\text{Me}}\text{N})\text{Cu}(\text{CH}_3\text{CN})][\text{PF}_6]$ (**41**).

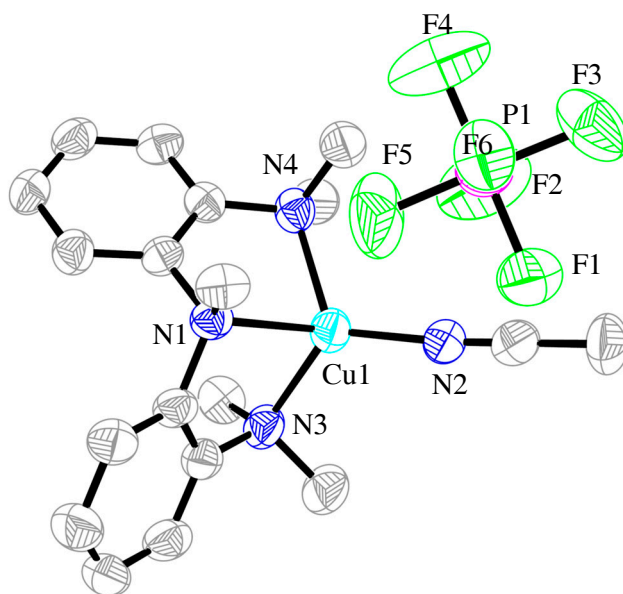
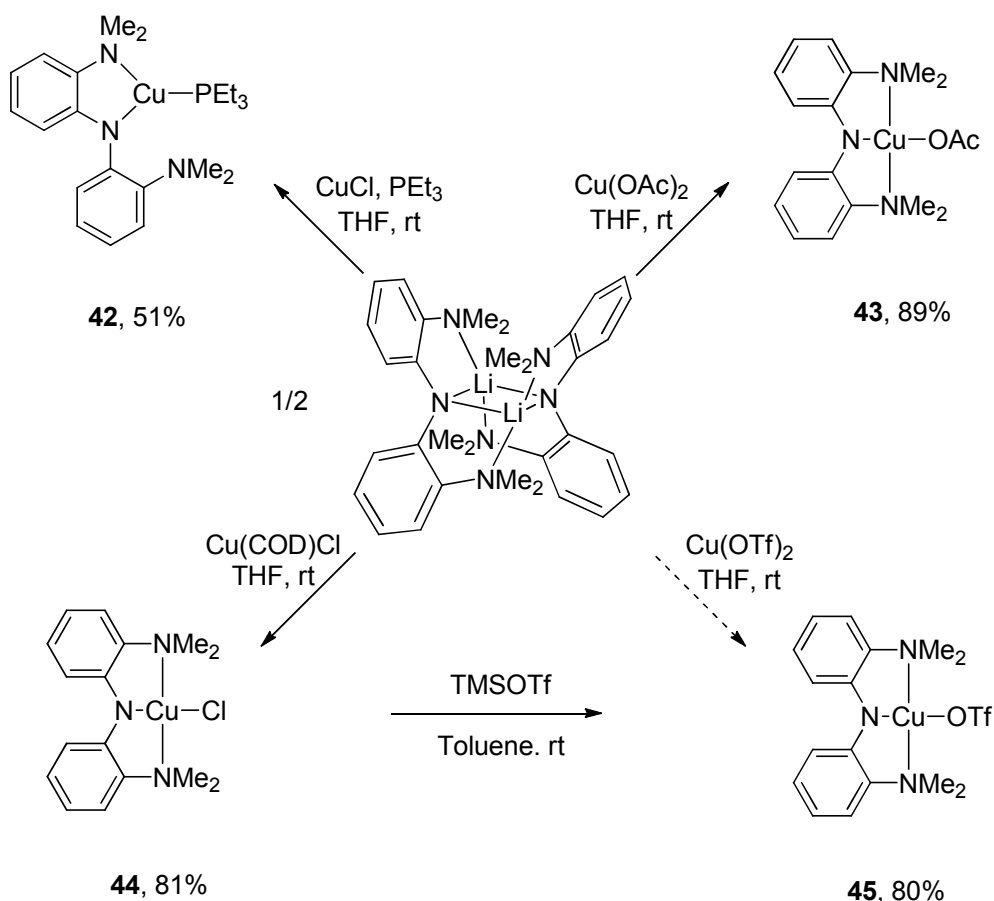


Figure 6. Crystal structure of complex $[(^{\text{Me}}\text{N}_2^{\text{Me}}\text{N})\text{Cu}(\text{CH}_3\text{CN})][\text{PF}_6]$ (**41**).

Reaction of $[(^{\text{Me}}\text{N}_2\text{N})\text{Li}]_2$ with CuCl and PEt_3 yielded $[(^{\text{Me}}\text{N}_2\text{N})\text{Cu}(\text{PEt}_3)]$ (**42**) (Scheme 5). Complex **42** resembles the other Cu(I) complexes, and is a distorted trigonal planar ligand environment (Figure 7). The Cu-P(alkyl) distance is 2.15475(5) Å, which is longer than Cu-P(aryl) in **36**. Cu(II) complexes were also synthesized successfully. Reaction of $[(^{\text{Me}}\text{N}_2\text{N})\text{Li}]_2$ with $\text{Cu}(\text{OAc})_2$ yielded $[(^{\text{Me}}\text{N}_2\text{N})\text{Cu}(\text{OAc})]$ (**43**). The fourth coordination site is occupied by OAc^- , which binds to Cu in an $^1\eta$ fashion. It appears that Cu(I) complexes containing amino amide ligand need a phosphine ligand for stability. Mixing $\text{Cu}(\text{COD})\text{Cl}$ precursor and $[(^{\text{Me}}\text{N}_2\text{N})\text{Li}]_2$, and benefiting from a disproportionation reaction, Cu(II) complex **44** could be obtained in high yield. Reaction of $[(^{\text{Me}}\text{N}_2\text{N})\text{Li}]_2$ with $\text{Cu}(\text{OTf})_2$ yielded $[(^{\text{Me}}\text{N}_2\text{N})\text{Cu}(\text{OTf})]$ (**45**), however, the product contains LiOTf , which is hard to separate from **45**. Additionally, a ligand exchange reaction could produce **45** by stirring **44** with trimethylsilyl trifluoromethanesulfonate (TMSOTf) in toluene, which gives pure **45** in high yield (Scheme 5).



Scheme 5. Synthesis of the copper complexes **42-45**.

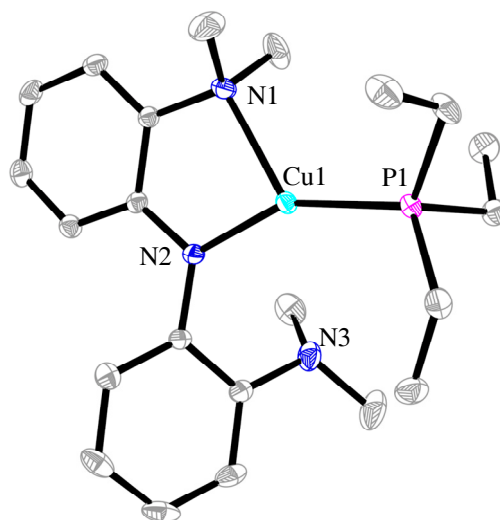


Figure 7. Crystal structure of complex $[(^{\text{Me}}\text{N}_2\text{N})\text{Cu}(\text{PEt}_3)]$ (**42**).

The coordination geometry of Cu(II) is approximately square-planar in all Cu(II) complexes (**43-45**) (Figure 8-10). The pincer NN_2 ligand binds to Cu(II) in the *mer* fashion which resembles N_2N -Ni complexes.^{51, 52} The Cu-O distance is slightly shorter in **43** (1.930(3) Å) than in **45** (2.001(4) Å). In general, the amide nitrogen atom is sp^2 hybridized, as the sum of the three bonds around it are all close to 360° . The Cu-N(amide) bonds are about 0.2 Å shorter than the corresponding Cu-N(amine) bonds. The key structural parameters for all the copper complexes are summarized in Table 1 and 2.

Table 1. Selected bond lengths for copper complexes.^a

Complex	Cu-N (amide)	Cu-N (amine)	Cu-P	Cu-X
36 $[(^{\text{Me}}\text{N}_2\text{N})\text{Cu}(\text{PPh}_3)]$	1.9406(16)	2.1339(16)	2.1492(6)	-
37 $[(\text{NNO})\text{Cu}(\text{PPh}_3)]$	1.925(2)	2.106(2)	2.1383(9)	-
38 $[(^{\text{Me}}\text{N}^{\text{Me}}\text{N}'\text{N})\text{Cu}(\text{PPh}_3)]$	1.910(3)	2.177(3)	2.1535(14)	-
39 $[(^{\text{H}}\text{NN})\text{Cu}(\text{PPh}_3)]$	1.908(3)	2.142(3)	2.1392(10)	-
40 $[(\text{NP})\text{Cu}(\text{PPh}_3)_2]$	2.027(3)	-	2.3016(12) Cu-P(NP) 2.2727(12) Cu-P(PPh_3) _{av.}	-
41 $[(^{\text{Me}}\text{N}_2^{\text{Me}}\text{N})\text{Cu}(\text{CH}_3\text{CN})][\text{PF}_6]$	-	2.168(4) Cu1-N1 2.111(5) Cu1-N3 2.123(5) Cu1-N4	-	1.869(5) Cu-N (CH_3CN)

Table 1. (Continued)

Complex	Cu-N (amide)	Cu-N (amine)	Cu-P	Cu-X
42 [(^{Me} N ₂ N)Cu(PEt ₃)]	1.9244(13)	2.2013(15)	2.1547(5)	-
43 [(^{Me} N ₂ N)Cu(OAc)]	1.892(4)	2.082(4) _{av.}	-	1.930(3)
44 [(^{Me} N ₂ N)CuCl]	1.887(3)	2.084(3) _{av.}	-	2.1991(11)
45 [(^{Me} N ₂ N)Cu(OTf)]	1.892(4)	2.0083(3)	-	2.001(4)

^a Distances are in Angstroms. Averaged bond distances were used in cases where there is more than one bond of the same given type. ^b X is the fourth ligand on Cu aside from the tridentate ligand chelate.

Table 2. Selected bond angles for copper complexes. ^a

Complex	N(amine)- Cu-N(amide)	N(amide)- Cu-P	P-Cu- N(amine)	A-Cu-B (Additional)	Geometry
36 [(^{Me} N ₂ N)Cu(PPh ₃)]	85.00(6)	143.42(5)	131.34(5)	-	Trigonal-Planar
37 [(NNO)Cu(PPh ₃)]	85.41(9)	141.81(7)	132.56(6)	-	Trigonal-Planar
38 [(^{Me} N ^{Me} N'N)Cu(PPh ₃)]	83.57(12)	156.89(9)	119.54(9)	-	Trigonal-Planar
39 [(^H NN)Cu(PPh ₃)]	84.83(10)	152.30(8)	121.45(8)	-	Trigonal-Planar
40 [(NP)Cu(PPh ₃) ₂]	-	85.10(9) P(NP)	111.22(9) N1-Cu1-P2 108.46(9) N1-Cu1-P3	113.85(4) P1-Cu1-P2 114.05(4) P1-Cu1-P3 118.90(4) P2-Cu1-P3 128.94(18) N1-Cu1-N2 82.34(16) N1-Cu1-N3 83.04(16) N1-Cu1-N4 123.33(18) N2-Cu1-N3 116.04(19) N2-Cu1-N4 113.36(17) N3-Cu1-N4	Tetrahedral
41 [(^{Me} N ₂ ^{Me} N)Cu(CH ₃ CN)][PF ₆]	-	-	-	-	Tetrahedral
42 [(^{Me} N ₂ N)Cu(PEt ₃)]	83.34(5)	152.63(4)	123.98(4)	-	Trigonal-Planar
43 [(^{Me} N ₂ N)Cu(OAc)]	83.20(15) _{av.}	-	-	96.71(15) _{av.} O-Cu- N(amine)	Square-Planar
44 [(^{Me} N ₂ N)CuCl]	82.74(12) _{av.}	-	-	93.38(9) _{av.} Cl-Cu- N(amine)	Square-Planar
45 [(^{Me} N ₂ N)Cu(OTf)]	86.63(8)	-	-	93.36(8) O-Cu- N(amine)	Square-Planar

^a Bonds angles are in degrees. The geometry was approximated.

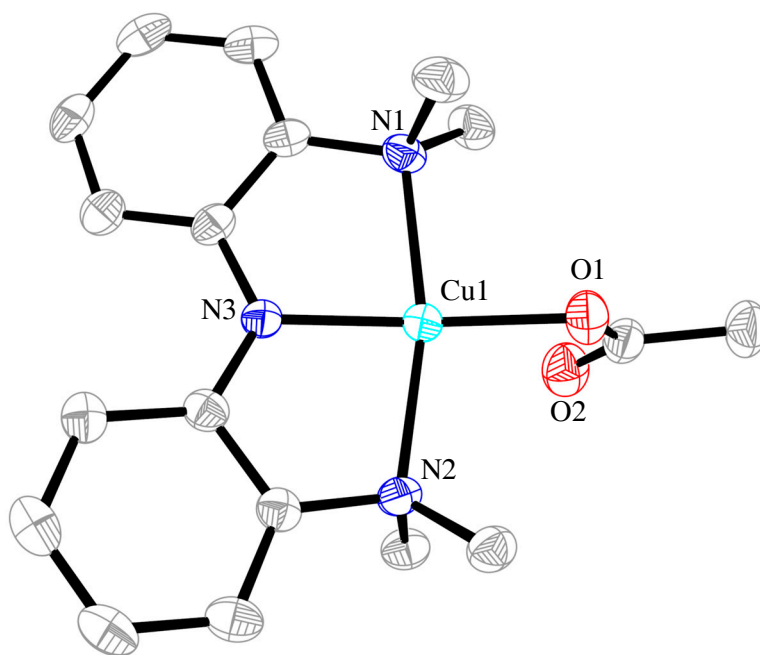


Figure 8. Crystal structure of complex $[(^{\text{Me}}\text{N}_2\text{N})\text{Cu}(\text{OAc})]$ (**43**).

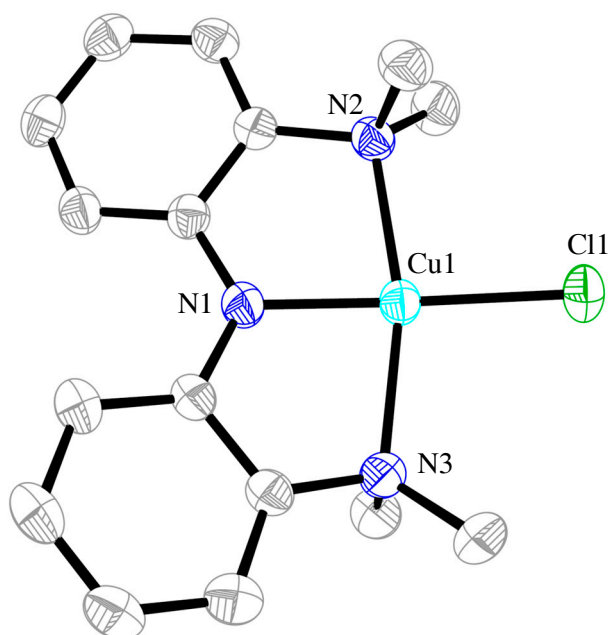


Figure 9. Crystal structure of complex $[(^{\text{Me}}\text{N}_2\text{N})\text{CuCl}]$ (**44**).

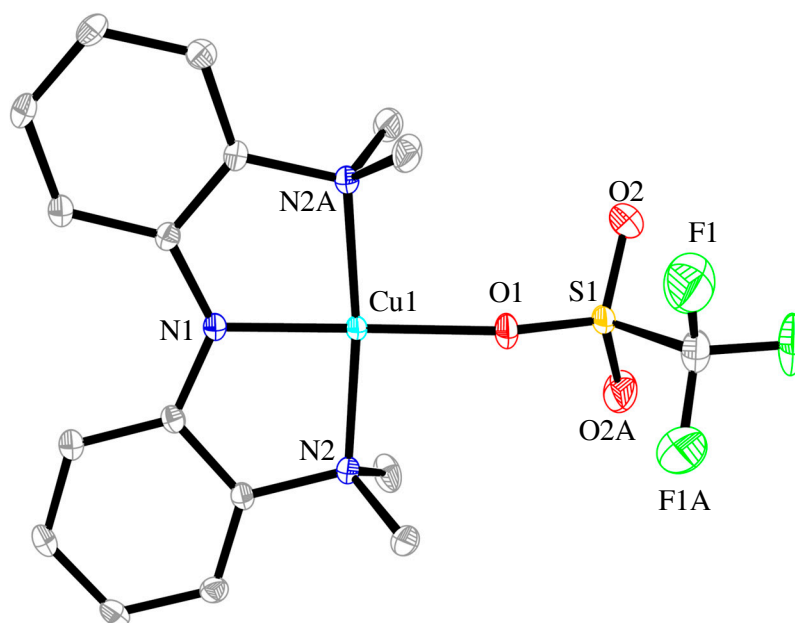
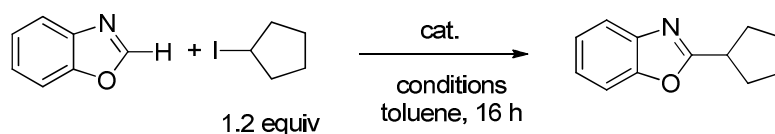


Figure 10. Crystal structure of complex $[(^{\text{Me}}\text{N}_2\text{N})\text{Cu}(\text{OTf})]$ (**45**).

4.3 Optimization of the coupling reaction conditions between benzoxazole and cyclopentyl iodide

Complex **36** was used as a test catalyst to optimize the reaction conditions for the coupling of benzoxazole with cyclopentyl iodide (Table 3). It turned out to be a good catalyst for direct alkylation. The Ni/Cu based method, which was efficient for direct coupling of azoles with primary alkyl halides,⁴⁶ was inefficient for this reaction. After attempts at modification, it gave a maximum yield of 4% (entry 1, Table 3). Replacing $[(^{\text{Me}}\text{N}_2\text{N})\text{NiCl}]$ (**1**) with **36** improved the yield to 32% (entry 2, Table 1). Increasing the loading of **36** to 10 mol % further increased the yield to 50% (entry 3, Table 3). The yields were similar when the reactions were run at 80°C or 100°C. ^tBuONa and toluene were the best base and solvent combination. Other combinations such as ^tBuOLi/dioxane, ^tBuOLi/DMF, and Cs₂CO₃/toluene gave no or inferior yields. Interestingly, without CuI as co-catalyst, the yield was only 11% (entry 4, Table 3). CuI alone did not catalyze the reaction (entry 5, Table 3).

Table 3. Optimization of Conditions for the Coupling of Benzoxazole with Cyclopentyl-I.^a

Entry	Catalysts	Conditions	Yield (%) ^b
1	5 mol % [(^{Me} N ₂ N)NiCl] and 5 mol % CuI	1.4 equiv ^t BuONa, 140 °C	4
2	5 mol % [(^{Me} N ₂ N)Cu(PPh ₃)] (36) and 5 mol % CuI	1 equiv ^t BuONa, 100 °C	32
3	10 mol % 36 and 5 mol % CuI	1.2 equiv ^t BuONa, 80 °C or 100 °C	50
4	10 mol % 36	1.2 equiv ^t BuONa, 80 °C	11
5	5 mol % CuI	1.2 equiv ^t BuONa, 80 °C	0
6	10 mol % 36 and 5 mol % CuI	5 mol % or 0.2 equiv BDMAEE, 1.2 equiv ^t BuONa, 100 °C	77
7	10 mol % 36	0.2 equiv BDMAEE, 1.2 equiv ^t BuONa, 80 °C	87/80^c
8	15 mol % CuI	0.2 equiv BDMAEE, 1.2 equiv ^t BuONa, 80 °C	62
9	10 mol % [Cu(Phen)(PPh ₃) ₂]NO ₃ or Cu(S(CH ₃) ₂)Br or [Cu(PPh ₃)Cl] ₄	0.2 equiv BDMAEE, 1.2 equiv ^t BuONa, 80 °C	57-61
10	10 mol % [(^{Me} N ₂ N)NiCl] and 5 mol % CuI	0.2 equiv BDMAEE, 1.2 equiv ^t BuONa, 80 °C	10
11	none	0.2 equiv BDMAEE, 1.2 equiv ^t BuONa, 80 °C	0
12	6.5 mol % [(BDMAEE)Cu ₂ I ₂]	0.2 equiv BDMAEE, 1.2 equiv ^t BuONa, 80 °C	61
13	10 mol % 36	0.2 equiv TMEDA, 1.2 equiv ^t BuONa, 80 °C	44
14	15 mol % CuI	0.2 equiv TMEDA, 1.2 equiv ^t BuONa, 80 °C	0
15	10 mol % [(TMEDA)CuI]	1.2 equiv ^t BuONa, 80 °C	0

Table 3. (Continued)

Entry	Catalysts	Conditions	Yield (%) ^b
16	10 mol % [(NNO)Cu(PPh ₃)] (37)	0.2 equiv BDMAEE, 1.2 equiv ^t BuONa, 80 °C	75
17	10 mol % [(^{Me} N ^{Me} N ^{Me} N)Cu(PPh ₃)] (38)	0.2 equiv BDMAEE, 1.2 equiv ^t BuONa, 80 °C	71
18	10 mol % [(^H NN)Cu(PPh ₃)] (39)	0.2 equiv BDMAEE, 1.2 equiv ^t BuONa, 80 °C	77
19	10 mol % [(NP)Cu(PPh ₃) ₂] (40)	0.2 equiv BDMAEE, 1.2 equiv ^t BuONa, 80 °C	5
20	10 mol % [(^{Me} N ₂ ^{Me} N)Cu(CH ₃ CN)] [PF ₆] (41)	0.2 equiv BDMAEE, 1.2 equiv ^t BuONa, 80 °C	61
21	10 mol % [(^{Me} N ₂ N)Cu(PEt ₃)] (42)	0.2 equiv BDMAEE, 1.2 equiv ^t BuONa, 80 °C	73
22	10 mol % [(^{Me} N ₂ N)CuCl] (44)	0.2 equiv BDMAEE, 1.2 equiv ^t BuONa, 80 °C	67

^aSee the experimental part for details. ^bGC yield relative to benzoxazole. ^cIsolated yield.

In the previous studies of Ni-catalyzed Kumada-type coupling reactions, our group found that bis[(2-(*N,N*-dimethylaminoethyl)]ether (BDMAEE, previously abbreviated as O-TMEDA) often promoted the catalysis.^{54,55} Out of curiosity, the effect of BDMAEE was tested for direct alkylation. To our delight, addition of 5 mol% or 0.2 equiv of BDMAEE led to a coupling yield of 77% (entry 6, Table 3). Slightly lower yields were obtained when the loadings of BDMAEE were between 1 to 5 equiv. Lowering the temperature from 100 to 80°C further increased the yield to 87% (entry 7, Table 3). CuI was no longer necessary under these conditions. When **36** was replaced by CuI (15 mol %), the yield decreased to 62%. When another soluble Cu(I) complex, [Cu(Phen)(PPh₃)₂]NO₃ (phen = phenanthroline) or Cu(S(CH₃)₂)Br or [Cu(PPh₃)Cl]₄ was used as precatalyst, the yield was about 60% (entry 9, Table 3). These results indicate a superior catalytic activity for complex **1**. On the other hand, [(^{Me}N₂N)NiCl] was still a poor catalyst even with BDMAEE as additive (compare entries 1 and 10, Table 3). A control experiment showed that without a Cu catalyst, BDMAEE did not catalyze the coupling (entry 11, Table 3). Finally, a preparative reaction under the optimized conditions (entry 7, Table 3) gave the alkylated product in an isolated yield of 80%.

As BDMAEE was essential for achieving high yields in the Cu-catalyzed direct alkylation, its roles were investigated. Obviously BDMAEE is a potential ligand. When CuI or Cu(S(CH₃)₂)Br was used as pre-catalyst (entries 8 and 9, Table 3), the active catalyst was most likely a Cu-BDMAEE complex. Reaction of CuI with BDMAEE produced a copper complex that appeared to be [(BDMAEE)Cu₂I₂], according to NMR and elemental analysis (Figure 11 and 12). Using this complex as catalyst, the coupling of benzoxazole with cyclopentyl iodide had a yield of 61%, similar to that obtained using CuI or Cu(S(CH₃)₂)Br in conjunction with BDMAEE. However, BDMAEE was not a ligand when complex **36** was used as catalyst, as no reaction occurred between **36** and BDMAEE. Furthermore, using **36** as catalyst, the yield was significantly higher (87%) than using [(BDMAEE)Cu₂I₂] as catalyst. Under these conditions, BDMAEE must play another important role. It is possible that BDMAEE partially solubilizes the inorganic base and promotes the deprotonation of azole. It is also possible that BDMAEE facilitates the transmetallation of azole anions to the Cu center in **36**. These roles might be replaced by CuI, albeit with a lower efficiency. In fact, the combination of **36** and CuI gave a coupling yield of about 50% (entry 3, Table 1), much higher than that of 11% using **36** alone (entry 4, Table 3). TMEDA (tetramethylethylenediamine) was another poor substitute for BDMAEE, resulting in a yield of 40% (entry 13, Table 3). The combination of CuI and TMEDA alone was not catalytically active (entries 14 and 15, Table 3).

Other new copper complexes were tested under the optimized conditions. The trigonal-planar amino amide copper complexes (**37-39**) whose structures are similar to that of **36**, had slightly lower yields (71%-77%) than **36** (entries 16-18, Table 3). [(NP)Cu(PPh₃)₂] (**40**) was inefficient for the reaction (entry 19, Table 3). Surprisingly, [[(^{Me}N₂^{Me}N)Cu(CH₃CN)][PF₆] (**41**), which has labile acetonitrile ligands which may dissociate from copper(I) to generate one free coordination site, also gave lower yield (61%) (entry 20, Table 3). The yield using [(^{Me}N₂N)Cu(PEt₃)] (**42**) was lower than using **36** (entry 21, Table 3), indicating that PPh₃ may be involved in the catalytic cycle. The yield of [(^{Me}N₂N)CuCl] (**44**), which contains Cu(II) ion and ^{Me}N₂N ligand, was lower than **36** (entry 22, Table 3). From these results, it was clear that **36** was the best catalyst. It is possible that electronic property of the ^{Me}N₂N ligand best fits the catalytic system. It is also possible that the hemilabile ^{Me}N₂N ligands could potentially act as tridentate ligands which stabilize the one of active catalyst intermediates better than others.

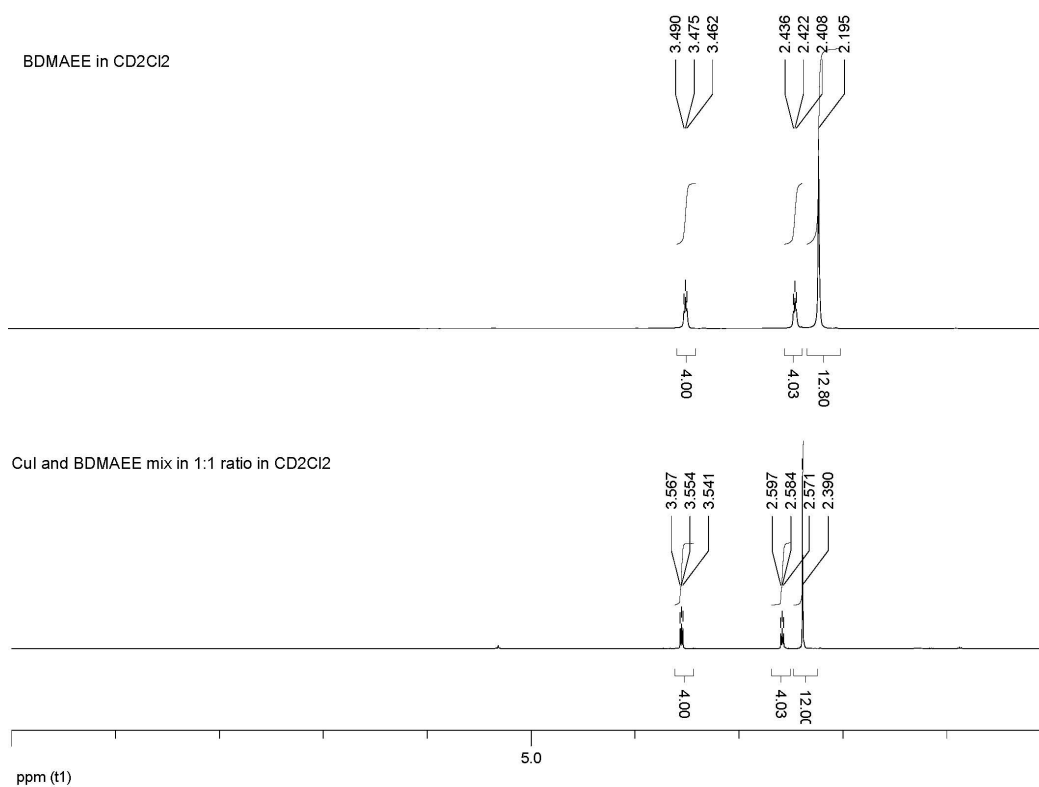


Figure 11. ¹H NMR spectra of BDMAEE and Cu-BDMAEE complex.

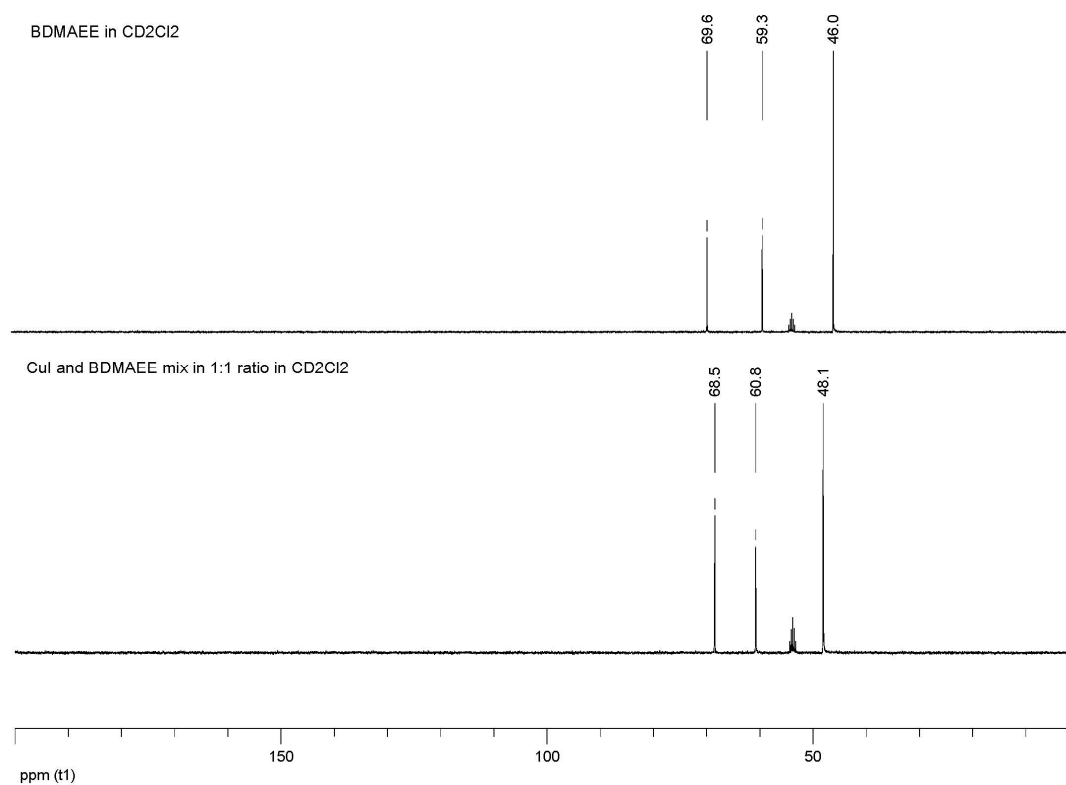


Figure 12. ¹³C NMR spectra of BDMAEE and Cu-BDMAEE complex.

4.4 Scope of the copper-catalyzed alkylation of benzoxazoles

The scope of the Cu-catalyzed alkylation of benzoxazoles was explored (Table 4). Cycloheptyl- and cyclooctyl-I were coupled to benzoxazole in high yields (entries 1-2, Table 4). Acyclic secondary alkyl iodides were also suitable substrates, and the reactions were insensitive to the length of the alkyl chains (entries 3-7, Table 4). Secondary alkyl bromides could also be coupled (entries 8-10, Table 4). Addition of a catalytic amount of CuI increased the yield substantially, probably because CuI mediated an I/Br exchange reaction.⁵⁷ Substituted benzoxazoles could also be alkylated in high yields (entries 11-16, Table 4). Both electron-donating Me and MeO groups and electron-withdrawing Cl and Br groups were tolerated. The aryl-Cl and aryl-Br moieties in the products (entries 14 and 15, Table 4) leave room for further functionalization by traditional cross coupling methods. Other iodide sources were not as effective for C-Br activation (entries 1 and 2, Table 5). Cl/I exchange was difficult for secondary alkyl chlorides under these conditions (entries 3 and 4, Table 5). Interestingly, for an unknown reasons, the coupling of primary alkyl halides was not efficient (entries 5-7, Table 5). Fortunately, such coupling can be achieved using previously reported Ni-catalysts.^{43,46,47}

Table 4. Scope of Cu-catalyzed alkylation of benzoxazoles.^a

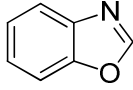
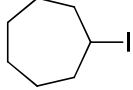
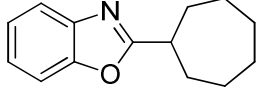
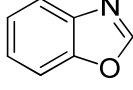
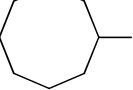
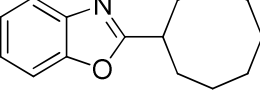
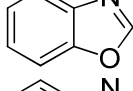
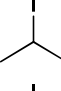
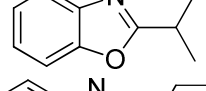
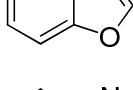
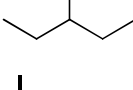
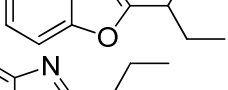
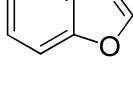
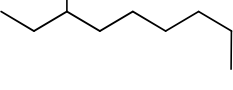
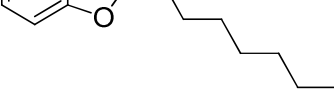
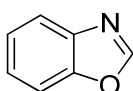
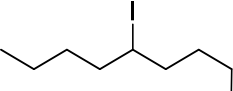
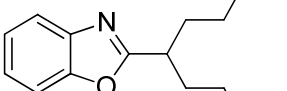
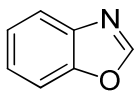
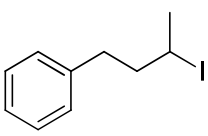
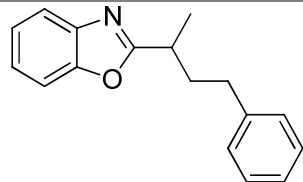
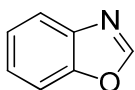
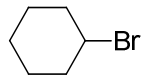
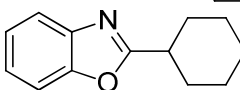
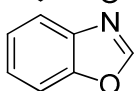
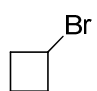
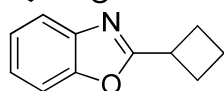
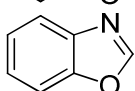
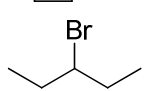
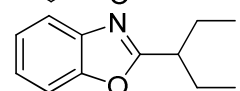
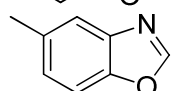
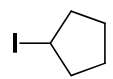
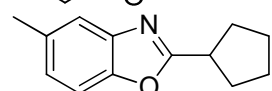
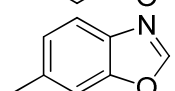
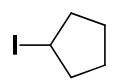
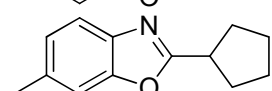
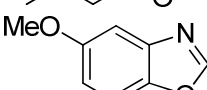
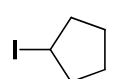
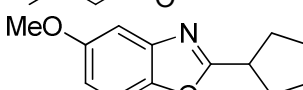
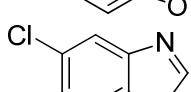
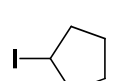
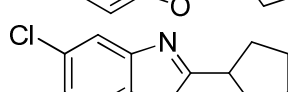
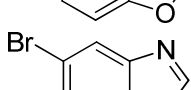
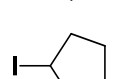
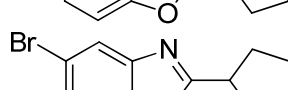
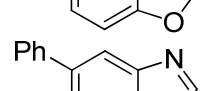
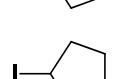
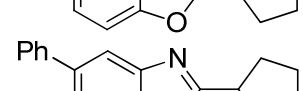
Entry	Azole	Alkyl-X	Product	Yield (%) ^b
1				73
2				75
3				81
4				71
5				81
6				82

Table 4. (Continued)

Entry	Azole	Alkyl-X	Product	Yield (%) ^b
7				76
8				66 ^c
9				57
10				60 ^c
11				63
12				62
13				64
14				73
15				69
16				64

^a 80°C for alkyl-I and 100°C for alkyl-Br. See experimental part for details. ^b Isolated yield. ^c 10 mol % **36** + 20 mol % CuI + 40 mol % BDMAEE were used.

Table 5. Additional entries for the coupling of alkyl halides with benzoxazole.

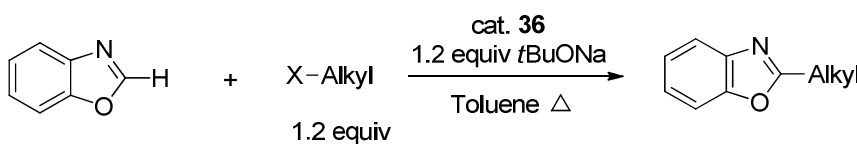
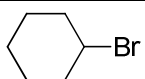
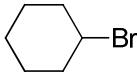
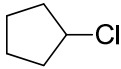
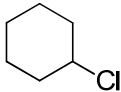
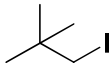
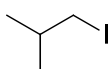
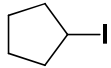
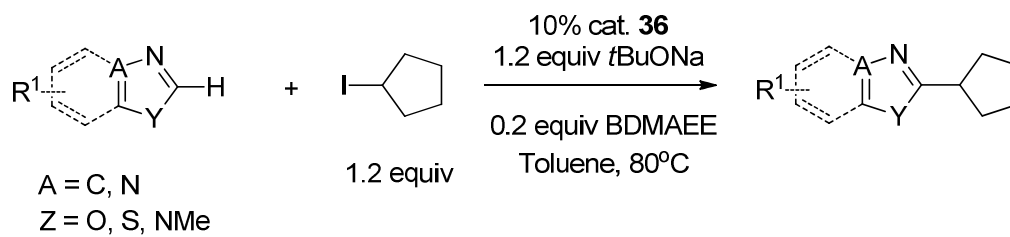
				
Entry	Alkyl-X	Catalyst, additive	Temperature, time	Yield ^[a]
1		10 mol % 36 , 0.2 equiv NaI 1 equiv BDMAEE	80°C, 16 h	trace

Table 5. (Continued)

Entry	Alkyl-X	Catalyst, additive	Temperature, time	Yield ^[a]
2		10 mol % 36 , 0.2 equiv NH ₄ I 0.2 equiv BDMAEE	120°C, 16 h	0
3		10 mol % 36 , 0.2 equiv BDMAEE	100°C, 16 h	trace
4		10 mol % 36 , 5 mol % CuI, 0.2 equiv BDMAEE	100°C, 16 h	0
5	Octyl-I	10 mol % 36 , 0.2 equiv BDMAEE	80°C, 16 h	trace
6		10 mol % 36 , 0.2 equiv BDMAEE	100°C, 16 h	37
7		20 mol % 36 , 0.2 equiv BDMAEE	100°C, 16 h	54
8		10 mol % 36 , 0.2 equiv BDMAEE, 10 equiv Hg	100°C, 16 h	74

^a GC yield.

Benzoxazoles bearing some particular functional group (ester, nitro, nitrile) at 5-position could not be coupled efficiently (entries 1-3, Table 6). This might be due to the coordination of donor atoms of the functional groups to the metal in the catalyst. For the 5- and 6-methyl substituted benzoxazoles, good yields could be obtained (entries 11 and 12, Table 3). However, only trace amount of the 4-methyl derivative coupling product was observed (entry 4, Table 6). This might be due to steric problem which affects the deprotonation of benzoxazole with the copper species.⁵⁸ Oxazolo[4,5-*b*]pyridine failed to couple with cyclopentyl iodide, which indicated that there may be a compromise between the acidity at 2-position of benzoxazole and the ability to coordinate with copper species.⁵⁹ For non-fused azoles (entries 7-12, Table 6), 1-methyl-1*H*-benzo[*d*]imidazole (entry 13, Table 6) and benzothiazole (entry 14, Table 6), the yields were 0% which may be caused by their weaker acidity.⁵⁹⁻⁶¹

Table 6. Limitations for the coupling of heterocycles.

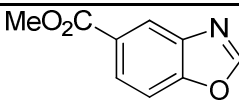
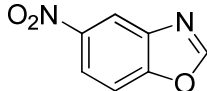
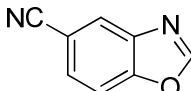
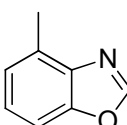
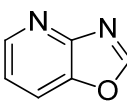
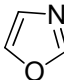
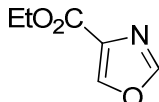
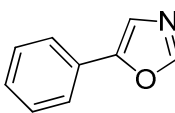
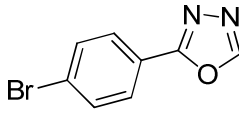
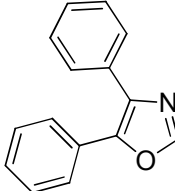
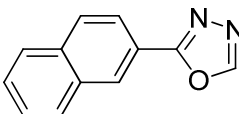
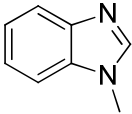
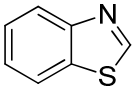
Entry	Heteroarenes	Yield ^[a]
1		15
2		0
3		0
4		trace
6		0
7		0 ^[b]
8		0 ^[b]
9		0
10		0 ^[b]
11		0 ^[b]
12		0

Table 6. (Continued)

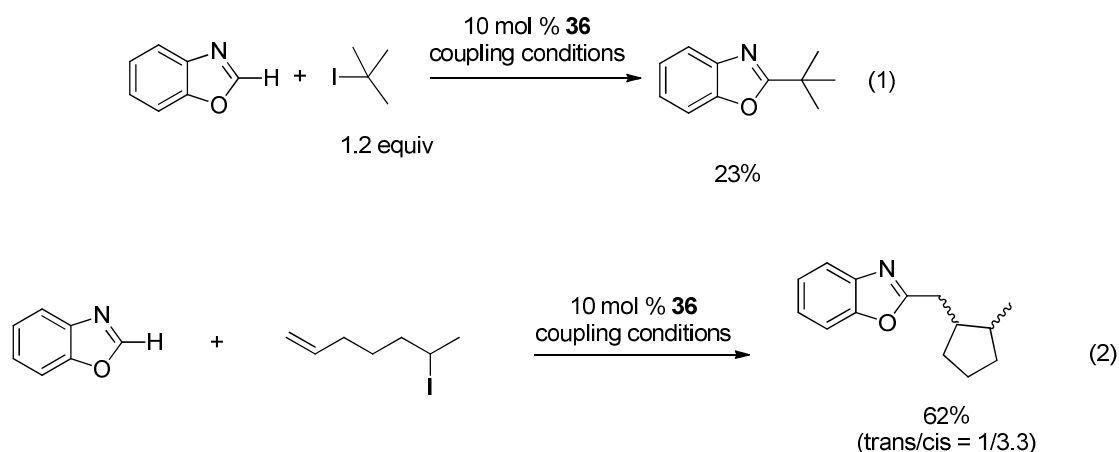
Entry	Heteroarenes	Yield ^[a]
13		0
14		0 ^[b]

^a GC yield. ^b The reaction temperature was 100°C.

4.5 Mechanistic investigations

The catalytic cycle of the Cu-catalyzed alkylation reaction might be similar to those proposed for Cu-catalyzed direct arylation and alkynylation of aromatic heterocycles.^{6,7,13} The azoles are deprotonated and transmetalated to Cu, and the resulting organometallic Cu species react with alkyl halides to give the coupling products. Previously, Ni particles were found to be the active species for Ni-catalyzed direct alkylation by a Hg-test experiment.⁴⁶ A similar Hg-test was conducted for the Cu catalysis. Thus, the coupling of benzoxazole with cyclopentyl-I was conducted in the presence of 10 equiv of Hg. The yield was 74%, close to the value obtained in the absence of Hg (entry 8, Table 5). This result suggests, albeit does not prove, that homogeneous Cu complexes are the active species.

Several experiments were carried out to probe the activation process of alkyl halides. Coupling of benzoxazole with ^tButyl-I gave a yield of 23% (eq. 1, Scheme 6). While the yield is too low to be synthetically useful, the result rules out the possibility of a S_N2-process for the alkylation. The reaction of benzoxazole with 6-iodohept-1-ene gave the ring-closed product in a yield of 62% (eq. 2, Scheme 6). This result indicates that the activation of secondary alkyl halides occurs via a radical process. Furthermore, the recombination of the resulting secondary carbon radical with the catalyst is slower than the ring-closing rearrangement of the hept-6-en-2-radical, which has a first-order rate constant of about 10⁵ s⁻¹.⁶² When the coupling of benzoxazole with cyclopentyl-I was conducted in the presence of 1 equiv of a radical inhibitor, TEMPO, the yield was zero. This result is consistent with a radical mechanism for the alkylation.



Scheme 6. Alkylation reactions using mechanistic probes; Isolated yields are reported.

4.6 Conclusions

In conclusion, we have developed a Cu-catalyzed direct alkylation of benzoxazoles. While the scope is limited and remains to be improved, to the best of our knowledge, this is the first time that non-activated secondary alkyl halides have been used as electrophiles. The well-defined Cu complex **36** is the best catalyst. The higher efficiency of **36** relative to other copper catalysts might result from the hemilabile property of the pincer ligand, which will be the subject of future exploration. The alkylation is promoted by a catalytic amount of BDMAEE. A similar promotion might be found for other C-H functionalization reactions.

4.7 Experimental section

4.7.1 Chemicals and Reagents

All manipulations were carried out under an inert N₂(g) atmosphere using standard Schlenk or glovebox techniques. Solvents were purified using a two-column solid-state purification system (Innovative Technology, NJ, USA) and transferred to the glove box without exposure to air. Deuterated solvents were purchased from Cambridge Isotope Laboratories, Inc., and were degassed and stored over activated 3 Å molecular sieves. Unless otherwise noted, all other reagents and starting materials were purchased from commercial sources and used without further purification. Liquid compounds were degassed by standard freeze-pump-thaw procedures prior to use. The following chemicals were prepared according to literature procedure: **2H**,⁵¹ **7H**,⁶³ Li complex [(^{Me}N₂N)Li]₂,⁵¹ [(^{Me}N₂N)NiCl]₂,⁵¹ [Cu(PPh₃)Cl]₄,⁶⁴⁻⁶⁶ Cu(COD)Cl,⁶⁷ Cu(tmeda)I,^{68,69} iodocycloheptane (entry 1, table 4), iodocyclooctane (entry 2, table 4), 3-iodopentane (entry 4, table 4), 3-iodononane (entry 5, table 4), 5-iodononane (entry 6, table 4), (3-iodobutyl)benzene (entry 7, table 4),⁶³ azoles

(entry 13 and 16, table 4, entry 1-6, 9-12, table 6)^{70,71} 6-iodo-1-heptene (Scheme 6).⁷² The synthetic method of **5H** was described in experimental part of chapter 2.

4.7.2 Physical methods

The ¹H, ³¹P and ¹³C NMR spectra were recorded at 293 K on a Bruker Avance 400 spectrometer. ¹H NMR chemical shifts were referenced to residual solvent as determined relative to Me₄Si (δ = 0 ppm). The ³¹P{¹H} chemical shifts were reported relative to 85% H₃PO₄. The ¹³C{¹H} chemical shifts were reported in ppm relative to the carbon resonance of CDCl₃ (77.0 ppm), C₆D₆ (128.1 ppm), CD₂Cl₂ (53.9 ppm). GC measurement was conducted on a Perkin-Elmer Clarus 400 GC with a FID detector. HRESI-MS measurements were conducted at the EPFL ISIC Mass Spectrometry Service with a Micro Mass QTOF Ultima spectrometer. Elemental analyses were performed on a Carlo Erba EA 1110 CHN instrument at EPFL. X-ray diffraction studies were carried out in the EPFL Crystallographic Facility. The data collections for both crystal structures were performed at low temperature using Mo K_{α} radiation on a Bruker APEX II CCD diffractometer equipped with a kappa geometry goniometer. The data were reduced by EvalCCD⁷³ and then corrected for absorption.⁷⁴ The solution and refinement was performed by SHELX.⁷⁵ The structure was refined using full-matrix least-squares based on F^2 with all non hydrogen atoms anisotropically defined. Hydrogen atoms were placed in calculated positions by means of the “riding” model.

4.7.3 Synthetic methods for ligands and copper complexes

Synthesis of *N*¹-(2-methoxyphenyl)-*N*²,*N*²-dimethylbenzene-1,2-diamine (NNOH), **32H**:

A 250 mL reaction vessel was charged with Pd₂(dba)₃ (1.36 g, 1.49 mmol), bis(diphenylphosphino)-ferrocene (DPPF) (1.65 g, 2.97 mmol), NaO^tBu (9.84 g, 98 mmol) and toluene (100 mL) under a dinitrogen atmosphere. 2-Bromoanisole (13.65 g, 73 mmol) and 2-amino-*N,N*-dimethylaniline (9.95 g, 73 mmol) were added to the reaction mixture. The resulting brown solution was vigorously stirred for 2 days at 110 °C. The solution was then cooled to room temperature and filtered through Celite. Removal of the solvent yielded a black liquid which was then purified by flash chromatography (silica-gel, hexane/ EtOAc 30:1) to afford the product as a light yellow oil. Yield: 14.90 g, 84%. ¹H NMR (400 MHz, CDCl₃): 7.37-7.46 (m, 2H), 7.08-7.14 (m, 1H), 6.95-7.05 (m, 1H), 6.84-6.95 (m, 5H), 3.92 (s, 3H), 2.71 (s, 6H). ¹³C NMR (100 MHz, CDCl₃): 148.9, 143.3, 137.3, 132.7, 123.6, 120.7, 120.1, 119.8, 119.3, 115.3, 115.3, 110.6, 55.6, 43.9. HR-MS (ESI): calculated for

(C₁₅H₁₈N₂O, M+H), 243.1497; found, 243.1499. Anal. Calcd for C₁₅H₁₈N₂O : C , 74.35; H, 7.49; N, 11.56. Found: C, 74.44; H, 7.43; N, 11.20.

Synthesis of 2-(diphenylphosphino)-*N*-phenylaniline (NPH), **33H**:

ⁿBuLi (100 mmol, 1.6 M in hexane) was slowly added to a solution of 2-bromo-*N*-phenylbenzenamine (50 mmol, 12.40 g) in Et₂O (200 mL) at -60 °C. The mixture was stirred for 2 h and warmed to ambient temperature and stirred for 16 h again. After cooling this solution to -60 °C, ClPPh₂ (18.4 mL, 100 mmol) was added, and the resulting reaction mixture was stirred for 2h and warmed to room temperature again. After 16 h, the suspension was evaporated to dryness, redissolved in MeOH (500 mL), and acidified with concentrated HCl (20 mL). After stirring for 1 h, the solution was neutralized with an excess of Na₂CO₃ (42.40 g, 400 mmol) and evaporated to dryness. The crude product was obtained by extraction with CH₂Cl₂ and further purified by flash chromatography (silica-gel, hexane/ EtOAc 50:1) to afford the product as a white solid. Yield: 15.37 g, 87%. ¹H NMR (400 MHz, CDCl₃): 7.39-7.43 (m, 10H), 7.23-7.38 (m, 4H), 6.87-7.01 (m, 5H), 6.28 (d, *J* = 6.0 Hz, 1H). ¹³C NMR (100 MHz, CDCl₃): 146.8, 146.6, 142.7, 135.4, 135.4, 134.6, 134.6, 133.8, 133.6, 130.0, 129.2, 128.9, 128.7, 128.6, 124.5, 124.4, 121.4, 121.1, 121.0, 119.0, 116.6, 116.6. ³¹P NMR (162 MHz, CDCl₃): -18.95. HR-MS (ESI): calculated for (C₂₄H₂₀NP, M+H), 354.1412; found, 354.1417. Anal. Calcd for C₂₄H₂₀NP : C , 81.57; H, 5.70; N, 3.96. Found: C, 81.74; H, 5.68; N, 3.86.

Synthesis of *N,N*-bis(2-dimethylaminophenyl)methylamine (^{Me}N₂^{Me}N), **34**:

A THF solution (300 mL) of **2H** (10.216 g, 40.0 mmol) was added to KH (1.845 g, 46.0 mmol) by portion. The reaction mixture was stirred for 2 hours at room temperature. After MeI (6.529 g, 46.0 mmol) was added to the above solution and stirred for overnight at room temperature. After removal of the solvent, the residue was added 100 mL water, and extracted with 100 mL×3 CH₂Cl₂. Removal of the solvent yielded the crude product which was then purified by flash chromatography (silica-gel, hexane/ EtOAc 30:1) to afford the product as a light yellow oil. Yield: 8.151 g, 76%. ¹H NMR (400 MHz, CDCl₃): 6.99-7.05 (m, 2H), 6.91-6.98 (m, 2H), 6.85-6.88 (m, 4H), 3.30 (s, 3H), 2.64 (s, 12H). ¹³C NMR (100 MHz, CDCl₃): 146.4, 143.4, 123.8, 122.3, 122.3, 119.5, 42.8, 36.2. HR-MS (ESI): calculated for (C₁₇H₂₃N₃, M+H), 270.1970; found, 270.1973. Anal. Calcd for C₁₇H₂₃N₃ : C , 75.80; H, 8.61; N, 15.60. Found: C, 76.00; H, 8.77; N, 15.51.

Synthesis of 2-bromo-*N*-phenylbenzenamine, **35**:⁷⁶

A 250 mL reaction vessel was charged with Pd₂(dba)₃ (1.36 g, 1.49 mmol), bis(diphenylphosphino)-ferrocene (DPPF) (1.65 g, 2.97 mmol), NaO^tBu (9.84 g, 98 mmol) and toluene (100 mL) under a dinitrogen atmosphere. 2-Bromo-aniline (12.56 g, 73 mmol) and iodobenzene (14.89 g, 73 mmol) were added to the reaction mixture. The resulting brown solution was vigorously stirred for 3 days at 100 °C. The solution was then cooled to room temperature and filtered through Celite. Removal of the solvent yielded a black liquid which was then purified by flash chromatography (silica-gel, hexane) to afford the product as a colourless oil. Yield: 15.91 g, 88%. ¹H NMR (400 MHz, CDCl₃): 7.57 (dd, *J* = 8.0, 1.6 Hz, 1H), 7.33-7.40 (m, 2H), 7.30 (dd, *J* = 8.4, 1.6 Hz, 1H), 7.16-7.23 (m, 3H), 7.06-7.11 (m, 1H), 6.75-6.80 (m, 1H), 6.13 (br. s, 1H). ¹³C NMR (100 MHz, CDCl₃): 141.5, 141.3, 132.9, 129.4, 128.0, 122.6, 120.8, 120.2, 115.7, 112.1. HR-MS (ESI): calculated for (C₁₂H₁₀BrN, M+H), 248.0075; found, 248.0083.

Synthesis of [(^{Me}N₂N)Cu(PPh₃)], **36**:

A THF solution (50 mL) of [(^{Me}N₂N)Li]₂ (3.92 g, 7.50 mmol) was added to a THF suspension (100 mL) of [Cu(PPh₃)Cl]₄ (5.42 g, 3.75 mmol). The reaction mixture was stirred for 1 h at room temperature. After removal of solvent, the residue was extracted with benzene (200 mL), and then was concentrated to *ca.* 20 mL. Addition of pentane (100 mL) afforded a light yellow precipitate, which was filtered, washed with additional pentane, and dried *in vacuo*. Yield: 7.50 g (86 %). Diffusion of pentane into a benzene solution of **36** afforded yellow crystals suitable for X-ray analysis. ¹H NMR (400 MHz, C₆D₆): 7.60 (d, *J* = 8.0 Hz, 2H), 7.32 (t, *J* = 8.8 Hz, 6H), 7.17-7.11 (m, 3H), 7.03-6.93 (m, 10H), 6.80 (t, *J* = 7.2 Hz, 2H), 2.49 (s, 12H). ¹³C NMR (100 MHz, C₆D₆): 150.8, 144.3, 134.2, 134.0, 133.6, 130.2, 129.0, 128.9, 125.4, 119.2, 118.8, 115.5, 45.9. ³¹P NMR (162 MHz, C₆D₆): 9.2. Anal. Calcd for C₃₄H₃₅N₃PCu: C, 70.39; H, 6.08; N, 7.24. Found: C, 70.06; H, 6.02; N, 7.10.

Synthesis of [(NNO)Cu(PPh₃)], **37**:

ⁿBuLi (11.2 mmol, 1.6 M in hexane) was slowly added to a THF solution (250 mL) of the ligand NNOH (2.580 g, 10.7 mmol) at room temperature. The reaction mixture was stirred for 1 h, and then this solution was added into a solution of [Cu(PPh₃)Cl]₄ (3.847 g, 2.7 mmo) in THF (25 mL). The resulting solution was stirred overnight and then evaporated in vacuum. The residue was extracted with benzene (100 mL), and then was filtered and concentrated to *ca.* 20 mL. Addition of pentane (100 mL) afforded a white precipitate, which was filtered,

washed with additional pentane, and dried *in vacuo*. Yield: 3.913 g (65%). Diffusion of pentane into a toluene solution of **37** afforded colourless crystals suitable for X-ray analysis. ^1H NMR (400 MHz, C_6D_6): 7.78 (d, $J = 7.6$ Hz, 1H), 7.32-7.43 (m, 6H), 7.22 (d, $J = 8.0$ Hz, 1H), 6.92-7.12 (m, 13H), 6.86 (d, $J = 8.0$ Hz, 1H), 6.55 (t, $J = 7.2$ Hz, 1H), 3.28 (s, 3H), 2.50 (s, 6H). ^{13}C NMR (100 MHz, C_6D_6): 154.6, 154.1, 145.4, 140.0, 134.1, 133.9, 133.8, 133.4, 130.2, 129.0, 128.9, 127.5, 126.4, 121.7, 120.0, 119.8, 113.2, 112.8, 111.2, 55.1, 48.0. ^{31}P NMR (162 MHz, C_6D_6): 9.424. Anal. Calcd for $\text{C}_{73}\text{H}_{72}\text{Cu}_2\text{N}_4\text{O}_2\text{P}_2$ ($2[\text{NNOCu}(\text{PPh}_3)] + \text{Toluene}$): C, 71.49; H, 5.92; N, 4.57. Found: C, 71.50; H, 5.84; N, 4.79.

Synthesis of $[(^{\text{Me}}\text{N}^{\text{Me}}\text{N}'\text{N})\text{Cu}(\text{PPh}_3)]$, **38**:

$^n\text{BuLi}$ (16 mmol, 1.6 M in hexane) was slowly added to a THF solution (150 mL) of the ligand $^{\text{Me}}\text{N}^{\text{Me}}\text{N}'\text{NH}$ (3.317 g, 16 mmol) at room temperature. The reaction mixture was stirred for 1 h, and then this solution was added into a solution of $[\text{Cu}(\text{PPh}_3)\text{Cl}]_4$ (3.516 g, 4 mmo) in THF (50 mL). The resulting solution was stirred overnight and then evaporated in vacuum. The residue was extracted with benzene (100 mL), and then was concentrated to *ca.* 20 mL. Addition of pentane (100 mL) afforded a light yellow precipitate, which was filtered, washed with additional pentane, and dried *in vacuo*. Yield: 6.200 g (73%). Diffusion of pentane into a toluene solution of **38** afforded light yellow crystals suitable for X-ray analysis. ^1H NMR (400 MHz, C_6D_6): 7.48-7.56 (m, 6H), 7.33 (t, $J = 7.2$ Hz, 1H), 6.94-7.06 (m, 11H), 6.55 (t, $J = 7.6$ Hz, 1H), 3.88 (t, $J = 6.4$ Hz, 2H), 2.94 (t, $J = 6.8$ Hz, 2H), 2.42 (s, 6H), 2.17 (s, 6H). ^{13}C NMR (100 MHz, C_6D_6): 156.6, 140.3, 134.1, 133.9, 133.5, 130.2, 129.0, 128.9, 128.4, 119.3, 109.6, 108.8, 64.9, 50.0, 47.6, 46.4. ^{31}P NMR (162 MHz, C_6D_6): 8.543. Anal. Calcd for $\text{C}_{30}\text{H}_{35}\text{CuN}_3\text{P}$: C, 67.71; H, 6.63; N, 7.90. Found: C, 67.90; H, 6.51; N, 7.47.

Synthesis of $[(^{\text{H}}\text{NN})\text{Cu}(\text{PPh}_3)]$, **39**:

$^n\text{BuLi}$ (15 mmol, 1.6 M in hexane) was slowly added to a THF solution (50 mL) of the ligand $^{\text{H}}\text{NNH}$ (3.185 g, 15 mmol) at room temperature. The reaction mixture was stirred for 1 h, and then this solution was added into a solution of $[\text{Cu}(\text{PPh}_3)\text{Cl}]_4$ (5.419 g, 3.75 mmo) in THF (100 mL). The resulting solution was stirred for 0.5 h and then evaporated in vacuum. The residue was extracted with benzene (100 mL), and then was filtered and concentrated to *ca.* 20 mL. Addition of pentane (100 mL) afforded a light yellow precipitate, which was filtered, washed with additional pentane, and dried *in vacuo*. Yield: 5.880 g (73%). Diffusion of pentane into a toluene solution of **39** afforded colourless crystals suitable for X-ray analysis. ^1H NMR (400 MHz, C_6D_6): 7.71-7.76 (m, 3H), 7.35-7.42 (m, 6H), 7.30 (t, $J = 7.2$

Hz, 2H), 7.06-7.10 (m, 1H), 6.89-7.02 (m, 11H), 6.58 (dt, $J = 7.6, 1.2$ Hz, 1H), 2.41 (s, 6H). ^{13}C NMR (100 MHz, C_6D_6): 156.1, 153.3, 141.1, 134.0, 133.9, 133.3, 132.9, 130.3, 129.3, 129.1, 129.0, 127.7, 124.3, 120.1, 118.6, 113.4, 112.4, 47.9. ^{31}P NMR (162 MHz, C_6D_6): 9.19. Anal. Calcd for $\text{C}_{32}\text{H}_{30}\text{CuN}_2\text{P}$: C, 71.56; H, 5.63; N, 5.22. Found: C, 71.75; H, 5.65; N, 5.29.

Synthesis of $[(\text{NP})\text{Cu}(\text{PPh}_3)_2]$, **40**:

$n\text{BuLi}$ (0.4 mmol, 1.6 M in hexane) was slowly added to a THF solution (10 mL) of the ligand NPH (**32H**) (0.142 g, 0.4 mmol) at room temperature. The reaction mixture was stirred for 1 h, and then this solution was added into a solution of $[\text{Cu}(\text{PPh}_3)\text{Cl}]_4$ (0.145 g, 0.1 mmol) and PPh_3 (0.105 g, 0.1 mmol) in THF (5 mL). The resulting solution was stirred overnight and then evaporated in vacuum. The residue was extracted with benzene (15 mL), and then was filtered and concentrated to *ca.* 2 mL. Addition of pentane (10 mL) afforded a yellow precipitate, which was filtered, washed with additional pentane, and dried *in vacuo*. Yield: 0.300 g (80%). Diffusion of pentane into a THF solution of **40** afforded yellow crystals suitable for X-ray analysis. ^1H NMR (400 MHz, CD_2Cl_2): 7.24-7.37 (m, 8H), 6.94-7.21 (m, 34H), 6.89-6.94 (m, 3H), 6.82 (t, $J = 7.6$ Hz, 2H), 6.58 (t, $J = 7.2$ Hz, 1H), 6.16-6.29 (s, 1H). ^{13}C NMR (100 MHz, CD_2Cl_2): 164.1, 163.9, 157.0, 136.4, 134.5, 134.4, 134.2, 133.1, 132.9, 131.7, 129.7, 128.9, 128.6, 128.6, 128.4, 128.3, 125.2, 118.5, 113.9, 113.3. ^{31}P NMR (162 MHz, CD_2Cl_2): -0.237, -13.606. Anal. Calcd for $\text{C}_{64.6}\text{H}_{59.4}\text{CuNO}_{0.4}\text{P}_3$ ($[\text{NPCu}(\text{PPh}_3)_2 + 0.4\text{THF} + 0.6\text{pentane}]$): C, 76.62; H, 5.91; N, 1.38. Found: C, 76.19; H, 5.66; N, 1.46.

Synthesis of $[(^{\text{Me}}\text{N}_2^{\text{Me}}\text{N})\text{Cu}(\text{CH}_3\text{CN})\text{PF}_6]$, **41**:

A CH_3CN solution (25 mL) of $^{\text{Me}}\text{N}_2^{\text{Me}}\text{N}$ (**34**) (1.347 g, 5 mmol) was added to a CH_3CN solution (25 mL) of $\text{Cu}(\text{CH}_3\text{CN})_4\text{PF}_6$ (1.864 g, 5 mmol). The reaction mixture was stirred overnight at room temperature. The solution was concentrated to *ca.* 20 mL. Addition of THF (150 mL) afforded a white precipitate, which was filtered, washed with additional pentane, and dried *in vacuo*. Yield: 1.680 g (65%). Diffusion of pentane into a dichloromethane solution of **41** afforded colourless crystals suitable for X-ray analysis. ^1H NMR (400 MHz, CD_2Cl_2): 7.47-7.52 (m, 2H), 7.42-7.47 (m, 2H), 7.30-7.38 (m, 4H), 3.37 (s, 3H), 3.00 (s, 6H), 2.57 (s, 6H), 2.24 (s, 3H). ^{13}C NMR (100 MHz, CD_2Cl_2): 148.4, 146.4, 128.5, 128.1, 125.2, 122.6, 116.7, 51.9, 50.4, 49.5, 2.9. ^{31}P NMR (162 MHz, CD_2Cl_2): -143.991 (septet). Anal. Calcd for $\text{C}_{19}\text{H}_{26}\text{CuF}_6\text{N}_4\text{P}$: C, 43.97; H, 5.05; N, 10.80. Found: C, 43.88; H, 4.99; N, 10.74.

Synthesis of [$(^{\text{Me}}\text{N}_2\text{N})\text{Cu}(\text{PEt}_3)$], **42**:

A THF solution (50 mL) of PEt_3 (2.360 g, 20 mmol) was added to a THF suspension (50 mL) of CuCl (0.990 g, 10 mmol). The reaction mixture was stirred for 1 h at room temperature. Then, a THF solution (30 mL) of [$^{\text{Me}}\text{N}_2\text{NLi}$] $_2$ (0.631 g, 5 mmol) was added to the above solution and stirred for overnight. After removal of solvent, the residue was extracted with benzene (50 mL), and then was filtered and evaporated all the solvent, and again the product was extracted with pentane, the solution concentrated to *ca.* 20 mL, and stored in fridge ($-20\text{ }^\circ\text{C}$) to recrystallize to afforded a colourless need crystals, which was filtered, and dried *in vacuo*. Yield: 2.220 g (51%). Recrystallization of **42** in pentane at $-20\text{ }^\circ\text{C}$ afforded colourless crystals suitable for X-ray analysis. ^1H NMR (400 MHz, C_6D_6): 7.24 (dd, $J = 7.2, 0.8\text{ Hz}$, 2H), 7.05-7.10 (m, 4H), 6.78 (dt, $J = 8.0, 1.2\text{ Hz}$, 2H), 2.65 (s, 12H), 0.98 (dq, $J_{\text{H-H}} = 7.6\text{ Hz}$, $J_{\text{P-H}} = 7.6\text{ Hz}$, 6H), 0.69 (dt, $J_{\text{H-H}} = 7.6\text{ Hz}$, $J_{\text{P-H}} = 16.8\text{ Hz}$, 9H) ppm. ^{13}C NMR (100 MHz, C_6D_6): 150.9, 144.0, 125.0, 119.2, 118.7, 115.3, 45.8, 17.7, 17.5, 8.9, 8.9 ppm. ^{31}P NMR (162 MHz, C_6D_6): -0.514 ppm. Anal. Calcd for $\text{C}_{22}\text{H}_{35}\text{CuN}_3\text{P}$: C, 60.60; H, 8.09; N, 9.64. Found: C, 60.85; H, 8.14; N, 9.53.

Synthesis of [$(^{\text{Me}}\text{N}_2\text{N})\text{Cu}(\text{OAc})$], **43**:

A THF solution (10 mL) of [$^{\text{Me}}\text{N}_2\text{NLi}$] $_2$ (0.131 g, 0.25 mmol) was added to a THF suspension (2 mL) of $\text{Cu}(\text{OAc})_2$ (0.091 g, 0.5 mmol). The reaction mixture was stirred overnight at room temperature. After removal of solvent, the residue was extracted with CH_2Cl_2 (10 mL), and then was filtered and concentrated to *ca.* 3 mL. Addition of pentane (15 mL) afforded a blue precipitate, which was filtered, washed with additional pentane, and dried *in vacuo*. Yield: 0.167 g (89%). Diffusion of pentane into a dichloromethane solution of **43** afforded blue crystals suitable for X-ray analysis. Anal. Calcd for $\text{C}_{18}\text{H}_{23}\text{CuN}_3\text{O}_2$: C, 57.35; H, 6.15; N, 11.15. Found: C, 57.59; H, 6.22; N, 11.36.

Synthesis of [$(^{\text{Me}}\text{N}_2\text{N})\text{CuCl}$], **44**:

A THF solution (40 mL) of [$^{\text{Me}}\text{N}_2\text{NLi}$] $_2$ (2.088 g, 8 mmol) was added to a THF suspension (40 mL) of $\text{Cu}(\text{COD})\text{Cl}$ (3.316 g, 16 mmol). The reaction mixture was stirred overnight at room temperature. After removal of solvent, the residue was extracted with CH_2Cl_2 (50 mL), and then was filtered and concentrated to *ca.* 10 mL. Addition of pentane (50 mL) afforded a blue precipitate, which was filtered, washed with additional pentane, and dried *in vacuo*. Yield: 2.287 g (81%). Diffusion of pentane into a toluene solution of **44** afforded blue

crystals suitable for X-ray analysis. Anal. Calcd for $C_{16}H_{20}ClCuN_3$: C, 54.39; H, 5.71; N, 11.89. Found: C, 54.18; H, 6.02; N, 11.56.

Synthesis of $[(^{Me}N_2N)Cu(OTf)]$, **45**:

A trimethylsilyl triflate (0.111 g, 0.5 mmol) was added to a toluene (10 mL) solution of **44** (0.141 g, 0.4 mmol). The reaction mixture was stirred overnight at room temperature. After removal of solvent, the residue was extracted with benzene (10 mL), and then the solution was concentrated to *ca.* 2 mL. Addition of pentane (10 mL) afforded the desired product, which was filtered, washed with additional pentane, and dried *in vacuo*. Yield: 0.150 g (80%). Diffusion of pentane into a toluene solution of **45** afforded red needle crystals suitable for X-ray analysis. Anal. Calcd for $C_{17}H_{20}CuF_3N_3O_3S$: C, 43.73; H, 4.32; N, 9.00. Found: C, 43.81; H, 4.21; N, 8.98.

Synthesis of $[(BDMAEE)Cu_2I_2]$

BDMAEE (120 mg, 0.75 mmol) was added to a dichloromethane suspension (7 mL) of CuI (143 mg, 0.75 mmol). After 3 min, CuI appeared to be dissolved. The reaction was stirred for 0.5 h, during which time a white powder started to precipitate. The solution was stirred overnight. The white solid was collected by filtration, washed with additional pentane, and dried *in vacuo*. Yield: 122 mg (60%). From elemental analysis, the CuI and BDMAEE ratio is 2 : 1, Anal. Calcd for $C_8H_{20}N_2OI_2Cu_2$: C, 17.76; H, 3.73; N, 5.18. Found: C, 17.74; H, 3.67; N, 5.01. The white solid product is not soluble in THF, CH_2Cl_2 , DMF, MeOH.

The reaction between CuI and BDMAEE was additionally monitored by NMR in CD_2Cl_2 before precipitation appeared (Figures 11 and 12). It appeared that a Cu-BDMAEE complex was formed in the solution.

4.7.4 Crystallographic details

(1) Complex **36** (rp600342)

A total of 44261 reflections ($-15 \leq h \leq 15$, $-16 \leq k \leq 16$, $-25 \leq l \leq 25$) were collected at $T = 100(2)$ K in the range of 3.21 to 27.50° of which 6669 were unique ($R_{int} = 0.0413$); $MoK\alpha$ radiation ($\lambda = 0.71073$ Å). The structure was solved by the direct methods. All non-hydrogen atoms were refined anisotropically, and hydrogen atoms were placed in calculated idealized positions. The residual peak and hole electron densities were 0.463 and -0.492 eÅ⁻³, respectively. The absorption coefficient was 0.829 mm⁻¹. The least squares refinement converged normally with residuals of $R(F) = 0.0346$, $wR(F^2) = 0.0726$ and a GOF = 1.083

($I > 2\sigma(I)$). $C_{34}H_{35}CuN_3P$, Mw = 580.16, space group $P2_1/c$, Monoclinic, $a = 12.1586(8)$, $b = 12.6802(16)$, $c = 19.525(4)$ Å, $\alpha = 90^\circ$, $\beta = 103.689(13)^\circ$, $\gamma = 90^\circ$, $V = 2924.8(7)$ Å³, $Z = 4$, $\rho_{\text{calcd}} = 1.318$ Mg/m³. CCDC number 860876 contains the supplementary crystallographic data for this complex. The data can be obtained free of charge from the Cambridge Crystallographic Data Center via www.ccdc.cam.ac.uk/data_request/cif.

(2) Complex 37 (rp700187)

A total of 12955 reflections ($-15 \leq h \leq 15$, $-27 \leq k \leq 27$, $-17 \leq l \leq 17$) were collected at $T = 140(2)$ K in the range of 2.14 to 27.69° of which 6701 were unique ($R_{\text{int}} = 0.0352$); $Mo_{K\alpha}$ radiation ($\lambda = 0.71073$ Å). The structure was solved by the direct methods. All non-hydrogen atoms were refined anisotropically, and hydrogen atoms were placed in calculated idealized positions. The residual peak and hole electron densities were 0.500 and -0.706 eÅ⁻³, respectively. The absorption coefficient was 0.802 mm⁻¹. The least squares refinement converged normally with residuals of $R(F) = 0.0499$, $wR(F^2) = 0.1261$ and a GOF = 1.061 ($I > 2\sigma(I)$). $C_{73}H_{72}Cu_2N_4O_2P_2$, Mw = 1226.37, space group $P2_1/n$, Monoclinic, $a = 11.969(6)$, $b = 21.048(8)$, $c = 13.447(4)$ Å, $\beta = 116.03(2)^\circ$, $V = 3044(2)$ Å³, $Z = 2$, $\rho_{\text{calcd}} = 1.338$ Mg/m³.

(3) Complex 38 (rp700492)

A total of 9464 reflections ($-12 \leq h \leq 13$, $-14 \leq k \leq 14$, $-17 \leq l \leq 17$) were collected at $T = 140(2)$ K in the range of 2.44 to 27.68° of which 5717 were unique ($R_{\text{int}} = 0.0468$); $Mo_{K\alpha}$ radiation ($\lambda = 0.71073$ Å). The structure was solved by the direct methods. All non-hydrogen atoms were refined anisotropically, and hydrogen atoms were placed in calculated idealized positions. The residual peak and hole electron densities were 0.632 and -0.812 eÅ⁻³, respectively. The absorption coefficient was 0.889 mm⁻¹. The least squares refinement converged normally with residuals of $R(F) = 0.0538$, $wR(F^2) = 0.1506$ and a GOF = 1.165 ($I > 2\sigma(I)$). $C_{30}H_{35}CuN_3P$, Mw = 532.12, space group $P-1$, Triclinic, $a = 9.998(5)$, $b = 11.276(4)$, $c = 13.478(6)$ Å, $\alpha = 104.93(3)^\circ$, $\beta = 102.89(3)^\circ$, $\gamma = 104.48(2)^\circ$, $V = 1352.8(10)$ Å³, $Z = 2$, $\rho_{\text{calcd}} = 1.306$ Mg/m³.

(4) Complex 39 (rp700013)

A total of 11399 reflections ($-14 \leq h \leq 14$, $-13 \leq k \leq 13$, $-31 \leq l \leq 31$) were collected at $T = 140(2)$ K in the range of 2.63 to 27.67° of which 6099 were unique ($R_{\text{int}} = 0.0497$); $Mo_{K\alpha}$ radiation ($\lambda = 0.71073$ Å). The structure was solved by the direct methods. All non-hydrogen

atoms were refined anisotropically, and hydrogen atoms were placed in calculated idealized positions. The residual peak and hole electron densities were 0.576 and -0.534 eA^{-3} , respectively. The absorption coefficient was 0.908 mm^{-1} . The least squares refinement converged normally with residuals of $R(F) = 0.0562$, $wR(F^2) = 0.1411$ and a GOF = 1.002 ($I > 2\sigma(I)$). $\text{C}_{32}\text{H}_{30}\text{CuN}_2\text{P}$, Mw = 537.09, space group $P2_1/n$, Monoclinic, $a = 10.881(2)$, $b = 10.151(2)$, $c = 24.022(5) \text{ \AA}$, $\beta = 93.20(3)^\circ$, $V = 2649.2(9) \text{ \AA}^3$, $Z = 4$, $\rho_{\text{calcd}} = 1.347 \text{ Mg/m}^3$.

(5) Complex 40 (rp700611)

A total of 23814 reflections ($-17 \leq h \leq 17$, $-31 \leq k \leq 31$, $-21 \leq l \leq 21$) were collected at $T = 140(2) \text{ K}$ in the range of 2.10 to 27.74° of which 12259 were unique ($R_{\text{int}} = 0.0776$); $\text{MoK}\alpha$ radiation ($\lambda = 0.71073 \text{ \AA}$). The structure was solved by the direct methods. All non-hydrogen atoms were refined anisotropically, and hydrogen atoms were placed in calculated idealized positions. The residual peak and hole electron densities were 0.432 and -0.702 eA^{-3} , respectively. The absorption coefficient was 0.548 mm^{-1} . The least squares refinement converged normally with residuals of $R(F) = 0.0646$, $wR(F^2) = 0.1449$ and a GOF = 0.975 ($I > 2\sigma(I)$). $\text{C}_{64.63}\text{H}_{59.50}\text{CuNO}_{0.38}\text{P}_3$, Mw = 1012.58, space group $P2_1/c$, Monoclinic, $a = 13.492(4)$, $b = 24.333(6)$, $c = 16.310(3) \text{ \AA}$, $\beta = 100.370(14)^\circ$, $V = 5267(2) \text{ \AA}^3$, $Z = 4$, $\rho_{\text{calcd}} = 1.277 \text{ Mg/m}^3$.

(6) Complex 41 (rp700482)

A total of 7195 reflections ($-9 \leq h \leq 9$, $-23 \leq k \leq 24$, $-15 \leq l \leq 15$) were collected at $T = 140(2) \text{ K}$ in the range of 2.54 to 24.55° of which 3700 were unique ($R_{\text{int}} = 0.0473$); $\text{MoK}\alpha$ radiation ($\lambda = 0.71073 \text{ \AA}$). The structure was solved by the direct methods. All non-hydrogen atoms were refined anisotropically, and hydrogen atoms were placed in calculated idealized positions. The residual peak and hole electron densities were 0.488 and -0.904 eA^{-3} , respectively. The absorption coefficient was 1.110 mm^{-1} . The least squares refinement converged normally with residuals of $R(F) = 0.0692$, $wR(F^2) = 0.1908$ and a GOF = 1.039 ($I > 2\sigma(I)$). $\text{C}_{19}\text{H}_{26}\text{CuF}_6\text{N}_4\text{P}$, Mw = 518.95, space group $P2_1/n$, Monoclinic, $a = 8.5040(17)$, $b = 20.598(4)$, $c = 12.908(3) \text{ \AA}$, $\beta = 97.91(3)^\circ$, $V = 2239.5(8) \text{ \AA}^3$, $Z = 4$, $\rho_{\text{calcd}} = 1.539 \text{ Mg/m}^3$.

(7) Complex 42 (rp700378)

A total of 81975 reflections ($-16 \leq h \leq 16$, $-27 \leq k \leq 27$, $-28 \leq l \leq 28$) were collected at $T = 100(2) \text{ K}$ in the range of 3.38 to 30.03° of which 6764 were unique ($R_{\text{int}} = 0.0545$); $\text{MoK}\alpha$

radiation ($\lambda = 0.71073 \text{ \AA}$). The structure was solved by the direct methods. All non-hydrogen atoms were refined anisotropically, and hydrogen atoms were placed in calculated idealized positions. The residual peak and hole electron densities were 0.415 and -0.386 e\AA^{-3} , respectively. The absorption coefficient was 1.021 mm^{-1} . The least squares refinement converged normally with residuals of $R(F) = 0.0356$, $wR(F^2) = 0.0659$ and a GOF = 1.144 ($I > 2\sigma(I)$). $\text{C}_{22}\text{H}_{35}\text{CuN}_3\text{P}$, Mw = 436.04 , space group $Pbca$, Orthorhombic, $a = 11.611(3)$, $b = 19.6963(13)$, $c = 20.290(4) \text{ \AA}$, $V = 4640.1(15) \text{ \AA}^3$, $Z = 8$, $\rho_{\text{calcd}} = 1.248 \text{ Mg/m}^3$.

(8) Complex 43 (rp700103)

A total of 3921 reflections ($-16 \leq h \leq 16$, $-11 \leq k \leq 11$, $-15 \leq l \leq 20$) were collected at $T = 140(2) \text{ K}$ in the range of 2.57 to 27.79° of which 3921 were unique ($R_{\text{int}} = 0.0000$); $\text{MoK}\alpha$ radiation ($\lambda = 0.71073 \text{ \AA}$). The structure was solved by the direct methods. All non-hydrogen atoms were refined anisotropically, and hydrogen atoms were placed in calculated idealized positions. The residual peak and hole electron densities were 0.686 and -1.366 e\AA^{-3} , respectively. The absorption coefficient was 1.297 mm^{-1} . The least squares refinement converged normally with residuals of $R(F) = 0.0598$, $wR(F^2) = 0.1870$ and a GOF = 1.155 ($I > 2\sigma(I)$). $\text{C}_{18}\text{H}_{23}\text{CuN}_3\text{O}_2$, Mw = 376.93 , space group $P2_1/c$, Monoclinic, $a = 12.752(5)$, $b = 8.435(4)$, $c = 15.840(5) \text{ \AA}$, $\beta = 90.86(2)^\circ$, $V = 1703.6(12) \text{ \AA}^3$, $Z = 4$, $\rho_{\text{calcd}} = 1.470 \text{ Mg/m}^3$.

(9) Complex 44 (rp700107)

A total of 7499 reflections ($-17 \leq h \leq 17$, $-10 \leq k \leq 10$, $-21 \leq l \leq 21$) were collected at $T = 140(2) \text{ K}$ in the range of 2.47 to 27.71° of which 4236 were unique ($R_{\text{int}} = 0.0380$); $\text{MoK}\alpha$ radiation ($\lambda = 0.71073 \text{ \AA}$). The structure was solved by the direct methods. All non-hydrogen atoms were refined anisotropically, and hydrogen atoms were placed in calculated idealized positions. The residual peak and hole electron densities were 0.906 and -0.867 e\AA^{-3} , respectively. The absorption coefficient was 1.319 mm^{-1} . The least squares refinement converged normally with residuals of $R(F) = 0.0527$, $wR(F^2) = 0.1509$ and a GOF = 1.177 ($I > 2\sigma(I)$). $\text{C}_{18.50}\text{H}_{26}\text{ClCuN}_3$, Mw = 389.41 , space group $P2_1/n$, Monoclinic, $a = 13.718(6)$, $b = 8.226(2)$, $c = 16.531(5) \text{ \AA}$, $\beta = 92.79(2)^\circ$, $V = 1863.2(11) \text{ \AA}^3$, $Z = 4$, $\rho_{\text{calcd}} = 1.388 \text{ Mg/m}^3$.

(10) Complex 45 (rp700485)

A total of 4270 reflections ($-8 \leq h \leq 8$, $-19 \leq k \leq 19$, $-25 \leq l \leq 25$) were collected at $T = 140(2) \text{ K}$ in the range of 2.76 to 27.65° of which 2365 were unique ($R_{\text{int}} = 0.0751$); $\text{MoK}\alpha$

radiation ($\lambda = 0.71073 \text{ \AA}$). The structure was solved by the direct methods. All non-hydrogen atoms were refined anisotropically, and hydrogen atoms were placed in calculated idealized positions. The residual peak and hole electron densities were 0.782 and -1.433 e\AA^{-3} , respectively. The absorption coefficient was 1.230 mm^{-1} . The least squares refinement converged normally with residuals of $R(F) = 0.0646$, $wR(F^2) = 0.1858$ and a GOF = 1.165 ($I > 2\sigma(I)$). $\text{C}_{17}\text{H}_{20}\text{CuF}_3\text{N}_3\text{O}_3\text{S}$, Mw = 466.96 , space group $Pnma$, Orthorhombic, $a = 6.961(4)$, $b = 14.770(5)$, $c = 19.704(7) \text{ \AA}$, $V = 2025.8(15) \text{ \AA}^3$, $Z = 4$, $\rho_{\text{calcd}} = 1.531 \text{ Mg/m}^3$.

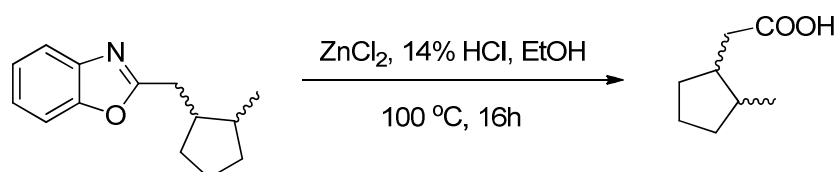
4.7.5 General procedures for Tables 3, 5, 6 and Scheme 6

A mixture of Cu catalyst (quantity shown in the corresponding table), BDMAEE or TMEDA (quantity shown in the corresponding table), $^t\text{BuONa}$ (quantity shown in the corresponding table), alkyl halide (0.6 mmol) and azole (0.5 mmol) was placed in a vial and 2 mL of toluene was added. The mixture was heated under N_2 during 16 h (temperature shown in the corresponding table). The reaction mixture was then cooled to room temperature, quenched with water (15 mL) and 1 mL of 1 M HCl , extracted with CH_2Cl_2 (3 times, 10 mL each), dried over Na_2SO_4 , filtered, and subjected to GC analysis. $60 \text{ }\mu\text{L}$ of dodecane was used as an internal standard.

4.7.6 General procedures for Table 4

A mixture of $[(^{\text{Me}}\text{N}_2\text{N})\text{Cu}(\text{PPh}_3)]$ (87 mg , 0.15 mmol), BDMAEE (24 mg , 0.15 mmol) $^t\text{BuONa}$ (173 mg , 1.8 mmol), Alkyl-X (1.8 mmol) and azole (1.5 mmol) was placed in a vial and 6 mL of toluene was added. Additional CuI (57 mg , 0.3 mmol) and BDMAEE (total 96 mg , 0.6 mmol) were added for coupling of alkyl-Br. The mixture was heated under N_2 during 16 h at $80 \text{ }^\circ\text{C}$ ($100 \text{ }^\circ\text{C}$ for alkyl-Br). The reaction mixture was then cooled to room temperature, quenched with 15 mL of water and 1 mL of 1 M HCl , extracted with CH_2Cl_2 (3 times, 20 mL each), dried over Na_2SO_4 , filtered, and finally evaporated under a reduced pressure. The residue was purified by flash chromatography on silica-gel.

4.7.7 Stereochemical assignment of ring-closed product (Scheme 6, eq. 2)

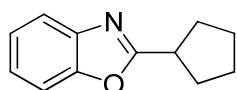


2-((2-methylcyclopentyl)methyl)benzoxazole (4) (108 mg, 0.5 mmol, major and minor ratio is 3.3 : 1 determined by ^1H NMR and 3.4 : 1 determined by GC) obtained from the reaction of benzoxazole coupling with 6-iodo-1heptene (scheme 6) was hydrolyzed using ZnCl_2 in 14% HCl aqueous and Ethanol mixture.⁴⁴ The major and minor hydrolysis products ratio is 3.3 : 1 determined by ^1H NMR. The ^1H and ^{13}C NMR of minor product are in good agreement with the reported data of 2-(*trans*-2-methylcyclopentyl)acetic acid,⁷⁷ which assign *trans* and *cis* isomers of 2-((2-methylcyclopentyl)methyl)benzoxazole ratio is 1:3.3.

2-(2-methylcyclopentyl)acetic acid: ^1H NMR (400 MHz, CDCl_3): 11.40 (br, 1H), 2.52 (dd, $J = 14.8, 4.8$ Hz, 0.23H, minor), 2.41 (dd, $J = 14.4, 6.0$ Hz, 0.77H, major), 2.35-2.04 (m, 2.54H), 2.00-1.17 (m, 6.46H), 0.99 (d, $J = 6.8$ Hz, 0.69H, minor), 0.83 (d, $J = 6.8$ Hz, 2.31H, major) ppm.

^{13}C NMR (100 MHz, CDCl_3) major: 180.4, 39.4, 36.0, 35.4, 33.1, 30.0, 22.5, 15.1 ppm; minor: 180.4, 43.7, 40.4, 39.0, 34.3, 32.3, 23.1, 18.9 ppm.

4.7.8 Detailed descriptions for products in Table 4



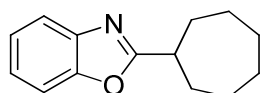
2-Cyclopentylbenzoxazole (Table 3, entry 7)⁷⁸:

Eluated from the column with hexane-diethyl ether (20:1) in 80% yield as a yellow liquid.

^1H NMR (400 MHz, CDCl_3): 7.69-7.64 (m, 1H), 7.48-7.45 (m, 1H), 7.31-7.26 (m, 2H), 3.44-3.32 (m, 1H), 2.25-2.12 (m, 2H), 2.10-1.99 (m, 2H), 1.91-1.79 (m, 2H), 1.79-1.67 (m, 2H).

^{13}C NMR (100 MHz, CDCl_3): 170.5, 150.7, 141.3, 124.2, 123.9, 119.4, 110.2, 38.8, 31.3, 25.6.

HRESI-MS: calculated for ($\text{C}_{12}\text{H}_{14}\text{NO}$, $\text{M}+\text{H}$), 188.1075; found, 188.1076.



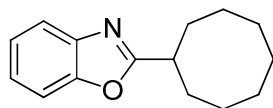
2-Cycloheptylbenzoxazole (Table 4, entry 1)⁷⁸:

Eluated from the column with hexane-diethyl ether (20:1) in 73% yield as a yellow liquid.

^1H NMR (400 MHz, CDCl_3): 7.69-7.62 (m, 1H), 7.46-7.40 (m, 1H), 7.27-7.20 (m, 2H), 3.15-3.08 (m, 1H), 2.20-2.13 (m, 2H), 1.97-1.86 (m, 2H), 1.84-1.73 (m, 2H), 1.68-1.50 (m, 6H).

^{13}C NMR (100 MHz, CDCl_3): 171.2, 150.5, 141.1, 124.1, 123.8, 119.4, 110.0, 39.6, 32.1, 28.2, 26.1.

HRESI-MS: calculated for ($\text{C}_{14}\text{H}_{18}\text{NO}$, $\text{M}+\text{H}$), 216.1388; found, 216.1397.

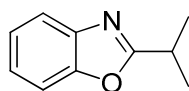
**2-Cycloheptylbenzoxazole (Table 4, entry 2)⁷⁸:**

Eluated from the column with hexane-diethyl ether (20:1) in 75% yield as a yellow liquid.

¹H NMR (400 MHz, CDCl₃): 7.67-7.64 (m, 1H), 7.47-7.41 (m, 1H), 7.28-7.22 (m, 2H), 3.21-3.15 (m, 1H), 2.16-2.09 (m, 2H), 2.02-1.94 (m, 2H), 1.80-1.69 (m, 2H), 1.67-1.49 (m, 8H).

¹³C NMR (100 MHz, CDCl₃): 171.4, 150.5, 141.1, 124.1, 123.8, 119.4, 110.1, 38.1, 29.6, 26.8, 25.9, 25.0.

HRESI-MS: calculated for (C₁₅H₂₀NO, M+H), 230.1545; found, 230.1543.

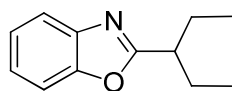
**2-Isopropylbenzoxazole (Table 4, entry 3)⁷⁹:**

Eluated from the column with pentane-diethyl ether (20:1) in 81% yield as a yellow liquid.

¹H NMR (400 MHz, CDCl₃): 7.72-7.66 (m, 1H), 7.51-7.46 (m, 1H), 7.32-7.27 (m, 2H), 3.31-3.19 (m, 1H), 1.47 (d, *J* = 6.8 Hz, 6H).

¹³C NMR (100 MHz, CDCl₃): 171.2, 150.6, 141.2, 124.3, 123.9, 119.5, 110.2, 28.8, 20.2.

HRESI-MS: calculated for (C₁₀H₁₂NO, M+H), 162.0919; found, 162.0920.

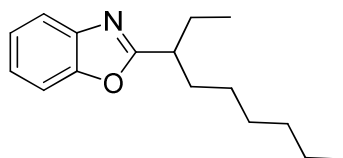
**2-(3-Pentyl)benzoxazole (Table 4, entry 4 or 10):**

Eluated from the column with hexane-diethyl ether (20:1) in 71% yield (starting from 3-iodopentane) and 60% yield (starting from 3-bromopentane) as a yellow liquid.

¹H NMR (400 MHz, CDCl₃): 7.70-7.65 (m, 1H), 7.48-7.43 (m, 1H), 7.29-7.22 (m, 2H), 2.90-2.82 (m, 1H), 1.95-1.73 (m, 4H), 0.89 (t, *J* = 7.2 Hz, 6H).

¹³C NMR (100 MHz, CDCl₃): 169.7, 150.5, 141.2, 124.1, 123.8, 119.5, 110.2, 43.3, 26.1, 11.7.

HRESI-MS: calculated for (C₁₂H₁₆NO, M+H), 190.1232; found, 190.1235.



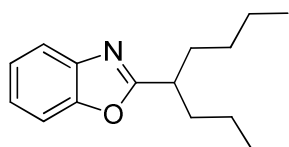
2-(3-Nonyl)benzoxazole (Table 4, entry 5):

Eluated from the column with hexane-diethyl ether (20:1) in 81% yield as a yellow liquid.

^1H NMR (400 MHz, CDCl_3): 7.70-7.65 (m, 1H), 7.49-7.43 (m, 1H), 7.30-7.23 (m, 2H), 2.98-2.89 (m, 1H), 1.93-1.70 (m, 4H), 1.32-1.22 (m, 8H), 0.91 (t, $J = 7.2$ Hz, 3H), 0.85 (t, $J = 7.2$ Hz, 3H).

^{13}C NMR (100 MHz, CDCl_3): 169.9, 150.6, 141.2, 124.1, 123.8, 119.5, 110.2, 41.8, 33.2, 31.6, 29.1, 27.2, 26.6, 22.5, 13.9, 11.7.

HRESI-MS: calculated for ($\text{C}_{16}\text{H}_{24}\text{NO}$, $\text{M}+\text{H}$), 246.1858; found, 246.1860.



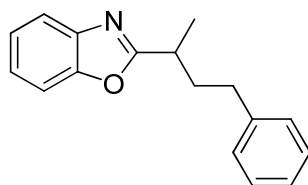
2-(5-Nonyl)benzoxazole (Table 4, entry 6)⁴⁴:

Eluated from the column with hexane-diethyl ether (20:1) in 82% yield as a yellow liquid.

^1H NMR (400 MHz, CDCl_3): 7.70-7.66 (m, 1H), 7.49-7.45 (m, 1H), 7.30-7.23 (m, 2H), 3.03-2.94 (m, 1H), 1.91-1.79 (m, 2H), 1.79-1.68 (m, 2H), 1.36-1.14 (m, 8H), 0.83 (t, $J = 6.8$ Hz, 6H).

^{13}C NMR (100 MHz, CDCl_3): 170.1, 150.5, 141.1, 124.1, 123.8, 119.5, 110.2, 40.2, 33.3, 29.5, 22.5, 13.8.

HRESI-MS: calculated for ($\text{C}_{16}\text{H}_{24}\text{NO}$, $\text{M}+\text{H}$), 246.1858; found, 246.1862.



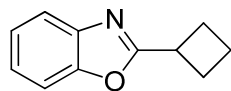
2-{2-(4-phenyl)butyl}benzoxazole (Table 4, entry 7):

Eluated from the column with hexane-diethyl ether (20:1) in 76% yield as a yellow liquid.

^1H NMR (400 MHz, CDCl_3): 7.75-7.70 (m, 1H), 7.54-7.48 (m, 1H), 7.37-7.25 (m, 4H), 7.23-7.17 (m, 3H), 3.25-3.13 (m, 1H), 2.76-2.65 (m, 2H), 2.38-2.25 (m, 1H), 2.10-1.97 (m, 1H), 1.50 (d, $J = 7.2$ Hz, 3H).

^{13}C NMR (100 MHz, CDCl_3): 170.3, 150.6, 141.4, 141.2, 128.4, 128.3, 125.9, 124.4, 124.0, 119.6, 110.3, 36.5, 33.6, 33.3, 18.4.

HRESI-MS: calculated for ($\text{C}_{17}\text{H}_{18}\text{NO}$, $\text{M}+\text{H}$), 252.1388; found, 252.1396.



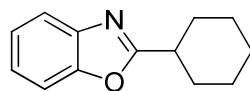
2-Cyclobutylbenzoxazole (Table 4, entry 9)⁷⁸:

Eluated from the column with pentane-diethyl ether (20:1) in 57% yield as a yellow liquid.

^1H NMR (400 MHz, CDCl_3): 7.71-7.64 (m, 1H), 7.51-7.45 (m, 1H), 7.32-7.25 (m, 2H), 3.85-3.72 (m, 1H), 2.63-2.40 (m, 4H), 2.22-2.00 (m, 2H).

^{13}C NMR (100 MHz, CDCl_3): 169.4, 150.8, 141.4, 124.4, 124.0, 119.6, 110.3, 33.4, 27.0, 18.8.

HRESI-MS: calculated for ($\text{C}_{11}\text{H}_{12}\text{NO}$, $\text{M}+\text{H}$), 174.0919; found, 174.0915.



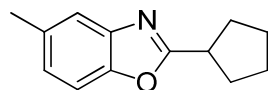
2-Cyclohexylbenzoxazole (Table 4, entry 8)⁷⁸:

Eluated from the column with pentane-diethyl ether (20:1) in 66% yield as a yellow liquid.

^1H NMR (400 MHz, CDCl_3): 7.70-7.65 (m, 1H), 7.50-7.43 (m, 1H), 7.32-7.24 (m, 2H), 3.00-2.91 (m, 1H), 2.19-2.12 (m, 2H), 1.90-1.84 (m, 2H), 1.76-1.64 (m, 3H), 1.50-1.25 (m, 3H).

^{13}C NMR (100 MHz, CDCl_3): 170.4, 150.5, 141.3, 124.3, 123.9, 119.6, 110.2, 37.9, 30.5, 25.8, 25.6.

HRESI-MS: calculated for ($\text{C}_{13}\text{H}_{16}\text{NO}$, $\text{M}+\text{H}$), 202.1232; found, 202.1236.



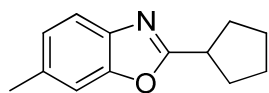
2-Cyclopentyl-5-methylbenzoxazole (Table 4, entry 11):

Eluated from the column with hexane-diethyl ether (20:1) in 63% yield as a yellow liquid.

^1H NMR (400 MHz, CDCl_3): 7.42 (s, 1H), 7.29 (d, $J = 8.4$ Hz, 1H), 7.03 (d, $J = 8.0$ Hz, 1H), 3.35-3.27 (m, 1H), 2.41 (s, 3H), 2.12-2.09 (m, 2H), 2.01-1.95 (m, 2H), 1.88-1.74 (m, 2H), 1.74-1.66 (m, 2H).

^{13}C NMR (100 MHz, CDCl_3): 170.4, 148.8, 141.3, 133.5, 125.1, 119.3, 109.4, 38.7, 31.2, 25.5, 21.3.

HRESI-MS: calculated for ($\text{C}_{13}\text{H}_{16}\text{NO}$, $\text{M}+\text{H}$), 202.1232; found, 202.1242.



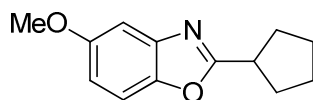
2-Cyclopentyl-6-methylbenzoxazole (Table 4, entry 12):

Eluated from the column with hexane-diethyl ether (20:1) in 62% yield as a yellow liquid.

^1H NMR (400 MHz, CDCl_3): 7.52 (d, $J = 8.0$ Hz, 1H), 7.26 (s, 1H), 7.09 (d, $J = 8.0$ Hz, 1H), 3.39-3.30 (m, 1H), 2.45 (s, 3H), 2.20-2.09 (m, 2H), 2.08-1.97 (m, 2H), 1.90-1.77 (m, 2H), 1.77-1.65 (m, 2H).

^{13}C NMR (100 MHz, CDCl_3): 170.0, 151.1, 139.1, 134.5, 125.0, 118.8, 110.4, 38.8, 31.3, 25.6, 21.6.

HRESI-MS: calculated for ($\text{C}_{13}\text{H}_{16}\text{NO}$, $\text{M}+\text{H}$), 202.1232; found, 202.1233.



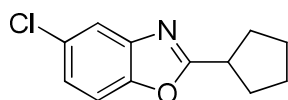
2-Cyclopentyl-5-methoxybenzoxazole (Table 4, entry 13):

Eluated from the column with hexane-diethyl ether (20:1 to 10:1) in 64% yield as a yellow liquid.

^1H NMR (400 MHz, CDCl_3): 7.32 (d, $J = 8.8$ Hz, 1H), 7.16 (d, $J = 2.8$ Hz, 1H), 6.86 (dd, $J = 8.0, 2.4$ Hz, 1H), 3.82 (s, 3H), 3.39-3.28 (m, 1H), 2.20-2.08 (m, 2H), 2.07-1.94 (m, 2H), 1.90-1.77 (m, 2H), 1.77-1.65 (m, 2H).

^{13}C NMR (100 MHz, CDCl_3): 171.4, 156.9, 145.4, 142.1, 112.5, 110.2, 102.8, 55.9, 38.9, 31.3, 25.6.

HRESI-MS: calculated for ($\text{C}_{13}\text{H}_{16}\text{NO}_2$, $\text{M}+\text{H}$), 218.1181; found, 218.1190.



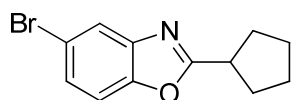
5-Chloro-2-cyclopentylbenzoxazole (Table 4, entry 14):

Eluated from the column with hexane-diethyl ether (30:1) in 73% yield as a yellow liquid.

^1H NMR (400 MHz, CDCl_3): 7.63 (d, $J = 2.0$ Hz, 1H), 7.38 (d, $J = 8.8$ Hz, 1H), 7.24 (dd, $J = 8.8, 2.0$ Hz, 1H), 3.41-3.30 (m, 1H), 2.22-2.10 (m, 2H), 2.07-1.95 (m, 2H), 1.92-1.79 (m, 2H), 1.79-1.66 (m, 2H).

^{13}C NMR (100 MHz, CDCl_3): 172.0, 149.2, 142.3, 129.3, 124.4, 119.4, 110.8, 38.8, 31.2, 25.6.

HRESI-MS: calculated for ($\text{C}_{12}\text{H}_{13}\text{ClNO}$, $\text{M}+\text{H}$), 222.0686; found, 222.0697.

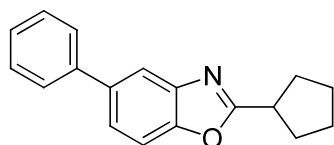
**5-Bromo-2-cyclopentylbenzoxazole (Table 4, entry 15):**

Eluated from the column with hexane-diethyl ether (20:1) in 69% yield as a yellow liquid.

^1H NMR (400 MHz, CDCl_3): 7.78 (d, $J = 2.0$ Hz, 1H), 7.38 (dd, $J = 8.4, 2.0$ Hz, 1H), 7.33 (d, $J = 8.8$ Hz, 1H), 3.41-3.30 (m, 1H), 2.22-2.09 (m, 2H), 2.07-1.95 (m, 2H), 1.91-1.78 (m, 2H), 1.78-1.65 (m, 2H).

^{13}C NMR (100 MHz, CDCl_3): 171.9, 149.8, 143.0, 127.3, 122.5, 116.6, 111.4, 38.8, 31.3, 25.7.

HRESI-MS: calculated for ($\text{C}_{12}\text{H}_{13}\text{BrNO}$, $\text{M}+\text{H}$), 266.0180; found, 266.0175.

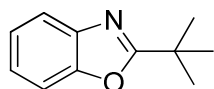
**2-cyclopentyl-5-phenylbenzoxazole (Table 4, entry 16):**

Eluated from the column with hexane-diethyl ether (20:1) in 64% yield as a yellow liquid.

^1H NMR (400 MHz, CDCl_3): 7.89 (s, 1H), 7.62 (d, $J = 7.2$ Hz, 2H), 7.52 (s, 2H), 7.46 (t, $J = 7.6$ Hz, 2H), 7.36 (t, $J = 7.2$ Hz, 1H), 3.45-3.37 (m, 1H), 2.20-2.18 (m, 2H), 2.12-2.04 (m, 2H), 1.98-1.82 (m, 2H), 1.77-1.66 (m, 2H).

^{13}C NMR (100 MHz, CDCl_3): 171.2, 150.3, 142.0, 141.2, 137.8, 128.8, 127.4, 127.0, 123.8, 118.0, 110.2, 38.9, 31.3, 25.7.

HRESI-MS: calculated for ($\text{C}_{18}\text{H}_{18}\text{NO}$, $\text{M}+\text{H}$), 264.1388; found, 264.1389.

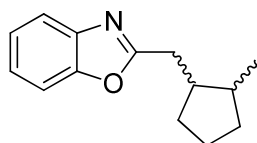
**2-(*Tert*-butyl)benzoxazole (Scheme 6, eq. 1)⁸⁰:**

Eluated from the column with pentane-diethyl ether (20:1) in 23% yield as a yellow liquid.

^1H NMR (400 MHz, CDCl_3): 7.71-7.67 (m, 1H), 7.51-7.45 (m, 1H), 7.33-7.25 (m, 2H), 1.47 (s, 9H).

^{13}C NMR (100 MHz, CDCl_3): 173.4, 150.8, 141.2, 124.3, 123.9, 119.7, 110.2, 34.1, 28.4.

HRESI-MS: calculated for ($\text{C}_{11}\text{H}_{14}\text{NO}$, $\text{M}+\text{H}$), 176.1075; found, 176.1083.



2-((2-methylcyclopentyl)methyl)benzoxazole (Scheme 6, eq. 2):

Eluated from the column with hexane-diethyl ether (20:1) in 62% yield as a yellow liquid.

^1H NMR (400 MHz, CDCl_3): 7.70-7.64 (m, 1H), 7.51-7.46 (m, 1H), 7.32-7.26 (m, 2H), 3.09 (dd, $J = 14.4, 4.8$ Hz, 0.23H, minor), 2.98 (dd, $J = 15.2, 6.8$ Hz, 0.77H, major), 2.79 (dd, $J = 15.2, 9.2$ Hz, 0.77H, major), 2.76 (dd, $J = 14.4, 8.8$ Hz, 0.23H, minor), 2.56-2.42 (m, 0.77H, major), 2.23-2.08 (m, 0.77H, major), 1.87-1.68 (m, 2.46H), 1.66-1.51 (m, 1.54H, major), 1.51-1.29 (m, 2H), 1.31-1.17 (m, 0.46H), 1.00 (d, $J = 6.8$ Hz, 0.69H, minor), 0.93 (d, $J = 7.2$ Hz, 2.31H, major).

^{13}C NMR (100 MHz, CDCl_3) major: 167.4, 150.7, 141.4, 124.2, 123.9, 119.4, 110.1, 41.2, 36.2, 33.0, 29.9, 29.6, 22.4, 15.1; minor: 167.4, 150.7, 141.4, 124.2, 123.9, 119.4, 110.1, 45.6, 40.5, 34.4, 33.2, 32.3, 23.1, 19.0.

HRESI-MS: calculated for ($\text{C}_{14}\text{H}_{18}\text{NO}$, $\text{M}+\text{H}$), 216.1388; found, 216.1383.

4.8 References and Notes

- (1) Eicher, T.; Hauptmann, S.; *The Chemistry of Heterocycles*, Wiley-VCH, Weinheim, **2003**.
- (2) Carey, J. S.; Laffan, D.; Thomson, C.; Williams, M. T.; *Org. Biomol. Chem.* **2006**, *4*, 2337-2347.
- (3) Kraft, A.; Grimsdale, A. C.; Holmes, A. B. *Angew. Chem., Int. Ed.* **1998**, *37*, 402-428.
- (4) Campeau, L. C.; Fagnou, K. *Chem. Commun.* **2006**, 1253-1264.
- (5) Phipps, R. J.; Grimster, N. P.; Gaunt, M. J. *J. Am. Chem. Soc.* **2008**, *130*, 8172-8174.
- (6) Daugulis, O.; Do, H. Q.; Shabashov, D. *Acc. Chem. Res.* **2009**, *42*, 1074-1086.
- (7) Cho, S. H.; Kim, J. Y.; Kwak, J.; Chang, S. *Chem. Soc. Rev.* **2010**, *40*, 5068-5083.
- (8) Ackermann, L.; Althammer, A.; Fenner, S. *Angew. Chem., Int. Ed.* **2009**, *48*, 201-204.
- (9) Join, B.; Yamamoto, T.; Itami, K. *Angew. Chem., Int. Ed.* **2009**, *48*, 3644-3647.
- (10) Besselievre, F.; Piguel, S. *Angew. Chem., Int. Ed.* **2009**, *48*, 9553-9556.
- (11) Brand, J. P.; Charpentier, J.; Waser, J. *Angew. Chem., Int. Ed.* **2009**, *48*, 9346-9349.
- (12) Turner, G. L.; Morris, J. A.; Greaney, M. F. *Angew. Chem., Int. Ed.* **2007**, *46*, 7996-8000.
- (13) Hirano, K.; Miura, M. *Synlett* **2011**, 294-307.

-
- (14) Matsuyama, N.; Hirano, K.; Satoh, T.; Miura, M. *Org. Lett.* **2009**, *11*, 4156-4159.
- (15) Hachiya, H.; Hirano, K.; Satoh, T.; Miura, M. *Angew. Chem., Int. Ed.* **2010**, *49*, 2202-2205.
- (16) Kitahara, M.; Hirano, K.; Tsurugi, H.; Satoh, T.; Miura, M. *Chem.-Eur. J.* **2010**, *16*, 1772-1775.
- (17) Messaoudi, S.; Brion, J. D.; Alami, M. *Eur. J. Org. Chem.* **2010**, 6495-6516.
- (18) For representative examples of direct alkylation of non-heterocyclic substrates, see ref. 19-25.
- (19) Ackermann, L.; Novak, P.; Vicente, R.; Hofmann, N. *Angew. Chem., Int. Ed.* **2009**, *48*, 6045-6048.
- (20) Ackermann, L.; Hofmann, N.; Vicente, R. *Org. Lett.* **2011**, *13*, 1875-1877.
- (21) Zhang, Y. H.; Shi, B. F.; Yu, J. Q. *Angew. Chem., Int. Ed.* **2009**, *48*, 6097-6100.
- (22) Shabashov, D.; Daugulis, O. *J. Am. Chem. Soc.* **2010**, *132*, 3965-3972.
- (23) Zhao, Y. S.; Chen, G. *Org. Lett.* **2010**, *13*, 4850-4853.
- (24) Altenhoff, G.; Wurtz, S.; Glorius, F. *Tetrahedron Lett.* **2006**, *47*, 2925-2928.
- (25) Eckhardt, M.; Fu, G. C. *J. Am. Chem. Soc.* **2003**, *125*, 13642-13643.
- (26) Frisch, A. C.; Beller, M. *Angew. Chem., Int. Ed.* **2005**, *44*, 674-688.
- (27) Netherton, M. R.; Fu, G. C. *Adv. Synth. Catal.* **2004**, *346*, 1525-1532.
- (28) Rudolph, A.; Lautens, M. *Angew. Chem., Int. Ed.* **2009**, *48*, 2656-2670.
- (29) Ackermann, L. *Chem. Commun.* **2010**, *46*, 4866-4877.
- (30) Hu, X. L. *Chem. Sci.* **2011**, *2*, 1867-1886.
- (31) Roberts, R. M.; Khalaf, A. A. *Friedel-Crafts Alkylation Chemistry. A century of Discovery*, Marcel Dekker, New York, **1984**.
- (32) Minisci, F.; Vismara, E.; Fontana, F. *Heterocycles* **1989**, *28*, 489-519.
- (33) Molander, G. A.; Colombel, V.; Braz, V. A. *Org. Lett.* **2011**, *13*, 1852-1855.
- (34) Bowman, W. R.; Storey, J. M. D. *Chem. Soc. Rev.* **2007**, *36*, 1803-1822.
- (35) Rueping, M.; Nachtsheim, B. J.; Scheidt, T. *Org. Lett.* **2006**, *8*, 3717-3719.
- (36) Kischel, J.; Jovel, I.; Mertins, K.; Zapf, A.; Beller, M. *Org. Lett.* **2006**, *8*, 19-22.
- (37) Wang, M. Z.; Wong, M. K.; Che, C. M. *Chem.-Eur. J.* **2008**, *14*, 8353-8364.
- (38) Nakao, Y.; Yamada, Y.; Kashihara, N.; Hiyama, T. *J. Am. Chem. Soc.* **2010**, *132*, 13666-13668.
- (39) Nakao, Y.; Kashihara, N.; Kanyiva, K. S.; Hiyama, T. *Angew. Chem., Int. Ed.* **2010**, *49*, 4451-4454.

-
- (40) Nakao, Y.; Idei, H.; Kanyiva, K. S.; Hiyama, T. *J. Am. Chem. Soc.* **2009**, *131*, 15996-15997.
- (41) Mukai, T.; Hirano, K.; Satoh, T.; Miura, M. *J. Org. Chem.* **2009**, *74*, 6410-6413.
- (42) Lewis, J. C.; Bergman, R. G.; Ellman, J. A. *Acc. Chem. Res.* **2008**, *41*, 1013-1025.
- (43) Zhao, X.; Wu, G. J.; Zhang, Y.; Wang, J. B. *J. Am. Chem. Soc.* **2011**, *133*, 3296-3299.
- (44) Yao, T.; Hirano, K.; Satoh, T.; Miura, M. *Angew. Chem., Int. Ed.* **2012**, *51*, 775-779.
- (45) Verrier, C.; Hoarau, C.; Marsais, F. *Org. Biomol. Chem.* **2009**, *7*, 647-650.
- (46) Vechorkin, O.; Proust, V.; Hu, X. L. *Angew. Chem., Int. Ed.* **2010**, *49*, 3061-3064.
- (47) Yao, T.; Hirano, K.; Satoh, T.; Miura, M. *Chem.-Eur. J.* **2010**, *16*, 12307-12311.
- (48) He, T.; Yu, L.; Zhang, L.; Wang, L.; Wang, M. *Org. Lett.* **2011**, *13*, 5016-5019.
- (49) Ackermann, L.; Barfusser, S.; Kornhaass, C.; Kapdi, A. R. *Org. Lett.* **2011**, *13*, 3082-3085.
- (50) Ackermann, L.; Punji, B.; Song, W. F. *Adv. Synth. Catal.* **2011**, *353*, 3325-3329.
- (51) Csok, Z.; Vechorkin, O.; Harkins, S. B.; Scopelliti, R.; Hu, X. L. *J. Am. Chem. Soc.* **2008**, *130*, 8156-8157.
- (52) Vechorkin, O.; Csok, Z.; Scopelliti, R.; Hu, X. L. *Chem.-Eur. J.* **2009**, *15*, 3889-3899.
- (53) Vechorkin, O.; Hu, X. L. *Angew. Chem., Int. Ed.* **2009**, *48*, 2937-2940.
- (54) Vechorkin, O.; Proust, V.; Hu, X. L. *J. Am. Chem. Soc.* **2009**, *131*, 9756-9766.
- (55) Vechorkin, O.; Scopelliti, R.; Hu, X. L. *Angew. Chem., Int. Ed.* **2011**, *50*, 11777-11781.
- (56) Vechorkin, O.; Barmaz, D.; Proust, V.; Hu, X. L. *J. Am. Chem. Soc.* **2009**, *131*, 12078-12079.
- (57) In the coupling reactions of alkyl bromides, trace amounts of alkyl iodides could be observed by GC in the product mixture.
- (58) Wertz, S.; Kodama, S.; Studer, A. *Angew. Chem., Int. Ed.* **2011**, *50*, 11511-11515.
- (59) Li, Y.; Xie, Y.; Zhang, R.; Jin, K.; Wang, X.; Duan, C. *J. Org. Chem.* **2011**, *76*, 5444-5449.
- (60) Guo, S.; Qian, B.; Xie, Y.; Xia, C.; Huang, H. *Org. Lett.* **2011**, *13*, 522-525.
- (61) Bordwell pK_a table, available at:
<http://www.chem.wisc.edu/areas/reich/pkatable/index.htm>
- (62) Fossey, J. S.; Lefort, D.; Sorba, J. *Free radicals in organic chemistry*, Wiley, **1995**.
- (63) Ren, P.; Vechorkin, O.; von Allmen, K.; Scopelliti, R.; Hu, X. L. *J. Am. Chem. Soc.* **2011**, *133*, 7084-7095.
- (64) Glockling, F.; Hooton, K. A.; *J. Chem. Soc.* **1962**, 2658-2661.
- (65) Jardine, F. H.; Rule, L.; Vohra, A. G. *J. Chem. Soc. A* **1970**, 238-240.

- (66) Cariati, F.; Naldini, L. *Gazzetta*, **1965**, 95, 3-15.
- (67) Cook, B. W.; Miller, R. G. J.; Todd, P. F. *J. Organometal. Chem.* **1969**, 19, 421-430.
- (68) Doyle, G.; Eriksen, K. A. *Organometallics* **1985**, 4, 2201-2206.
- (69) Engelhardt, L. M.; Papasergio, R. I.; White, A. H. *Aust. J. Chem.* **1984**, 37, 2207-2213.
- (70) Vechorkin, O.; Hirt, N.; Hu, X. L. *Org. Lett.* **2010**, 12, 3567-3569.
- (71) Joseph, J.; Kim, J. Y.; Chang, S. *Chem. Eur. J.* **2011**, 17, 8294-8298.
- (72) Meyer, C.; Marek, I.; Courtemanche, G.; Normant, J. F. *Tetrahedron* **1994**, 50, 11665-11692.
- (73) Duisenberg, A. J. M.; Kroon-Batenburg, L. M. J.; Schreurs, A. M. M. *J. Appl. Crystallogr.* **2003**, 36, 220-229.
- (74) Blessing, R. H. *Acta Crystallogr. A* **1995**, 51, 33-38.
- (75) Sheldrick, G. M. *Acta Crystallogr. A* **2008**, 64, 112-122.
- (76) Budén, M. E.; Vaillard, V. A.; Martin, S. E.; Rossi, R. A. *J. Org. Chem.* **2009**, 74, 4490-4498.
- (77) Deng, K.; Bensari-Bouguerra, A.; Whetstone, J.; Cohen, T. *J. Org. Chem.* **2006**, 71, 2360-2372.
- (78) In agreement with literature data: de Raadt, A.; Griengl, H.; Petsch, M.; Plachota, P.; Schoo, N.; Weber, H. *Tetrahedron: Asymmetry*, **1996**, 7, 473-490.
- (79) In agreement with literature data: Evindar, G.; Batey, R. A. *J. Org. Chem.* **2006**, 71, 1802-1808.
- (80) In agreement with literature data: Naidu, A. B.; Sekar, G. *Synthesis* **2010**, 579-586.

Concluding Remarks and Outlook

The Ni pincer complex [$(^{\text{Me}}\text{N}_2\text{N})\text{NiCl}$] (**1**) developed by our group showed high efficiency for cross coupling of non-activated and functionalized alkyl halides with alkyl Grignard reagents. One limitation of the reactions is the low efficiency for the coupling of secondary alkyl halides. Subsequently, the development of Kumada-type alkyl-alkyl cross-coupling was the starting point of this Ph.D thesis. Thirteen well-defined Ni(II) complexes were synthesized and structurally characterized. Many of these complexes are active for Kumada coupling of non-activated secondary alkyl halides. Using these complexes, it was possible to study the influence of coordination number, geometry, and spin state on the efficiency of catalysis. Another important outcome of this work is the development of two excellent new catalysts [$(^{\text{H}}\text{NN})\text{Ni}(\text{PPh}_3)\text{Cl}$] (**24**) and [$(^{\text{H}}\text{NN})\text{Ni}(2,4\text{-lutidine})\text{Cl}$] (**27**) for alkyl-alkyl Kumada coupling of non-activated secondary alkyl halides. The origin of their high efficiency was shown to be related to the steric properties of the ligands and the access to a transmetalation pathway. There are only a handful of catalysts known for alkyl-alkyl coupling of non-activated secondary alkyl halides, let alone well-defined catalysts. This work significantly expanded the available pool of catalysts for this challenging methodology, which is highly desirable in organic synthesis. The structure-activity study is an important step toward the understanding of this coupling reaction.

In an attempt to find a more synthetically useful pathway to the formation of tertiary and quaternary carbon centers, the reverse methodology was considered as an alternative. An efficient method for the cross-coupling of alkyl halides and tosylates with secondary and tertiary alkyl Grignard reagents was subsequently developed. Simple conditions such as a small loading of CuCl at room temperature in THF, and with no additives, are the big advantage of this methodology. It also shows broad substrate scope and good functional group tolerance.

In recent years, copper catalysts have become a promising area for C-H functionalization and cross-coupling reactions. In the last part of my thesis, ten copper complexes with newly designed ligands were synthesized and fully characterized. They were screened to test the alkylation of benzoxazoles by using secondary alkyl halides, which are desirable secondary alkyl electrophiles. The best catalyst is the copper(I) complex [$(^{\text{Me}}\text{N}_2\text{N})\text{Cu}(\text{PPh}_3)$] (**36**) which contains the bis-(amino)amide ($(^{\text{Me}}\text{N}_2\text{N})$) ligand. The reactions are promoted by bis[2-(N,N-dimethylamino)ethyl] ether.

As described here, some progress has been made in creating tertiary and quaternary carbon centers by nickel and copper-catalyzed cross-coupling reactions of alkyl electrophiles during the course of my thesis. However, there are several issues that still remain to be resolved: (1)

Although significant progress of Kumada type alkyl-alkyl cross-couplings has been made, coupling of alkyl chlorides is less studied. Alkyl chlorides are desirable alkylation reagents because of their wide availability and low cost relative to their iodo and bromo analogues, however they are less reactive due to the strong C-Cl bond compared to C-Br and C-I bonds. Thus, high functional group-tolerant Kumada couplings of non-activated alkyl chlorides should be developed. (2) As was found in the coordination chemistry of a series of bidentate and tridentate ligands, nickel and copper complexes with different coordination number, geometry, oxidation states (copper chemistry) and catalytic efficiency can be produced depending on the reaction conditions. Based on this observation, it will be advantageous to use well-defined catalysts for mechanistic investigations. (3) I develop three pathways to create tertiary and quaternary carbon centers by nickel and copper-catalyzed cross-coupling reactions. Application of this chemistry to catalysts possessing chiral ligands could result in formation of desired enantioselective products, and should be explored. (4) With regards to C-H functionalization by copper catalysis, significant improvements must be made to the catalytic system in order to broaden the scope of the substrates.

Curriculum Vitae

Peng Ren

EPFL SB ISIC LSCI, BCH 3207, CH 1024, Switzerland

Tel.: +41 (0)21 6939881 E-mail : peng.ren@epfl.ch

Date of Birth: Oct. 16, 1984

Place of Birth: Zhengzhou, Henan, P. R. China

Education

EPFL

Lausanne, Switzerland

- Ph.D. candidate in organometallic chemistry *Nov.2008-present*
- Synthesis of well-defined Ni-, Cu-, Ru-based coordination complexes, development of new synthetic methodology for cross coupling of non-activated alkyl halides and direct C-H functionalization.

Nankai UNIVERSITY

Tianjin, China

- Bachelor of Science *Sep.2004-July.2008*
- Synthesis and characterization of Metal-Organic Frameworks (MOFs).

Core Skills

-
- Proficient in working with air and moisture sensitive materials using both Schlenk techniques and Glove-Box.
 - Good skills in isolation, purification and structure elucidation of new compounds.
 - Extensive use of analytical techniques such as NMR, GC-MS, HPLC, UV-vis, MALDI-TOF. Familiar with Single-crystal X-Ray Diffraction, SQUID.
 - Software: Microsoft Office, Chemoffice, Origin, Diamond, Mercury.

Teaching Experience

-
- Research Assistant: mentored 3 master students and 1 research apprentice through project direction and laboratory training.
 - Teaching Assistant: Inorganic Chemistry, Organic Chemistry, Chemical Engineering.

Awards

-
- 2012
Swiss National Science Foundation fellowship for young researchers
 - 2012
Student Travel Award from the Swiss Academy of Science
 - 2012
Chinese government award for outstanding self-financed students abroad

Publications and Presentations

Ph.D. work

17. **Ren, P.**; Stern, L.A.; Hu, X.L.
Copper-Catalyzed Cross Coupling of Functionalized Alkyl Halides and Tosylates with Secondary and Tertiary Alkyl Grignard Reagents
Angew. Chem., Int. Ed. **2012**, *51*, 9110-9113.
16. Perez Garcia, P. M.; Franco, T. D.; Orsino, A.; **Ren, P.**; Hu, X. L.
Nickel-Catalyzed Diastereoselective Alkyl-Alkyl Kumada Coupling
Org. Lett., **2012**, *14*, 4286-4289.
15. Madhira, V. N.; **Ren, P.**; Vechorkin, O.; Hu, X.L.; Vicic, D.A.
Synthesis and Electronic Properties of a Pentafluoroethyl Derivatized Nickel Pincer Complex
Dalton Trans., **2012**, *41*, 7915-7919.
14. **Ren, P.**; Salihu, I.; Scopelliti, R.; Hu, X.L.
Cu-Catalyzed Alkylation of Benzoxazoles with Secondary Alkyl Halides
Org. Lett., **2012**, *14*, 1748-1751.
13. **Ren, P.**; Vechorkin, O.; Von Allmen, K.; Scopelliti, R.; Hu, X.L.
A Structure-Activity Study of Ni-Catalyzed Alkyl-Alkyl Kumada Coupling. Improved Catalysts for Coupling of Secondary Alkyl Halides.
J. Am. Chem. Soc., **2011**, *133*, 7084-7095.
12. **Ren, P.**; Vechorkin, O.; Csok, Z.; Salihu, I.; Scopelliti, R.; Hu, X.L.
Pd, Pt, and Ru Complexes of a Pincer Bis(amino)amide Ligand.
Dalton Trans., **2011**, *40*, 8906-8911.

Bachelor work

11. Han, T.; **Ren, P.**; Xu, N; Cheng, P; Liao, D.Z.; Yan, S.P.
Ferro/antiferromagnetic interactions transmitted by double bridged carboxylate groups in 2D mixed-ligand transition metal coordination polymers
Inorg. Chim. Acta, **2012**, doi:10.1016/j.ica.2012.01.019.
10. Liu, M.L.; **Ren, P.**; Shi, W.; Cui, J.Z.; Cheng, P.; Gao, H.L.
Synthesis, Structures and Magnetic Properties of 1D to 3D Coordinated Polymers Based on Series of Flexible Sulfide Ligands.
Inorg. Chim. Acta, **2011**, *378*, 56-65.
9. Zhao, L.M.; **Ren, P.**; Zhang, Z.J.; Fang, M.; Shi, W.; Cheng, P.
Synthesis, Crystal Structures and Fluorescence Properties of Four Mixed-Ligands Zn(II) and Cd(II) Coordination Compounds.
Science in China, Series B: Chemistry, **2009**, *52*, 1479-1484.
8. **Ren, P.**; Liu, M.L.; Zhang, J.; Shi, W.; Cheng, P.; Liao, D.Z.; Yan, S.P.
1D, 2D and 3D Luminescent Zinc(II) Coordination Polymers Assembled from Varying Flexible Thioether Ligands.
Dalton Trans., **2008**, *35*, 4711-4713.

7. **Ren, P.**; Xu, N.; Chen, C.; Song, H.B.; Shi, W.; Cheng, P.
Solvothermal Synthesis of 1D and 2D Cobalt(II) and Nickel(II) Coordination Polymers with 2,5-Dihydroxy-p-Benzenediacetic acid.
Inorg. Chem. Comm., **2008**, *11*, 730-732.
6. **Ren, P.**; Shi, W.; Cheng, P.
Synthesis and Characterization of Three-Dimensional 3d-3d and 3d-4f Heterometallic Coordination Polymers with High Thermal Stability.
Cryst. Growth & Des., **2008**, *8*, 1097-1099.
5. Chen, Z.; Fang, M.; **Ren, P.**; Li, X.H.; Zhao, B.; Shi, W.; Cheng, P.
Synthesis, Structure and Luminescent Property of Two New 2D Metal-Organic Frameworks Containing Lanthanide Ions.
Z. Anorg. Allg. Chem., **2008**, *634*, 382-386.
4. **Ren, P.**; Shi, W.; Cheng, P.
Unprecedented 7-Connected $3^6 \cdot 4^{13} \cdot 6^2$ Structural Topology: Praseodymium-Based Coordination Polymers Built from Mixed Carboxylate Ligands.
Inorg. Chem. Comm., **2008**, *11*, 125-128.
3. **Ren, P.**; Chen, P.K.; Xu, G.F.; Chen, Z.
Novel $(4^2 \cdot 8^4)(4^3 \cdot 6^3)_2(4^6 \cdot 6^3 \cdot 8^6)_2$ Topology Network Built Up from the Highly Connective Pyridine-2,4,6-Tricarboxylate Ligand,
Inorg. Chem. Comm., **2007**, *10*, 836-838.
2. Huang, Y.Q.; Ding, B.; Song, H.B.; Zhao, B.; **Ren, P.**; Cheng, P.; Wang, H.G.; Liao, D.Z.; Yan, S.P.
A Novel 3D Porous Metal-Organic Framework Based on Trinuclear Cadmium Clusters as a Promising Luminescent Material Exhibiting Tunable Emissions Between UV and Visible Wavelengths
Chem. Commun., **2006**, *47*, 4906-4908.
1. **Ren, P.**; Ding, B.; Shi, W.; Wang, Y.; Lu, T.B.; Cheng, P.
2D and 3D Sulfate-Water Supramolecular Networks Templated via Triazole-Nickel(II) Complexes.
Inorg. Chim. Acta, **2006**, *359*, 3824-3830.

Conference

- **Ren, P.**; Scopelliti, R.; Hu, X.L.
Nickel and Copper-Catalyzed Cross Coupling of Secondary Alkyl Halides
18th International Symposium on Homogeneous Catalysis, Toulouse **France**, July 2012.
- **Ren, P.**; Vechorkin, O.; Von Allmen, K.; Scopelliti, R.; Hu, X.L.
A Structure-Activity Study of Ni-Catalyzed Alkyl-Alkyl Kumada Coupling. Improved Catalysts for Coupling of Secondary Alkyl Halides.
XIX EuChemS Conference on Organometallic Chemistry, Toulouse **France**, July 2011.

